

Kinetic Modeling of Financial Market Models

Von der Fakultät für Mathematik, Informatik und Naturwissenschaften
der RWTH Aachen University zur Erlangung des akademischen Grades
eines Doktors der Naturwissenschaften genehmigte Dissertation

vorgelegt von

Torsten Trimborn, M.Sc.

aus

Viersen

Berichter: Prof. Dr. Martin Frank

Prof. Dr. Michael Herty

Prof. Dr. Lorenzo Pareschi

Tag der mündlichen Prüfung: 21.12.2017

Diese Dissertation ist auf den Internetseiten der Universitätsbibliothek verfügbar.

To my family

Nina, Zoe and Oscar

Acknowledgement

Special thanks belongs to my supervisor Martin Frank who constantly supported my research project, dating back to the start of my master thesis in 2012. His idealism, curiosity and open mindedness made it possible to work on this special topic. I enjoyed our endless discussions on mean field games and his sound advice in times of setbacks. I am grateful that he did not only took care of my scientific career but has also shaped my personal development.

I also wish to express my gratitude to Michael Herty. With him we started the journey of solving the riddle of mean field games in 2015. Thank you for your patience and your time to discuss all the obstacles I faced. I am very pleased for the opportunity to pursue my research and looking forward to the new destinations on this journey.

I would also like to thank Lorenzo Pareschi for his kind hospitality during my stays in Ferrara. Due to the fruitful cooperation in the past years I have gained further insights into kinetic modeling. In particular, I remember fondly the derivation of the microscopic portfolio model we did together at the blackboard in Ferrara.

I thank Stephan Martin for his support and advice during the early stage of my Ph.D. A lot of work in this study is based on early research I conducted with Stephan.

I am grateful to José Carrillo for sharing his knowledge in the rigorous derivation of mean field models. I would like to thank Erika Ábrahám for the opportunity to supervise seminars of computer scientists. Furthermore, I wish to express my gratitude to Prof. Kittsteiner, who was always open for discussions and supported my application forms. I thank Prof. Kamps for his support of my successful application for my scholarship.

All this work could be only achieved in a productive and friendly working environment which was created by my fellows at the MathCCES institute. Thank you for so many scientific and non-scientific discussions, which I will miss in the future. In particular, I would like to thank Graham Alldredge, Richard Barnard, Thomas Camminady, Maren Hattebur, Kerstin Küpper, Kai Krycki, Jonas Kusch, Julian Koellermeier, Philipp Otte, Teddy Pichard, Pascal Richter, Christina Roeckerath, Birte Schmidtmann, Maike Sube, Armin Westerkamp and Jannick Wolters for all the good times we shared. Special thanks go to my old office mates Richard Barnard and Pascal Richter. I will never forget the inspiring atmosphere in the office 325, the official break room next to the kitchen.

Thank you Pascal for your unbelievable enthusiasm which has always been a motivation to me. I am looking back to 5 great years in the best (and largest) Ph.D. office at RWTH University. Furthermore, special thanks to captain Philipp. I remember so many joyful experiences that I do not know where I should start. Thanks for your scientific advice, for proofreading, the joint projects, the cooking evenings and all the tedious discussions.

I wish to express my gratitude to all students I have supervised. Special thanks go to Max Beikirch, Simon Cramer and Emma Pabich for the time they invested in the SABCEMM project. Furthermore, I would like to thank my former student colleges Max Broelsch, Simone Küpper, Christian Lax, Andrea Seeger, Nina Thomas, Carl Troebs, Markus Tronnier, Jan Umlauft, Martin Voss, Kristin Wache, Sebastian Wolf and Simone Zucker. I am looking back to the afternoons we spent in the *Romanistik* and all the great events we experienced

together.

Thanks to Christoph Elsberger, Thorsten Klingen and Christian Lax for proofreading this document.

I acknowledge funding by the *Hans-Böckler-Stiftung* with financial support from the *Federal Ministry of Education and Research of Germany*. Their support made the realization of this project possible. I am glad for the possibility to participate in many seminars and a language school of the *Hans-Böckler-Stiftung*. I also thank the Graduiertenstipendium of RWTH Aachen University for financial support.

I would like to thank my parents for their emotional and financial support during my studies which made this work possible in the first place. Last but not least special thanks to the most important persons in my life, Nina, Zoe and Oscar. I am sorry for all the indulgence and patience you had to invest in the past half year. Sadly, I did not manage to accompany the pregnancy as I would have wanted. Thanks for your support, love and affection you give me, which has been the strongest motivation in the past months.

Abstract

The modeling of financial markets has a long tradition in economics and has developed into a significant and highly accepted field of research. Especially the financial crises of the last decade, namely the Global Financial Crisis of 2007 and the European Debt Crisis of 2009 have demonstrated the incapability of many standard financial market models to account for financial crashes or merely reproduce them. Stylized facts, observations in statistical data, are considered to play a prominent role in the emergence of financial crashes. More recent financial market models such as agent-based models can reproduce these stylized facts. These models are large dynamical systems studied by Monte Carlo simulations. They share many similarities with models from particle physics and substantially differ from classical financial market models. Agent-based models indicate that behavioral aspects in investors' investment decisions account for the existence of stylized facts. The disadvantage of these models, however, is the necessity to verify any results of the microscopic model by means of Monte Carlo simulations, which have the drawback of a slow convergence rate. Furthermore, it has been shown that many stylized facts in agent-based models are mere numerical artifacts. These disadvantages can be overcome by time continuous kinetic financial market models which can be studied analytically. Thus, steady state distributions can be analyzed and the origins of stylized facts can be proven. The centerpiece of this work is concerned with the derivation and the analysis of two kinetic financial market models. Econophysical agent-based models will be our starting point as they can replicate stylized facts. Our analysis will provide new insights on the origin of stylized facts as well as helping us to characterize the distribution of wealth and stock prices. We will derive a portfolio model of interacting financial agents. The agents face an optimization problem on the microscopic level. Model predictive control will be applied to simplify and solve the utility maximization before we derive the mean field limit. Interestingly, this method provides us with a mathematical connection between the two opponent economic concepts of modeling financial agents to be either rational or bounded rational. We will study the wealth and stock price distributions in detail and obtain analytically steady state solutions. The wealth distribution is always characterized by a lognormal distribution function. For the stock price distribution, we can either observe lognormal behavior in the case of long-term investors or a power-law in the case of high-frequency traders. The second model is a behavioral asset pricing model depicting agents' investment decisions either solely based on a trading strategy or additionally influenced by the behavioral herding pressure. We will show that quantitatively, the kinetic limit is an appropriate limit of the original econophysical model. Moreover, we can quantify that the emergence of stylized facts can be attributed to herding pressure and analyze the deterministic version of our kinetic system. The steady states are characterized and entropy bounds are derived which provide us with first explanations for the complex model behavior. A further aspect this work is concerned with is the theory of mean field limits. In the case of deterministic ODEs, we rigorously derive the mean field equations for a simple financial market model. Additionally, we study the case of a microscopic differential game, a new field of research called mean field games.

We derive the mean field game limit system for a large class of ODE models. In fact, we obtain a genuinely new class of models which has never been discussed in literature before. The last aspect we will present in this work is the SABCEMM software, a simulation tool for agent-based models and the first simulator specialized for econophysical agent-based computational financial market models. This tool is designed to enable an unbiased comparison between different models and to minimize the amount of coding needed in order to create new models. This code is written so efficiently that it enables a standard laptop to compute simulations with up to several millions of agents. We can conclude that kinetic theory is appropriate to approximate agent-based financial market models and that it allows for the discovery of new results in comparison to microscopic agent-based market models.

Preface

My personal interest in the kinetic modeling of financial markets has been awoken by a number of circumstances. The Global Financial Crisis of 2007 and the ongoing European Debt Crisis have shifted my attention to models of financial markets as they promise explanations for the emergence of these market crashes. Especially the negative impacts of crashes on the real economy such as high unemployment rates and recessions have been my personal motivation to devote myself to research in this field.

Martin Frank's lecture on *Transport Theory* at RWTH Aachen university in 2011 must be considered the starting point for my fascination with kinetic theory. Searching literature for an appropriate subject for my master thesis combining kinetic theory and financial market models, I found the paper *On a kinetic model for a simple market economy* by Cordier, Pareschi and Toscani [67], a work which succeeded to engage my interest in kinetic modeling of financial markets. Since then, I have been fascinated by this new field of research. At this point, I must emphasize that the application of kinetic theory to economic models must still be regarded a very recent development and a very special field of research although there has been an increasing number of contributions in the past years.

There are several rationales to the necessity of studying financial market models. Most importantly, classical financial market models, or standard models, fail to reproduce several statistical observations on financial markets and thus cannot account for real-life financial market phenomena. The most prominent example is the inequality of income first studied by Pareto [200]. So-called fat tails in the distribution of stock price returns must be considered a further example. The origins of these statistical observations remain widely unexplained [69]. Several studies indicate that these statistical artifacts play a crucial role in the creation of financial crashes [102, 151]. In order to investigate the reasons for market crashes, financial market models which are able to reproduce these statistical properties are a major concern.

In literature, there are more recent modern financial market models, agent-based computational financial market models, which enable the reproduction of these statistical observations, often called stylized facts. These models share many similarities with models from statistical physics and their dynamics are thus studied with the help of Monte Carlo simulations. In addition, these models are inspired by behavioral finance and do not model investors as perfect utility maximizers. The drawback of these models, however, is that these systems usually are large dynamical systems and their complexity necessitates computer simulations. Especially in the case of a large number of market participants, these simulations are very elaborate and thus very costly. Numerical issues must be considered an additional problem regarding these models. One example can be found in finite size effects observed in several agent-based models [93]. Stability problems, e.g. caused by stiff differential equations, are another issue.

Kinetic modeling enables the derivation of approximations of these large dynamical systems. More precisely, starting at the microscopic level with agent-based economic models, we derive time continuous kinetic PDE models, arriving at a significant reduction of computational costs. Notably, a kinetic PDE model enables us to perform a proper mathematical analysis and thus e.g. to analyze the wealth or stock price distribution. Finally, we want to point out, that such a reduced time continuous formulation helps us to prove the reasons for the

appearance of stylized facts in each model. This proves to be a significant advantage since computer simulations are usually the only feasible way of studying agent-based models. The challenges we are confronted with deriving kinetic financial market models are of various kind. On the microscopic level, the difference equations have to be translated into time continuous models. In order to exclude finite size effects, one has to run computationally expensive simulations considering many agents. The next step is concerned with the selection of the appropriate kinetic limit and the derivation of the kinetic equation. The quality of the kinetic approximation in comparison to the microscopic model should be quantified. Finally, a proper mathematical analysis of the kinetic model is required in order to gain insights into the model behavior. In summary, the modeling of kinetic financial market models covers a broad spectrum of mathematical disciplines, such as modeling, analysis and numerics.

Based on these observations, we derive and analyze two kinetic financial market models. Furthermore, we have developed the software tool SABCEMM (Simulate Agent-Based Computational Economic Market Models) which is a simulator for agent-based economic market models. Regarding kinetic limits, we study the mean field limit of a general class of differential games. These models are known as *mean field games* and are frequently applied in economic contexts.

In chapter 2, we will present the software tool SABCEMM which is designed to efficiently simulate agent-based computational economic market models. The tool was developed in C++ and its efficient coding allows us to simulate models with up to several millions of agents. Due to its object-oriented structure, this tool enables the user to design and compare multiple ABCEM models from a unified perspective. We will provide several examples of various agent-based models and exemplarily show finite-size effects in the Levy-Levy-Solomon model [155]. In addition, we will discuss the scaling behavior and the computational efficiency of the framework.

In chapter 3, our detailed discussion of the mean field limit will be preceded by a brief introduction to stochastic processes and kinetic theory. More precisely, we rigorously derive the mean field limit of a simple financial market model. This chapter will be concluded by an introduction to mean field games. In comparison to the previous setting, each agent faces an optimization problem while the state dynamics are given by ODEs. We will derive the mean field games limit system in detail for a large class of models. Finally, we will derive the mean field game system for a microscopic financial market model.

In chapter 4, we introduce a microscopic asset allocation model which has been inspired by the econophysical Levy-Levy-Solomon model [155]. In this model, the investment decisions of investors, derived by an optimization process, drives the stock price. The financial agents' investment decisions are approximated by model predictive control (MPC). Interestingly, the MPC approach reveals a mathematical connection between the two opponent economic concepts of modeling financial agents to be either rational or boundedly rational. In the next step, we will perform the mean field limit and derive the kinetic model. Furthermore, we will derive a moment model which is able to replicate the most prominent features of financial markets: oscillatory price behavior, booms and crashes. Due to our kinetic approach, we study the wealth and price distribution of the kinetic model as well.

In the concluding chapter, we will derive the mean field limit of the econophysical Cross model [71]. We will demonstrate that our kinetic model is appropriate to qualitatively approximate the original model. Thus, our model allows the replication of some stock price anomalies,

i.e. fat-tails of asset returns, uncorrelated stock price returns and volatility clustering. Interestingly, the reasons for these statistical artifacts can be attributed to psychological misperceptions (on behalf of the investors/financial agents). Finally, this model will be discussed analytically in order to understand the complex model behavior.

Several chapters of this work are based on papers which have been published with coauthors previously. Section two largely relies on [242] and was published with Philipp Otte, Simon Cramer, Max Beikirch, Emma Pabich and Martin Frank. My contribution to this paper is mainly concerned with the economic model, test cases and the interpretation of the results. Parts of section 3 are based on [240], which was published in cooperation with Michael Herty and Martin Frank. In this paper, we revisited and extended an earlier work of Michael Herty et al. [81]. A detailed formal derivation of the paper's general model as well as the design and computation of all examples constituted my personal contribution to this work. Furthermore, I modeled and derived the financial market model. Chapter 4 is based on [243], which was published with my coauthors Lorenzo Pareschi and Martin Frank. I contributed the work's fundamental concept, i.e. the application of MPC to a portfolio model, closely related to the model in [155]. Apart from the modeling of the microscopic portfolio model, I have been responsible for the application of the MPC methodology and the derivation of kinetic models. In addition, the analysis has been performed by myself but it relies on a paper by Pareschi and Maldarella [166]. Furthermore, I have been responsible for the conduction of all simulations. Finally, chapter 5 relies on [239], in which I mainly worked on the derivation of the mean field model and which was published with my coauthors Stephan Martin and Martin Frank. Moreover, I conducted the tests to quantify the validity of our kinetic approximation and computed all analytical results presented in this section.

Contents

1	Introduction	1
1.1	Motivation	1
1.2	Stylized Facts	3
1.3	Econophysics and Agent-Based Models	10
1.3.1	Modeling Agents	11
2	SABCEMM- A Simulation Framework for Agent-Based Computational Economic Market Models	13
2.1	Introduction	13
2.2	Abstract ABCEM Models	16
2.2.1	Market Mechanisms	19
2.2.2	Agent Design	21
2.2.3	Environment	22
2.3	Results	22
2.3.1	Cross Model	23
2.3.2	LLS Model	30
2.3.3	Harras Model	35
2.4	Software Architecture	36
2.4.1	Numerical Core	38
2.4.2	Features	40
2.4.3	Computational Aspects	42
2.4.4	Conclusion	46
2.5	Appendix	47
2.5.1	Models	47
2.5.2	Parameter Sets	51
3	Kinetic Theory and Applications to Financial Market Models	54
3.1	Stochastic Processes to PDEs	54
3.1.1	Stochastic Differential Equations	54
3.1.2	Kolmogorov Equations	56
3.1.3	Application to Stock Price SDEs	58
3.1.4	Long Time Asymptotics	62
3.2	Kinetic Theory	64
3.2.1	Applications to Financial Market Models	69
3.3	Mean Field Limit	72
3.3.1	Microscopic Economic Model	72
3.3.2	Mean Field Limit of Microscopic Economic Model	77
3.3.3	Stochastic Mean Field Limit	87
3.4	Mean Field Games	90
3.4.1	Introduction	90
3.4.2	Main Results	92
3.4.3	Derivation of Main Results	96
3.4.4	Examples	106
3.4.5	Conclusion	110

4 Portfolio Optimization and Model Predictive Control	111
4.1 Introduction	111
4.2 Microscopic Model	113
4.3 MPC for Microscopic Model	115
4.4 Mean Field Limit of Feedback Controlled Model	117
4.4.1 Moment Model	119
4.4.2 Marginals of Mean Field Portfolio Equation	124
4.5 Feedback Controlled Model with Noise	125
4.5.1 Mean Field Limit	126
4.5.2 Marginals of Diffusive Mean Field Portfolio Equation	128
4.6 Stock Price as Random Process	129
4.6.1 Long-term investors	130
4.6.2 High-frequency Traders	131
4.7 Numerics	134
4.8 Conclusion	139
4.9 Appendix	140
4.9.1 Moment Model	140
4.9.2 Parameters of Moment Simulation	141
4.9.3 Marginals of Mean Field Portfolio Model	141
4.9.4 Marginals of Diffusive Mean Field Portfolio Model	142
4.9.5 Asymptotic Limit of Boltzmann Model	142
4.9.6 Parameters of Simulations	144
5 Mean Field Limit of a Behavioral Financial Market Model	145
5.1 Introduction	145
5.2 The Original Model	147
5.2.1 Microscopic Simulations	149
5.3 Kinetic Particle Model	150
5.3.1 Microscopic Simulations of Kinetic Particle Model	152
5.4 Kinetic Model	152
5.5 Numerics	155
5.5.1 Deterministic Stock Price Equation	157
5.5.2 Monte Carlo Solver	159
5.6 Qualitative Behavior of the Model	160
5.7 Conclusion and Outlook	165
5.8 Appendix	167
5.8.1 Numerics	167
5.8.2 Qualitative Studies	169
6 Conclusion and Outlook	172
6.1 SABCEMM	172
6.2 Mean Field Limit and Mean Field Games	173
6.3 Portfolio Optimization and Model Predictive Control	173
6.4 Behavioral Financial Market Model	174
6.5 Economic Perspectives	174
References	176

1 Introduction

The objective of this work is to derive and analyze kinetic financial market models. With kinetic models, we refer to time continuous models defined by partial differential equations (PDEs) which we derive from microscopic dynamics as known from kinetic theory. On the microscopic level, we consider agent-based econophysical financial market models. These models are large non-linear dynamical systems. Each financial agent is modeled by an ordinary differential equation (ODE) or stochastic differential equation (SDE). In order to derive the kinetic PDE model we need to perform a kinetic limit. The limit describes the shift from a finite number of agents to an infinite number of agents. Thus, the evolution of agents is described by a density function defined as the solution of the corresponding PDE.

In this work we will provide a study of the mean-field limit. This work's centerpiece is the derivation and analysis of two kinetic financial market models. The advantage of kinetic financial market models compared to their microscopic counterparts is the possibility to study them analytically. Furthermore, such PDE models make it possible to discover wealth or stock price distributions. In addition, the kinetic limit leads to a huge reduction in dimensions and thus to a reduction of computational costs as well.

Brief introductions into kinetic theory, the mathematical concepts relevant to this work and into agent-based financial market models are given. We extensively motivate the importance of such modern financial market models, especially in the context of the great socio-economic implications of financial crashes in our globalized and industrialized world.

1.1 Motivation

The modeling of financial markets has a long tradition in economics and dates back to the early works of Bachelier [17]. This research field is known as *quantitative finance* or *financial mathematics*. On the mathematical side, there have been remarkable contributions by Itô [127] on stochastic diffusion processes. Regarding modeling, the most influential work was published by Black, Scholes and Merton in the 1970s [49]. Black and Scholes derived a model for option pricing [26] while Merton analyzed the risks of interest rates [182] and contributed to the theory of option pricing as well [181].

The general interest in financial market models can be attributed to many rationales: Investors want to predict stock prices and crashes, insurance companies want to reduce their investment risks and politicians aim to have a valid regularization.

Especially in the last decade, the focus of many scientists and economic practitioners has shifted to the modeling of financial markets. The reason are the several financial crises in the past years, most notably the *Global Financial Crisis* 2007 and the *European Debt Crisis* in 2009. Further examples of stock market crashes in the last century are the *Great Depression 1929*, the *Energy Crisis in the 1970s* and the *Black Monday 1987*. Such crises have always had a negative impact on the real economy and have yielded to high unemployment rates. For example, the unemployment rate during the Great Depression rose in the United States to 25 %. Financial crashes seem to be a natural, recurring event in global financial markets. This has already been discovered in the 19th century by Owen [194] and Sismondi [217] and has led to the theory of business cycles. Interestingly, Owen claimed that the *inequality of*

wealth seems to play an important role in the creation of market crashes. Furthermore, this early theory of business cycles and financial crashes has even influenced the work of Marx [153].

Such a theory of business cycles seems to indicate that a rational explanation for the succession of booms and crashes exists. Examples are the *industrial revolutions, wars or monetary policies*. These arguments guide us to the *efficient market hypothesis* (EMH) proposed by Fama in 1970 [100]. The EMA claims that financial markets are rational. This means that the stock price always reflects the fair market price and incorporates all available information. Classical financial market models like the Black and Scholes model are built on the assumption of a rational market.

There are several studies which raise doubt regarding the EMH [129]. Especially the field of *behavioral finance*, where financial agents are not acting purely rational but are rather influenced by psychological biases, contradict the EMH [29, 211].

Since the 1970s, econometricians have been observing statistical characteristics of stock price data they observed all over the world on different time scales. These statistical facts are often coined *financial market anomalies*, but we prefer the term *stylized facts*. The most prominent example is the inequality of wealth and income, which was discovered by Pareto in 1897 [200]. Further examples are *fat-tails of asset returns* and *volatility clustering*, which we will discuss in detail later. At this point, we want to stress that these *stylized facts* cannot be explained by the EMH [163]. In fact several studies indicate that stylized facts play a prominent role in the creation of market crashes [151]. Thus, in order to gain insights into the origin of financial crashes, one needs to understand the reasons for the existence of stylized facts. This leads us to the statement that a good financial market model has to be capable to replicate stylized facts in financial data. Unfortunately, the classical or standard financial market models fail to replicate stylized facts, since they consider representative agents in the spirit of the EMH [163]. The failure of most models to understand and explain the Global Financial Crisis in 2007 has been pointed out by many authors [61, 102].

Alternative attempts to these classical models have been emerging from the representative agent paradigm since the 1990s. These models rather focus on the interaction of many agents and consider behavioral aspects as well. Furthermore, these models are closely connected to the complex models of interacting particles, originally studied in statistical physics. Hence, it is not a coincidence that many physicists started to apply physical theories like percolation theory or kinetic theory to economic issues. This popular field of research is known as *econophysics*. One part of econophysics is preoccupied with agent-based financial market models. These models consist of many interacting financial agents. The evolution of macroscopic quantities such as the stock price is studied through Monte Carlo simulations. These modern financial market models are capable to reproduce stylized facts. In fact, several models show that psychological biases of investors cause the appearance of stylized facts. Hence, we can conclude that these modern models can help to study the origin of stylized facts. Furthermore, these models also enable researchers to study the impact of new regularizations on these artificial stock markets. Thus, agent-based models can help politicians to construct effective measures of regularization. The importance of these agent-based models has been pointed out by several authors [102, 163]. In the next section, we will discuss agent-based financial

market models in more detail.

Finally, we want to point out that financial crashes, as well as the inequality of wealth, have not only economic but also social and socio-political implications. After the Global Financial Crisis in 2007, there have been many demonstrations against the banks and financial institutions all over the world. Many citizens of the western hemisphere even doubt the effectiveness of the capitalistic system. Studies point out that inequality of wealth leads to democratic instabilities [220, 137]. In fact, recent studies reveal an increase of the global wealth inequality in the past decades [204, 205]. In addition, the international monetary fund has proposed that high wealth inequities may have a negative impact on economic growth [76].

In conclusion, we want to sharpen the message to: the study of financial markets and the discovery of the origins of stylized facts is of significant importance for the further existence of the western capitalist democracies.

1.2 Stylized Facts

As pointed out previously, agent-based models aim at the reproduction of artificial financial data which has the same characteristics, respectively *anomalies*, as real world financial data. The label *anomalies* is not well chosen because it implies that there are no scientific explanations for those characteristics [163]. We thus prefer the term *stylized facts* as those can be explained to be universal market properties which can be observed at stock markets all over the world [209].

There are at least thirty known stylized facts, we refer to [56, 163] for a short summary. The evidence of those *stylized facts* has been shown by econometricians in the last decades. Probably the oldest known *stylized fact* is the power law behavior of the income distribution obtained by Vilfredo Pareto. Furthermore, we want to introduce and explain the most prominent *stylized facts*: *fat tails in asset returns*, *absence of autocorrelation* in stock returns and *volatility clustering*.

Wealth distribution In 1897, Vilfredo Pareto proposed an inverse power law for the income (wealth) distribution of employees (agents) [200]:

$$F_c(w) = \int_w^\infty f(w^*) dw^* \sim w^{-\mu}.$$

Here f denotes the probability density function of employees (agents) to have an income (wealth) w and F_c is the complementary cumulative density function. In honor of Pareto, the corresponding distribution, which has exactly this power-law behavior, is named after him. The Pareto density function is given by:

$$f(x) = \begin{cases} \mu x_0^\mu x^{-\mu-1} & x \geq x_0, \\ 0, & x < x_0, \end{cases}$$

with a scale parameter x_0 and a shape parameter (often called Pareto index) $\mu > 0$. The cumulative density function is given by

$$F(x) = \begin{cases} 1 - \left(\frac{x_0}{x}\right)^\mu & x \geq x_0, \\ 0, & x < x_0, \end{cases}$$

and the complementary cumulative density function can be observed directly by the relation

$$F_c(x) := P(X > x) = 1 - P(X \leq x) = 1 - F(x).$$

Pareto mistakenly believed that there is an universal exponent $\mu \approx 1.5$ which fits the income distribution in every society [67]. In 1932, Gibrat stated that the Pareto distribution is only valid for high incomes and that a lognormal probability density is correct regarding the middle-income range [190, 108].

More recent studies, mostly of physicists, indicate that the appropriate distribution below the threshold x_0 is the Gibbs distribution [86]. Economists often prefer the lognormal distribution and the question of the correct distribution is still subject of vivid debate [190].

The exponent μ of the income distribution is estimated e.g. for the USA around $\mu_{USA} \approx 1.7 \pm 0.1$, for the United Kingdom $\mu_{UK} = 2.0 - 2.3$ [87] and for Japan $\mu_J \approx 2$ [106].

There definitely is much interest in wealth distributions from a social point of view. A society's degree of inequality can directly be deduced from the wealth distribution. The Pareto distribution is defined by the parameters x_0 and μ which may characterize the inequality in each country. The questions of inequality in different countries, respectively national economies, is not only discussed in scientific society but also in politics and economy. The international monetary fund (IMF) claims that too much inequality in a society has negative impact on its economic growth [193]. One can approximately assume that 85% of the wealth is owned by 10% of the population [77]. In Germany, the richest 0.1% of the population own 23% of the entire property [16]. In addition, the income inequality has grown globally between 1910 and 1992 [13].

Such heavy tailed distributions do not only appear in the context of wealth and income distributions but also in the case of stock returns [161]. This phenomenon is called *fat-tails of asset returns*. Before we study this stylized fact in detail, we want to quantify fat or heavy tailed distributions mathematically.

What are fat or heavy tails? We want a distinction which is not always made in literature between a heavy tailed and fat-tailed distribution. Heuristically, we can state that a distribution has a heavy tail if the tail is heavier than exponential.

Definition 1.2.1. *The distribution of a random variable X with distribution function F and complementary distribution function F_c is heavy tailed if*

$$\lim_{x \rightarrow \infty} e^{\lambda x} F_c(x) = \infty, \quad \forall \lambda > 0,$$

holds.

Example 1.2.1 (Weibull distribution). $X \sim Wei(\alpha, k)$, $0 < k < 1$, $\alpha > 0$. Then for $x \geq 0$

$$\lim_{x \rightarrow \infty} e^{\lambda x} e^{-\left(\frac{x}{\alpha}\right)^k} = \infty.$$

There are many more heavy tailed distributions: e.g. Pareto, Log-Normal, Cauchy, Fréchet distribution.

Furthermore, the fat-tailed distributions are a subclass of the heavy tailed distributions.

Definition 1.2.2. *The distribution of a random variable X with distribution function F is fat tailed if*

$$F_c(x) \sim x^{-\mu}, \text{ as } x \rightarrow \infty, \mu > 0.$$

Examples: Pareto distribution, Inverse-Gamma distribution, Lévy distribution

Fat tails in stock return The modeling of stock markets dates back to the PhD thesis of Louis Bachelier (1900) [17]. Bachelier modeled the price dynamics in the following way [7].

$$S(t + \Delta t) = S(t) + \eta(t), \quad \eta(t) \sim \mathcal{N}(0, \Delta t \sigma^2).$$

Later, the stock price increments have been replaced by relative price changes or logarithmic increments. These price changes are called returns and are defined by:

$$r_{\Delta t}(t) := \log(S(t + \Delta t)) - \log(S(t)) = \log\left(\frac{S(t + \Delta t)}{S(t)}\right).$$

This improved model is called geometric Brownian motion and can heuristically be written as

$$r_{\Delta t}(t) = \eta(t), \quad \eta(t) \sim \mathcal{N}(0, \Delta t \sigma^2),$$

or to be mathematical precise and using Itô's interpretation of the stochastic integral, one has the following stochastic differential equation (SDE).

$$dS = \rho S dt + \sigma S dW,$$

where W is a Wiener process also known as Brownian motion. Here ρ and σ are positive constants, which describe the drift and the volatility of this stochastic process. This model is nowadays still the basic model of price dynamics and is also used in the famous Black-Scholes model for option pricing.

The assumption of normally distributed returns is in fact wrong, which has been discovered more than 50 years ago. Many empirical findings in literature state that statistical tests reject the null hypothesis of normally distributed returns at a high significance level [7]. The first notable discussion of power laws in financial data dates back to the seminal paper of Mandelbrot in 1963 [169]. In this paper, Mandelbrot analyzed cotton futures and showed that the returns are not normally distributed. Furthermore, Mandelbrot observed that the tail of the stock returns (denoted by r) follows the Pareto law.

$$P(|r| > x) \sim x^{-\mu}.$$

Finally, Mandelbrot stated the famous stable paretian or Levy stable distributions and claimed that this is the more appropriate model of stock returns. This family of paretian distributions does not have a general analytic form but can be described by their characteristic functions [95]. The distribution is defined by four parameters, the most important of which is the Pareto index (or characteristic exponent) μ . Mandelbrot estimated the tail index for cotton

prices to be approximately $\mu \approx 1.7$ [169]. In the same year, E. Fama supported Mandelbrot's hypothesis and observed a tail index of $\mu \approx 1.7$ for the Dow Jones industrial average [99]. The hypothesis of paretian distributions restricts the power-law of stock returns to be in the range $\mu \in (0, 2]$, which means divergence of the second moment [161]. More recent studies of return distributions [171] indicate a finite second moment which disagrees with the hypothesis of stable paretian distributions [161, 7]. One reason for the different results can definitely be found in the computational limitations of the 1960s. Mandelbrot studied a dataset of approximately 2000 observation which is quite small compared to datasets of high frequency data of $10^6 - 10^7$ observations in the last decade [95]. Nowadays, one assumes the tail index to be around three ($\mu_S \approx 3$) [161] but one has even found a tail index larger than three for different indices [95]. More detailed studies of the return distribution reveal that a tail index $\mu \approx 3$ is correct for Δt between one minute and four days [113]. Interestingly, the return distribution shows slow convergence to gaussian behavior for Δt larger than four days and up to one month. This characteristic can be considered to be a *stylized fact* itself and is called *aggregational gaussianity* [62]. Furthermore, Gopikrishnan et al. [113] observe that the scaling properties break down if one shuffles the time series and thus destroys possible time dependencies. Thus, one can conclude that scaling behavior is in some sense caused by time dependencies [95]. Examples of modern models of stock return distributions are e.g. the student-t distribution, the truncated Lévy flight or hyperbolic distributions, see [7] for a short summary. The question of the right distribution of stock returns remains an open question, although his knowledge is crucial for many applications like portfolio selection or value-at-risk estimations [95].

One question we have not answered so far is: how we can measure the fatness of the

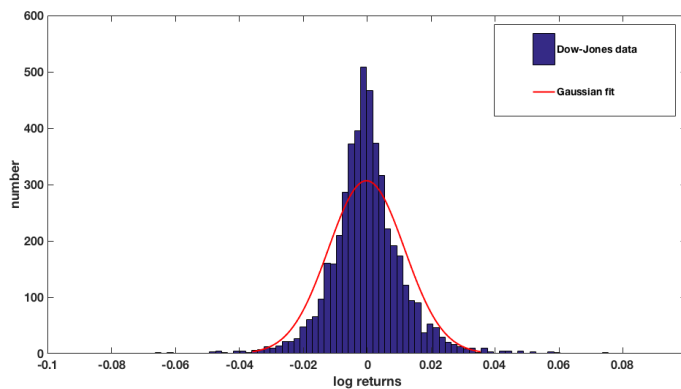


Figure 1: Stock return of daily Dow-Jones data (09.2005-9.2015).

tail, respectively the distinctions to the gaussian distribution? Probably the most famous method to measure the deviations from gaussian behavior is to measure the *excess kurtosis* of a distribution. The definition is given as the normalized fourth moment minus a correction term [7].

$$\kappa := \frac{E((r - \bar{r})^4)}{\sigma^4} - 3,$$

where $\bar{r} := E(r)$ and $\sigma^2 := E((x - \bar{r})^2)$. The correction term is needed to obtain gaussian behavior for $\kappa = 0$ (called *mesokurtic*). Excess kurtosis measures the fatness of the tail and the peak at the mean. One has *leptokurtic* behavior in the case $\kappa > 0$ which means such distributions have a higher peak around the mean and a heavier tail than the normal distribution (see figure 1). Consequently, a *platykurtic* distribution ($\kappa < 0$) has a lower peak around the mean and thinner tails than the normal distribution. For example, the excess kurtosis of daily DAX returns (03.01.1986-30.12.2005) is computed to be $\kappa = 5.84$ [95]. One obvious disadvantage of the measure is that one has to assume a priori the convergence of the fourth moment, which is not guaranteed. In this study, we will often make use of quantile-quantile plots (qq-plots) to visualize the fat-tail behavior. The qq-plots we use in this work fit the empirical distribution function e.g. the stock return data to a gaussian distribution.

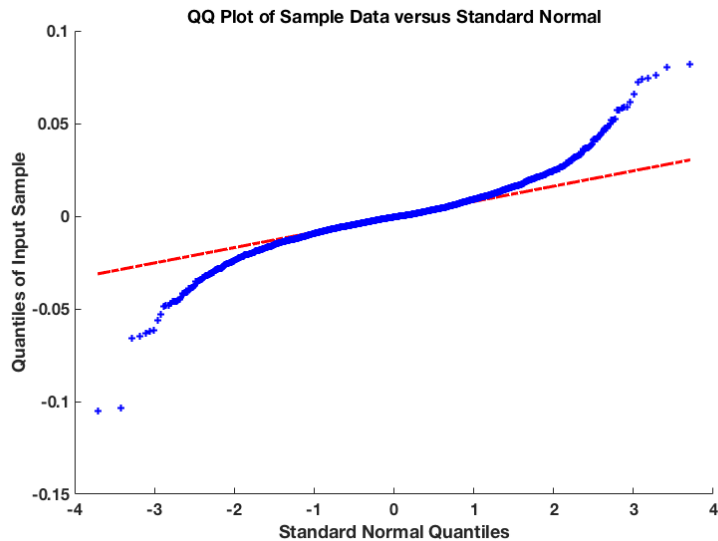


Figure 2: Stock return of daily Dow Jones data (09.2005-9.2015).

Absence of autocorrelation One further famous *stylized fact* is the absence of linear autocorrelation in stock returns. The autocorrelation function of returns is defined as:

$$\begin{aligned} C(l) := \text{Corr}(r_{\Delta t}(t + l), r_{\Delta t}(t)) &= \frac{\text{Cov}((r_{\Delta t}(t + l), r_{\Delta t}(t)))}{E((r_{\Delta t}(t) - \bar{r})^2)} \\ &= \frac{E((r_{\Delta t}(t + l) - \bar{r})(r_{\Delta t}(t) - \bar{r}))}{E((r_{\Delta t}(t) - \bar{r})^2)}, \quad l > 0. \end{aligned}$$

The correlation is given by the normalized covariance of two random variables and $C(l) \in [-1, 1]$ holds. The previous definition presumes that the random variables $r_{\Delta t}(t)$ and $r_{\Delta t}(t+l)$ are identically distributed and have the same expected value. The autocorrelation function depends on the time delay or time shift called *lag* ($l > 0$) of the random variable.

Empirical findings indicate that the autocorrelation function decays to zero within a few minutes [62] (see figure 3). For practical purposes one can assume that there is no linear

correlation for $l \geq 15$ (minutes) [65], which means that $C(l) \approx 0$. This characteristics of stock returns are often cited to support the EMH [56]. Heuristically, one can explain this behavior of stock return very easily. New information can cause linear correlations but trading strategies based on correlations (called *statistical arbitrage*) reduce these correlations and thus after several minutes (approximately 15 minutes), the market has reacted to informations respectively correlations and the autocorrelation is zero again [62].

Furthermore, one can even observe negative correlations in very short time lags [62]. This behavior is often assigned to the bid-ask spread since the prices can bounce on the tick level between these two extremes [40].

Notice that $C(l) = 0$ only indicates no linear autocorrelation but no linear dependencies does not imply independence of the considered random variables. In fact there are nonlinear dependencies in stock returns, one example is *volatility clustering* in stock returns.

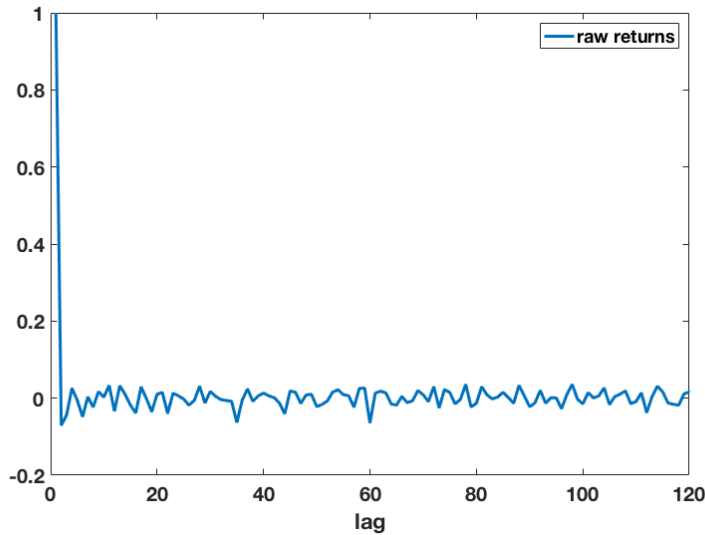


Figure 3: Autocorrelation function of daily Dow-Jones data (09.2005-9.2015).

Volatility clustering The last *stylized fact*, we discuss in detail is *volatility clustering*. This phenomenon was first described by Mandelbrot [169] in 1963. He observed:

Large changes tend to be followed by large changes, of either sign, and small changes tend to be followed by small changes [169].

This behavior indicates some kind of nonlinear dependency respectively correlation in the serial data of returns. The correlations can be verified by the positive autocorrelation of absolute returns or squared returns [62, 161]. Thus, we can immediately conclude that log returns are not well modeled by a random walk [62]. This *stylized fact* is also often called *volatility persistence* [95] or the *(G)ARCH* effect [63, 210]. This correlation raises the question whether stock returns are partially predictable and if the knowledge of correlations in financial data might be useful for trading strategies [95]. More generally, one can define the following

correlation function as measure for volatility clustering [62]

$$C_q(l) = \text{Corr}(|r_{\Delta t}(t+l)|^q, |r_{\Delta t}(t)|^q), \quad l > 0,$$

which considers arbitrary powers $q > 0$ of the stock return. We call the autocorrelation function defined above the *multi-scaled autocorrelation function*, which satisfies [161, 170]:

$$C_q(l) \approx l^{-\beta(q)}.$$

Interestingly, there is a nonlinear dependence of the scaling parameter β on the power q [84]. A similar behavior of turbulent fluids is known from statistical physics, where multi-fractal models are used [161]. A further interesting fact is that the highest correlation of the multi-scaled autocorrelation function for a fixed lag is observed for absolute returns $q = 1$ [84]. Thus, one can conjecture that absolute returns are more predictable than other powers of return [161]. Empirical studies reveal that $\beta \in [0.2, 0.4]$ holds for $q \in \{1, 2\}$ [65].

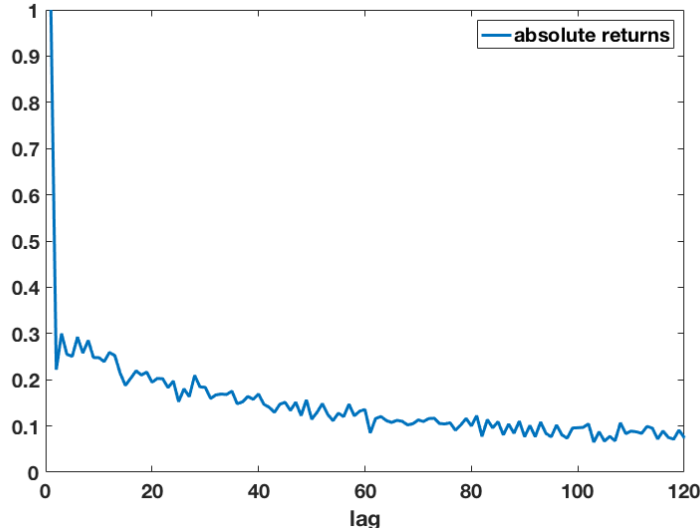


Figure 4: Autocorrelation function of absolute returns (daily Dow-Jones data 09.2005-9.2015).

Stylized facts for physicists From the perspective of physicists, these *stylized facts* can be viewed as *scaling laws* [163]:

Statistical physics has determined that physical systems which consist of a large number of interacting particles obey universal laws that are independent of the microscopic details. This progress was mainly due to the development of scaling theory. Since economic systems also consist of a large number of interacting units, it is plausible that scaling theory can be applied to economics [227]

Although these *stylized facts* are “almost universally accepted among economists and physicists” [166], a “satisfactory explanation in standard theories of financial markets is still lacking” [166] [195].

Lux emphasizes that “stochastic models of interacting agents” [163] seem to be “able to provide generic explanations for the ‘deeper’ anomalies of fat-tails and volatility clustering” [163]. He also points out that these models are closer “in spirit to models of multi-particle interaction in physics than to traditional asset-pricing models” [163].

1.3 Econophysics and Agent-Based Models

The research field of *econophysics* is a rather new field of research and dates (approximately) back to the early 1990s. The neologism *econophysics* has been coined by Stanley [225] and describes an interdisciplinary field of several disciplines. The core aspect of *econophysics* is the application of tools of statistical mechanics and physical theories to economic questions [226]. In the recent years, this new field of research has become very popular and has gained a rapidly increasing community [31].

Examples of such physical theories are *kinetic gas theory*, *percolation theory* or the *Ising model*. A widespread tool of statistical physics utilized in many econophysical models are Monte Carlo simulations. The areas of applications of econophysics are very broad, examples include financial markets, wealth distributions, auctions, company growth and business networks.

The origins of econophysics date many years back. Early computer simulations of market models can be found in studies of Stigler in the 1960s [209, 229]. In practice, many inventions in economics date back to interdisciplinary cooperations between economists and mathematicians or physicists. One example is the development of game theory, mainly influenced by von Neumann and Morgenstern. A further example is the collaboration between Black and Scholes. In addition, we want to point out that the first nobel laureate Tinbergen studied physics and mathematics. This reveals that a great amount of economic research is naturally developed by interdisciplinary groups of physicists, mathematicians and economists. In that respect, the new discipline econophysics must be regarded a natural development. We refer to [172, 216] for a general introduction to the field *econophysics*.

One important branch of econophysics are *agent-based economic market models*. These models consider complex microscopic interactions of financial agents. The dynamics of these large systems are simulated by Monte Carlo simulations. The goal is to replicate realistic macroscopic economic data and to study the connections between the microscopic model and the output data. To be more precise, these models explore the connection between the agents’ model, the market design and the existence of stylized facts. Often, these models are very similar to physical models in statistical physics and do not share many similarities to classical financial market models.

The starting point of the first *modern multi-agent model* [209] is probably the market crash of 20% at the US stock market in 1987. This extreme *anomaly* known as *Black Monday*, which economists failed to provide an explanation for, encouraged the economists Kim and Markowitz to design an agent-based model [140]. They tried to discover connections between agents who follow a portfolio insurance strategy and the volatility of the market with the help of Monte Carlo simulations.

There are many elaborated surveys about agent-based economic models, for example [95, 56,

209, 190, 121, 125, 222]. The great advantage of agent-based models compared to traditional models is the possibility to design complex agents and study the interaction of those by computer simulations. As the name reveals, the modeling of the agent is the key aspect of these models. Modeling financial agents has a long tradition in economics and dates back the work of Smith [219]. Recent developments in the field of behavioral finance had a significant influence on agent-based models most. In the next section, we will provide a short overview of agent modeling and introduce the concept of *bounded rational agents* which is used in most agent-based models.

1.3.1 Modeling Agents

The question of modeling financial agents is actually concerned with the simulation of processes of choice. Thus, in the case of a financial market, agents are faced with the decision to buy, hold or sell a stock (good) or to be flat in the market. The theory of choice is known in economics as *decision theory* or *utility theory*. Besides early contributions of Bentham, Gossen and Depuit, modern utility theory has been developed by Walras and Menger [228]. These early studies focused on proper utility measures and utility maximization. Notable contributions on the mathematization of utility models have been published by Edgeworth [91].

In the context of financial market models respectively agent-based models, we are especially interested in the theory of *expected utility* also known as *expected utility hypothesis*. This theory deals with the modeling of the decision process of persons under uncertain outcomes. The first example of a problem of choice under uncertainties has been given by Bernoulli in 1713 with the famous St. Petersburg paradox. In the 1930s and 1940s, the expected utility hypothesis has been put on a solid mathematical foundation by the mathematician von Neumann and economist Morgenstern. In 1944, they published the famous von Neumann-Morgenstern utility theorem [247] which precisely defines when a decision maker is *rational*, i.e. if a utility function and the corresponding maximum exist.

The model of rational expectation of financial agents has been rigorously defined by Muth in 1961 [187] and is known as the *rational expectation hypothesis*. It says that the agents' expectation (e.g. of the future stock price) is equal to the true expected value of the economic asset. Thus, the agents' expectations may deviate from the correct value but is true on the average. This theory became the dominant macroeconomic approach after Lucas used it in his famous *Lucas critique* in 1976 [159, 95]. Furthermore, the *rational expectation hypothesis* is the foundation of the famous *efficient market hypothesis* by E. Fama [100].

As discussed earlier, market models of rational agents are not able to explain and reproduce stylized facts. For that reason agent-based models do not follow the rational expectation hypothesis, they follow the ansatz of boundedly rational agents. Thus, also behavioral aspects are considered in the decision making of the agents.

Bounded Rational Agents The concept of *boundedly rational agents* has been introduced by Simon [212, 213]. Like the theory of expected utility, this is a model of the agents' choice. Bounded rational agents do not only act rational but partly irrational. Mathematically, they do not solve an optimization problem, but rather look for a satisfactory solution which is near the optimum. This can be supported by the fact that the computational resources,

respectively the time to solve the optimization problem are limited in real world application [95]. Furthermore, it is well known that fund managers often prefer to apply heuristics than to solve a highly complex optimization problem. One extension of this model has been derived by Rubinstein [206]. The concept of bounded rational agents is heavily influenced and supported by *behavioral finance*. Thus, the deviations of financial agents to the optimal solution can be accounted for behavioral biases of agents. Probably the most famous theory in behavioral finance is the so called *prospect theory* which has been established by Kahnemann and Tversky in their seminal paper *Prospect Theory: An Analysis of Decision under Risk* in 1979. Prospect theory deals with the decision making of agents under uncertain outcomes. It attempts to approximate real-life heuristics of decision makers which are influenced by psychological effects. In some sense, this theory can be seen as an extension of the expected utility theory.

2 SABCEMM- A Simulation Framework for Agent-Based Computational Economic Market Models

We introduce the simulation tool *SABCEMM* (Simulate Agent-Based Computational Economic Market Models) for agent-based computational economic market (ABC^EM) models. Our simulation tool is implemented in C++ and we can easily run ABC^EM models with up to several million agents. Thanks to the object-oriented software design, this tool enables the user to design and compare multiple ABC^EM models from a unified perspective. Thus, one can easily change the market mechanism or agent types. This makes it possible to quantitatively compare ABC^EM models e.g. regarding the ability of each model to reproduce *stylized facts*. We present a qualitative study of three known ABC^EM models and several variants of those. Furthermore, we discuss finite-size effects and time discretizations of ABC^EM models. Finally, we show the great impact of different random number generators on the run time of ABC^EM models and even on the qualitative output of the model. The code can be downloaded from GitHub <https://github.com/SABCEMM/SABCEMM>, such that all results can be reproduced by the reader.

2.1 Introduction

Over the last two decades, the new research field of *Econophysics* benefited from a rapidly increasing community and gained lots of momentum [31]. Due to several financial crises, the interest in new financial market models has risen, not only in the scientific society [102, 32] but especially in the work of practitioners like Trichet [238] and Bernanke [22]. One subject of *Econophysics* are so called agent-based computational economic market (ABC^EM) models. These models resemble an artificial market of interacting financial agents usually analyzed with the help of Monte Carlo simulations.

Many classical financial market models are based on the *Efficient Market Hypothesis*(EMH) originally introduced by Fama [168]. The EMH faces extensive criticism and controversial discussions are carried out still [167]. One reason for this is that the existence of market anomalies, usually named *stylized facts*, cannot be explained using the EMH. *Stylized facts* are statistical observations in financial data which can be documented on different time scales and for various stock markets all over the world. The *stylized fact* probably best known is the inequality of income and wealth which was first discovered by Pareto in 1897 [201]. Heavy tails in stock return distribution and volatility clustering, originally identified by Mandelbrot in 1963 [169], are additional examples of *stylized facts*. For further discussion of *stylized facts*, we refer to [62, 162].

Stylized facts seem to play a major role in the emergence of financial crises [69] and the need to investigate the origins of *stylized facts* has been emphasized by several authors [102]. The common goal of ABC^EM models is to replicate financial data containing *stylized facts* and thus to discover reasons for their appearance. Thus ABC^EM models can help to better understand the emergence of financial crashes.

ABC^EM models indicate that stylized facts are introduced due to behavioral aspects and psychological misperceptions of agents. ABC^EM models are heavily influenced by *behavioral finance* [133] and do not share many similarities with classical financial market models. The

investors within ABCEM models, usually called agents, do not follow the *homo oeconomicus* [184] paradigm of rational utility maximizers. They are rather modeled as *bounded rational agents* in the sense of Simon [212, 213].

In the last decade there have been many contributions of new ABCEM models. We only present a short overview over the most influential ABCEM models: the Levy-Levy-Solomon model [155], the Lux-Marchesi model [164, 165], the Brock-Hommes model [37, 38], and the Cont-Bouchaud model [64]. ABCEM models describe a diverse field of applications. Several models focus on the creation of crises (cf. [140, 135, 115]) while others try to explore the influence of new regulations of policy makers on the market behavior (cf. [232, 75]). We refer interested readers to reviews [150, 31, 50, 222, 125, 121, 209, 94, 56] for a general introduction to ABCEM models.

Until now, there is no satisfactory explanation for the appearance of *stylized facts* [165, 162]. Several alternative hypotheses to the EMH have been postulated. Examples for these hypothesis include the *Adaptive Market Hypothesis* [158, 94] and the *Interacting Agent Hypothesis* [164, 165, 94], which give a partial answer to this question.

Generally, ABCEM models suffer from the drawback of painting a limited picture of reality. In fact, an explanation of stylized facts in one model does not necessarily hold true in another model. In addition, critics might argue that all the results are based on computer simulations and cannot be trusted blindly. This is a severe issue and earlier studies [93, 254, 52, 143, 119] have shown that the obtained *stylized facts* in many models are only numerical artifacts. More precisely, these studies revealed that for example the very influential Lux-Marchesi model and the Levy-Levy-Solomon model exhibit finite size effects [93, 254]. Finite size effects generally describe that different numbers of agents may lead to qualitatively different model outputs. In addition, ABCEM models are often described by difference equations, for example the models presented in [115, 155, 37, 60]. Difference equations are generally difficult to analyze, although they may have a large variety of bifurcation types and can create chaotic behavior. Examples of ABCEM models, which have been studied with respect to bifurcations and chaotic behavior are presented in [37, 60]. Difference equations can be derived as numerical approximations of ordinary differential equations (ODEs) and stochastic differential equations (SDEs). The advantage of time-discretized ODEs is the possibility of studying their behavior on different time scales. Thus, in the context of ABCEM models, this enables us to analyze the stylized facts on different time levels. In addition, a proper time discretization may help to overcome stability issues e.g. in case of stiff ODEs. Furthermore, such a discretization may help reduce the sensitivity of the ABCEM model to distinct parameters. For these reasons, we derive time continuous models in section 2.3.2 and simulate their numerical approximations. Finally, one faces the challenge that Monte Carlo simulations have in general a poor convergence rate and that a large amount of samples is required in order to obtain reliable results. Nevertheless, we want to emphasize that many ABCEM models are far too complex to study them by analytical methods and therefore computer simulations present the only feasible way.

While a huge amount of ABCEM models is presented in literature, to our knowledge a unified model and perspective on ABCEM models is missing. Furthermore, there is no objective comparison between different models possible, since the models are implemented in different languages and simulated on different machines. In addition, we experienced difficulties

while reproducing the results published in literature, we refer to section 2.3.3. This may have several reasons. First of all ABCEM models are usually non-linear dynamical systems, very sensitive to their parameters. Secondly, ABCEM models heavily depend on random numbers and thus it is impossible to reproduce published results exactly. Finally, many publications provide incomplete information regarding the implementation details, e.g. initial values of model quantities.

These obstacles motivate us to establish a simulation tool for ABCEM models. This software framework allows for implementation of many different ABCEM models with a minimal amount of coding. This goal is achieved by providing an object-oriented framework implemented in C++. Another advantage of well-implemented C++ code is the computational speed which enables us to run models with up to several million agents on a Laptop. Accordingly we have derived an unified model of ABCEM models which is the basis of our software SABCEMM (Simulate Agent-Based Computational Economic Market Models). The main building blocks are agents and market mechanisms. We would like to point out that the SABCEMM tool enables the user to carry out a fair comparisons between different models. In addition, the framework allows for running models with numerous random number generators. We emphasize that the object-oriented software design enables the user to easily add and test new models by interchanging agents or market types.

We encourage readers to implement their ABCEM models in our framework. Our goal with the SABCEMM tool is to help to reveal the reasons for the creation of stylized facts. In addition, to aid reproducibility we publish the code and all examples discussed in this publication under an open source license.

We have implemented three ABCEM models in our framework, namely the Levy-Levy-Solomon (LLS) model [155], the Cross model [71] and the Harras model [115]. We carry out several experiments to analyze the computational efficiency of the SABCEMM framework. Furthermore, we study the impact of different random number generators on the model output and the computational efficiency as well. We also discuss numerical aspect of ABCEM models by also carrying out experiments with large numbers of agents. In addition, we present a proper time discretization of the LLS model and discuss the drawbacks of difference equations. Finally, we show the great flexibility of our framework by interchanging the market mechanism of the Cross model. We have conducted unit tests and qualitative tests of the model output to verify our implementation.

The outline of the paper is as follows: In the next section we properly define a unified model from economic perspective. The core part of the paper is a discussion of the Cross, LLS and Harras model presented in section 3. Besides simulations of the original models, we study special versions of each model. Then in section 4, we present the software architecture and analyze the SABCEMM software with respect to computational efficiency. This includes scaling behavior and the impact of different random number generators. We finish this paper with a short conclusions of this work.

2.2 Abstract ABCEM Models

In this section, we introduce a framework allowing to categorize and to abstract ABCEM models. All models consist of at least one type of financial *agent* and a price adjustment mechanism. Here, the agent type describes the strategy an investor follows when acting on a market and interacting with other market participants. The other market participant might follow the same or a different strategy, i.e. be of the same or of a different agent type, respectively. In addition, we only consider models with at least two agents, i.e. investors, which even holds true for very stylized models like [64] or [37].

The obvious second building block is the *market mechanism*, which consists of the *clearance mechanism* and a method of computing the *excess demand*. Here, the clearance mechanism describes how the price of a good or a stock in each ABCEM model is adjusted. The excess demand denotes the aggregated supply and demand of all agents. More precisely the excess demand is defined as the sum of agents' supply subtracted from agent's demand. Since the clearance mechanism should equalize supply and demand, it depends on the excess demand of all market participants. Obviously, the actions of all market participants is coupled through the price, respectively the excess demand.

Finally, we introduce a third aspect called *environment*. With environment we denote an additional coupling of the agents besides the global market price. A prominent example of such a coupling is the herding behavior, implemented in many ABCEM models. Though such a component is not a necessary part of an ABCEM model, it is used in many models. The reason for the prominent role of such an environment is that the additional coupling admits the major role in the formation of *stylized facts*. Our meta-model is outlined in figure 5. Before we discuss each building block separately, we present the SABCEMM model. First, we properly define an agent:

Definition 2.2.1. *An agent is characterized by three aspects:*

1. *a set of private pieces of information used in the investment decision process;*
2. *a set of public pieces of information used in the investment decision process; and*
3. *the investment decision process.*

Now, assume a set of N agents, where agent i takes their own set of J_i pieces of information, the private pieces of all remaining $N - 1$ agents and the set of J_{ex} public pieces of information into account in their investment decision process. We denote the set of all information used in the investment decision process by $\Omega \subseteq \mathbb{R}^{\sum_{i=1}^N J_i + J_{ex}}$. The investment decision process is defined by the map:

$$\left. \begin{aligned} A_i : \Omega &\rightarrow \mathbb{R}^{J_i} \times \mathbb{R}, \\ \omega &\mapsto A_i(\omega), \end{aligned} \right\}$$

where the map A_i maps onto a new set of private pieces of information used in its next investment decision process (representing an update of the set of private pieces of information) and a price, which needs to coincide for all agents.

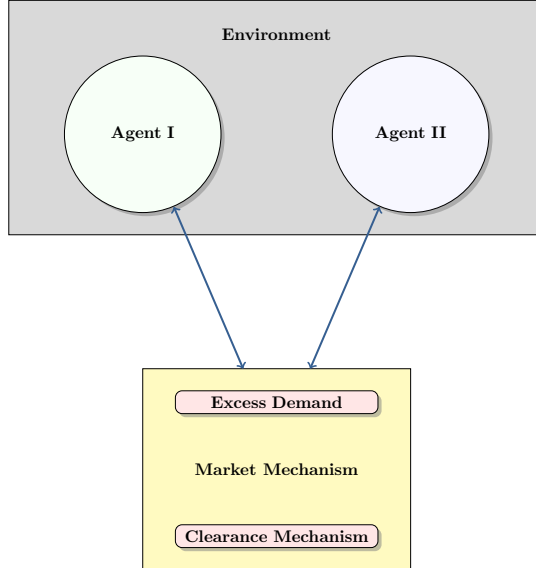


Figure 5: Schematic picture of our model.

Acknowledging that this definition of agents is rather abstract and general, we provide following remarks and examples to motivate and clarify this definition.

Remark 2.2.1. *The private pieces of information are called private as they are held and updated by a distinct agent only. Still, these information may be accessed and used by all remaining agents as well. These factors may especially include an opinion on the state of the market, a history of previous decisions and a history of previous returns.*

Remark 2.2.2. *The set of public pieces of information may represent publicly available information induced into the market which is not private to each agent, such as news. In the case of a rational market, the external information also contains the price derived in the previous iteration of the fix point iteration.*

Remark 2.2.3. *The definition of the set of all admissible pieces of information used in the investment decision process Ω includes not only the agent's private knowledge alongside publicly available information but also the private knowledge of all other agents trading at the market. This way, the effects of a coupling via an environment are built into the definition of agents.*

Remark 2.2.4. *For agents not utilizing the concept of coupling via an environment, the*

investment decision process can be written as:

$$\left. \begin{aligned} A_i : \Omega &\rightarrow \mathbb{R}^{J_i} \times \mathbb{R}, \\ \omega &\mapsto A_i(f_{i,1}, \dots, f_{i,J_i}; f_{ex,1}, \dots, f_{ex,J_{ex}}), \end{aligned} \right\}$$

where $f_{i,j}$ ($j = 1, \dots, J_i$) denote the private pieces of information of agent A_i and $f_{ex,j}$ ($j = 1, \dots, J_{ex}$) the publicly pieces of information, respectively. Note, that models only including agents not utilizing environment coupling are inherently parallelizable.

In order to visualize the coupling via an environment, we present the following example using a coupling based on the average of one of the private pieces of information.

Example 2.2.1. Assume a set of $N \in \mathbb{N}$ agents each equipped with a set of only three private pieces of information:

1. the wealth of the agent;
2. the stock held by the agent; and
3. the opinion of the agent on the stock.

Further, assume that the decision of each agent is based on the stock price as external piece of information, their individual private pieces of information and the average opinion of all agents. Then, the decision process can be written as:

$$\left. \begin{aligned} A_i : \Omega &\rightarrow \mathbb{R}^3 \times \mathbb{R}, \\ \omega &\mapsto A_i \left(S, w_i, q_i, \sigma_i, \frac{1}{N} \sum_{k=1}^N \sigma_k \right), \end{aligned} \right\}$$

where S denotes the stock price, w_i , q_i and σ_i denote the wealth, stock and opinion of agent A_i , respectively.

Based on the definition of agents provided above, we now introduce the notion of agent types allowing for an easier discussion of ABCEM models.

Definition 2.2.2. Assume two agents A_i and A_j with $i \neq j$ are defined in such a way that their behavior depends only on their private pieces of information, the public pieces of information, information obtained by averaging private pieces of information of all agents and private pieces of information of a small subset of other agents (the neighborhood). In addition, assume that agents A_i and A_j use the same set of pieces of information in their investment decision process and that their investment decision process coincide for permutations of input vector ω for which private pieces of information for agents A_i and A_j are swapped. Then, we say that these agents are of the same agent type.

Next, we define the market mechanism consisting of *excess demand* and the *clearance mechanism*.

Definition 2.2.3. The global excess demand ED of N agents is defined as the average of the agents' microscopic excess demands $ed_i \in \mathbb{R}$:

$$ED(S) := \frac{1}{N} \sum_{i=1}^N ed_i(S).$$

The quantity ed_i is the agent's aggregated demand and depends on the stock price S , thus $ed_i = 0$ corresponds to no orders of the i -th agent. A positive value $ed_i > 0$ represents a buy order, whereas a negative $ed_i < 0$ reflects a sell order. Our model does not prescribe the explicit form of ed_i .

Example 2.2.2. In [115] a reasonable choice is given by:

$$ed_i(S) = \sigma_i(S) \frac{\gamma_i(S) w_i(S)}{S},$$

with investment position $\sigma_i \in \{-1, 0, 1\}$, investment fraction $\gamma_i \in [0, 1]$, wealth $w_i \geq 0$ and market price S .

Definition 2.2.4. The SABCEMM framework provides two possible clearance mechanism.

i) Rational market:

$$ED(S) \stackrel{!}{=} 0.$$

ii) Irrational market:

$$S_{k+1} = K(S_k, ED, \eta).$$

Notice that the rational market is a root-finding problem, whereas the irrational market is a numerical approximation of a differential equation. The general form of the irrational market (defined by the function K) does not only include explicit discretizations schemes but may also include exponential integrators to approximate the equation.

Example 2.2.3. One example of a rational market is given by

$$0 \stackrel{!}{=} \frac{1}{N} \sum_{i=1}^N \sigma_i(S) \frac{\gamma_i(S) w_i(S)}{S}.$$

A further example of an irrational market reads

$$S_{k+1} = S_k + \frac{\Delta t}{N \lambda} \sum_{i=1}^N \sigma_i(S) \frac{\gamma_i(S) w_i(S)}{S}.$$

In the remainder of this section, we discuss each building block separately in order to provide insight into the theoretical background of each modeling aspect. In addition, we provide some examples of popular agent types and market mechanisms in ABCEM models.

2.2.1 Market Mechanisms

In this section we motivate the market mechanism of our meta-model. The origin of the *general equilibrium theory*, namely that demand matches supply, dates back to John Locke, James Denham-Steuart and Adam Smith. In the 19th century, the general equilibrium theory has been further developed by Antoine Cournot, Carl Menger and León Walras. Probably the most influential model in the general equilibrium theory has been introduced by Léon Walras [251]. The model considers an auctioneer, who determines the price in a so called *tâtonnement* process. Here, one assumes a *rational market* in the sense that we have perfect information and no transaction costs. There are further developments of the *general equilibrium theory*

due to McKenzie, Arrow and Debreu in the 1950s. We refer to the book [248] for a general discussion. The equilibrium can heuristically be expressed as:

$$\sum_{i=1}^N v_i^S(S, t) = \sum_{i=1}^N v_i^D(S, t),$$

where $N \in \mathbb{N}$ denotes the number of market participants and $v^{(\cdot)}(S, t)$ the volume of stocks or goods each agent demands respectively offers at a certain price S . The equilibrium price S_{eq} is then simply given as the price, where supply matches demand. From a mathematical perspective, this results in a fixed point problem, for which existence of a solution often is not a priori guaranteed and which is usually difficult to solve.

The general equilibrium theory is criticized (e.g. [117, 3]) due to the restricted nature of the assumption of a *rational* market which seems to be often violated in real world economics. In addition, there is an ongoing discussion whether market prices represent an equilibrium. For example, Beja and Hakansson [19] point out that observed prices are usually not identically to the equilibrium prices. This is due to the *tâtonnement* process taking too long, such that the computed solution is again in disequilibrium.

This has lead to the theory of market prices in disequilibrium [19, 116, 78] in which the price adjustment speed is finite and the actual market price represents a price in disequilibrium. Before we can present the disequilibrium model of Beja and Goldman [19], we need to define the *aggregated excess demand* ED (see for example [173, 80, 221]). In essence the excess demand denotes the sum of the demand subtracted by the sum of supply. A positive excess demand represents non cleared buy orders and a negative excess demand non cleared sell orders.

The disequilibrium model by Beja and Goldman [19] reads:

$$\frac{d}{dt} P = H(ED(P)), \quad P := \log(S), \quad (1)$$

where S denotes the price of the stock, good or security and ED the *aggregated excess demand*. Furthermore, the function H is assumed to be a monotone increasing function, which vanishes at zero. The function H might be nonlinear which is supported by several studies [40, 139, 64]. Beja and Goldman approximate model (1) by a first order linearization of H (Taylor expansion of H with $\dot{H}(0) = \frac{1}{\lambda}$):

$$\frac{d}{dt} P = \frac{1}{\lambda} ED(P), \quad (2)$$

where constant $\lambda > 0$ is interpreted as the market depth [139]. Mathematically, such a linearization of the function H is a good approximation for small values of ED . In fact, studies of Farmer et al. [64, 101] indicate a linear trading impact for small price changes. In addition, Beja and Goldaman add white noise to their model (2) to cover random errors or external news. Hence, the clearance mechanism is given by:

$$\frac{d}{dt} P = \frac{1}{\lambda} ED(P) + \eta, \quad \eta \sim \mathcal{N}(0, 1). \quad (3)$$

Thus the ordinary differential equation (1) has become the stochastic differential equation (3). The stochastic differential equation is properly defined as an integral equation and can be interpreted in the Itô or Stratonovich sense.

Mathematically, the process of transforming the algebraic demand supply equation

$$0 = ED(P). \quad (4)$$

into the differential equation (2) can be interpreted as relaxation, where the rate of relaxation is given by the market depth λ . The excess demand is usually measured in wealth or number of stocks. Thus, the right hand side of (2) is a rate due to the multiplication with the market depth. Hence, the most general model in this context is

$$dS = F(S, ED) dt + G(S, ED) dW, \quad (5)$$

with Wiener process W and arbitrary functions F and G . We use the usual notation for Itô stochastic differential equations. Many market mechanism of ABCEM models are special cases of model (5), for example the models presented in [78, 9, 160, 57, 58, 59, 60, 51, 253, 11, 115, 223, 136, 196, 33, 64, 71, 72, 70, 82, 103, 164, 165, 79].

Discretization All ABCEM models can be regarded as a time discrete versions of time continuous models. The simplest discretization is the Euler-Maruyama method. Applying the Euler-Maruyama method to equation (5), we obtain:

$$S(t + \Delta t) = S(t) + \Delta t F(S(t), ED(t)) + \sqrt{\Delta t} G(S(t), ED(t)) \eta, \quad \eta \sim \mathcal{N}(0, 1) \quad (6)$$

for a fixed time $t > 0$ and time step $\Delta t > 0$. In the case of a fully deterministic model, the numerical scheme (6) is identical to the standard Euler method.

From a mathematical perspective, we stress that more sophisticated numerical methods for equation (5) exist, which may improve the quality of approximation remarkably. In particular for the case of stiff ODEs, one should use implicit solvers to prevent stability problems.

Still, in the ABCEM literature one usually finds explicit discretizations of type (6). Often, the numerical approximation is rescaled and fixed such that the time step is set to one. Hence, in ABCEM literature, we are rather faced with difference equations of the following type

$$S_{k+1} = S_k + \bar{F}(S_k, ED_k) + \bar{G}(S_k, ED_k) \eta,$$

than differential equations where $k \in \mathbb{N}$ is an index of the discretized time steps ($S_k = S(t + k \Delta t)$ for a fixed initial time t and time step $\Delta t > 0$).

2.2.2 Agent Design

In this section, we discuss the design of agents for ABCEM models. The agents are designed as *bounded rational agents* in the sense of Simon [212, 213]. This means that the investors rather build their investment decisions on heuristics (behavioral rules) than a perfect utility maximization. Mathematically, they do not solve an optimization problem, but derive a satisfactory solution near the optimum by their trading rules. Such suboptimal trading strategies

are astonishingly good approximations of the real investment process [94, 233]. Furthermore, the heuristic trading rules often incorporate psychological aspects in the investment decision. For an introduction to the discipline *behavioral finance* we refer the interested reader to an article by Kahnemann [133].

Examples of such heuristic trading strategies are the two investor types: *chartists* (technical trader) and *fundamentalists*. A fundamentalist investor believes that there exist a fair price for a good or stock and that the market price will converge to this value. For a given fundamental value S^f and a monotonically increasing function D_i one may define

$$ed_i(S) := D_i(S_i^f - S).$$

In contrast to the fundamentalist, the *chartists* forecast the future price by extrapolating past values. In the simplest setting the chartist may only consider the last stock prices.

$$ed_i(S) = D_i(S_k - S_{k-1}).$$

Examples of ABCEM models, which consider chartists or fundamentalists are [154, 59, 37, 38, 59, 105].

2.2.3 Environment

In this section, we introduce the third aspect of our framework: the environment. Alternatively, the environment could also be named coupling and represents the crucial ingredient of many ABCEM models.

The first environment frequently used is the *herding mechanism*. Possibly, Kirman [141] was the first who used herding. Herding makes investors flock together and creates high correlations among the financial agents. This leads to rapid up or down movement in the market price and non-Gaussian price behavior. Several models have implemented the herding mechanism e.g. [8, 142, 141, 71, 105].

The second coupling mechanism frequently used in ABCEM models is a switching mechanism between different agent groups. Switching allows agents to change investment strategy resulting in a varying weight of implemented investment strategies. Thus the price behavior is often mainly influenced by one investment strategy. The switch or more precisely the switching rate is often triggered by a *fitness measure*. A *fitness measure* of an investor, respectively the investor group, is usually a comparison of past or actual profits of the different investment strategies. Thus, such a switching mechanism again creates additional correlation among agents. Prominent examples are [37, 38, 105, 164].

Nevertheless we have to point out that there are other environments in ABCEM models which seem to create stylized facts. Examples are agent interactions on lattice topologies or couplings through global information streams [253, 115].

2.3 Results

In this section we present simulations of the Cross, LLS and Harras model. We discuss each model separately and demonstrate the advantages of our simulation framework. Thus, we

study the behavior of the LLS and Cross model in the case of many agents. This way, we investigate if the models may exhibit finite-size effects. Furthermore, we demonstrate the flexibility of our framework by creating new models and adding features to the Cross model. In addition, we introduce a time continuous version of the LLS Model and discuss the resulting model behavior.

Finally, we want to emphasize that we provide the reader with all necessary information to reproduce the results. Thus we define in detail the implemented models, present all parameter values and the initial states of each model in the appendix 2.5.1. We ran our simulations on an Intel Xeon 64 bit architecture. Input files for all simulations can be found <https://github.com/SABCEMM/SABCEMM>. Furthermore, our simulation data is published as well [241].

2.3.1 Cross Model

This section presents results for the Cross model which is inspired by the Ising model [126] from physics. In the Cross model, each agent is characterized by his position, long $\sigma_i = +1$ or short $\sigma_i = -1$ in the market, respectively. Their investment propensity is determined by two tensions: one related to rational agent behavior and the other to irrational agent behavior. They both mimic the role of temperature in the Ising model. The irrational agent behavior takes into account the herding propensity of financial investors. The price process is driven through the change of the excess demand and is additionally perturbed by white noise. The authors Cross et al. show that their model can replicate the most prominent stylized facts of financial markets, namely fat-tails, uncorrelated price returns and volatility clustering. For further modeling details, we refer to [71, 72]

In our simulations, we obtain the same qualitative results as presented in [71, 72]. As figure 6 reveals, the price dynamic is influenced heavily by the evolution of the excess demand over time. Furthermore, the absence of raw price returns can be verified by figure 8. In addition, figure 7 reveals the fat-tail in asset returns. By adding the *heteroskedasticity parameter* θ , one couples the noise with the excess demand. This leads to volatility clustering as we can see in figure 8. A detailed introduction of the model can be found in appendix 2.5.1.

Many Agents In [72] the authors claim that their model has no finite size effects. All their simulations are performed with only 100 agents. In order to verify their statement, we analyze the model with different numbers of up to five million agents. We ran our simulations with 10,000 time steps in order to have a sufficiently large sample size. Our simulations (see figures 9, 10 and 11) support the findings of Cross et al. Thus, we obtain no qualitative difference between the model outputs conducted with 100 or five million agents.

New Models This section presents new variants of the Cross model. We consider the Cross agents in combination with new market mechanisms. In addition, we modify the Cross agents by adding a wealth evolution to each agent. The main purpose of these example is to show how easy new models can be created using SABCEMM. Certainly, it is still necessary to implement each new agent type or market mechanism once. Then, the change of a few lines in the SABCEMM `input file` defines a new model. Nevertheless, we want to emphasize that our software tool does not check the sanity of any choice of the user.

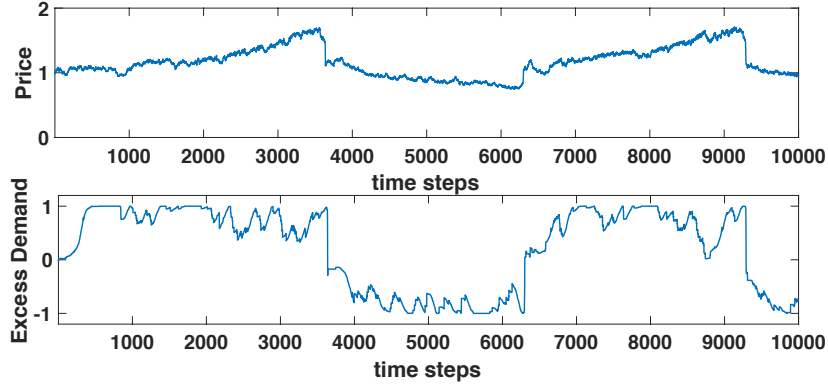


Figure 6: Cross base model. Parameters as in table 5

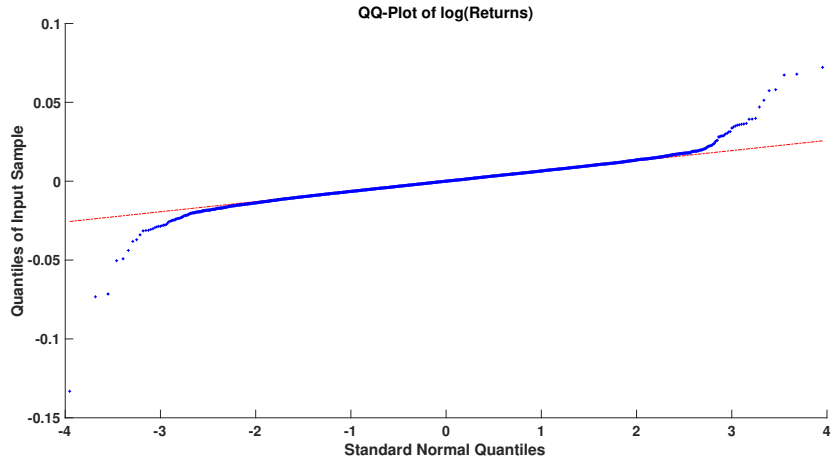


Figure 7: Cross base model. Parameters as in table 5. QQ-Plot of log-returns.

Wealth Evolution We consider the original Cross model as defined in appendix 2.5.1. We add a wealth evolution of the type

$$w_i(t + \Delta t) = w_i(t) + \Delta t \left[(1 - \gamma) r + \gamma \frac{S(t) - S(t - \Delta t)}{\Delta t S(t)} \right] w_i(t),$$

to each Cross agent $i = 1, \dots, N$. The positive constant $r > 0$ denotes the interest rate and $\gamma \in (0, 1)$ a fixed fraction of stock investments for all agents. The goal was to study the influence of the non-Gaussian return distribution on the wealth distribution. With increasing γ , we obtain an increasing excess kurtosis of the wealth distribution. In fact the excess kurtosis approaches the excess kurtosis of the stock price, which is approximately 6. In figure

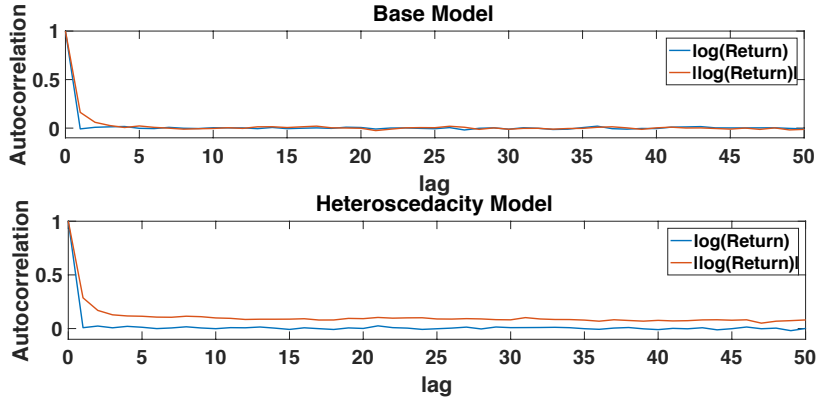


Figure 8: Autocorrelation of log-returns and absolute log-returns in the base model (upper graph, parameters see table 5) and full model (parameters see table 5 except $\theta = 2$).

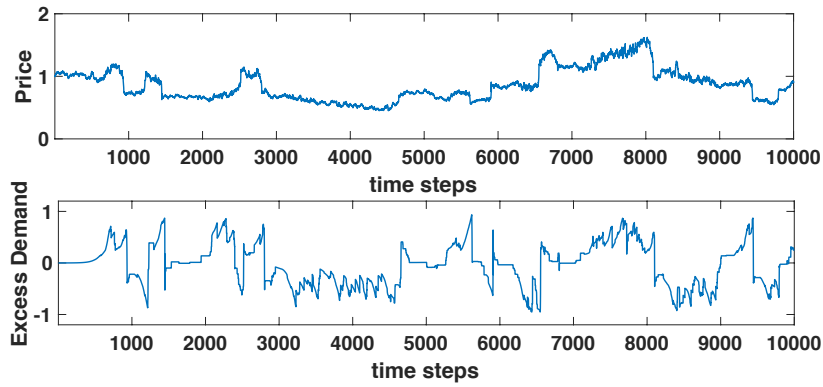


Figure 9: Cross model with five million agents. Parameters as in table 5, except $N = 5,000,000$ and $\theta = 2$.

12 we have averaged the results over 200 runs. The qq-plot figure 14 clearly shows the fat-tail behavior for a fixed $\gamma = 1$.

Furthermore, we could generalize the microscopic excess demand of the Cross agents by adding a wealth dependency. This would lead to an additional coupling between wealth and stock price behavior. We leave this question open for further research.

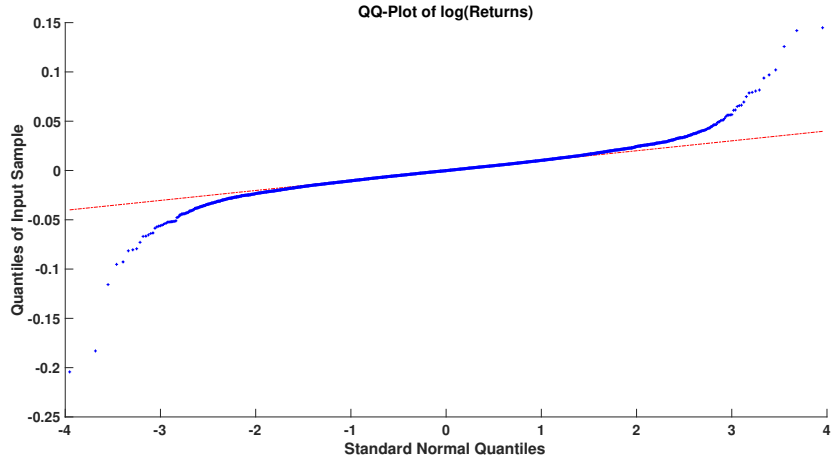


Figure 10: Cross model with five million agents. Parameters as in table 5, except $N = 5,000,000$ and $\theta = 2$.

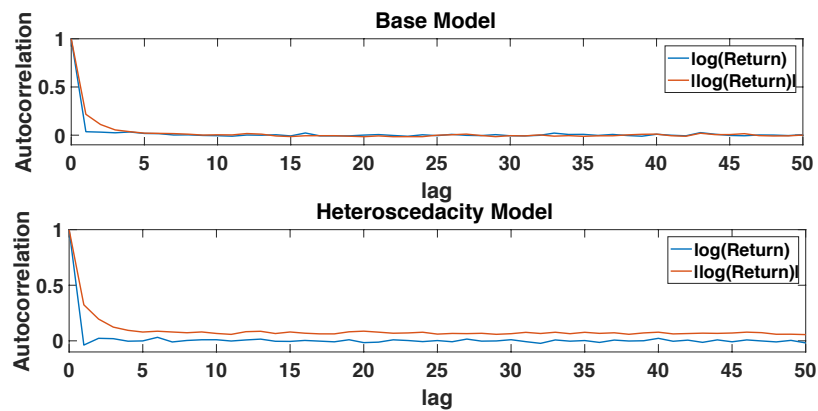


Figure 11: Autocorrelation of log-returns and absolute log-returns in the base model (upper graph, parameters see table 5) and full model (parameters see table 5 except $\theta = 2$). Both with $N = 5,000,000$

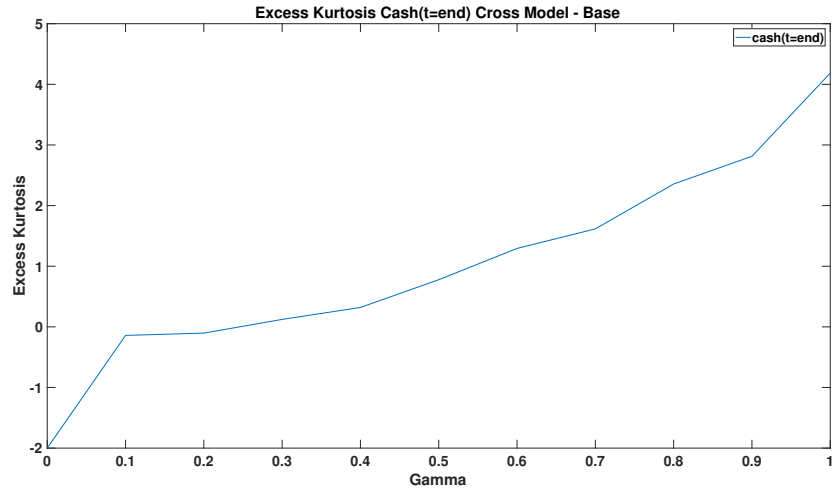


Figure 12: Excess kurtosis for the wealth at final time of the Cross model. Parameters as in table 5 with $w_i(t = 0) = 1$ and $r = 0.01$.

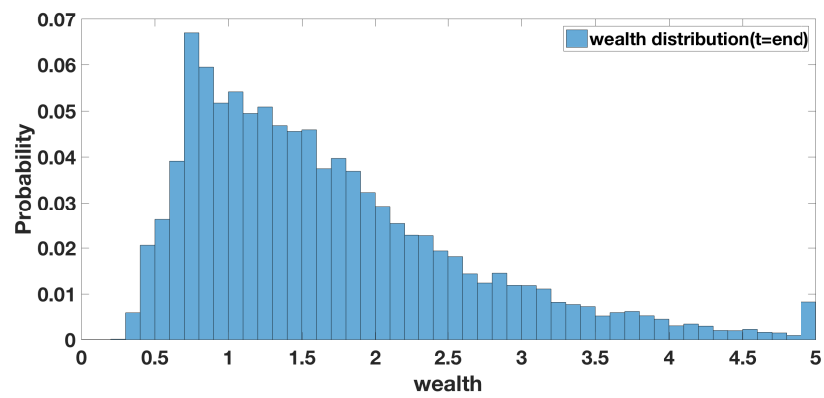


Figure 13: Histogram of the wealth distribution at final time. Parameters as in table 5 with $w_i(t = 0) = 1$ and $r = 0.01$.

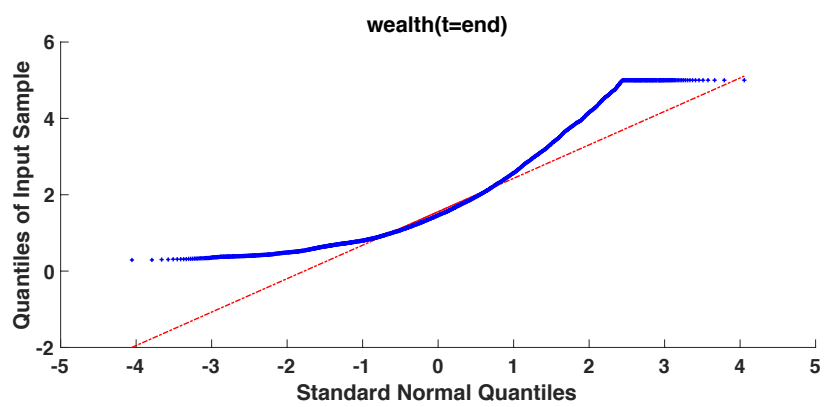


Figure 14: QQ-Plot of the wealth distribution. Parameters as in table 5 with $w_i(t = 0) = 1$ and $r = 0.01$.

SDE Discretization In this section, we again consider the Cross agents, but we change the clearance mechanism. We set the pricing rule to be

$$S(t + \Delta t) = S(t) + \Delta t F_{Cross}(S, ED) + \sqrt{\Delta t} S(t) (1 + \theta |ED|) \eta, \quad \eta \sim \mathcal{N}(0, 1).$$

In fact we have chosen the Euler-Maruyama discretization of the SDE:

$$dS = F_{Cross}(S, ED) dt + S (1 + \theta |ED|) dW,$$

where W is a Wiener process and the SDE should be interpreted in the Itô sense. For our first simulation, we set the drift operator F to read:

$$F_{Cross}^1(S, ED) := S(t) \frac{d}{dt} ED(t).$$

As the figures 15 and 16 reveal, the behavior of this model is identical to the original Cross model. Thus, we have obtained a pricing rule which is a proper time discretization of a time continuous model.

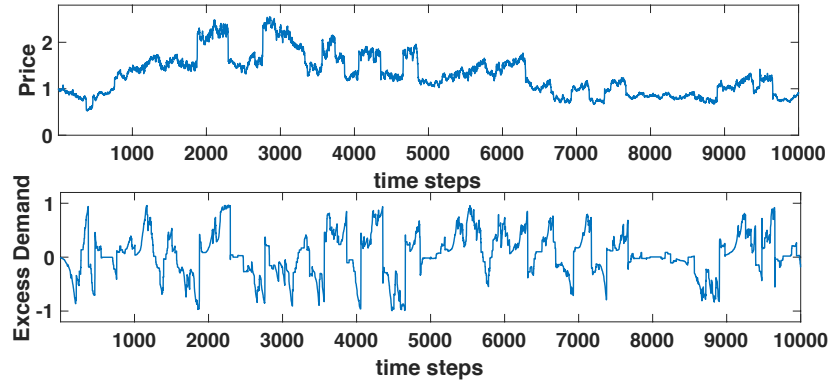


Figure 15: Cross agents with SDE pricing rule. Parameters as in table 5 except $\theta = 2$.

In a second test we set the drift coefficient to

$$F_{Cross}^2(S, ED) := S(t) ED(t).$$

We study the different impact of the two models on the stock price behavior. Our studies reveal that the choice F_{Cross}^2 leads to Gaussian price behavior. We measured this with the excess kurtosis, which we averaged over 100 runs. This is an interesting result, since it reveals the great influence of the drift coefficient on the stock price behavior.

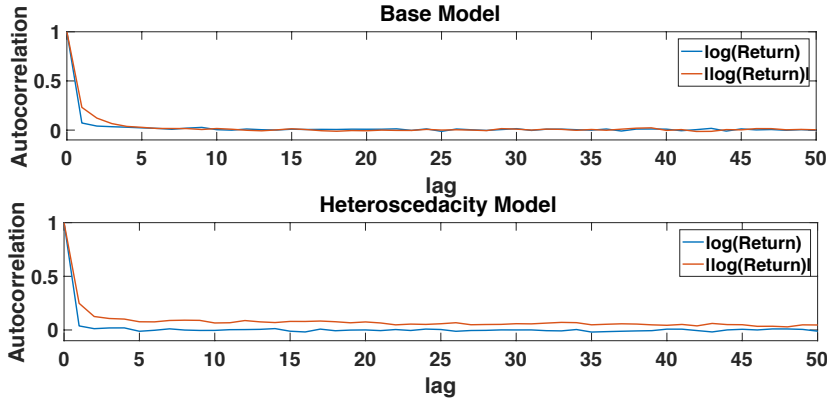


Figure 16: Autocorrelation of log-returns and absolute log-returns in the base model (upper graph, parameters see table 5) and full model (parameters see table 5 except $\theta = 2$). We obtain the same behavior as previously in section 2.3.1.

	excess kurtosis
$F_{Cross}^1, \theta = 0$	27.0434
$F_{Cross}^1, \theta = 2$	22.5530
$F_{Cross}^2, \theta = 0$	-0.0044
$F_{Cross}^2, \theta = 2$	1.2580

Table 1: Averaged excess kurtosis over 100 runs with different drift functions.

2.3.2 LLS Model

In this section, we present results for the LLS model which is one of the earliest and most influential econophysical ABCEM models. In addition, the LLS model is an example for a *rational market*, i.e. the price is determined through a fixed point iteration (compare equation (9)). The LLS model is subject to critical discussions in literature [254]. We discuss these crucial findings in detail in this section.

The LLS model considers the wealth evolution of the financial agents. Every agent has to decide in each time step which fraction of wealth he wants to invest in stocks with the remaining wealth being invested in a safe bond. The investment decision is determined by a utility maximization. For modeling details we refer to [155, 156, 157, 154].

We define the model and parameter sets in detail in appendix 2.5.1, which is the identical choice as in the earlier studies [156, 157]. We consider only one type of financial agent. The agent has a fixed memory span of $m = 15$. Figure 17 shows the simulation in the case of

no noise added on the investment decision and with noise added. We observe that the noise leads to oscillatory behavior, which coincides with earlier findings in [156]. Figure 18 shows results for three types of agents with different memory spans $m_1 = 10$, $m_2 = 141$, $m_3 = 256$. The results are qualitatively identical to the results in [157].

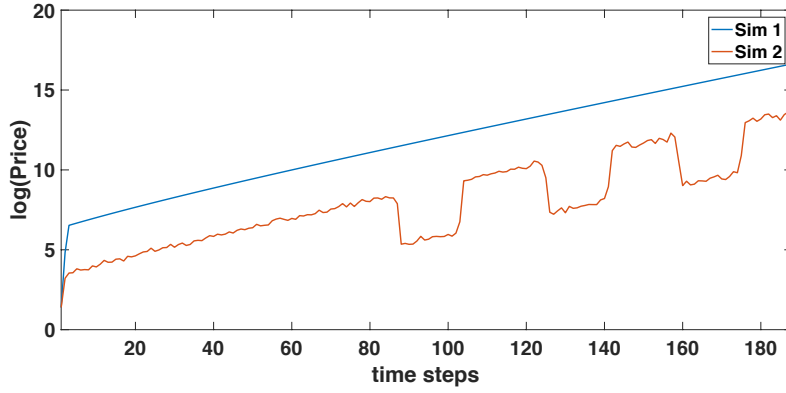


Figure 17: Price evolution of the LLS model with noise $\sigma_\gamma = 0.2$ (red) and without noise $\sigma_\gamma = 0$ (blue). Parameters as in table 6

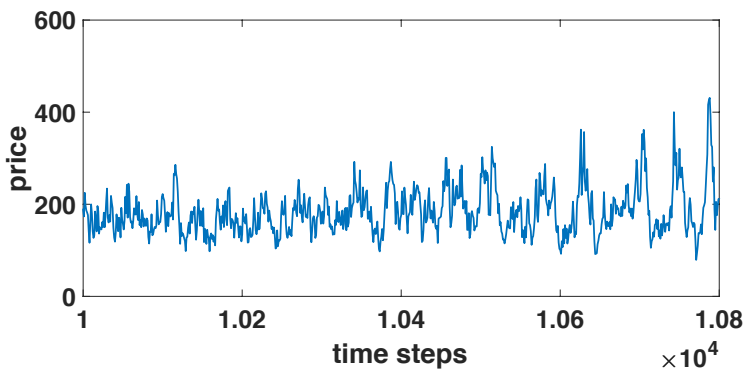


Figure 18: Price evolution of the LLS model with three different investor types. Parameters as in table 7

Finite Size Effects It was discovered earlier that the LLS model exhibits finite size effects [254]. In our simulations, we identify two different kinds of effects caused by different number of agents. Our simulations are conducted first with 100 agents and then with 1,000 agents. First, we obtain that chaotic price behavior becomes regular and Gaussian by increasing the number of agents. The Gaussian stock return behavior can be seen in figure 19. Secondly, Levy at al. [157] claimed that the investor group with the maximum memory becomes the dominant one, meaning they own the maximum amount of wealth. In our simulations, the wealth evolution of different agent groups changes with varying number of agent, as the figures 20 and 21 reveal. Thus, we can conclude that the qualitative output of the model changes with respect to the number of agent, which is an undesirable model characteristic.

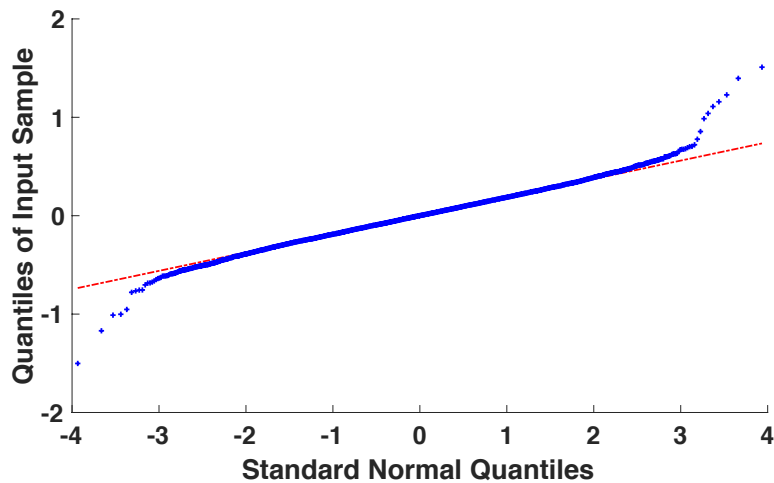


Figure 19: QQ-Plot of log-returns. Simulation conducted with 1,000 agents and the parameters are set as in table 7 with $\sigma_\gamma = 0.2$.

Discussion of Model Behavior The simulation in figure 17 reveals that the deterministic model is characterized by a constant investment proportion. The optimal investment proportion is always located at the boundaries $\gamma \in \{0.01, 0.99\}$, determined through the initialization of the return history. This is an absolutely reasonable result, thus the wealth evolution in the original LLS model [155] is linear

$$w_{k+1} = w_k + (1 - \gamma_k) r + \gamma_k w_k \frac{S_{k+1} - S_k + D_k}{S_k}, \quad (7)$$

and the chosen logarithmic utility function is monotonically increasing. In fact, additive noise on the optimal solutions leads to oscillatory behavior. Thus, the investors change between the two possible extreme investments of being fully invested in stocks or bonds. We point out that the noise level is crucial in order to obtain this behavior. Figure 22 illustrates the model output for different noise levels.

Nevertheless figure 18 seems to indicate chaotic price behavior. The previous simulations (see figures 19, 20 and 21) clearly reveal Gaussian distributed stock returns and finite size

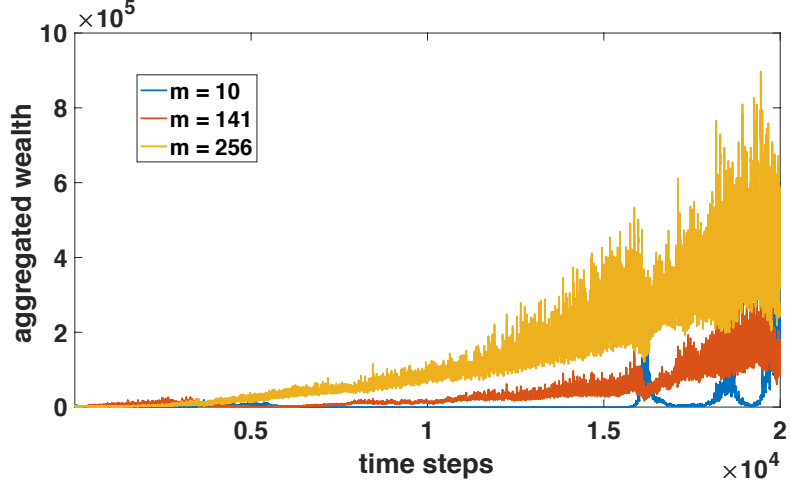


Figure 20: Aggregated wealth of three equally sized agent groups. The total number of agents is 99, for further parameters we refer to table 7.

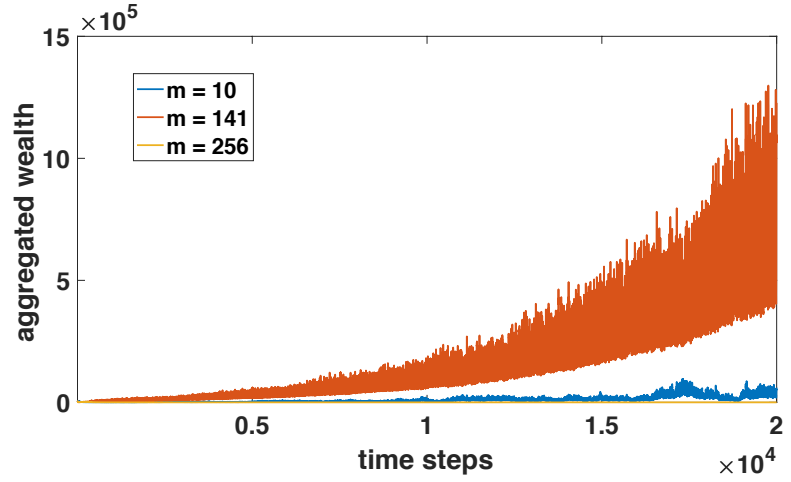


Figure 21: Aggregated wealth of three equally sized agent groups. The total number of agents is 999, for further parameters we refer to table 7.

effects as well. In our simulations we obtain that also in the noisy case approximately 90% of the investment decisions (pre-noise) are located at the boundaries. Mathematically this is an unsatisfying result. In order to gain more insights into the model mechanism we study the corresponding time continuous model.

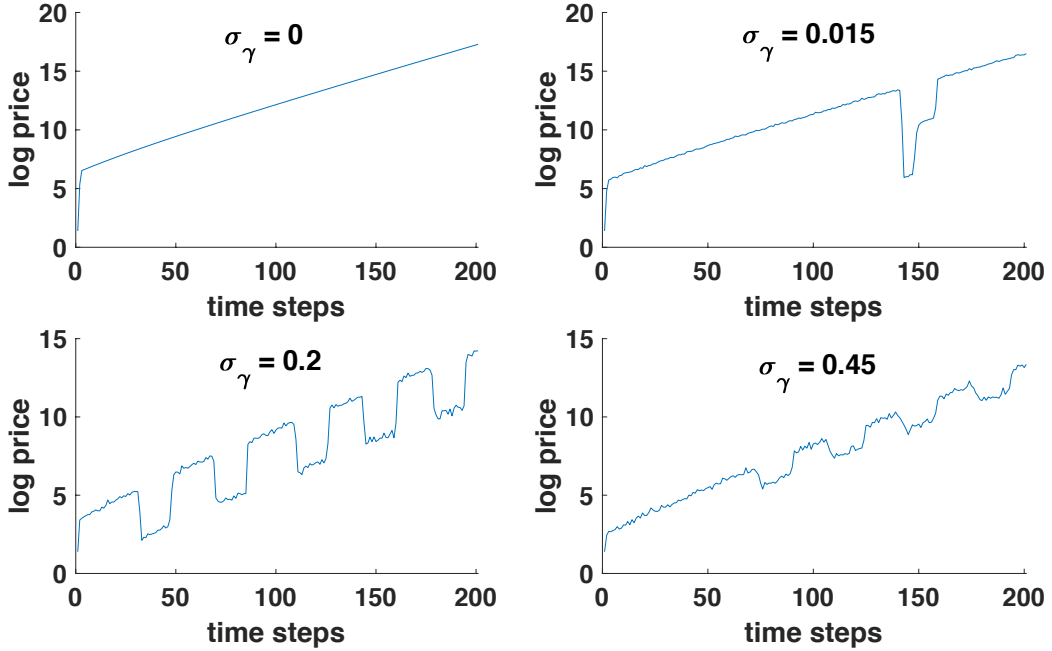


Figure 22: Simulations of the basic LLS model with varying noise levels. Parameters as set in table 6.

Time Continuous Version The time continuous version of the wealth evolution (7) is given by

$$w(t + \Delta t) = w(t) + \Delta t \left[(1 - \gamma(t)) r + \gamma(t) \frac{\frac{S(t+\Delta t) - S(t)}{\Delta t} + D(t)}{S(t)} \right] w(t). \quad (8)$$

Notice that the bond return r and the stock return $\frac{\frac{S(t)-S(t-\Delta t)}{\Delta t}+D(t)}{S(t-\Delta t)}$ are rates and thus scale in time. The equation (8) is the Euler discretization of the ODE:

$$\frac{d}{dt}w(t) = (1 - \gamma(t)) r w(t) + \gamma(t) \frac{\frac{d}{dt}S(t) + D(t)}{S(t)} w(t).$$

In order to study the time continuous version of the model, we need to properly define the scaling of the investor. We want to emphasize that several reasonable time scales exist. First, we study the case when the memory variable m_i scales with time, which means: $\bar{m}_i := \frac{m_i}{\Delta t}$. The results for different time steps can be seen in figure 23.

Interestingly, for sufficiently small Δt the optimal investment decisions are all located in the interior of the interval $[0.01, 0.99]$. This can be explained by the very small optimization horizon and the smoothing effect of a large return history. For $\Delta t = 0.1$ the percentage of

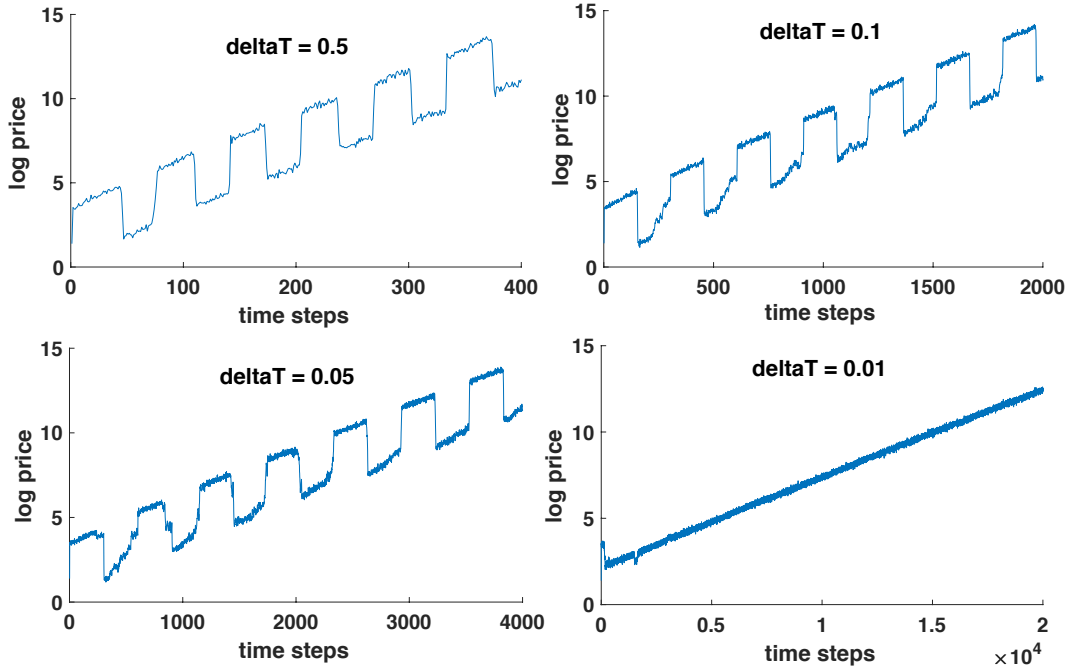


Figure 23: Simulations of time continuous LLS model with scaled memory variable and different time discretizations. Further parameters as defined in table 6 with $\sigma_\gamma = 0.2$.

extreme decisions reduces to 72% and for $\Delta t = 0.01$ all optimal investment decisions are located in the interior. Here, we have averaged our results over 100 runs. From modeling perspective the results are not interesting, thus the price exhibits Gaussian behavior as well.

Further, we might assume that the investor's memory does not scale with time. Our simulations prove that the characteristics of oscillating prices can be obtained on all chosen time levels (see figure 24). An averaging over 100 runs also indicates that the percentage of extreme decisions remain approximately around 90% for any chosen time discretization. The possibility to study further scales of the LLS model is left for future research.

2.3.3 Harras Model

The Harras model is inspired by phase transitions observed in the Ising model [126], as previously the Cross model. The goal of the authors is to investigate the development of crashes and bubbles. The investment decision of each agent is based on their expectation of future price behavior. To be more precise, their opinion is determined by three types of information: private information, global information like news and friendship information. The friendship information is implemented through microscopic interactions on a lattice topology of agents. This introduces spatial correlations among the different investors. The topology is a good example for an environment as introduced in section 2.2. Besides their opinion the agents in

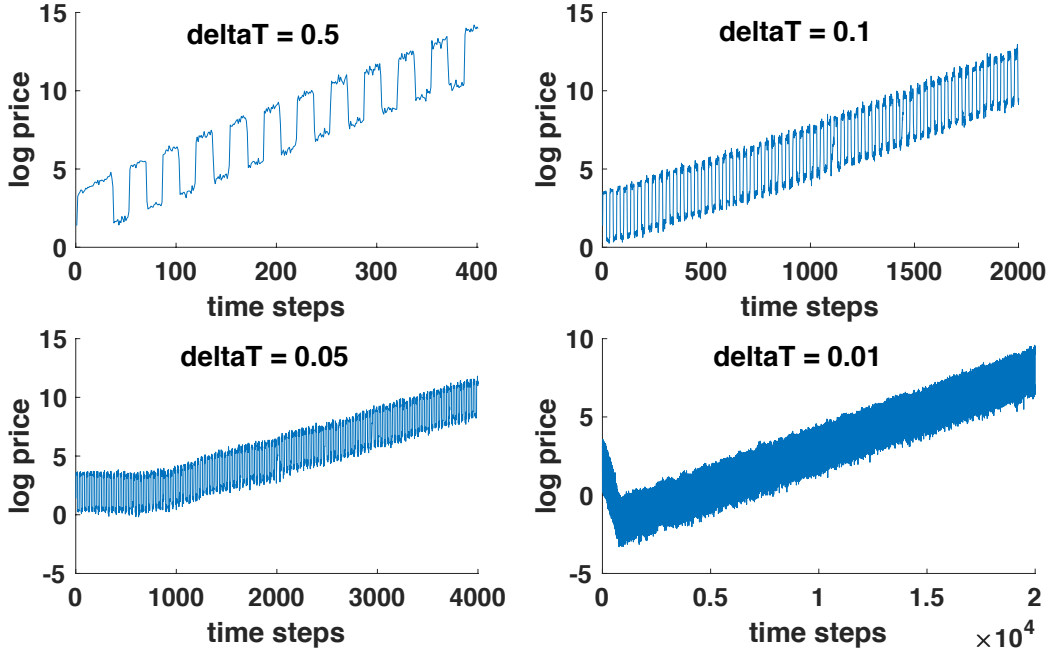


Figure 24: Simulations of time continuous LLS model with fixed memory variable and different time discretizations. Further parameters as defined in table 6 with $\sigma_\gamma = 0.2$.

the Harras model are equipped with their personal wealth and their number of stocks. These quantities are aggregated in the excess demand, that drives the market price in a deterministic fashion. For further modeling details we refer to the original model [115].

In their simulations the authors have obtained that depending on the weight of the friendship information the price behavior rapidly changes. Above a certain threshold the model develops bubbles and price crashes, called *dragon-kings* by Harras and Sornette. Furthermore, the authors show that the model can generate fat-tails in asset returns and volatility clustering as well.

We cannot reproduce all results of Harras and Sornette. We observe fat-tails in asset returns and volatility clustering (see figure 26). We cannot observe bubbles and crashes as presented in [115]. The differences maybe caused by incomplete information regarding the parameter settings and modeling details. We refer to the appendix 2.5.1 for details.

2.4 Software Architecture

In this section, we provide a bird's eye view on our simulation software SABCEMM (Simulate Agent Based Computational Economic Market Models). It allows an easy and straight for-

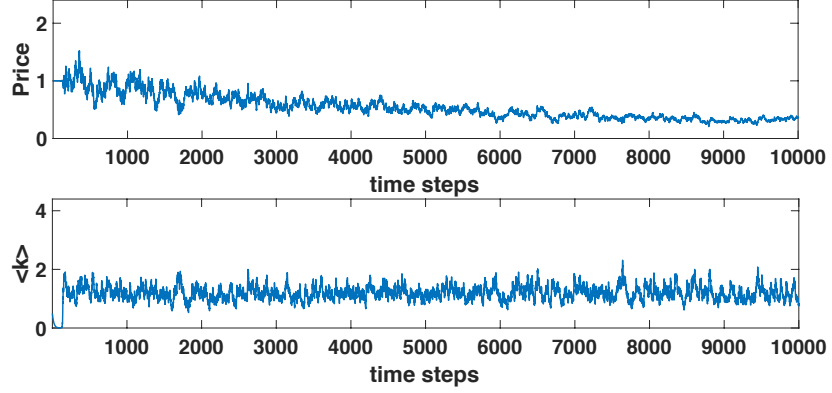


Figure 25: Harras model with no friendship information ($C_1 = 0$). Parameters as in table 8.

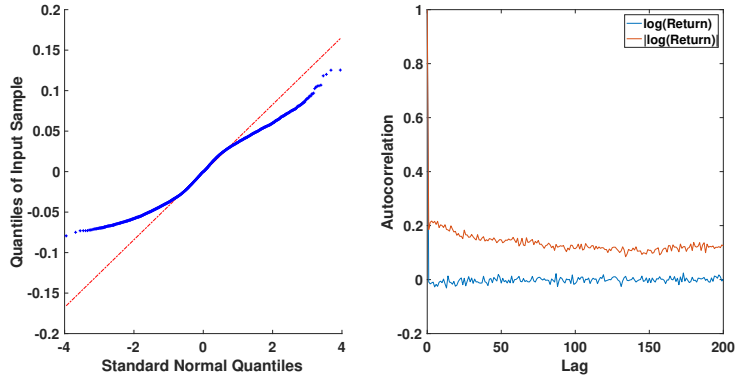


Figure 26: Harras model with no friendship information ($C_1 = 0$). Parameters as in table 8.

ward implementation of the general ABCEM model introduced in section 2.2. First, in section 2.4.1, the building blocks of the numerical core of the SABCEMM simulation software are laid out. Then, we note on some important features of our software in section 2.4.2. Finally, in section 2.4.3, we present results for scalability and efficiency of our code showing that the code is suited for simulation of models including more than 3 millions of agents.

An object-oriented design of the SABCEMM simulation software allows implementation of Dijkstra's [83] principle of *separation of concerns*. More precisely, we follow a class based object-oriented programming approach as described in [207]. In our specific case the object-orientation enables the user to test and implement new econophysical models with minimal additional coding in the SABCEMM framework.

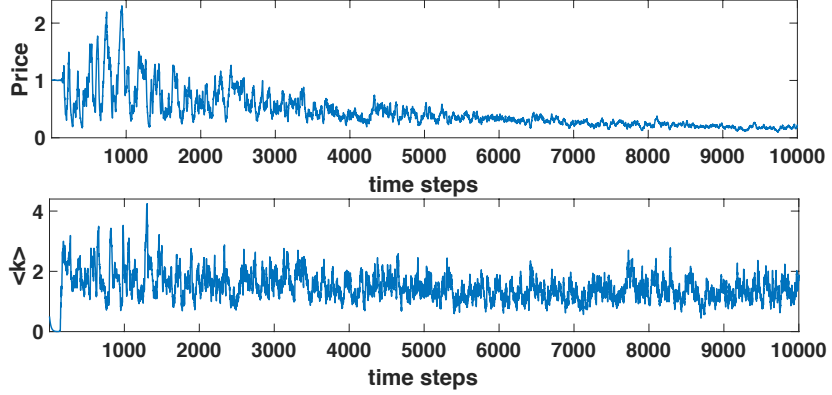


Figure 27: Harras model with friendship information ($C_1 = 4$). Parameters as in table 8 except $C_1 = 4$.

2.4.1 Numerical Core

In this section, we present the design of the numerical core of the SABCEMM simulation software, i.e. the design of those parts of the software used in the simulation loop itself. The three main building blocks of the numerical core and the main workhorses of the simulation are abstracted into abstract classes: `Agent`, `ExcessDemandCalculator` and `PriceCalculator`. The model to be simulated is then implemented using specialized subclasses of these building blocks vastly reducing the cost for implementation of new econophysical models. The interaction of the building blocks is orchestrated by the class `StockExchange`. The building blocks of the numerical core are visualized as class diagram in figure 28.

The Abstract Class Agent The abstract class `Agent` defines the general interface, i.e. those general characteristics of all agent types required for simulation. In order to comply to [115, 71, 155, 156], every agent type needs the following member variables:

- `Stock` is the amount of stocks an agent holds at a distinct time. In more sophisticated models like [115] agents can buy/sell varying amounts of stock.
- `Cash` is the amount of money the agent has available. In simple models this is called wealth since there is no distinction between stocks owned and disposable cash.
- The `Decision` can generally take the three discrete values $\{-1, 0, 1\}$ which stand for sell/no/buy order.
- `Trading Volume` is the amount of stocks the agent wants to buy or sell.

Noted that not all characteristics are relevant for all models, i.e. some might be set to one/zero to avoid repetition of code. In addition, every agent type needs to implement the following methods:

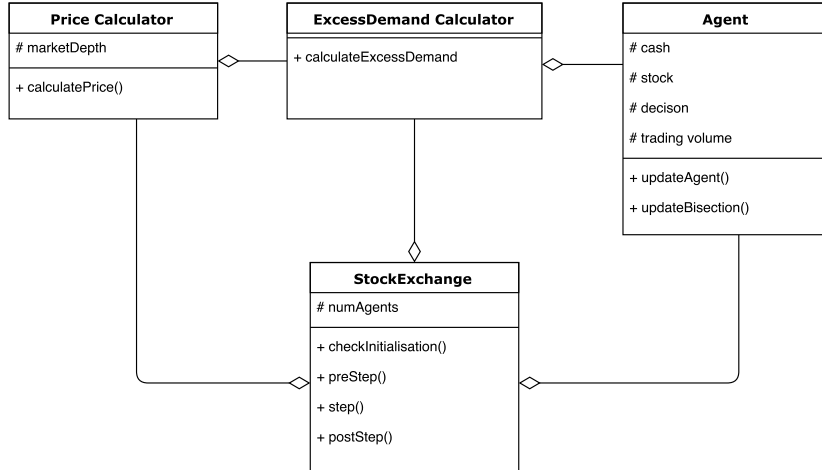


Figure 28: Class diagram of the numerical core.

- `updateAgent()` does all necessary computations to migrate the agent from one time step to the next one, e.g. revise his `Decision` and update `Cash`/ `Stock`.
- `updateBisection()` is needed in a rational market only. While searching the next price some of the agent's quantities have to be adapted while others have to remain unchanged.

Note that for models with agents relying on an environment (see section 2.2) the environment needs to be integrated into the specialization of the `Agent` class.

Example 2.4.1. *The agents as defined by [115] are grouped on a virtual square lattice with periodic boundary conditions, such that each agent has four neighbors (for details see appendix 2.5.1). Consequently the corresponding specialization of the `Agent` class can manage a neighborhood.*

The Abstract Class `PriceCalculator` defines the general interface of all implementations of the computation of the new price of a stock. The method `calculatePrice` determines the new stock price at each time step. Each of the price mechanisms presented in section 2.2 is implemented in a subclass of the abstract class `PriceCalculator`.

The Abstract Class `ExcessDemandCalculator` describes the interface to every class implementing a method for calculating the excess demand in a model (compare section 2.2). The Excess Demand represents the coupling element between the agent and the price. The method `calculateExcessDemand` iterates over all agents and collects their microscopic excess demand to calculate the global excess demand. Note that the `PriceCalculator` relies on the excess demand to find the new stock price.

The Class `StockExchange` represents the interaction between the agents, the price calculator and the excess demand calculator. Its interface includes the following member variable and methods:

- Member variable `Agents` represents a list containing all agents trading at a stock exchange.
- Method `preStep()` is called before a step is carried out. It allows implementation of housekeeping tasks, such as collecting data for tracking before a time step is carried out.
- Method `postStep()` is called after the time step is carried out. It allows implementation of housekeeping tasks, such as collecting data for tracking after a time step is carried out.
- In method `step()`, the price calculator is called to determine a new price. This invokes the excess demand calculator first to determine the excess demand. With the new price all agents are then updated.

Figure 29 shows a flow chart of how the different classes work together.

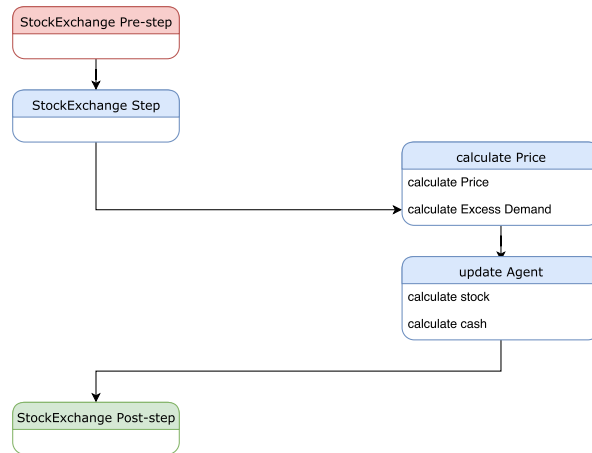


Figure 29: Flow chart of the numerical core.

2.4.2 Features

The goal of the SABCEMM framework is to allow for simple implementation of different ABCEM models while allowing fast simulations with larger numbers of agents and providing easy access to simulation results for evaluation of the implemented models. Keeping this in mind we have added some features to our framework.

Input File In order to mix and match different agent types or examine different parameter settings a great number of simulations is necessary. Additionally the simulations have to be repeated multiple times to examine the influence of randomness on the simulation results. In order to allow for easy configuration, simulation parameters are defined in input files formatted in XML. These text based files are easy to parse for humans and can easily be saved, ideally using some method of version control, to be reused and to regenerate results. In addition, parameter studies can be carried out easily by using scripting languages to assemble the required input files.

Output To evaluate possibly thousands of simulations it is important to save the output in a way which is later easily accessible for analysis. SABCEMM offers two formats for output files. In the basic version everything is saved in `csv` files in a dedicated folder. This method does not rely on third party software and is possible on all computers. A more sophisticated possibility is to save the entire results of a simulation in a `HDF5` file. An `HDF5` file offers an internal structure for data similar to file systems and is a self-describing format. This allows proper readability of the results stored in an `HDF5` file. In addition, the `HDF5` format allows us to also store the input `XML` used for a simulation within the `HDF5` output file. Hence, the output contains all the information necessary to analyze an ABCEM model which aids in ensuring correct documentation of simulation results. Note that the `HDF5` file format can easily be read using MATLAB and Excel (using the PyHexad Excel Add-in PyHexadGit).

Random Number Generators As seen in section 2.4.3 the ABCEM models rely heavily on the generation of random numbers. The SABCEMM framework supports multiple random number generators, namely the NAG library [189], the Intel Math Kernel Library (MKL) [68] and the random generator of the C++ library. While the random generator offered by the C++ library has the advantage that it is shipped with every C++ compiler we advise strongly against any standard older than C++11. The quality of the random numbers generated by older standards do not meet our requirements. The Intel MKL library and the NAG library have to be provided by the user at compile time. The version depends on what software is installed on your system. We rely on the Intel@Math Kernel Library 11.3.3 for Linux to provide our random numbers if not otherwise noted. As shown in figure 2.4.3 it is very fast when using the batch mode. The SABCEMM framework allows the user to choose the library best suited to his needs.

Testing With ever increasing complexity of software systems, the importance of software testing has become more and more evident. This has led to great advances in testing theory [188]. Generally, in large scale and complex problems bugs are easily mistaken for features of the simulation and vice versa. Therefore, the interpretation of results requires a flawless implementation. In order to ensure correctness of the SABCEMM framework, testing is included for framework code. Usually, numerical simulations are tested against their respective analytical solutions. However, finding analytical solutions for ABCEM models is only possible for extremely simplified versions. Finding that simplified implementations work correctly does not guarantee the correctness in general cases. Also, every model we consider heavily relies on random numbers. As random generators are allowed to behave differently on different platforms, programming languages or even different compilers, simulations are still not reproducible if the random seed is known. Therefore, we use a different approach to testing.

- For each model, we calculate one time step by hand. Whenever the model draws a random number, we usually use the same constant for each agent or use a deterministic number generator (we could draw numbers linearly from a range or similar). Initial values are determined from a real random draw (but they could also be chosen arbitrarily). We use a minimum number of agents to keep time and effort low. As those tests are well integrated into SABCEMM and `GoogleTest` [1], they are completely automatable. Large changes in implementation may require that the by-hand calculation is modified or redone.

- Complex models are prototyped in IPython [202] and later implemented in SABCEMM. Random numbers can be precomputed and used in both programs, which ensures that both programs work on the same input. In theory, that would allow for an exact comparison of the programs' outputs. However, the output formats are not compatible yet and IPython and C++ may respond differently to numerical effects. As such, the comparison must be done manually. A typical approach is comparing key variables between the implementations in the last time step.
- As a weaker criterion, we also compare our results to plots given in the corresponding papers. As outlined above, foreign results are not (easily) reproducible, which is why only qualitative comparisons are feasible.

While testing cannot prove the absence of mistakes in implementation, we encourage all users of the SABCEMM framework to also test their own contributions.

2.4.3 Computational Aspects

We now analyze how the runtime of simulations scales with the number of agents and number of time steps. From figures 30 and 31, we find a linear scaling of the Cross model with regard to the number of time steps and number of agents used in the simulation. This is an expected result and seems to be a universal observation for our tool. Although the example in figure 30 is conducted with the Cross model, we observe linear scaling for the Harras and LLS mode with respect to time steps, as well. Figure 32 reveals linear scaling of the LLS model with respect to the number of agents. For every data point we averaged the runtime of 100 simulations. We used the most basic setup relying on the standard C++ random number generator and using .csv files as an output. One can consider this the worst case. Using the random generator from the Intel MKL and output in HDF5 files we achieve even faster runtimes. An example is given in figure 4.

Finally, we compare the performance of our tool with implementations within MATLAB programming environment. Here, we compare the object-oriented SABCEMM simulation software implemented in the C++ programming language with the initial object-oriented implementation of the Cross model and a non-object-oriented implementation of the LLS model both implemented in the MATLAB programming environment. From figures 30, 31 and 32, we obtain the good performance of the SABCEMM framework. For the Cross model, we have a speedup up the factor of 100, for increasing number of agents and number of time steps as well. For the LLS model, SABCEMM times stay well below MATLAB times for up to 10,000 agents. However, given the data in figure 32, we can predict that the MATLAB implementation will eventually outperform SABCEMM. There are two advantages of the MATLAB implementation: First, the structure of LLS allows for an implementation in vector notation, giving MATLAB the opportunity for optimization. Second, on our 4-core machine, MATLAB exploits multiple cores to speed up its calculations, whereas SABCEMM is yet single-threaded.

Random Number Generator As mentioned before, many ABCEM models heavily utilize random numbers. Hence, quality and efficiency of random number generators directly influence the quality of simulation results. In this section, we investigate two aspects related to generation of random numbers: efficient generation of large amounts of random numbers and

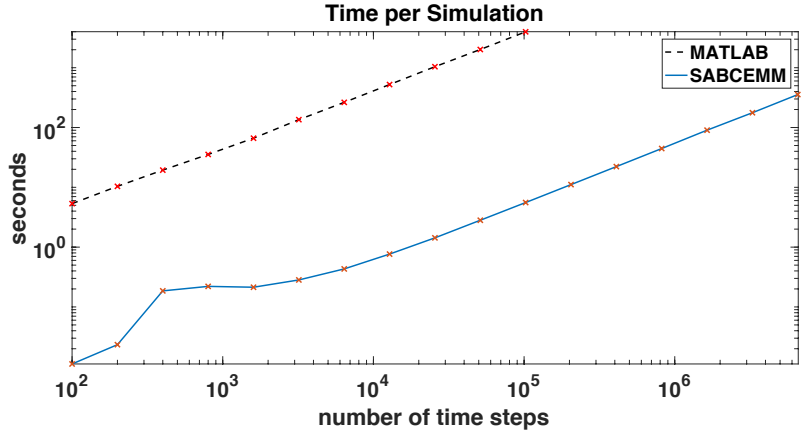


Figure 30: Scaling of the Cross Model with respect to the number of time steps. Parameters as in table 5. The time steps are varied according to the plot.

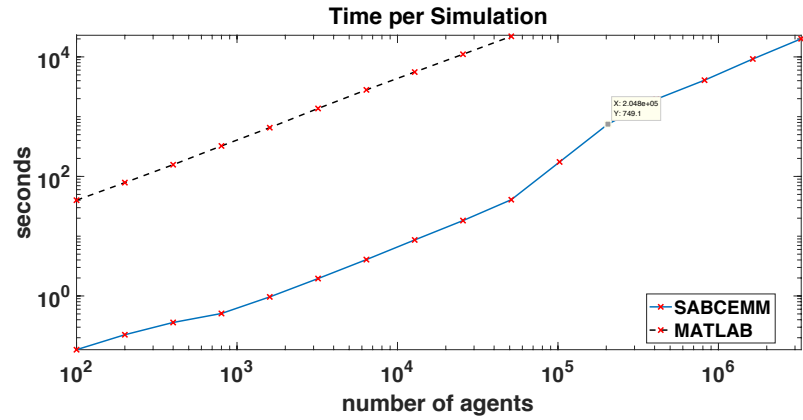


Figure 31: Scaling of the Cross model with respect to the number of agents. Parameters as in table 5. The parameter N is varied according to the plot.

influences of different random number generators on simulation results.

To stress the importance of efficiently generating large amounts of random numbers, we assume a simulation with 10,000 time steps. This provides a sufficiently large sample size for proper statistical analysis. In addition, we assume that the market mechanism requires one

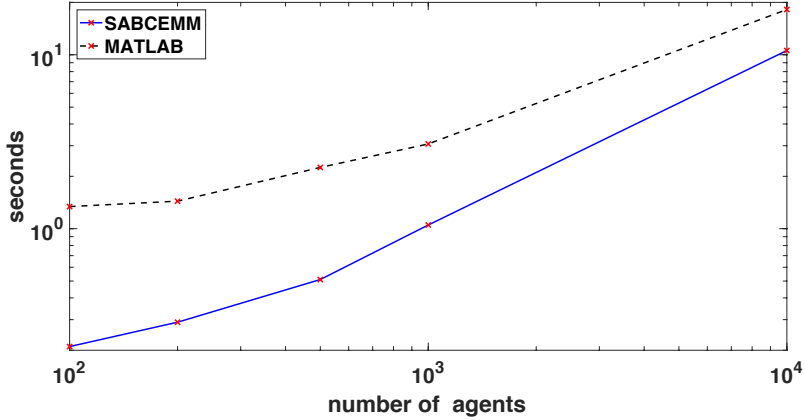


Figure 32: Scaling of the LLS model with respect to the number of agents. Parameters as in table 6 with $\sigma_\gamma = 0.2$. The parameter N is varied according to the plot.

number of agents	number of random numbers per agent and time step		
	1	2	3
100	1,010,000	2,010,000	3,010,000
1,000	10,010,000	20,010,000	30,010,000
10,000	100,010,000	200,010,000	300,010,000

Table 2: Example calculation of needed random numbers.

random number per time step. Table 2 presents the number of random number needed for varying number of agents and different amounts of random numbers needed for each agent per time step. From table 2, we see that even for the small number of 100 agents we already need one million random numbers.

In order to avoid the overhead implied by invoking the random number generator every time a random number is required during the simulation, we introduce the possibility to generate a pool of random numbers into the SABCEMM simulation software. Figure 33 reveals the speed of each generator regarding the creation of different pool sizes.

Random numbers then can be drawn from this pool instead of being computed on the fly. In addition, it is also possible to calculate random numbers on the fly the moment they are required. Table 3 summarizes the change of runtime of the Harras model with respect to the C++ sequential and MKL batch random number generator.

From this, we can easily see that pooling of random numbers is well-suited to reduce the overall runtime of simulations carried out using the SABCEMM simulation software. Finally, table 4 shows considerable speed up by utilizing the MKL batch random number generator.

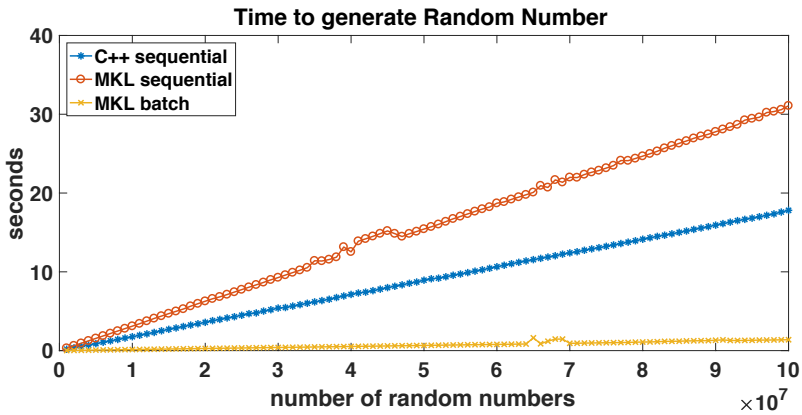


Figure 33: Time needed to generate a variety of random numbers.

Amount of		Runtime for the simulations		Generating random numbers	
Agents	Random Numbers	C++ sequential	MKL batch	C++ sequential	MKL batch
2,500	25,040,002	8.65 sec	5.61 sec	4.46 sec	0.346 sec
5,041	50,480,494	18.39 sec	13.25 sec	8.99 sec	0.697 sec
7,569	75,790,830	28.46 sec	20.34 sec	13.50 sec	1.047 sec
10,000	100,130,002	39.52 sec	30.63 sec	17.84 sec	1.383 sec

Table 3: Runtime of the Harras model with respect to varying number of agents and different random number generators. Further parameters are set to the values in table 8.

We obtain a maximal speed up of 35% of the total simulation time.

Amount of		Speed up	
Agents	Random Numbers	of the simulations	for generating random numbers
2,500	25,040,002	35 %	92 %
5,041	50,480,494	29 %	92 %
7,569	75,790,830	28 %	92 %
10,000	100,130,002	22 %	92 %

Table 4: Speed up of the Harras model due to the MKL batch random number generator.

A very important aspect is the influence of the random numbers regarding the qualitative results of the model. We tested this by utilizing a quite unreliable random number generator.

For this purpose we have chosen the `RANDU` generator, which is known to have a poor performance [118]. We have run the `RANDU` generator on a processor implementing the ARMv7 32 bit architecture. For our comparison, we have chosen the standard C++ random number generator on processors implementing the Intel 64 (also named AMD64 and x86_64) 64 bit architecture.

Exemplary, we run a simulation of the LLS model. Figure 34 reveals that the change of random number generator drastically changes the qualitative model output. Thus, we may conclude that models sensitive to the choice of random variable, generate different model outputs with respect to different random number generators.

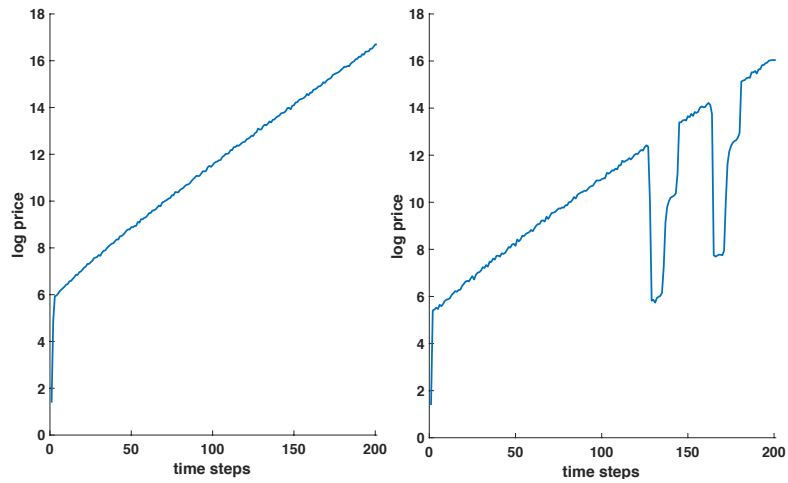


Figure 34: Simulations of the LLS model conducted with different random number generators. Left hand side, a run with the C++ random number generator on a 64 bit architecture, right hand side, a run with the `RANDU` generator on a 32 bit architecture. Parameters as in table 6 with $\sigma_\gamma = 0.01$.

2.4.4 Conclusion

We have introduced the software framework SABCEMM. The motivation for this simulator was the lack of a unified simulation approach in literature. SABCEMM is to our knowledge the first simulator for ABCEM models. The software tool enables the user to compare ABCEM models. Furthermore, the object-orientation enables the user to easily add and create new models with a minimum amount of coding. Especially, we want to emphasize that the framework was built and coded efficiently such that it is possible to run simulations of several million agents in an appropriate time.

In fact the simulation framework is built for a very general ABCEM model, we have introduced in section 2.2. We have motivated the model from economic perspective and have shown the huge adaptability of the model. In section 2.3 we demonstrated the great sim-

ulation possibilities provided by the SABCEMM framework. We presented our simulation results of the Cross, LLS and Harras model. Especially, we have shown the great flexibility of the framework. Thus, we have created new variants of the Cross model and did a proper comparison between two different market mechanisms. In addition, we have critically discussed the LLS model with respect to finite size effects and the investment decisions.

In section 2.4 we presented the software architecture, scaling behavior and efficiency of our model. Our tests indicate a linear scaling of our simulation framework with respect to the number of time steps and agents. Furthermore, we obtained that SABCEMM performs faster than two naive MATLAB implementations. We investigated the effect of random numbers with respect to computation time and qualitative output. Our examples indicate that a good and clever integration of a random number generator can reduce the run time up to 35%. Furthermore, we obtained qualitative differences in the model output of the LLS model due to a bad random number generator. This leads us to conclude that a proper choice of random number generator is essential, in order to obtain reliable simulation results.

Finally, we want to describe possible improvements in order to speed up simulations. Above all, parallelization of SABCEMM with respect to the number of agents seems to be a reasonable improvement of our tool. As we expect synchronization costs to be constant, the parallel efficiency should increase with the complexity of the model. In addition, an improvement of SABCEMM can be accomplished by speed up the generation of random numbers. This could be achieved by performing the generation of random numbers in parallel. Random number generation is almost perfectly parallelizable because of low synchronization overhead.

The authors hope that the simulation framework SABCEMM helps to efficiently simulate, test and compare ABCEM models. This goal can be only achieved by implementing more models into the framework. Hence, we want to encourage the reader to do so. The authors, an interdisciplinary group of mathematicians, physicists, engineers and computer scientists are open for any suggestions for improvements and welcome any questions regarding the SABCEMM tool.

2.5 Appendix

2.5.1 Models

Cross Model We present the Cross model as defined in [71]. We assume a fixed number of $N \in \mathbb{N}$ agents. Each agent decides in each time step, whether he wants to be long or short in the market. Thus, the investment propensity σ_i , $1 \leq i \leq N$ of each agent switches between $\sigma_i = \pm 1$. The excess demand of all investors at time $[0, \infty)$ is then defined as:

$$ED(t) := \frac{1}{N} \sum_{i=1}^N \sigma_i(t).$$

Furthermore, the model introduces two pressures, the *herding pressure* and the *inaction pressure*, which control the switching mechanism.

The *inaction pressure* is defined by the interval

$$I_i = \left[\frac{m_i}{1 + \alpha_i}, m_i (1 + \alpha_i) \right],$$

where m_i denotes the stock price of the last switch of agent i and $\alpha_i > 0$ is the so called *inaction threshold*. The *herding pressure* is given by:

$$\begin{cases} c_i(t + \Delta t) = c_i(t) + \Delta t |ED(t)|, & \text{if } \sigma_i(t) ED(t) < 0 \\ c_i(t + \Delta t) = c_i(t), & \text{otherwise.} \end{cases}$$

In addition, one defines the *herding threshold* β_i . The thresholds are chosen once randomly from an i.i.d. random variable, which is uniformly distributed.

$$\begin{aligned} \alpha_i &\sim \text{Unif}_c(A_1, A_2), \quad A_2 > A_1 > 0, \\ \beta_i &\sim \text{Unif}_c(B_1, B_2), \quad B_2 > B_1 > 0. \end{aligned}$$

The constants B_1 and B_2 have to scale with time, since they correspond to the time units an investor can resist the herding pressure.

$$\begin{aligned} B_1 &:= b_1 \cdot \Delta t, \\ B_2 &:= b_2 \cdot \Delta t. \end{aligned}$$

Switching mechanism The switching is then induced if

$$c_i > \beta_i \text{ or } S(t) \notin I_i.$$

After a switch the herding pressure is reset to zero and the inaction interval gets updated as well. The stock price is then driven by the excess demand:

$$\begin{aligned} S(t + \Delta t) &= S(t) \exp\{(1 + \theta |ED(t)|) \sqrt{\Delta t} \eta(t) + \kappa \Delta t \frac{\Delta ED(t)}{\Delta t}\}, \\ \sqrt{\Delta t} \eta &\sim \mathcal{N}(0, \Delta t) \\ \Delta ED(t) &:= \frac{1}{N} \sum_{i=1}^N \sigma_i(t) - \frac{1}{N} \sum_{i=1}^N \sigma_i(t - \Delta t), \end{aligned}$$

where κ denotes the market depth and $\Delta t > 0$ the time step.

Cross model extensions: One alternative pricing function is given by:

$$S(t + \Delta t) = S(t) + \Delta t \kappa \frac{\Delta ED(t)}{\Delta t} S(t) + \sqrt{\Delta t} F_{Cross}(S, ED) S(t) \eta,$$

Furthermore, we have added the wealth evolution, for a fixed interest rate $r > 0$ and fixed investment fraction $\gamma \in (0, 1)$:

$$w_i(t + \Delta t) = w_i(t) + \Delta t \left[(1 - \gamma) r + \gamma \frac{S(t) - S(t - \Delta t)}{\Delta t S(t)} \right] w_i(t).$$

LLS Model We have implemented the model as defined in [155, 156]. As described in section 2.3.2 we have added the correct time scale to the model. In order to obtain the original model one needs to set $\Delta t = 1$.

The model considers $N \in \mathbb{N}$ financial agents who can invest $\gamma_i \in [0.01, 0.99]$, $i = 1, \dots, N$ of their wealth $w_i \in \mathbb{R}_{>0}$ in a stocks and have to invest $1 - \gamma_i$ of their wealth in a safe bond with interest rate $r \in (0, 1)$. The investment propensities γ_i are determined by a utility maximization and the wealth dynamic of each agent at time $t \in [0, \infty)$ is given by

$$w_i(t) = w_i(t - \Delta t) + \Delta t \left((1 - \gamma_i(t - \Delta t)) r w_i(t - \Delta t) + \gamma_i(t - \Delta t) w_i(t - \Delta t) \underbrace{\frac{\frac{S(t) - S(t - \Delta t)}{\Delta t} + D(t)}{S(t)}}_{=:x(S, t, D)} \right).$$

The dynamics is driven by a multiplicative dividend process. Given by:

$$D(t) := (1 + \Delta t \tilde{z}) D(t - \Delta t),$$

where \tilde{z} is a uniformly distributed random variable with support $[z_1, z_2]$. The price is fixed by the so called *market clearance condition*, where $n \in \mathbb{N}$ is the fixed number of stocks and $n_i(t)$ the number of stocks of each agent.

$$n = \sum_{i=1}^N n_i(t) = \sum_{k=1}^N \frac{\gamma_k(t) w_k(t)}{S(t)}. \quad (9)$$

The utility maximization is given by

$$\max_{\gamma_i \in [0.01, 0.99]} E[\log(w(t + \Delta t, \gamma_i, S^h))].$$

with

$$E[\log(w(t + \Delta t, \gamma_i, S^h))] = \frac{1}{m_i} \sum_{j=1}^{m_i} U_i \left((1 - \gamma_i(t)) w_i(t, S^h) (1 + r\Delta t) + \gamma_i(t) w_i(t, S^h) (1 + x(S, t - j\Delta t, D) \Delta t) \right).$$

The constant m_i denotes the number of time steps each agent looks back. Thus, the number of time steps m_i and the length of the time step Δt defines the time period each agent extrapolates the past values. The superscript h indicates, that the stock price is uncertain and needs to be fixed by the market clearance condition. Finally, the computed optimal investment proportion gets blurred by a noise term.

$$\gamma_i(t) = \gamma_i^*(t) + \epsilon_i,$$

where ϵ_i is distributed like a truncated normally distributed random variable with standard deviation σ_γ .

Utility maximization Thanks to the simple utility function and linear dynamics we can compute the optimal investment proportion in the cases where the maximum is reached at the boundaries. The first order necessary condition is given by:

$$f(\gamma_i) := \frac{d}{dt} E[\log(w(t + \Delta t, \gamma_i, S^h))] = \frac{1}{m_i} \sum_{j=1}^{m_i} \frac{\Delta t (x(S, t - j\Delta t, D) - r)}{\Delta t (x(S, t - j\Delta t, D) - r) \gamma_i + 1 + \Delta t r}.$$

Thus, for $f(0.01) < 0$ we can conclude that $\gamma_i = 0.01$ holds. In the same manner, we get $\gamma_i = 0.99$, if $f(0.01) > 0$ and $f(0.99) > 0$ holds. Hence, solutions in the interior of $[0.01, 0.99]$ can be only expected in the case: $f(0.01) > 0$ and $f(0.99) < 0$. This coincides with the observations in [209].

Harras model We present the Harras model as defined in [115].

We consider N financial agents where each agent is equipped with a personal opinion $\psi_i(t_k)$, and t_k denotes a discrete time step. The personal opinion is created through the personal information of each agent $\epsilon_i(t_k)$, public information $n(t_k)$ and the expected action of the surrounded neighbor j by the agent i , $E_i[\sigma_j(t_k)]$, $\sigma_j \in \{-1, 0, 1\}$. The opinion of the i -th agent at time t_k reads:

$$\psi_i(t_k) = c_{1,i} \sum_{j=1}^4 k_{ij}(t_{k-1}) E[\sigma_i(t_k)] + c_{2,i} u(t_{k-1}) n(t_k) + c_{3,i} \epsilon_i(t_k). \quad (10)$$

During the evaluation of our simulations we noticed a significant difference in the magnitude of the price's volatility. Our investigation leads us to the conclusion that the opinion of the i -th agent at time t_k should instead be:

$$\psi_i(t_k) = c_{1,i} \frac{1}{4} \sum_{j=1}^4 k_{ij}(t_{k-1}) E[\sigma_i(t_k)] + c_{2,i} u(t_{k-1}) n(t_k) + c_{3,i} \epsilon_i(t_k).$$

The weights $(c_{1,i}, c_{2,i}, c_{3,i})$ are chosen initially for each agent from three uniformly distributed random variables on the domains $[0, C_l]$, $l \in \{1, 2, 3\}$. The private and public information $\epsilon_i(t_k), n(t_k)$ are modeled as standard normally distributed i.i.d. random variables. The agents are grouped on a virtual square lattice with periodic boundary conditions, such that each agent has four neighbors. We update of the opinion of each agent is performed in each time step in random order. The additional factor k_{ij} weights the predicted action of the j -th agent based on the past performance. In the same manner the factor u weights the public information stream. The update rule of these weighting factors is given by:

$$u(t_k) = \alpha u(t_{k-1}) + (1 - \alpha) n(t_{k-1}) \frac{ED(t_k)}{\sigma_{ED}(t_k)},$$

$$k_{i,j}(t_k) = \alpha k_{i,j}(t_{k-1}) + (1 - \alpha) E_i[\sigma_j(t_{k-1})] \frac{ED(t_k)}{\sigma_{ED}(t_k)},$$

with the constant $0 < \alpha < 1$ and the volatility

$$\sigma_{ED}^2(t_k) = \alpha \sigma_{ED}^2(t_{k-1}) + (1 - \alpha) (ED(t_{k-1}) - \langle ED(t_k) \rangle)^2,$$

$$\langle ED(t_k) \rangle = \alpha \langle ED(t_{k-1}) \rangle + (1 - \alpha) ED(t_{k-1}),$$

where the brackets $\langle \cdot \rangle$ denote the expected excess demand ED . The agent's action on the market is then determined by a threshold of each agent. The threshold $\bar{\psi}_i$ is drawn from a uniform distribution in the interval $[0, \Omega]$. The trading decision of each agent is characterized by $\sigma_i = \pm 1$, where $\sigma_i = 1$ represents a buy order and $\sigma = -1$ a sell order. We have

$$\sigma_i(t_k) = \begin{cases} 1, & \psi_i(t_k) > \bar{\psi}_i, \\ -1, & \psi_i(t_k) < -\bar{\psi}_i, \\ 0, & \text{else.} \end{cases}$$

Furthermore, each agent tracks his number of stocks q_i and the cash w_i and thus the trading volume $v_i(t_k)$ of each agent (in units of stocks) is given by

$$v_i(t_k) = \begin{cases} g \frac{w_i(t_k)}{S(t_k)}, & \sigma_i = 1, \\ g q_i(t_k), & \sigma = -1. \end{cases}$$

Here, $S(t_k)$ denotes the stock price and $g \in (0, 1)$ a fixed fraction of wealth each agent wants to invest in stocks. The stock price is then driven by the excess demand $ED(t_k)$

$$\log(S(t_k)) = \log(S(t_{k-1})) + ED(t_{k-1}),$$

where ED is defined as:

$$ED(t_k) := \frac{1}{\lambda N} \sum_{i=1}^N \sigma_i(t_k) v_i(t_k).$$

The constant $\lambda > 0$ represents the market depth. Finally, we want to state the update mechanism of w_i and q_i .

$$\begin{aligned} w_i(t_k) &= w_i(t_{k-1}) - \sigma_i(t_{k-1}) v_i(t_{k-1}) S(t_k), \\ q_i(t_k) &= q_i(t_{k-1}) + \sigma_i(t_{k-1}) v_i(t_{k-1}). \end{aligned}$$

Unknown implementation details: While implementing the model from [115], we were missing some crucial implementation details. First of all, no information was given concerning the initialization of most variables. We choose them according to table 8. Further the term $E[\sigma_i(t_k)]$ used during the calculation of the opinion (10) is not defined. We assume this to be the decision σ_i of agent i . Since the update of the agents is done in random order σ_i can either be $\sigma_i(t_{k-1})$ if the agent i has yet to be updated or $\sigma_i(t_k)$ if the agent i has already been updated. This assumption was later confirmed by Harras via mail correspondence. Furthermore, the update order can not be deduced from the publication [115]. We have ordered the process as defined through the previously introduced discrete time steps.

2.5.2 Parameter Sets

Cross Model

LLS Model The initialization of the stock return is performed by creating an artificial history of stock returns. The artificial history is modeled as a Gaussian random variable with mean μ_h and standard deviation σ_h . Furthermore, we have to point out that the increments of the dividend is deterministic, if $z_1 = z_2$ holds. We used the C++ standard random number generator for all simulations of the LLS model if not otherwise stated.

Harras Model

Parameter	Value
N	1000
A_1	0.1
A_2	0.3
b_1	25
b_2	100
$w_i(t = 0)$	$1 \quad \forall 1 \leq i \leq N$
time steps	10,000
Δt	$4 \cdot 10^{-5}$
κ	0.2
θ	0
$S(t = 0)$	1

Variable	Initial Value
$ED(t = 0)$	$\frac{1}{N} \sum_{i=1}^N \gamma_i(0)$
$c_i(t = 0)$	$B_1 + \text{rand}(B_2 - B_1), \forall 1 \leq i \leq N$
$m_i(t = 0)$	$S(t = 0), \forall 1 \leq i \leq N$
$\sigma_i(t = 0)$	$\text{Unif}_d(\{-1, 1\})$

(a) Parameters of Cross model.

(b) Initial values of Cross model.

Table 5: Cross basic setting.

Parameter	Value
N	100
m_i	15
σ_γ	0 or 0.2
r	0.04
$z_1 = z_2$	0.05
Δt	1
time steps	200

Variable	Initial Value
μ_h	0.0415
σ_h	0.003
$\gamma(t = 0)$	0.4
$w_i(t = 0)$	1000
$n_i(t = 0)$	100
$S(t = 0)$	4
$D(t = 0)$	0.2

(a) Parameters of LLS model.

(b) Initial values of LLS model.

Table 6: Basic setting of the LLS model.

Parameter	Value
N	99
m_i	$10, 1 \leq i \leq 33$ $141, 34 \leq i \leq 66$ $256, 67 \leq i \leq 99$
σ_γ	0.2
r	0.0001
$z_1 = z_2$	0.00015
Δt	1
time steps	20,000

Variable	Initial Value
μ_h	0.0415
σ_h	0.003
$\gamma_i(t = 0)$	0.4
$w_i(t = 0)$	1000
$n_i(t = 0)$	100
$S(t = 0)$	4
$D(t = 0)$	0.004

(a) Parameters of LLS model.

(b) Initial values of LLS model.

Table 7: Setting for the LLS model (3 agent groups).

Parameter	Value	Variable	Initial Value
C_1	0	$k_{ij}(t = 0)$	Unif_c(0, 1)
C_2	1	$E_i[\sigma_j(t = 0)]$	Unif_d({-1, 0, 1})
C_3	1	$\sigma_{ED}^2(t = 0)$	0.1
Ω	2	$\langle ED(t = 0) \rangle$	0
g	0.02	$ED(t = 0)$	0
α	0.95	$ED(t = -1)$	0
$w_i(t_0)$	1 $\forall 1 \leq i \leq N$	$u_i(t = -1)$	0
$q_i(t_0)$	1 $\forall 1 \leq i \leq N$	$u_i(t = 0)$	0
N	2500	$v_i(t = 0)$	0
λ	0.25	$\sigma_i(t = 0)$	0
$S(t = 0)$	1		
$q_i(t = 0)$	1 $\forall 1 \leq i \leq N$		
time steps	10,000		

(a) Parameters in the Harras model.

(b) Initial values Harras.

Table 8: Harras basic setting.

3 Kinetic Theory and Applications to Financial Market Models

This chapter is devoted a mathematical introduction to the theory we will apply in the next chapters. Firstly, we give an introduction into stochastic diffusion processes and the corresponding Kolmogorov equations. We illustrate the translation of a stochastic differential equation (SDE) into a Kolmogorov equation by the means of simplified price adjustments introduced in the previous chapter. Secondly, we give a short introduction to kinetic theory and provide a concise overview of relevant literature regarding kinetic models of financial markets. We then extensively study the mean field limit with an example of a simple financial market model. Finally, we give an introduction to the new theory mean field games. Again, we demonstrate the presented theory by applying it to a simple econophysical model.

3.1 Stochastic Processes to PDEs

We begin this section with an introduction to stochastic differential equations (SDEs) and probabilistic representation formulas of this diffusion processes. In a next step, we will apply the presented theory to simple SDEs we already observed in the previous chapter.

3.1.1 Stochastic Differential Equations

In the previous chapter, we have heuristically written the SDEs as ordinary differential equation with white noise.

$$\dot{X}(t) = F(t, X(t)) + G(t, X(t)) \eta, \quad X(t) = x, \quad \eta \sim \mathcal{N}(0, 1).$$

Mathematically, this notation does not make sense. One can imagine that the solution X of the previous SDE is a stochastic process and nowhere differentiable. Thus, we should interpret a SDE always as an integral equation.

$$X(t + \tau) = X(t) + \int_t^{t+\tau} F(s, X(s)) ds + \int_t^{t+\tau} G(s, X(s)) d\eta.$$

We still need to define the integral $\int_t^{t+\tau} G(s, X(s)) d\eta$ properly. It turns out that we need a generalization of the Lebesgue, respectively the Stieltjes integral. Possible generalizations are the **Itô** and the **Stratonovich** integrals. We refer to the lecture notes of Evans [98] for an introduction to SDEs. In this study, we only consider the **Itô** stochastic integral. Before we can define the **Itô** integral, we need to define the Wiener process.

Definition 3.1.1. A real-valued stochastic process $W(t)$, $t \geq 0$ is called Brownian motion or Wiener process if

- i) $W(0) = 0$, a.s.,
- ii) $W(t) - W(s) \sim \mathcal{N}(0, t - s)$, $\forall t \geq s \geq 0$,
- iii) for all times $0 < t_1 < t_2 < \dots < t_n$, the random variables $W(t_1), W(t_2) - W(t_1), \dots, W(t_n) - W(t_{n-1})$ are independent

Definition 3.1.2. A process I is called step process if there exists a partition $P = \{0 = t_0 < t_1 < \dots < t_m = T\}$ such that

$$I(t) \equiv I_k, \quad \text{for } t_k \leq t < t_{k+1} \quad (k = 1, \dots, m - 1),$$

holds.

Then, we can define the Itô stochastic integral.

Definition 3.1.3. *Let I be a step process, then*

$$\int_0^T I \, dW := \sum_{k=0}^{m-1} I_k (W(t_{k+1}) - W(t_k)),$$

is the Itô stochastic integral of I on the interval $(0, T)$.

We want to approximate arbitrary functions G by a step process I such that we can generalize the stochastic integral for arbitrary functions G . We have the following lemma:

Lemma 3.1.1. *If G is sufficiently regular, there exists a sequence of bounded step processes G_n such that*

$$E \left(\int_0^T |G - G_n|^2 \, dt \right) \rightarrow 0,$$

holds.

Definition 3.1.4. *The Itô stochastic integral of the process G is defined as:*

$$\int_0^T G \, dW := \lim_{n \rightarrow \infty} \int_0^T G_n \, dW.$$

The Itô stochastic integral has the following properties.

Theorem 3.1.1. *For all constants $a, b \in \mathbb{R}$ and for integrable functions G, H , we have*

$$i) \int_0^T a G + b H \, dW = a \int_0^T G \, dW + b \int_0^T H \, dW,$$

$$ii) E \left(\int_0^T G \, dW \right) = 0,$$

$$iii) E \left(\left(\int_0^T G \, dW \right)^2 \right) = E \left(\int_0^T G^2 \, dW \right),$$

$$iv) E \left(\int_0^T H \, dW \int_0^T G \, dW \right) = E \left(\int_0^T HG \, dW \right).$$

We want to emphasize that

$$\int_t^{t+\tau} 1 \, dW = W(t + \tau) - W(t),$$

holds, which immediately follows from the definition. We symbolically use the abbreviation

$$dX(t) = F(t, X(t)) \, dt + G(t, X(t)) \, dW, \quad X(t) = x, \quad (11)$$

for the integral equation

$$X(t + \tau) = X(t) + \int_t^{t+\tau} F(s, X(s)) \, ds + \int_t^{t+\tau} G(s, X(s)) \, dW(s).$$

Finally, we want to present the Itô chain rule and product rule which can be again found in [98].

Theorem 3.1.2. *We assume that the real-valued stochastic process X satisfies the stochastic differential*

$$dX = F(X, t) \, dt + G(X, t) \, dW,$$

for F, G Lipschitz continuous. Assume $u : \mathbb{R} \times [0, T] \rightarrow \mathbb{R}$ is continuous and that $\frac{\partial u}{\partial t}, \frac{\partial u}{\partial x}, \frac{\partial^2 u}{\partial x^2}$ exist and are continuous.

$$Y(t) := u(X(t), t).$$

Then Y has the stochastic differential

$$\begin{aligned} dY &= \frac{\partial u}{\partial t} \, dt + \frac{\partial u}{\partial x} \, dX + \frac{1}{2} \frac{\partial^2 u}{\partial x^2} G^2(X, t) \, dt \\ &= \left(\frac{\partial u}{\partial t} + \frac{\partial u}{\partial x} F(X, t) + \frac{1}{2} \frac{\partial^2 u}{\partial x^2} G^2(X, t) \right) dt + \frac{\partial u}{\partial x} G(X, t) \, dW. \end{aligned}$$

This formula is also called Itô's chain rule or Itô formula.

Furthermore, we want to state Itô's product rule.

Theorem 3.1.3. *Suppose we have*

$$\begin{cases} dX_1 = F_1 \, dt + G_1 \, dW, \\ dX_2 = F_2 \, dt + G_2 \, dW, \end{cases}$$

for Lipschitz continuous functions $F_i, G_i, i = 1, 2$. Then

$$d(X_1 X_2) = X_1 \, dX_2 + X_2 \, dX_1 + G_1 G_2 \, dt,$$

holds.

3.1.2 Kolmogorov Equations

The SDE (11) defines a diffusion process which can be associated to a second order differential operator. The resulting partial differential equations describe the averaged evolution of the stochastic process. Heuristically, one can state that the SDE defines the *random characteristic curve* of the associated PDE. This makes it possible to solve the PDE numerically solely by solving the corresponding SDE. This numerical method is known as Monte Carlo method and is a very powerful tool to solve many types of partial differential equations. We refer to [198] for an introduction. The next section can be regarded as a small summary of probabilistic representations of diffusion processes and is based on the book by Lapeyre, Pardoux and Sentis [147].

Infinitesimal Generator First, we introduce the *Kolmogorov operator* and its dual operator on measures. Secondly, we will shortly introduce the *infinitesimal operator* of a diffusion process and finally derive the forward Kolmogorov (better known as Fokker-Planck equation) and the backward or retrograde Kolmogorov equation. We do not present any proofs and refer to the book by Lapeyre, Pardoux and Sentis [147].

The *Kolmogorov operator* P_t is defined as

$$P_t f = E[f(X_t)],$$

where X_t is a unique solution of our SDE (11) and f an arbitrary differential function. The *Kolmogorov operator* satisfies the semigroup property:

$$P_{t+s} f = P_t P_s f.$$

The dual operator or adjoint operator of the *Kolmogorov operator* P_t^* acting on the space of probability measures $\mathcal{P}(\mathbb{R})$ is defined by:

$$\int f \, d(P_t^* \mu) = \int P_t f \, d\mu, \quad \mu \in \mathcal{P}(\mathbb{R}),$$

one might use the abbreviation $\langle P_t^* \mu, f \rangle = \langle \mu, P_t f \rangle$ for the previous identity. We define the *infinitesimal operator* of a diffusion process as follows:

Theorem 3.1.4. *Given the solution X_t^x of the SDE (11) with initial condition $X(0) = x$ and a twice differentiable function f with bounded derivatives, the function $t \mapsto E[f(X^x(t))]$ is differentiable and*

$$\frac{d}{dt} E[f(X^x(t))] \Big|_{t=0} = Af(x),$$

holds with the infinitesimal operator A

$$Af(x) := \frac{G^2(t, x)}{2} \frac{\partial^2}{x^2} f(x) + F(t, x) \frac{\partial}{\partial x} f(x).$$

Furthermore, we want to state the following result which can be seen as a simple version of the famous *Feynman-Kac theorem*.

Theorem 3.1.5. *Given a continuous function g and we assume that $u(t, x)$ satisfies*

$$\begin{cases} u(T, x) = g(x), & x \in \mathbb{R}, \\ (\partial_t u + Au)(t, x) = 0, & (t, x) \in [0, T] \times \mathbb{R}. \end{cases}$$

Then

$$u(t, x) = E[g(X^x(T-t))],$$

holds.

Notice that the previous theorem gives a representation formula for parabolic equations with final conditions called *backward Kolmogorov equations*. Finally, we want to derive parabolic equations with initial conditions. As in the case of the *Kolmogorov operator*, we need to derive

the adjoint operator of the *infinitesimal generator* acting on the dual space of measures. The adjoint operator A^* is defined by:

$$A^*f(x) = \frac{1}{2} \frac{\partial^2(G^2(t, x) f(x))}{\partial x^2} - \frac{\partial(F(t, x) f(x))}{\partial x},$$

and satisfies for twice differentiable functions f and g

$$\int_{\mathbb{R}} (Af)(x) g(x) dx = \int_{\mathbb{R}} f(x) (A^*g)(x) dx.$$

We get:

Theorem 3.1.6. *We assume that the law of the random variable $X(t)$ has a sufficiently regular density function $p(t, x)$. Then the density function satisfies*

$$\begin{cases} \partial_t p(t, x) = A^*p(t, x), & t \geq 0, x \in \mathbb{R}, \\ p(0, x) = p_0(x), & a. s. \text{ in } x. \end{cases}$$

This parabolic PDE is nothing else than the famous *Fokker-Planck equation*. We summarize the findings in figure 35.

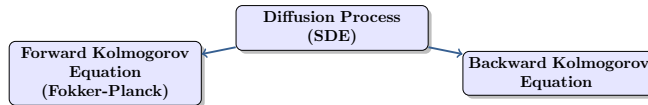


Figure 35: Probabilistic representation formulas for diffusion processes.

3.1.3 Application to Stock Price SDEs

In the previous chapter, we already introduced the *economic equilibrium theory* proposed by Léon Walras in 1874 [249]. As explained in the previous chapter, we model the excess demand by:

$$ED(S, \gamma, w, \Phi, t) := \frac{1}{N} \sum_{i=1}^N \Phi_i(t) \frac{\gamma_i(t) w_i(t)}{S(t)},$$

$$\Phi \in \{-1, 0, 1\}, \gamma_i \in (0, 1), w_i, t > 0, N \in \mathbb{N}.$$

Thus, the excess demand is nothing else than the averaged aggregated demand of all market participants.

- Φ_i characterizes the expected stock price movement of the i th investor
- γ is the fraction of wealth each investor wants to invest

- w_i is the wealth of each investor
- the fraction $v_i := \frac{\gamma_i w_i}{S}$ is the volume or amount of stocks each investor wants to buy or sell

Notice that all these quantities w_i, Φ_i, γ_i also depend on the stock price itself. In practice, Φ_i and γ_i should be determined by the strategy of each financial investor, respectively by a maximization process. Thus, the equilibrium price at time t is determined by:

$$ED(S) \stackrel{!}{=} 0. \quad (12)$$

Here, we have neglected the further dependencies of the excess demand for simplicity. Notice that the auctioneer would need to know the demand functions (Φ_i, γ_i, w_i) of all financial agents to solve this equation. This does not seem to be very realistic since no investor wants to publish his strategy.

Mathematically, we are faced with a root finding problem which is generally quite difficult to solve. Many agent-based econophysical models consider generalizations of the equilibrium model of Walras. These models are called disequilibrium models [19] and only coincide in special cases with the solution of the corresponding equilibrium model. Mathematically, these models are nothing else than the relaxation of the algebraic equation (12). The dynamic can be described by:

$$\dot{S} = \lambda ED(S) S. \quad (13)$$

where λ is the relaxation parameter, which can be economically interpreted as the inverse *market depth*. This seems to be a more realistic model of the stock price evolution, since the stock prices move towards the equilibrium also if they never reach it.

One can generalize the previously introduced model if one considers market imperfections which are usually modeled by adding Gaussian white noise. Adding the noise to (12) and then performing the relaxation we get:

$$dS = \lambda ED(S) S dt + \lambda S dW. \quad (14)$$

where W is the Wiener process. Here, we have neglected the possible relaxation constant λ in the diffusion term. The same procedure can be conducted with log prices P .

Examples of the Excess Demand We want to have a look at two examples of different excess demands in the literature of agent-based economic market models. First, we want to look at the excess demand introduced in the famous Levy-Levy-Solomon model [155]. The excess demand is given by:

$$ED_{LLS}(S) := \frac{1}{n} \sum_{i=1}^N \frac{\gamma_i w_i}{S} - 1.$$

The natural numbers n and N are the fixed amount of stocks and financial agents and $\gamma_i \in (0, 1)$ the fraction of wealth each agents wants to invest. In the Levy-Levy-Solomon model, the investment propensity γ_i is determined by an utility maximization process which also

depends on the current and past stock prices. Another example of a different excess demand can be found in Harras and Sornette [115]

$$ED_H(S) := \frac{1}{N} \sum_{i=1}^N \Phi_i \frac{c w_i}{S},$$

where $c \in (0, 1)$ is a positive constant, $w_i > 0$ the wealth of each agent and $\Phi_i \in \{-1, 0, 1\}$ the position of each investor in the market. The position Φ_i of each investor is determined in the model by spin dynamics influenced by a nonlinear dynamical system.

Model Simplifications In this section, we are interested in the structure of the resulting stock price equations. We thus simplify the previously introduced excess demands in the following way.

$$\begin{aligned} ED_{LLS}(S(t), t) &= \frac{m(t)}{S(t)} - 1, \quad m(t) > 0, \\ ED_H(S(t), t) &= \frac{h(t)}{S(t)}, \quad h(t) \in \mathbb{R}. \end{aligned}$$

Obviously, we neglect all further nonlinear dependencies of the stock price equation. The stock price equations are:

$$dS = \lambda (m - S) dt + S dW \tag{15}$$

$$dS = \lambda h dt + S dW. \tag{16}$$

Connection to other Models The SDE (15) can be interpreted as a special case of the *Cox-Ingersoll-Ross model* which is a well known *one factor interest rate models* in mathematical finance. Furthermore, equations of type (15) arise in the context of kinetic financial market models, e.g. [166] and as well in chapter 4 of this study.

Solutions We will use the Itô formula (theorem 3.1.2) and Itô product rule (theorem 3.1.3) to derive the solutions of our SDEs. Furthermore, we add to both SDEs the following initial condition:

$$S(0) = S_0.$$

We start to study the solutions of the SDE (16).

$$dS(t) = \lambda h(t) dt + S dW,$$

We make the ansatz

$$S(t) = X(t) Y(t),$$

and assume that

$$\begin{aligned} dX &= X dW, \quad X(0) = 1, \\ dY &= A dt + B dW, \quad Y(0) = S(0), \end{aligned}$$

holds. Then the Itô product rule tells us that

$$\begin{aligned} dS &= X \, dY + Y \, dX + B \, X \, dt \\ &= X \, (A \, dt + B \, dW) + Y \, X \, dW + B \, X \, dt \end{aligned}$$

holds. Thus, we require

$$X \, (A + B) \, dt + X \, B \, dW = \lambda \, h \, dt,$$

which is satisfied if we choose A and B to be:

$$\begin{aligned} A(t) &= \frac{\lambda \, h(t)}{X}, \\ B(t) &= 0. \end{aligned}$$

Thus, the processes X and Y are given by:

$$\begin{aligned} X(t) &= \exp\left\{-\frac{t}{2} + W(t)\right\}, \\ Y(t) &= S(0) + \int_0^t \frac{\lambda \, h(s)}{X(s)} \, ds. \end{aligned}$$

Hence, the solution of the SDE (16) is:

$$S(t) = \exp\left\{-\frac{t}{2} + W(t)\right\} \left(S(0) + \int_0^t \frac{\lambda \, h(s)}{\exp\left\{-\frac{s}{2} + W(s)\right\}} \, ds \right).$$

The SDE (15) is given by

$$dS(t) = \lambda \, [m(t) - S(t)] \, dt + S \, dW.$$

Performing the same ansatz as before, we get:

$$\begin{aligned} dX &= -\lambda \, X \, dt + X \, dW, \quad X(0) = 1, \\ dY &= A \, dt + B \, dW, \quad Y(0) = S(0). \end{aligned}$$

Thus for $dS = d(XY)$ we obtain:

$$\begin{aligned} dS &= X \, dY + Y \, dX + B(t) \, X \, dt \\ &= X \, [A \, dt + B \, dW] + Y \, [-\lambda \, X \, dt + X \, dW] + B \, X \, dt. \end{aligned}$$

Hence, we require

$$X \, [A + B] \, dt + X \, B \, dW = \lambda \, m \, dt,$$

which is fulfilled for:

$$\begin{aligned} A(t) &= \frac{\lambda \, m(t)}{X(t)}, \\ B(t) &= 0. \end{aligned}$$

Then are the solutions given by

$$X(t) = \exp\{W(t) - (\lambda + \frac{1}{2}) t\},$$

$$Y(t) = S(0) + \int_0^t \frac{\lambda m(s)}{X(s)} ds,$$

and we obtain our process S .

$$\begin{aligned} S(t) = & S(0) \exp\{W(t) - (\lambda + \frac{1}{2}) t\} + \\ & \exp\{W(t) - (\lambda + \frac{1}{2}) t\} \int_0^t \lambda m(s) \exp\{-W(s) + (\lambda + \frac{1}{2}) s\} ds. \end{aligned}$$

3.1.4 Long Time Asymptotics

We have seen that the solutions of the SDEs (15) and (16) exist. In order to study the long time behavior of our models, we search for steady states of the corresponding forward Komogorov (Fokker-Planck) equations. The *adjoint infinitesimal generators* of our SDEs are given by:

$$A^* f(t, x) = \frac{1}{2} \frac{\partial^2}{\partial s^2} (s^2 f(t, s)) - \frac{\partial}{\partial s} (\lambda (m(t) - s) f(t, s)), \quad (17)$$

$$A^* f(t, x) = \frac{1}{2} \frac{\partial^2}{\partial s^2} (s^2 f(t, s)) - \frac{\partial}{\partial s} (\lambda h(t) f(t, s)). \quad (18)$$

Here, the operator (17) corresponds to the SDE (15) and the generator (18) to the equation (16). We have to set the infinitesimal generator of our processes to zero.

$$A_\infty^* f_\infty(s) = 0.$$

We assume that the limits

$$\begin{aligned} \lim_{t \rightarrow \infty} m(t) &= \bar{m}, \\ \lim_{t \rightarrow \infty} h(t) &= \bar{h}, \end{aligned}$$

exist. We get:

$$\begin{aligned} 0 &= \frac{1}{2} \frac{\partial^2}{\partial s^2} (s^2 f(t, s)) - \frac{\partial}{\partial s} (\lambda (\bar{m} - s) f(t, s)), \\ 0 &= \frac{1}{2} \frac{\partial^2}{\partial s^2} (s^2 f(t, s)) - \frac{\partial}{\partial s} (\lambda \bar{h} f(t, s)). \end{aligned}$$

The steady state distributions are given by:

$$f_\infty(s) = c_1 + \frac{c_2}{s^{2+2\lambda}} \exp\left\{-\frac{2\lambda \bar{m}}{s}\right\}, \quad (19)$$

$$f_\infty(s) = c_1 + \frac{c_2}{s^2} \exp\left\{-\frac{2\lambda \bar{h}}{s}\right\}, \quad (20)$$

Here, we have implicitly assumed that the solution of the corresponding Fokker-Planck models (17) (18) converge to the steady state distributions. This is in general not clear but can be proven for special Fokker-Planck models. We refer to several studies of Toscani [12, 234, 107]. Interestingly, the steady states distributions (19) (20) are special cases of the *inverse Gamma distribution*. We want to define the inverse Gamma distribution or Amoroso distribution:

Definition 3.1.5. *We define the inverse Gamma distribution (or Amoroso distribution) with shape parameter a and scale parameter b to be:*

$$f(x) := \begin{cases} \frac{b^a}{\Gamma(a)} \frac{1}{x^{a+1}} \exp\left\{-\frac{b}{x}\right\}, & x \geq 0, \\ 0, & x < 0, \end{cases}$$

where Γ denotes the gamma function.

We want to point out that this distribution asymptotically satisfies a power-law.

$$f(x) \sim \frac{1}{x^{a+1}}.$$

For this reason, the inverse Gamma distribution plays a prominent role in kinetic financial market models. This distribution has been discovered as wealth or stock price distribution [166, 67, 66, 198]. Furthermore, this distribution has been obtained as steady state distribution of kinetic opinion formation models [198].

3.2 Kinetic Theory

This introduction to kinetic theory is partially based on the lecture *Transport Theory* given by Martin Frank at RWTH university between 2009-2017 and the same-titled lecture notes.

Kinetic theory describes gases as a large system of interacting atoms. This theory dates back to the early works of Daniel Bernoulli 1738, James Maxwell 1859 and Ludwig Boltzmann 1871. Starting on the microscopic level with Newton's equation of motion, kinetic theory aims to describe macroscopic quantities such as velocity, pressure and temperature. Kinetic models are usually formulated on the mesoscopic level. This means, instead of considering the position $x \in \mathbb{R}^3$ and velocity $v \in \mathbb{R}^3$ of one molecule, one zooms out and rather describes the moving atoms by their statistical probability. Thus, the seven dimensional density function $f = f(t, x, v)$ describes the probability to find a particle at time $t \geq 0$ at position x with velocity v . On the microscopic level, Newton's equations of motion determine the evolution of particles. The i th particle $i = 1, \dots, N$ with mass m_i moving in a force field F satisfies the ODEs

$$\begin{cases} \dot{x}_i(t) = v_i(t), \\ \dot{v}_i(t) = \frac{1}{m_i} F_i(t, \mathbf{x}(t), \mathbf{v}(t)), \end{cases} \quad (21)$$

where $t \in [0, \infty)$ with space variable $\mathbf{x} := (x_1, \dots, x_N)^T \in \mathbb{R}^{3N}$ and velocities $\mathbf{v} = (v_1, \dots, v_N(t)) \in \mathbb{R}^{3N}$. In order to obtain a mesoscopic description, one considers the limit of infinitely particles. In the most simple setting of no particle interactions and identical particles, we derive the kinetic equation in one dimension. In this case, the force field F only depends on the velocity and position of the i -th molecule. We obtain N identical ODEs and assume that $(x^*(t), v^*(t))$ is the unique solution. We then define the *empirical measure* as a point mass at the position of our particle.

$$f(t, x, v) := \delta(x - x^*(t)) \delta(v - v^*(t)).$$

Since f can be only understood in the distributional sense, we consider

$$\langle \phi, f \rangle := \int \int \phi(x, v) f(t, x, v) dx dv. \quad (22)$$

for an arbitrary test function $\phi(x, v)$. For arbitrary density functions, the quantity (22) is called observable quantity. Then, we compute the time evolution of our observable (22).

$$\begin{aligned} \frac{d}{dt} \langle \phi, f \rangle &= \frac{d}{dt} \phi(x^*(t), v^*(t)) \\ &= \partial_x \phi(x^*(t), v^*(t)) \frac{d}{dt} x^*(t) + \partial_v \phi(x^*(t), v^*(t)) \frac{d}{dt} v^*(t) \\ &= \partial_x \phi(x^*(t), v^*(t)) v^*(t) + \partial_v \phi(x^*(t), v^*(t)) \frac{1}{m} F(t, x^*(t), v^*(t)) \\ &= \int \int \left(v \partial_x \phi(x, v) + \frac{1}{m} F(t, x, v) \partial_v \phi(x, v) \right) f(t, x, v) dx dv \\ &= - \left\langle \phi(x, v), v \partial_x (f(t, x, v)) + \partial_v \left(\frac{1}{m} F(t, x, v) f(t, x, v) \right) \right\rangle \end{aligned}$$

Thus, we have derived the weak form of the PDE

$$\partial_t f(t, x, v) + v \cdot \partial_x f(t, x, v) + \partial_v \left(\frac{1}{m} F(t, x, v) f(t, x, v) \right) = 0$$

In the case of a divergence free force field F , the previous PDE coincides with the *Liouville equation*. The Liouville equation describes the time evolution of a classical Hamiltonian system. If we add microscopic interactions to the microscopic model, the Liouville equation is no longer valid. In the case of binary interactions, one needs to add a collision operator to the Liouville equation. The Boltzmann equation, originally formulated by Boltzmann [28], describes the evolution of rarefied gases.

$$\partial_t f(t, x, v) + v \cdot \nabla_x f(t, x, v) = Q(f, f), \quad (23)$$

where the advection models the free transportation of particles and the integral operator $Q(f, f)$ the particle interactions. The collision operator

$$Q(f, f) := \int_{S^2} \int_{\mathbb{R}^3} K((v - w) \cdot n) [f(v') f(w') - f(v) f(w)] dw dn,$$

where S^2 denotes the unit sphere and $K > 0$ is the interaction kernel ensures the relaxation towards the local Maxwellian equilibrium [48, 198]. The interaction kernel K does not depend on the velocity in the case of Maxwellian molecules, which leads to a huge simplification. The unique equilibrium distribution, often called Maxwellian is given by:

$$M(x, v, t) := \rho(t, x) \frac{1}{(2 \pi T(t, x))^{\frac{3}{2}}} \exp \left\{ -\frac{|v - U(t, x)|^2}{2 T(t, x)} \right\}$$

where the Maxwellian itself depends on the macroscopic quantities mass $\rho(t, x)$, velocity $U(t, x)$ and temperature $T(t, x)$

$$\rho := \int f dv, \quad U := \frac{1}{\rho} \int v f dv, \quad T := \frac{1}{3 \rho} \int (v - U)^2 f dv.$$

One further characteristic of the Boltzmann equation can be found in the conserved quantities. A conserved quantity is defined by

$$\frac{d}{dt} q(t) = 0,$$

where $q(t) := \int \int \phi(v) f(t, x, v) dx dv$ is a special observable quantity since the ϕ only depends on velocity v . In case of the Boltzmann equation, a conserved quantity needs to satisfy

$$\int \int \phi(v) Q(f, f) dx dv = 0.$$

Examples are mass ρ , momentum m and kinetic energy E , where momentum and energy are defined as

$$\begin{aligned} m_i(t) &:= \int \int v_i f(t, x, v) dx dv, \quad i = \{1, 2, 3\} \\ E(t) &:= \frac{1}{2} \int \int \|v\|^2 f(t, x, v) dx dv. \end{aligned}$$

A closely related concept of conserved quantities can be found in the collision invariants. A collision invariant $\phi(v)$ of the Boltzmann equation has to satisfy

$$\int \phi(v) Q(f, f) dv = 0.$$

Thus, all collision invariants define a corresponding conserved quantity. Furthermore, one can show that all collision invariants of the Boltzmann equation are given by

$$\phi(v) \in \text{span}\{1, v_1, v_2, v_3, \|v\|^2\}.$$

In addition, the integro-differential equation (23) satisfies the remarkable property of decreasing entropy. The result is known as H theorem and was the first analytical proof of the second principle of thermodynamics [48, 198]. The entropy is defined as

$$H(t) := \int \int f(t, x, v) \log(f(t, x, v)) dx dv.$$

Then, the H theorem states that

$$\frac{d}{dt} H(t) \leq 0,$$

holds and $\frac{d}{dt} H(t) = 0$ if and only if f is a Maxwellian. Mathematically, the entropy is a Lyapunov functional of the Boltzmann equation.

The second kinetic model we want to present is the linear Boltzmann equation, often called transport equation. It can be regarded as a simplification of the highly-nonlinear Boltzmann equation and models the interaction of a particle with a random background. The model reads

$$\partial_t f(t, x, v) + v \cdot \nabla_x f(t, x, v) = L(f),$$

where the interaction operator is given by

$$L(f) := \int k(v, v') (f(v') - f(v)) dv',$$

with interaction kernel $k > 0$. One special choice of the linear operator L would be $L_M(f) := Q(M, f)$. The concept of collision invariants and conserved quantities translates one to one to the linear Boltzmann equation. In addition, the linear Boltzmann equation satisfies the H theorem as well.

The last kinetic model we want to present is the Vlasov equation introduced in 1930. The Vlasov equation models a system of point particles with mass m and charge q , ϵ_0 is the dielectric permittivity of vacuum in plasma. The model is given by

$$\begin{aligned} \frac{\partial f}{\partial t} + v \cdot \nabla_x f + \frac{1}{m} F[f](t, x) \cdot \nabla_v f &= 0, \\ F[f](t, x) &= - \int f(y, v, t) K(x, y) dv dy, \\ K(x, y) &:= \frac{q^2}{4\pi \epsilon_0} \frac{x - y}{|x - y|^3}. \end{aligned}$$

In comparison to the Boltzmann equation which models binary collisions, the Vlasov equation considers interacting particles through a field. Looking again at our Newton equations (21), this corresponds to the choice:

$$F_i(t, \mathbf{x}, \mathbf{y}) := \frac{1}{N} \sum_{k=1, k \neq i}^N K(x_i, y_k).$$

Before we summarize the most important kinetic limits starting from microscopic particle dynamics, we give a short overview of the different levels of modeling.

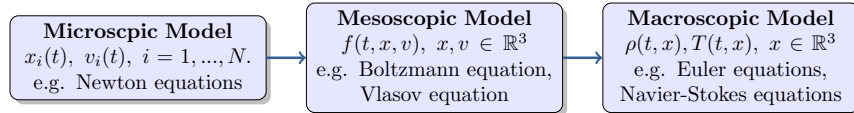


Figure 36: Schematic picture of different modeling levels.

The different limits of microscopic dynamics have their origin in the different particle interactions in microscopic systems, e.g. the different interactions in rarefied gas and plasma. The classifications of these limits are usually given in terms of a reference space-time scale. Following Spohn [224] we list the different *pure* limit cases.

- i) *Hydrodynamic Limit*: e.g. Euler equations, Navier-Stokes equations,
- ii) *Low Density Limit (Boltzmann-Grad Limit)* : e.g. Boltzmann equation,
- iii) *Weak Coupling Limit*: e.g. Landau equation
- iv) *Mean Field Limit*: e.g. Vlasov equation.

For all these differential equations mentioned above it took many years for scientists to give a rigorous derivation from particle systems. The Boltzmann equation, for example, established in 1872 by Ludwig Boltzmann, was rigorously derived by Lanford in 1975 [146] at least for short times. Furthermore, Spohn [224] emphasizes that a rigorous derivation of particle dynamics to the time evolution on a mesoscopic scale was first investigated in the *mean field limit* case by Kac in 1953 [131]. Even today, there are many open questions. A very active research topic is to obtain connections between each of those four limiting equations. One example is the possibility of passing from the Boltzmann equation in the *grazing limit* to the Landau equation [6]. A further example are the *hydrodynamic limits* of the Boltzmann equation [208] where one can derive the Euler and Navier-Stokes equation out of the Boltzmann equation. A not comprehensive overview of kinetic equations and limits is given in figure 37.

All kinetic equations need to be considered as models because they are still an approximation of the large microscopic particle systems. By large particles systems, we refer to particle numbers between $10^{10} \sim 10^{60}$ which is the case in classical applications such as gases or plasmas. The necessity of considering kinetic models in order to describe and study such large interacting particle systems is obvious: the computational effort to solve the microscopic ODE systems is inexpressibly large and beyond the scope of any supercomputer.

The popularity of kinetic theory in current research can be explained by the rich variety of important applications. In essence, kinetic theory can help to study any large system of interacting particles or agents as long the microscopic dynamics can be well described by differential equations. Besides the classical applications of kinetic modeling in physical and engineering, there are many new fields in social and natural sciences. Popular examples are radiotherapy [104], traffic [120], opinion formation [237], bacteria [138], flocking phenomena [47], cell behavior [53] and economic applications [198]. In the next section, we want to give an overview of the application of kinetic theory for economic models.

3.2.1 Applications to Financial Market Models

The models of Bouchaud and Mézard [34], Slanina [218], Dragulescu and Jokavenko [86] and a model of Chatterjee et al. [55] are probably the first kinetic models dealing with financial applications.

The model by Bouchaud and Mézard considers microscopic wealth interactions of mean field type. The authors can derive the corresponding Fokker-Planck equation and compute steady state wealth distributions of inverse Gamma type.

The model by Slanina considers binary wealth interactions of agents and the authors derive Boltzmann-like equations. Furthermore, they can compute self-similar solutions of inverse gamma type.

The model by Dragulescu and Jokavenko and as well the model by Chatterjee et al. also consider pairwise wealth interactions of financial agents. They show that the interactions of agents lead to a steady wealth profile which is given in both cases by the Boltzmann-Gibbs distribution.

The authors of the previous cited papers are all physicists. The first mathematicians who started to work on kinetic models with economic applications are Lorenzo Pareschi and Giuseppe Toscani. They both worked in a large research project dealing with the conjecture by Ernst and Brito [96, 97, 198] to obtain self-similar solutions with fat-tails in space homogeneous models with inelastic scattering [198]. Then, by pure coincidence, Pareschi and Toscani have discovered the work of Slanina and were attracted by the similarities between statistical physics and economic theory [198]. Their motivation was to put the results from Slanina and as well the conjecture from Ernst and Brito on a solid mathematical foundation [198]. The first publication of Pareschi and Toscani on this subject was in 2005, a kinetic model of wealth interactions [67]. Already one year later, Pareschi and Toscani have investigated the creation of power-laws in the steady state distributions in a general space homogeneous Boltzmann model [197]. The model can be written as

$$\partial_t f(t, v) = Q^+(f, f)(t, v) - f(t, v)$$

with the gain operator

$$Q^+(f, f)(t, v) = \frac{1}{2} \int_{\mathbb{R}} \int_{\mathbb{R}} f(t, w_1) f(t, w_2) (\delta(v - w'_1) + \delta(v - w'_2)) dw_1 dw_2,$$

where δ denotes the dirac delta. The microscopic interactions from (v, w) to (v', w') are defined as

$$\begin{aligned} w'_1 &= p w_1 + q w_2, & p > q > 0, \\ w'_2 &= q w_1 + p w_2. \end{aligned}$$

This work [197] has provided a rigorous mathematical explanation for the creation of fat-tails in steady state profiles. Based on this work by Pareschi and Toscani, there have been many new contributions to this new field of kinetic research. Examples are [88, 25, 89, 176, 198, 18, 175, 236, 90]. The second type of model which has been extensively used in the context of financial market models is a homogeneous linear Boltzmann model of the following type.

$$\partial_t f(t, v) = L^+(f)(t, v) - \sigma f(t, v),$$

with $\sigma > 0$ and the linear gain operator

$$L^+(f)(t, v) := g * f(t, v)$$

where g is the probability distribution function of the background and $*$ denotes the usual convolution operator. Examples of kinetic models with this kind of linear Boltzmann-like equation are [166, 235, 199, 66]. We want to highlight the models [66, 166], which are inspired by econophysical financial market models and do not simply consider binary trades between agents. This is the root we want to follow in this work. Thus, we will consider microscopic models, identical or very close to their original econophysical counterpart and translate them into kinetic models.

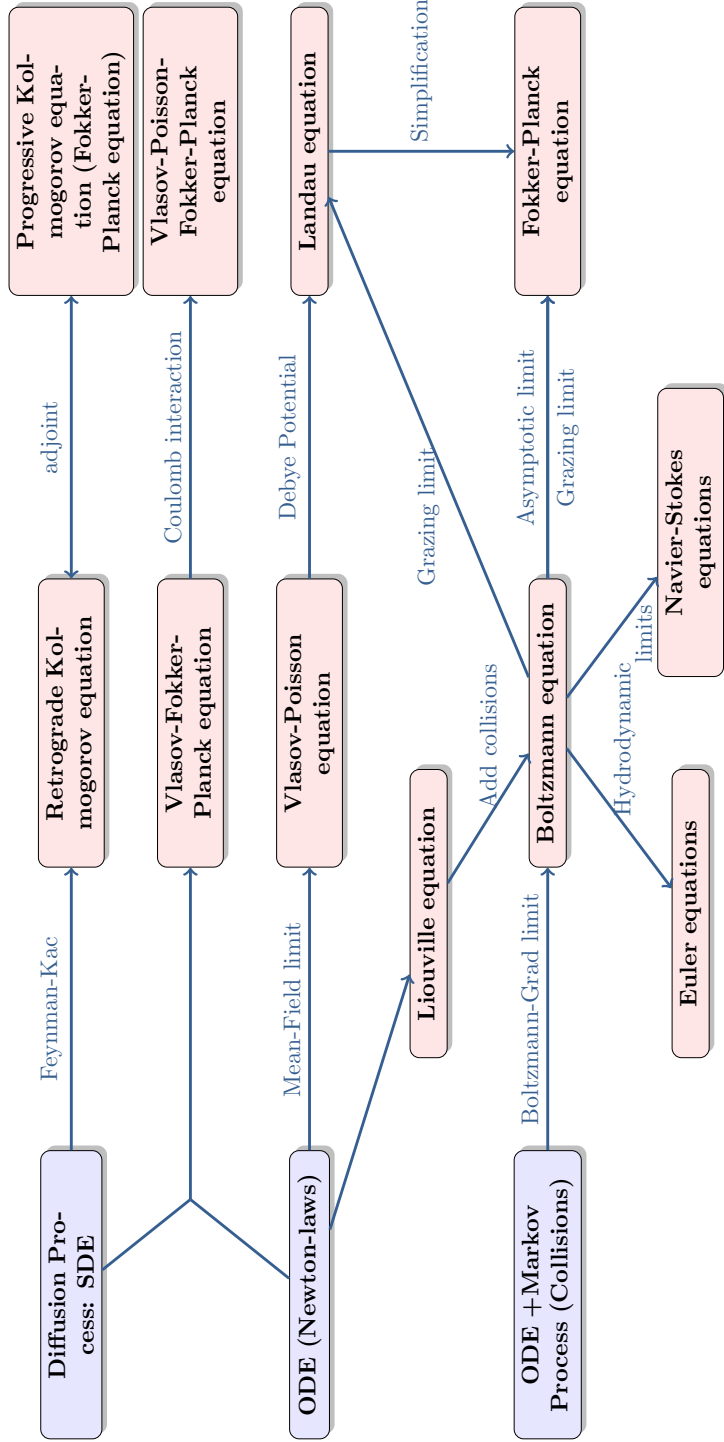


Figure 37: Chart of several kinetic equations and limits.

3.3 Mean Field Limit

Mean field theory dates back to early work of Pierre Curie [74] and Pierre Weiss [252] on phase transition at the beginning of the last century. Possibly the first mean field model, the Ising model, which describes the magnetization of ferromagnets, was formulated by Ernst Ising in 1925 [126]. Another very prominent mean field model is the Vlasov equation. The Vlasov equation, first investigated by Vlasov in 1938 [245], models the time evolution of particles in plasma.

It is mathematically interesting to notice that the mean field limit, i.e. the limit of the microscopic particle system to the mesoscopic evolution equation, can be proven rigorously. This could be first proven by Kac in 1953 [131]. Further classical results of mean field limits are [85, 35, 192, 224]. More recent reviews of known results are [111, 112, 128]. Recently, mean field theory has shifted in the focus of attention of many researchers again thanks to the new applications in social science and biology. Popular fields of applications are herding phenomena [46], animal aggregations [39], opinion formation [4] and economics [218].

In this section, we rigorously derive the mean field equation of an econophysical financial market model. We apply the Dobrushin method [85] for our derivation. The proofs are inspired by the review of Golse [112].

3.3.1 Microscopic Economic Model

This economic microscopic model is based on the econophysical Levy-Levy-Solomon (LLS) model first introduced in [155]. The authors Pareschi et al. [66] introduced a kinetic market model closely related to the LLS model. In this section, we want to derive a rigorous mean field approach for a toy model which is a simplified version of the LLS model. Our model considers $N \in \mathbb{N}$ financial agents who can invest $\gamma_i \in (0, 1)$, $i = 1, \dots, N$ of their wealth $w_i \in \mathbb{R}_{>0}$ in a stock S and have to invest $1 - \gamma_i$ of their wealth in a safe bond with interest rate $r \in (0, 1)$. The investment propensities γ_i are constants and the wealth dynamic of each agent at time $t \in [0, \infty)$ is given by

$$\dot{w}_i(t) = (1 - \gamma_i) r w_i(t) + \gamma_i w_i(t) \frac{\dot{S}(t) + d(t)}{S(t)}, \quad w_i(0) = w_i^0, \quad i = 1, \dots, N.$$

We assume that the dividend $d : \mathbb{R} \rightarrow \mathbb{R}_{\geq 0}$ is continuously differentiable and the derivative $|\dot{d}| \leq B$, $B > 0$ is bounded. Furthermore, we assume that the dividend is not random. The stock price is given by the *market clearance condition*

$$S(t) = \frac{1}{N} \sum_{k=1}^N \gamma_k w_k(t).$$

Remark 3.3.1. Compared to the classical theory of statistical physics where the interaction potential $V(\cdot, \cdot)$ depends on the position of two particles, our potential, the market clearance condition depends on the investment propensity and wealth of every agent.

From the perspective of mean field theory this model is a first-order model, called an aggregation equation, with the additional constraints of investment proportions and stock price.

$$\begin{cases} \dot{w}_i(t) = (1 - \gamma_i) r w_i(t) + \gamma_i w_i(t) \frac{\dot{S}(t) + d(t)}{S(t)}, \\ w_i(0) = w_i^0, \\ S(t) = \frac{1}{N} \sum_{k=1}^N \gamma_k w_k(t), \quad i = 1, \dots, N. \end{cases}$$

So far we have no explicit ODE system because the right hand side of our differential equation depends on the differential of the stock price.

ODE System We want to derive the matrix form of our system. The stock price $S(t)$, $t \in [0, \infty)$ is:

$$S(t) = \frac{1}{N} \sum_{k=1}^N \gamma_k w_k(t) = \frac{1}{N} \boldsymbol{\gamma}^T \mathbf{w}(t), \quad \mathbf{w}(t) \in \mathbb{R}_{>0}^{N \times 1}, \quad \boldsymbol{\gamma} = (\gamma_1, \dots, \gamma_N)^T \in (0, 1)^N.$$

The wealth dynamics can be rewritten in matrix form as:

$$\dot{\mathbf{w}}(t) = \text{diag}((\mathbf{e} - \boldsymbol{\gamma}) r) \mathbf{w}(t) + \text{diag}(\boldsymbol{\gamma}) \mathbf{w}(t) \frac{\boldsymbol{\gamma}^T \dot{\mathbf{w}}(t) + d(t)}{\boldsymbol{\gamma}^T \mathbf{w}(t)} N,$$

where $\mathbf{e} := (1, \dots, 1)^T \in \mathbb{R}^N$. This is equivalent to:

$$\underbrace{\left(\mathbf{I} - \text{diag}(\boldsymbol{\gamma}) \frac{\mathbf{w}(t) \boldsymbol{\gamma}^T}{\boldsymbol{\gamma}^T \mathbf{w}(t)} \right)}_{=: \boldsymbol{\Sigma}(\mathbf{w}(t))} \dot{\mathbf{w}}(t) = \text{diag}((\mathbf{e} - \boldsymbol{\gamma}) r) \mathbf{w}(t) + \frac{N}{\boldsymbol{\gamma}^T \mathbf{w}(t)} \text{diag}(d(t) \boldsymbol{\gamma}) \mathbf{w}(t),$$

where $\mathbf{I} \in \mathbb{R}^{N \times N}$ is the identity matrix. Thus, the question if we have an explicit ODE system reduces to the questions if the matrix $\boldsymbol{\Sigma}(\mathbf{w}(t))$ is invertible.

Matrix inversion The matrix can be written as:

$$\boldsymbol{\Sigma}(\mathbf{w}(t)) = \begin{pmatrix} 1 - \frac{\gamma_1^2 w_1}{\boldsymbol{\gamma}^T \mathbf{w}(t)} & -\frac{\gamma_2 \gamma_1 w_1}{\boldsymbol{\gamma}^T \mathbf{w}(t)} & \cdots & -\frac{\gamma_n \gamma_1 w_1}{\boldsymbol{\gamma}^T \mathbf{w}(t)} \\ -\frac{\gamma_1 \gamma_2 w_2}{\boldsymbol{\gamma}^T \mathbf{w}(t)} & \ddots & & \vdots \\ \vdots & & \ddots & -\frac{\gamma_n \gamma_{n-1} w_{n-1}}{\boldsymbol{\gamma}^T \mathbf{w}(t)} \\ -\frac{\gamma_1 \gamma_n w_n}{\boldsymbol{\gamma}^T \mathbf{w}(t)} & -\frac{\gamma_2 \gamma_n w_n}{\boldsymbol{\gamma}^T \mathbf{w}(t)} & \cdots & 1 - \frac{\gamma_n^2 w_n}{\boldsymbol{\gamma}^T \mathbf{w}(t)} \end{pmatrix}$$

We compute the inverse of the matrix $\boldsymbol{\Sigma}(\mathbf{w}(t))$ and use the method presented in [185]. We can write the matrix as:

$$\boldsymbol{\Sigma}(\mathbf{w}(t)) = \mathbf{I} - \mathbf{P}(\mathbf{w}(t)),$$

where $\mathbf{P}(\mathbf{w}(t))$ is given by:

$$\mathbf{P}(\mathbf{w}(t)) := \begin{pmatrix} \frac{\gamma_1 w_1(t)}{\boldsymbol{\gamma}^T \mathbf{w}(t)} \\ \vdots \\ \frac{\gamma_n w_n(t)}{\boldsymbol{\gamma}^T \mathbf{w}(t)} \end{pmatrix} \quad (\gamma_1 \quad \gamma_2 \quad \cdots \quad \gamma_n).$$

The $\|\cdot\|_1$ of the matrix $\mathbf{P}(\mathbf{w}(t))$ is given by:

$$\|\mathbf{P}(\mathbf{w}(t))\|_1 = \max_{j=1,\dots,N} \sum_{i=1}^N |p_{ij}| = \max\{\gamma_1, \dots, \gamma_n\} < 1, \quad \gamma_i \in (0, 1).$$

Hence, the matrix $\Sigma^{-1}(\mathbf{w}(t))$ exists and has a Neumann series expansion.

$$\Sigma^{-1}(\mathbf{w}(t)) = (\mathbf{I} - \mathbf{P}(\mathbf{w}(t)))^{-1} = \sum_{k=0}^{\infty} \mathbf{P}^k(\mathbf{w}(t)).$$

Furthermore, the matrix $\mathbf{P}(\mathbf{w}(t))$ has rank one and for all positive integers n we can write

$$\mathbf{P}^n(\mathbf{w}(t)) = \alpha^{n-1} \mathbf{P}(\mathbf{w}(t)), \quad \alpha := \text{trace}(\mathbf{P}(\mathbf{w}(t))) = \frac{1}{\gamma^T \mathbf{w}(t)} \sum_{i=1}^N \gamma_i^2 w_i(t).$$

Thus, we can rewrite the series as:

$$\Sigma^{-1}(\mathbf{w}(t)) = \mathbf{I} + \sum_{k=0}^{\infty} \alpha^k \mathbf{P}(\mathbf{w}(t)).$$

We then use that $|\alpha| < 1$ and simply sum the series.

$$\Sigma^{-1}(\mathbf{w}(t)) = \mathbf{I} + \frac{1}{1-\alpha} \mathbf{P}(\mathbf{w}(t)).$$

Explicit ODE system Thus, our explicit ODE system reads

$$\begin{cases} \dot{\mathbf{w}}(t) = \Sigma^{-1}(\mathbf{w}(t)) \text{ diag}((\mathbf{e} - \boldsymbol{\gamma}) r) \mathbf{w}(t) + \frac{N}{\boldsymbol{\gamma}^T \mathbf{w}(t)} \Sigma^{-1}(\mathbf{w}(t)) \text{ diag}(d(t) \boldsymbol{\gamma}) \mathbf{w}(t), \\ \mathbf{w}(0) = \mathbf{w}^0, \end{cases}$$

where $\boldsymbol{\gamma} = (\gamma_1, \dots, \gamma_N)^T \in (0, 1)^N$ and $\mathbf{w}(t) \in \mathbb{R}_{>0}^N$. The differential equation is equivalent to

$$\begin{aligned} \dot{\mathbf{w}}(t) &= r \cdot \left(\mathbf{I} + \frac{1}{1-\alpha} \mathbf{P}(\mathbf{w}(t)) \right) \cdot ((1 - \gamma_1)w_1(t), \dots, (1 - \gamma_N)w_N(t))^T \\ &\quad + \frac{d(t) N}{\boldsymbol{\gamma}^T \mathbf{w}(t)} \left(\mathbf{I} + \frac{1}{1-\alpha} \mathbf{P}(\mathbf{w}(t)) \right) \cdot (\gamma_1 w_1(t), \dots, \gamma_N w_N(t))^T, \end{aligned}$$

and can be simplified to

$$\begin{aligned} \dot{\mathbf{w}}(t) &= r \cdot \left(((1 - \gamma_1)w_1(t), \dots, (1 - \gamma_N)w_N(t))^T + \frac{\sum_{j=1}^N (1 - \gamma_j) \gamma_j w_j(t)}{(1 - \alpha) \boldsymbol{\gamma}^T \mathbf{w}(t)} (\gamma_1 w_1(t), \dots, \gamma_N w_N(t))^T \right) \\ &\quad + \frac{d(t) N}{\boldsymbol{\gamma}^T \mathbf{w}(t)} \left((\gamma_1 w_1(t), \dots, \gamma_N w_N(t))^T + \frac{\sum_{j=1}^N \gamma_j^2 w_j(t)}{(1 - \alpha) \boldsymbol{\gamma}^T \mathbf{w}(t)} (\gamma_1 w_1(t), \dots, \gamma_N w_N(t))^T \right). \end{aligned}$$

Then, we obtain for the i th component of this system:

$$\begin{aligned}\dot{w}_i &= r((1 - \gamma_i)w_i(t) + \gamma_i w_i(t)) \\ &\quad + \gamma_i w_i(t) \frac{d(t)}{\gamma^T \mathbf{w}(t)} N \left(1 + \frac{\sum_{j=1}^N \gamma_j^2 w_j(t)}{\sum_{j=1}^N (1 - \gamma_j) \gamma_j w_j(t)} \right).\end{aligned}$$

Thus, we get for each agent $i = 1, \dots, N$,

$$\dot{w}_i(t) = rw_i(t) + \frac{\gamma_i w_i(t) d(t)}{\frac{1}{N} \sum_{j=1}^N (1 - \gamma_j) \gamma_j w_j(t)}, \quad w_i(0) = w_i^0,$$

where $\gamma_i \in (0, 1)$, $w_i \in \mathbb{R}_{>0}$.

Existence and uniqueness Clearly, the potential singularity in the second term of the right-hand side might cause difficulties. We thus want to ensure that

$$\frac{1}{N} \sum_{j=1}^N (1 - \gamma_j) \gamma_j w_j(t) > 0, \quad \forall t \in [0, \infty),$$

holds to obtain existence and uniqueness on $t \in [0, \infty)$. We define for an arbitrary but fixed number of agents $N \in \mathbb{N}$ the function

$$F : \mathbb{R}_{>0}^N \times [0, \infty) \rightarrow \mathbb{R}^N, \quad (w_1, \dots, w_N, t)^T \mapsto \begin{pmatrix} rw_1 + \frac{\gamma_1 w_1 d(t)}{\frac{1}{N} \sum_{j=1}^N (1 - \gamma_j) \gamma_j w_j} \\ \vdots \\ rw_N + \frac{\gamma_N w_N d(t)}{\frac{1}{N} \sum_{j=1}^N (1 - \gamma_j) \gamma_j w_j} \end{pmatrix}.$$

The function $F(\mathbf{w}, t)$ is continuously differentiable for all $\mathbf{w} = (w_1, \dots, w_N)^T$. Thus, the function $F(\mathbf{w}, t)$ is locally Lipschitz. We have for $i, j = 1, \dots, N$:

$$DF_{i,j} = -\frac{\gamma_i w_i d(t) \frac{1}{N} \gamma_j (1 - \gamma_j)}{\left(\frac{1}{N} \sum_{k=1}^N (1 - \gamma_k) \gamma_k w_k \right)^2} + \delta_{ij} \left(r + \frac{\gamma_j d(t)}{\frac{1}{N} \sum_{k=1}^N (1 - \gamma_k) \gamma_k w_k} \right)$$

We define a weighted $\|\cdot\|_{1w}$ norm:

$$\|\mathbf{x}\|_{1w} := \frac{1}{N} \sum_{i=1}^N \gamma_i (1 - \gamma_i) |x_i|, \quad \mathbf{x} \in \mathbb{R}^{N \times 1}.$$

Thus, we can rewrite the Matrix $\mathbf{D}\mathbf{F}$:

$$DF_{i,j} = -\frac{\gamma_i w_i d(t) \frac{1}{N} \gamma_j (1 - \gamma_j)}{\|\mathbf{w}\|_{1w}^2} + \delta_{ij} \left(r + \frac{\gamma_j d(t)}{\|\mathbf{w}\|_{1w}} \right).$$

We get:

$$\|\mathbf{DF}\|_1 = \max_{\|\mathbf{x}\|_{1w}=1} \|\mathbf{DF} \mathbf{x}\|_{1w} = \max_{j=1,\dots,N} \frac{1}{N} \sum_{i=1}^N \gamma_i (1 - \gamma_i) |DF_{i,j}|.$$

Then, we can immediately deduce the inequality

$$\|\mathbf{DF}\|_1 \leq d(t) \left(\frac{\|\mathbf{w}\|_{1w}}{\|\mathbf{w}\|_{1w}^2} + \frac{1}{\|\mathbf{w}\|_{1w}} \right) + r,$$

and obtain as Lipschitz constant:

$$L := \left(r + \max_{t \in [0, t_1]} d(t) \cdot \max_{w \in (a, a+\epsilon)^N} \frac{2}{\|\mathbf{w}\|_{1w}} \right).$$

We have for $\mathbf{w}, \tilde{\mathbf{w}} \in (a, a+\epsilon)^N \subset \mathbb{R}_{>0}^N, \epsilon > 0, t \in [0, t_1] \subset [0, \infty)$:

$$\|F(\mathbf{w}, t) - F(\tilde{\mathbf{w}}, t)\| \leq L \|\mathbf{w} - \tilde{\mathbf{w}}\|.$$

Obviously, the Lipschitz constant L blows up if we run in the singularity and we thus cannot state a global Lipschitz constant. Furthermore, L is decreasing with respect to a for fixed $\epsilon > 0$, which is the lower interval boundary of our wealth variable. The initial conditions of our ODE system are positive $w_i^0 > 0$ and by assumption $\gamma_i \in (0, 1)$. Hence, the Picard-Lindelöf theorem gives us existence and uniqueness on an interval $[0, t_1]$, $t_1 \in (0, \infty)$. Especially

$$\frac{1}{N} \sum_{j=1}^N (1 - \gamma_j) \gamma_j w_j(t) \geq \underbrace{\frac{1}{N} \sum_{j=1}^N (1 - \gamma_j) \gamma_j w_j(0)}_{=: \Gamma_N} > 0, \quad \forall t \in [0, t_1].$$

holds. Therefore, we can apply the Picard-Lindelöf theorem iteratively on the intervals $[t_k, t_{k+1}], k \geq 1$. The Lipschitz constant is not increasing for each interval (growth of dividend is bounded). Hence, we get inductively existence and uniqueness on $[0, \infty)$.

Growth result We want to give a growth result of our ODE system and apply the differential form of the Gronwall inequality. For $i = 1, \dots, N$

$$\dot{w}_i(t) \leq w_i(t) \left(r + \frac{d(t)}{\Gamma_N} \right), \quad \forall t \in [0, \infty),$$

holds and thus

$$w_i(t) \leq w_i(0) \exp \left\{ \int_0^t r + \frac{d(x)}{\Gamma_N} dx \right\}, \quad \forall t \in [0, \infty).$$

The limit of infinitely many agents As we have shown in the previous section, the inequality

$$\frac{1}{N} \sum_{j=1}^N (1 - \gamma_j) \gamma_j w_j(t) \geq \Gamma_N, \quad \forall t \in [0, \infty)$$

holds. In the limit, we assume

$$\lim_{N \rightarrow \infty} \Gamma_N = \Gamma > 0.$$

This assumption is closely related to the well known *Boltzmann-Grad* limit. Economically, we assume that the average amount of investments in stocks is finite.

Distance estimate We can apply the Gronwall inequality and observe for two solutions $w(t), \bar{w}(t)$ at time $t \in [0, \infty)$ the distance estimate:

$$|w_i(t) - \bar{w}_i(t)| \leq |w_i(0) - \bar{w}_i(0)| \exp \left\{ t r + \frac{1}{\Gamma_N} \int_0^t d(s) ds \right\}.$$

This estimate depends on the number of agents. In the mean field limit, we are interested in the limit of infinite agents and thus consider $N \rightarrow \infty$. We obtain:

$$|w_i(t) - \bar{w}_i(t)| \leq |w_i(0) - \bar{w}_i(0)| \exp \left\{ t r + \frac{1}{\Gamma} \int_0^t d(s) ds \right\}.$$

This estimate does not depend on N , the number of agents. Furthermore, this distance estimate is essential to observe rigorous convergence results in the mean field limit.

3.3.2 Mean Field Limit of Microscopic Economic Model

Before we can derive the mean field limit, we need to define the empirical measure.

Definition 3.3.1. Given a vector $\mathbf{x} := (x_1, \dots, x_N)^T \in \mathbb{R}^{dN}$, $x_i := (x_i^1, \dots, x_i^d) \in \mathbb{R}^d$, $i = 1, \dots, N$ then the empirical measure (or atomic probability measure) $\mu_{\mathbf{x}}^N$ is defined as

$$\mu_{\mathbf{x}}^N(x^1, \dots, x^d) = \frac{1}{N} \sum_{i=1}^N \delta(x^1 - x_i^1) \cdot \dots \cdot \delta(x^d - x_i^d).$$

By $\mathcal{P}(\mathbb{R}_{>0} \times (0, 1))$, we denote the space of probability measures on $\mathbb{R}_{>0} \times (0, 1)$. Then, the empirical measure associated to the solutions $X_N := (w_1(t), \gamma_1, w_2(t), \gamma_2, \dots, w_N(t), \gamma_N)$, $t \in [0, \infty)$ is

$$\mu_{X_N}^N : [0, \infty) \rightarrow \mathcal{P}(\mathbb{R}_{>0} \times (0, 1)),$$

given by:

$$\mu_{X_N}^N(t) := \mu_{X_N}^N(t, w, \gamma) = \frac{1}{N} \sum_{k=1}^N \delta(w - w_k(t)) \delta(\gamma - \gamma_k).$$

We use the explicit ODE to derive the mean field limit. We consider a test function $\phi \in$

$C_c^1(\mathbb{R}_{>0} \times (0, 1))$ and we compute

$$\begin{aligned}
\frac{d}{dt} \langle \mu_{X_N}^N(t), \phi(w, \gamma) \rangle &= \frac{1}{N} \sum_{k=1}^N \frac{d}{dt} \phi(w_k(t), \gamma_k) \\
&= \frac{1}{N} \sum_{k=1}^N \frac{\partial}{\partial w} \phi(w_k(t), \gamma_k) \cdot \dot{w}_k(t) \\
&= \frac{1}{N} \sum_{k=1}^N \frac{\partial}{\partial w} \phi(w_k(t), \gamma_k) \cdot \left(r w_k(t) \right. \\
&\quad \left. + \frac{\gamma_k w_k(t) d(t)}{\frac{1}{N} \sum_{j=1}^N (1 - \gamma_j) \gamma_j w_j(t)} \right) \\
&= \left\langle \mu_{X_N}^N(t), \frac{\partial}{\partial w} \phi(w, \gamma) \cdot r w \right\rangle \\
&\quad + \left\langle \mu_{X_N}^N(t), \frac{\partial}{\partial w} \phi(w, \gamma) \cdot \frac{\gamma w d(t)}{\frac{1}{N} \sum_{j=1}^N (1 - \gamma_j) \gamma_j w_j(t)} \right\rangle.
\end{aligned}$$

Furthermore, we define

$$\begin{aligned}
F[\mu_{X_N}^N](t) &:= \frac{1}{N} \sum_{k=1}^N (1 - \gamma_k) \gamma_k w_k(t) \\
&= \langle \mu_{X_N}^N(t), (1 - \gamma) \gamma w \rangle \\
&= \int_{\mathbb{R}_{>0}} \int_0^1 w \gamma (1 - \gamma) \mu_{X_N}^N(\gamma, w, t) d\gamma dw,
\end{aligned}$$

and we thus get:

$$\frac{d}{dt} \langle \mu_{X_N}^N(t), \phi(\gamma, w) \rangle = \left\langle \mu_{X_N}^N(t), \frac{\partial}{\partial w} \phi(w, \gamma) \left[r w + \frac{\gamma w d(t)}{F[\mu_{X_N}^N](t)} \right] \right\rangle.$$

Then, we integrate by parts in γ and w and obtain:

$$\left\langle \frac{\partial \mu_{X_N}^N}{\partial t} + \frac{\partial}{\partial w} \left(\left[r w + \frac{\gamma w d(t)}{F[\mu_{X_N}^N](t)} \right] \mu_{X_N}^N \right), \phi \right\rangle = 0.$$

Such a PDE is called *mean field PDE*. In order to prove the mean field limit, we apply the method originally used by Dobrushin [85]. The first step is to define the *mean field characteristic flow* of our mean field PDE and prove existence and uniqueness. Before we do so, we have to give a short definition of the so called *push-forward* operator.

Definition 3.3.2. Given two measurable spaces (X, \mathcal{A}) and (Y, \mathcal{B}) , a measurable map

$$\Phi : (X, \mathcal{A}) \rightarrow (Y, \mathcal{B}),$$

and a measure μ on (X, \mathcal{A}) . Then the push-forward of μ under Φ is the measure on (Y, \mathcal{B}) defined by:

$$\Phi \# \mu(B) = \mu(\Phi^{-1}(B)), \quad \forall B \in \mathcal{B}.$$

Lemma 3.3.1. For each $\xi \in \mathbb{R}_{>0} \times (0, 1)$ and each Borel probability measure μ^0 , which satisfies

$$0 < \int \xi'_2(1 - \xi'_2) \xi'_1 \mu^0(d\xi'_1, d\xi'_2) < \infty,$$

there exist a unique solution denoted by

$$[0, \infty) \ni t \mapsto W(t, \xi^0, \mu^0) \in \mathbb{R}_{>0} \times (0, 1),$$

of class C^1 of the problem

$$\begin{cases} \dot{W}(t, \xi, \mu^0) = \begin{pmatrix} \dot{W}_1(t, \xi, \mu^0) \\ \dot{W}_2(t, \xi, \mu^0) \end{pmatrix} = \begin{pmatrix} r W_1(t, \xi, \mu^0) + \frac{W_1(t, \xi, \mu^0)}{\int \xi'_2(1 - \xi'_2)} \frac{W_2(t, \xi, \mu^0)}{\xi'_1} \frac{d(t)}{\mu(t, d\xi'_1, d\xi'_2)} \\ 0 \end{pmatrix}, \\ \mu(t) = W(t, \cdot, \mu^0) \# \mu^0, \\ W(0, \xi, \mu^0) = \xi = \begin{pmatrix} \xi_1 \\ \xi_2 \end{pmatrix}. \end{cases}$$

The operator $\#$ is the push-forward of the measure μ^0 under W .

Proof. We have

$$c := \int \xi'_2(1 - \xi'_2) \xi'_1 \mu^0(d\xi'_1, d\xi'_2) < \infty,$$

and define the weighted L_w^1 space

$$L_w^1 := \left\{ z : \mathbb{R}_{>0} \times (0, 1) \rightarrow \mathbb{R}^2 \text{ measurable function, } \int_{\mathbb{R}_{>0} \times (0, 1)} |z(y)| y_2(1 - y_2) \mu^0(dy_1, dy_2) < \infty \right\}.$$

The weight is a positive measurable function and thus our space is a Banach space. Then, we define the sequence $(W^n)_{n \geq 0}$

$$\begin{cases} W^{n+1}(t, \xi) = \begin{pmatrix} W_1^{n+1}(t, \xi) \\ W_2^{n+1}(t, \xi) \end{pmatrix} = \begin{pmatrix} \xi_1 + \int_0^t r W_1^n(s, \xi) + \frac{W_1^n(s, \xi)}{\int W_2^n(s, \xi)(1 - W_2^n(s, \xi))} \frac{W_2^n(s, \xi)}{W_1^n(s, \xi)} \frac{d(s)}{\mu^0(d\xi'_1, d\xi'_2)} ds \\ \xi_2 \end{pmatrix}, \\ W^0(t, \xi) = \xi = \begin{pmatrix} \xi_1 \\ \xi_2 \end{pmatrix}, \quad \xi_2 \in (0, 1), \quad \xi_1 > 0. \end{cases}$$

The second component of our ODE system does not change over time, we thus have:

$$W_2^n(t, \xi) = \xi_2, \quad \forall n \in \mathbb{N}.$$

We use the special structure of our original N -particle ODE system to observe:

$$\begin{aligned}
& \|W^{n+1}(t, \cdot) - W^n(t, \cdot)\|_{L_w^1} = \|W_1^{n+1}(t, \cdot) - W_1^n(t, \cdot)\|_{L_w^1} \\
& \leq \int_0^t r \|W_1^n(s, \xi) - W_1^{n-1}(s, \xi)\|_{L_w^1} ds + \\
& \quad \int_0^t \max_{y \in [0, t]} |d(y)| \left\| \frac{W_1^n(s, \cdot)}{\int \xi'_2(1 - \xi'_2) W_1^n(s, \xi') \mu^0(d\xi'_1, d\xi'_2)} \right\|_{L_w^1} ds \\
& \quad - \frac{W_1^{n-1}(s, \cdot)}{\int \xi'_2(1 - \xi'_2) W_1^{n-1}(s, \xi') \mu^0(d\xi'_1, d\xi'_2)} \|_{L_w^1} ds \\
& \stackrel{(\star)}{\leq} \int_0^t \left(r + \max_{y \in [0, t]} |d(y)| L \right) \|W_1^n(s, \cdot) - W_1^{n-1}(s, \cdot)\|_{L_w^1} ds \\
& \leq \int_0^t \dots \int_0^t \left[\left(r + \max_{y \in [0, t]} |d(y)| L \right) \right]^n \|W_1^1(s, \cdot) - W_1^0(s, \cdot)\|_{L_w^1} ds.
\end{aligned}$$

We have to discuss the local Lipschitz constant L . We define the operator

$$\hat{F}[g] = \frac{g(\xi)}{\int g(\xi') \xi'_2(1 - \xi'_2) \mu^0(d\xi'_1, d\xi'_2)},$$

where $g \in L_w^1$. The Gâteaux derivative of this operator is given by:

$$\begin{aligned}
d\hat{F}(g; \psi) &= \frac{d}{dh} \hat{F}[g + h\psi] \Big|_{h=0} = \frac{\psi}{\int g(\xi') \xi'_2(1 - \xi'_2) \mu^0(d\xi'_1, d\xi'_2)} - \\
&\quad \frac{g \int \psi(\xi') \xi'_2(1 - \xi'_2) \mu^0(d\xi'_1, d\xi'_2)}{\left(\int g(\xi') \xi'_2(1 - \xi'_2) \mu^0(d\xi'_1, d\xi'_2) \right)^2}
\end{aligned}$$

We have to discuss the operator norm of the Gâteaux derivative.

$$\begin{aligned}
& \sup_{\|\psi\|_{L_w^1}=1} \left\| \frac{\psi}{\int g(\xi') \xi'_2(1 - \xi'_2) \mu^0(d\xi'_1, d\xi'_2)} - \frac{g \int \psi(\xi') \xi'_2(1 - \xi'_2) \mu^0(d\xi'_1, d\xi'_2)}{\left(\int g(\xi') \xi'_2(1 - \xi'_2) \mu^0(d\xi'_1, d\xi'_2) \right)^2} \right\|_{L_w^1} \\
& \leq \sup_{\|\psi\|_{L_w^1}=1} \left\| \frac{\psi}{\int g(\xi') \xi'_2(1 - \xi'_2) \mu^0(d\xi'_1, d\xi'_2)} \right\|_{L_w^1} + \left\| \frac{g \int \psi(\xi') \xi'_2(1 - \xi'_2) \mu^0(d\xi'_1, d\xi'_2)}{\left(\int g(\xi') \xi'_2(1 - \xi'_2) \mu^0(d\xi'_1, d\xi'_2) \right)^2} \right\|_{L_w^1} \\
& \leq \sup_{\|\psi\|_{L_w^1}=1} \frac{\|\psi\|_{L_w^1}}{\|g\|_{L_w^1}} + \frac{\|g\|_{L_w^1}}{\|g\|_{L_w^1}^2} \|\psi\|_{L_w^1} = \underbrace{\frac{2}{\|g\|_{L_w^1}}}_{=: L} < \infty
\end{aligned}$$

for a fixed function $g \in L_w^1$.

If we return to our original inequality (\star) , we can apply the previous computations. We observe a local Lipschitz constant L . Starting from the initial density $W^0(t, \cdot) \in L_w^1$ which satisfies

$$\frac{1}{\|W_1^0(t, \cdot)\|_{L_w^1}} < \infty,$$

we can deduce that we never run in the singularity zero. The reason for this is the construction of the sequence, respectively the structure of our ODE. The right hand side of our ODE is positive and thus our solution, respectively the sequence, remains positive.

The dividend is not bounded by definition. Thus, we can obtain for every time interval $[0, T]$, $T \in \mathbb{R}_{>0}$ a constant M ,

$$M := r + \max_{y \in [0, T]} |d(y)| L, \quad L := \frac{2}{\|W_1^0(t, \cdot)\|_{L_w^1}},$$

such that the previous inequality (\star) holds. Furthermore, we have the inequality

$$\begin{aligned} & \|W^1(s, \xi) - W^0(s, \xi)\|_{L_w^1} = \|W_1^1(t, \xi) - W_1^0(s, \xi)\|_{L_w^1} \\ &= \int_0^s \left| r\xi_1 + \frac{\xi_1 \xi_2 d(y)}{\int \xi'_2(1-\xi'_2) \xi'_1 \mu^0(d\xi'_1, d\xi'_2)} dy \right| \xi_2(1-\xi_2) \mu^0(d\xi_1, d\xi_2) \\ &\leq \int_0^t \int \left| r\xi_1 + \frac{\xi_1 d(y)}{\int \xi'_2(1-\xi'_2) \xi'_1 \mu^0(d\xi'_1, d\xi'_2)} \right| \xi_2(1-\xi_2) d\mu^0(d\xi_1, d\xi_2) dy \\ &\leq \left(rc + \max_{y \in [0, t]} |d(y)| 1 \right) t. \end{aligned}$$

and finally observe:

$$\|W^{n+1}(t, \cdot) - W^n(t, \cdot)\|_{L_w^1} \leq \left(rc + \max_{y \in [0, t]} |d(y)| \right) \frac{(M t)^n}{n!}$$

Hence, we have

$$W^n(t, \cdot) \rightarrow W(t, \cdot),$$

uniformly in L_w^1 and $t \in [0, T]$. Furthermore, $W \in C(\mathbb{R}_{>0} \times (0, 1), L_w^1)$ satisfies

$$\begin{cases} W(t, \xi) = \begin{pmatrix} W_1(t, \xi) \\ W_2(t, \xi) \end{pmatrix} = \begin{pmatrix} \xi_1 + \int_0^t r W_1(s, \xi) + \frac{W_1(s, \xi) W_2(s, \xi) d(s)}{\int W_2(s, \xi)(1-W_2(s, \xi)) W_1(s, \xi) \mu^0(d\xi'_1, d\xi'_2)} ds \\ \xi_2 \end{pmatrix}, \end{cases} \quad (24)$$

As next step, we prove the uniqueness of our solutions. We assume that $W(t, \xi), \tilde{W}(t, \xi)$ are two solutions. The uniqueness in the second component is obvious because both solutions have to satisfy the initial conditions. In the first component, we deduce the following inequality.

$$\begin{aligned} & \|W_1(t, \xi) - \tilde{W}_1(t, \xi)\|_{L_w^1} \leq \int_0^t r \|W_1(s, \xi) - \tilde{W}_1(s, \xi)\|_{L_w^1} ds \\ &+ \int_0^t \xi_2 \left\| \frac{d(s) W_1(s, \xi)}{\int W_1(s, \xi') \xi_2(1-\xi_2) \mu^0(d\xi')} - \frac{d(s) \tilde{W}_1(s, \xi)}{\int \tilde{W}_1(s, \xi') \xi_2(1-\xi_2) \mu^0(d\xi')} \right\|_{L_w^1} ds \\ &\leq \int_0^t (r + d(s) L) \|W_1(s, \xi) - \tilde{W}_1(s, \xi)\|_{L_w^1} ds \end{aligned}$$

Then, we immediately observe uniqueness by applying the Gronwall inequality. The integrant in equation (24) is continuous and thus the function $t \mapsto W(t, \xi)$ is of class C^1 on $[0, T]$ and satisfies

$$\begin{cases} \frac{\partial}{\partial t} W(t, \xi) = \left(r W_1(t, \xi) + \frac{W_1(t, \xi) W_2(t, \xi)}{\int W_2(t, \xi)(1 - W_2(t, \xi)) W_1(t, \xi) \mu^0(d\xi'_1, d\xi'_2)} \frac{d(t)}{W_1(t, \xi) \mu^0(d\xi'_1, d\xi'_2)} \right) \\ W(0, \xi) = \xi. \end{cases}$$

We then finally substitute

$$\begin{aligned} w' &= W_1(t, \xi'), \\ \gamma' &= W_2(t, \xi'), \end{aligned}$$

and the integral in the denominator is given by:

$$\int W_1(t, \xi') W_2(t, \xi') (1 - W_2(t, \xi')) \mu^0(d\xi') = \int w' \gamma' (1 - \gamma') \underbrace{W(t, \cdot) \# \mu^0(d\xi')}_{=\mu(t)}$$

Thus, we have shown the existence and uniqueness of a solution of our mean field characteristic equation. \square

The idea of the Dobrushin estimate is to derive a stability estimate for the mean field characteristic flow $W(t, \xi^0, \mu^0)$. To measure the stability, we need some kind of distance. The best distance for this application is probably the *Wasserstein* or *Monge-Kantorovich* distance. Let $\mathcal{P}_\lambda(\mathbb{R}^d)$, $\lambda \geq 1$ be the space of all Borel probability measures on \mathbb{R}^d with finite momentum of order λ , i.e.

$$\int_{\mathbb{R}^d} |x|^\lambda \mu(dx) < \infty.$$

Furthermore, we define the set $\Pi(\nu, \mu)$ to be the set of all probability measures on $\mathbb{R}^d \times \mathbb{R}^d$ with marginals $\nu, \mu \in \mathcal{P}_\lambda(\mathbb{R}^d)$. This means:

$$\pi \in \Pi(\nu, \mu) \iff \int_{\mathbb{R}^d \times \mathbb{R}^d} (\phi(x) + \psi(y)) \pi(dx dy) = \int_{\mathbb{R}^d} \phi(x) \nu(dx) + \int_{\mathbb{R}^d} \psi(y) \mu(dy),$$

where $\phi, \psi \in C(\mathbb{R}^d)$ and $\psi(x) = \phi(x) = O(|x|^\lambda)$, as $|x| \rightarrow \infty$. We can then simply define the Wasserstein distance to be:

Definition 3.3.3. For each $\lambda \geq 1$ and $\nu, \mu \in \mathcal{P}_\lambda(\nu, \mu)$, the Wasserstein distance $dist_{W,\lambda}(\nu, \mu)$ between the measures ν and μ is defined by

$$dist_{W,\lambda}(\nu, \mu) = \inf_{\pi \in \Pi(\nu, \mu)} \left(\int_{\mathbb{R} \times \mathbb{R}} |x - y|^\lambda \pi(dx dy) \right)^{\frac{1}{\lambda}}.$$

As next step, we state and prove the Dobrushin stability estimate.

Theorem 3.3.1. Let μ_1^0 and μ_2^0 two measures on $\mathbb{R}_{>0} \times (0, 1)$ which satisfy

$$0 < \int_{\mathbb{R}_{>0}} \int_0^1 \xi'_1 \xi'_2 (1 - \xi'_2) \mu_i^0(d\xi'_1, d\xi'_2) < \infty,$$

$i \in \{1, 2\}$. Then, the measures

$$\mu_i(t) = W(t, \cdot, \mu_i^0) \# \mu_i^0,$$

where W is the mean field characteristic flow defined in lemma 3.3.1 satisfy

$$dist_{W,1}(\mu_1(t), \mu_2(t)) \leq e^{M|t|} dist_{W,1}(\mu_1^0, \mu_2^0),$$

where $M > 0$ is a positive constant and $t \in [0, T]$.

Proof. Let $\xi, \tilde{\xi} \in \mathbb{R}_{>0} \times (0, 1)$ and the measures μ_i^0 satisfy

$$0 < \int_{\mathbb{R}_{>0}} \int_0^1 \xi'_1 \xi'_2 (1 - \xi'_2) \mu_i^0(d\xi'_1, d\xi'_2) < \infty,$$

then we have:

$$\begin{aligned} W(t, \xi, \mu_1^0) - W(t, \tilde{\xi}, \mu_2^0) &= \xi - \tilde{\xi} \\ &\quad \int_0^t r W_1(s, \xi, \mu_1^0) - r W_1(s, \tilde{\xi}, \mu_1^0) + \frac{\xi_2 W_1(s, \xi, \mu_1^0) d(s)}{\int \xi'_1 \xi'_2 (1 - \xi'_2) \mu_1(s, d\xi'_1, d\xi'_2)} - \frac{\tilde{\xi}_2 W_1(s, \tilde{\xi}, \mu_2^0) d(s)}{\int \tilde{\xi}'_1 \tilde{\xi}'_2 (1 - \tilde{\xi}'_2) \mu_2(s, d\tilde{\xi}'_1, d\tilde{\xi}'_2)} ds \end{aligned}$$

Then, we do a substitution in the integrals in the denominator and since $\mu_i(t) = W(t, \cdot, \mu_i^0) \# \mu_i^0$ we observe e.g. for $i = 1$:

$$\int \xi'_1 \xi'_2 (1 - \xi'_2) \mu_1(s, d\xi'_1, d\xi'_2) = \int W_1(s, \xi', \mu_1^0) \xi'_2 (1 - \xi'_2) \mu_1^0(d\xi'_1, d\xi'_2)$$

We then use the Lipschitz continuity again. By abuse of notation, we use the same notation for our constant although they differ due to different norms we consider.

$$|W(t, \xi, \mu_1^0) - W(t, \tilde{\xi}, \mu_2^0)| \leq |\xi - \tilde{\xi}| + \underbrace{(r + \max_{y \in [0, t]} |d(y)| L)}_{=: M} \int_0^t |W(s, \xi, \mu_1^0) - W(s, \tilde{\xi}, \mu_2^0)| ds$$

Then, we integrate with respect to the measure $\pi^0 \in \Pi(\mu_1^0, \mu_2^0)$ and use Fubini:

$$\begin{aligned} \int |W(t, \xi', \mu_1^0) - W(t, \tilde{\xi}', \mu_2^0)| \pi^0(d\xi', d\tilde{\xi}') &\leq \int |\xi' - \tilde{\xi}'| \pi^0(d\xi', d\tilde{\xi}') \\ &\quad + M \int_0^t \int |W(s, \xi', \mu_1^0) - W(s, \tilde{\xi}', \mu_2^0)| \pi^0(d\xi', d\tilde{\xi}') ds \end{aligned}$$

We define:

$$D[\pi^0](t) := \int |W(t, \xi', \mu_1^0) - W(t, \tilde{\xi}', \mu_2^0)| \pi^0(d\xi', d\tilde{\xi}').$$

Thus, we can rewrite the inequality above to be

$$D[\pi^0](t) \leq D[\pi^0](0) + M \int_0^t D[\pi](s) ds,$$

and can deduce by the Gronwall inequality that

$$D[\pi^0](t) \leq D[\pi^0](0) e^{M t},$$

holds. We then define the map

$$\Phi_t : (\xi, \tilde{\xi}) \mapsto (W(t, \xi, \mu_1^0), W(t, \tilde{\xi}, \mu_2^0))$$

and

$$\Phi_t \# \pi^0 = \pi(t) \in \Pi(\mu_1(t), \mu_2(t)),$$

since $\pi^0 \in \Pi(\mu_1^0, \mu_2^0)$ and $W(t, \cdot, \mu_i^0) \# \mu_i^0 = \mu_i(t)$ for all $t \in [0, T]$. Hence, we have

$$\begin{aligned} dist_{W,1}(\mu_1(t), \mu_2(t)) &= \inf_{\pi \in \Pi(\mu_1(t), \mu_2(t))} \int |\xi - \tilde{\xi}| \pi(d\xi, d\tilde{\xi}) \\ &\leq \inf_{\pi^0 \in \Pi(\mu_1^0, \mu_2^0)} \int |W(t, \xi, \mu_1^0) - W(t, \tilde{\xi}, \mu_2^0)| \pi^0(d\xi, d\tilde{\xi}) \\ &= \inf_{\pi^0 \in \Pi(\mu_1^0, \mu_2^0)} D[\pi^0](t) \\ &\leq e^{M t} \inf_{\pi^0 \in \Pi(\mu_1^0, \mu_2^0)} D[\pi^0](0) \\ &= e^{M t} dist_{W,1}(\mu_1^0, \mu_2^0), \end{aligned}$$

which gives the result. The first inequality is delicate. In essence, one switches from the infimum over the couplings $\Pi(\mu_1(t), \mu_2(t))$ to the infimum over $\Pi(\mu_1^0(t), \mu_2^0(t))$ due to the choice of one transformation. Since the set $\Pi(\mu_1^0(t), \mu_2^0(t))$ is possibly smaller than $\Pi(\mu_1(t), \mu_2(t))$, the infimum becomes larger. \square

As a consequence of this stability estimate, we can derive the mean field limit rigorously.

Theorem 3.3.2. *Let f^0 be a probability density on $\mathbb{R}_{>0} \times (0, 1)$ such that*

$$0 < \int_{\mathbb{R} \times (0,1)} w \gamma (1 - \gamma) f^0(w, \gamma) dw d\gamma < \infty.$$

Then the Cauchy problem for the mean field PDE

$$\begin{cases} \frac{\partial}{\partial t} f(t, w, \gamma) + \frac{\partial}{\partial w} \left(r w f(t, w, \gamma) + \frac{\gamma w d(t)}{\int w' \gamma' (1 - \gamma') f(t, w, \gamma') dw' d\gamma'} f(t, w, \gamma) \right) = 0, \\ f(0, w, \gamma) = f^0, \end{cases}$$

$w \in \mathbb{R}_{>0}$, $\gamma \in (0, 1)$, $t \in [0, T]$, $T \in \mathbb{R}_{>0}$, has a unique weak solution in $C(\mathbb{R}_{>0} \times (0, 1), L^1(\mathbb{R}_{>0} \times (0, 1)))$. Then the ODE system with initial conditions $X_N^0 = (w_1^0, \gamma_1, \dots, w_N^0, \gamma_N)$

$$\begin{cases} \dot{w}_i(t) = rw_i(t) + \frac{\gamma_i w_i(t) d(t)}{\frac{1}{N} \sum_{j=1}^N (1-\gamma_j) \gamma_j w_j(t)}, \\ w_i(0) = w_i^0, \end{cases}$$

where $\gamma_i \in (0, 1)$, $w_i \in \mathbb{R}_{>0}$ has a unique solution denoted by $X_N = (w_1(t), \gamma_1, \dots, w_N(t), \gamma_N)$, $t \in [0, T]$. If the empirical measure

$$\mu_{X_N^0} = \frac{1}{N} \sum_{i=1}^N \delta(w - w_i(0)) \delta(\gamma - \gamma_i),$$

satisfies

$$dist_{W,1}(\mu_{X_N^0}, f^0) \rightarrow 0, \quad \text{as } N \rightarrow \infty,$$

then

$$\mu_{X_N} \rightharpoonup f(t, \cdot) \mathcal{L}, \quad \text{as } N \rightarrow \infty,$$

in the weak topology of probability measures, where \mathcal{L} denotes the Lebesgue measure on $\mathbb{R}_{>0} \times (0, 1)$. Furthermore, the convergence rate is given by:

$$dist_{W,1}(\mu_{T_t X_N^0}, f(t, \cdot) \mathcal{L}) \leq e^{M-t} dist_{W,1}(\mu_{X_N^0}, f^0) \rightarrow 0,$$

as $N \rightarrow \infty$ for each $t \in [0, T]$.

Proof. We sketch the main arguments and follow the steps of Golse [112].

- We use lemma 3.3.1 to observe:

$$f(t, \cdot) \mathcal{L} = X(t, \cdot, f^0 \mathcal{L}) \# f^0 \mathcal{L}, \quad \forall t \in \mathbb{R}.$$

Thus, we can immediately conclude the uniqueness of the solution of the Cauchy problem in $C(\mathbb{R}_{>0} \times (0, 1), L^1(\mathbb{R}))$ for the mean field PDE.

- By Dobrusin's stability estimate we get:

$$dist_{W,1}(\mu_{X_N}, f(t, \cdot, \cdot) \mathcal{L}) \leq e^{M|t|} dist_{W,1}(\mu_{X_N^0}, f^0).$$

- By assumption

$$dist_{W,1}(\mu_{X_N^0}, f^0) \rightarrow 0, \quad \text{as } N \rightarrow \infty,$$

and thus

$$dist_{W,1}(\mu_{X_N}, f(t, \cdot, \cdot) \mathcal{L}) \rightarrow 0, \quad \text{as } N \rightarrow \infty,$$

holds.

- We consider $\phi \in Lip(\mathbb{R}_{>0} \times (0, 1))$ and for each $\pi \in \Pi(\mu_{X_N}, f(t, \cdot) \mathcal{L})$ one has

$$\begin{aligned} & \left| \int_{\mathbb{R}_{>0} \times (0, 1)} \phi(w, \gamma) \mu_{X_N}(dw, d\gamma) - \int_{\mathbb{R}_{>0} \times (0, 1)} \phi(w', \gamma') f(t, w', \gamma') dw' d\gamma' \right| \\ &= \left| \int_{\mathbb{R}_{>0} \times (0, 1)} \int_{\mathbb{R}_{>0} \times (0, 1)} \phi(w, \gamma) - \phi(w', \gamma') \pi(dw, d\gamma, dw', d\gamma') \right| \\ &\leq Lip(\phi) \int_{\mathbb{R}_{>0} \times (0, 1)} \int_{\mathbb{R}_{>0} \times (0, 1)} |w - w'| + |\gamma - \gamma'| \pi(dw, d\gamma, dw', d\gamma'), \end{aligned}$$

and thus

$$\begin{aligned} & \left| \int_{\mathbb{R}_{>0} \times (0, 1)} \phi(w, \gamma) \mu_{X_N}(dw, d\gamma) - \int_{\mathbb{R}_{>0} \times (0, 1)} \phi(w', \gamma') f(t, w', \gamma') dw' d\gamma' \right| \\ &\leq Lip(\phi) \inf_{\pi \in \Pi(\mu_{X_N}, f(t, \cdot) \mathcal{L})} \int_{\mathbb{R} \times \mathbb{R}} \int_{\mathbb{R} \times \mathbb{R}} |w - w'| + |\gamma - \gamma'| \pi(dw, d\gamma, dw', d\gamma') \\ &= Lip(\phi) dist_{W,1}(\mu_{X_N}, f(t, \cdot) \mathcal{L}) \rightarrow 0, \end{aligned}$$

holds as $N \rightarrow \infty$.

- The inequality above holds for $\phi \in C_c^1(\mathbb{R}_{>0} \times (0, 1))$ and thus

$$\int_{\mathbb{R}_{>0} \times (0, 1)} \phi(w, \gamma) \mu_{X_N}(dw, d\gamma) \rightarrow \int_{\mathbb{R}_{>0} \times (0, 1)} \phi(w, \gamma) f(t, w, \gamma) dx,$$

also holds for $\phi \in C_c(\mathbb{R}_{>0} \times (0, 1))$ as $N \rightarrow \infty$, because $C_c^1(\mathbb{R}_{>0} \times (0, 1))$ is dense in $C_c(\mathbb{R}_{>0} \times (0, 1))$.

- Finally, one can apply the so called “portmanteau theorem” to observe

$$\mu_{X_N} \rightharpoonup f(t, \cdot) \mathcal{L}, \quad \text{as } N \rightarrow \infty.$$

in the weak topology of probability measures.

□

Numerics Finally, we want to test our limit result and show that the limit PDE approximates the microscopic dynamics very well. We have implemented an explicit Euler method to solve the microscopic ODE system. The PDE model is solved by the finite difference method with an upwind scheme. The microscopic simulation has been conducted with 10.000 agents.

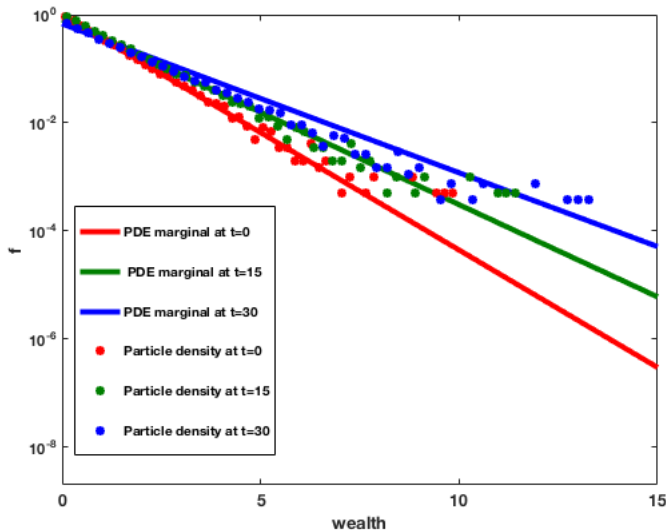


Figure 38: Comparison of the wealth distribution with an initial exponential distribution.

3.3.3 Stochastic Mean Field Limit

In this section, we want to provide a brief outlook on the situation when the microscopic process of interacting agents is prescribed by SDEs. Thus, the microscopic interaction may be given by:

$$dX_i = F_i(t, \mathbf{X}) dt + G_i(t, \mathbf{X}) dW_i, \quad 1 \leq i \leq N, \quad X_i \in \mathbb{R}, \quad \mathbf{X} \in \mathbb{R}^N, \quad N \in \mathbb{N}, \quad (25)$$

where W_i is a Wiener process and the SDE needs to be interpreted in the Itô sense. The rigorous derivation of the mean field limit in the case of stochastic diffusion processes dates back to McKean [177]. Further classical results on this topic are Méléard [178] and Sznitman [230]. We also want to refer to a more recent result by Bolley et al. [27]. In this study, Bolley et al. weaken the usual assumption of Lipschitz continuous drift and diffusion functions F_i, G_i to locally Lipschitz functions.

We do not intent to look into details and only want to heuristically describe the limit process.

In a first step, one proves the convergence of the particle model to the system of McKean-Vlasov equations. Then, one has a system of independent and identically distributed processes and can derive the corresponding forward Kolmogorov (Fokker-Planck) equation.

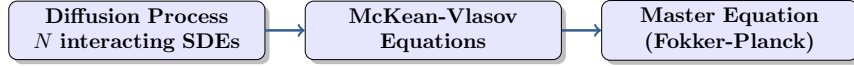


Figure 39: Schematic representation of the stochastic mean field limit.

Finally, we want to give an example of this limit process. The mean field limit of the following example has been rigorously analyzed by Bolley et al. [27].

Example 3.3.1. *We consider a stochastic version of the famous swarming model by Cucker-Smale [73]. The microscopic system reads:*

$$\begin{aligned} dX_t^i &= V_t^i \ dt, \\ dV_t^i &= \sqrt{2} \ dW_t^i - \frac{1}{N} \sum_{j=1}^N H(X_t^i - X_t^j, V_t^i - V_t^j) \ dt, \quad 1 \leq i \leq N, \end{aligned}$$

with the interaction potential:

$$H(X_t^i - X_t^j, V_t^i - V_t^j) := \frac{V_t^j - V_t^i}{(1 + |X_t^i - X_t^j|)^\gamma}, \quad \gamma \geq 0.$$

The processes of N interacting individuals $(X_t^i, V_t^i)_{t \geq 0}$ behave in the mean field limit $N \rightarrow \infty$ like the processes $(\bar{X}_t^i, \bar{V}_t^i)_{t \geq 0}$, which are solutions to the McKean-Vlasov Equations:

$$\begin{aligned} d\bar{X}_t^i &= \bar{V}_t^i \ dt, \\ d\bar{V}_t^i &= \sqrt{2} \ dW_t^i - H * f_t(\bar{X}_t^i, \bar{Y}_t^i) \ dt, \quad f_t = \text{law}(\bar{X}_t^i, \bar{Y}_t^i), \end{aligned}$$

where $*$ denotes the convolution. The processes $(\bar{X}_t^i, \bar{V}_t^i)_{t \geq 0}$ with $i \geq 0$ are independently and identically distributed processes and the law $f_t = f(t, x, y)$ satisfies the following PDE.

$$\partial_t f(t, x, y) + v \cdot \nabla_x f(t, x, v) = \Delta_v f(t, x, v) + \nabla_v \cdot ([H * f](t) f(t, x, v)).$$

Outlook We want to finish this section with further research questions inspired by financial market applications. As pointed out in the previous chapter, it is commonly accepted to model the stock price evolution by stochastic differential equations coupled with the wealth dynamics of financial agents. We want to state an explicit example and want to emphasize that such systems naturally arise in economic applications.

Example 3.3.2. *We may consider N financial agents equipped with a personal wealth $w_i > 0$, $i = 1, \dots, N$ which always invest a fixed fraction $\gamma_i \in (0, 1)$ of their wealth in stocks. The stock price S is determined by a SDE and driven by the excess demand. We define the excess demand to be:*

$$ED(S, \mathbf{w}) = \frac{1}{N} \sum_{i=1}^N \frac{\gamma_i w_i}{S} - c_0, \quad c_0 > 0, \quad \mathbf{w} := (w_1, \dots, w_N)^T \in \mathbb{R}^N$$

Then the microscopic system reads

$$\begin{aligned} dw_i &= \gamma_i \frac{dS + D}{S} w_i dt, \\ dS &= \lambda ED(t, \mathbf{w}, S) S dt + S dW, \end{aligned} \tag{26}$$

where $D > 0$ is the dividend, λ the inverse market depth and $\frac{dS+D}{S}$ the stock return of the investment in stocks.

In comparison to the microscopic model (25), the mean field limit of example 3.3.2 is non-standard. To our knowledge, there are no rigorous results for the mean field limit for models of the type (26). The reason is that in the classical case one considers N interacting SDEs, whereas the model (26) consist of N deterministic ODEs interacting with one SDE. A proper derivation of the mean field limit in example 3.3.2 may help to understand the price and wealth dynamics in many econophysical models.

3.4 Mean Field Games

Mean field game theory studies the behavior of a large number of interacting individuals in a game theoretic setting. This research field, popularized in the mathematical community by Lasry and Lions [148], has received a lot of attention in the past decade. In this work, we derive the mean field game PDE system from deterministic microscopic agent dynamics. The dynamics are given by a general ODE which defines a large class of differential games. This class of differential games has been studied by Bressan [36] in the case of a finite number of players. We use the concept of Nash equilibria and apply dynamic programming to derive the mean field limit equation. We extensively study the scaling behavior of our system and observe new reasonable configurations. We show that well known mean field game limit systems are a subclass of our model. We motivate the novel scales with an example of an agent-based financial market model, inspired by the econophysical Levy-Levy-Solomon [154] model. We want to point out that our derivation is only formal and tries to be as comprehensible as possible to the reader. To some extent, this work can be also regarded as an introduction to mean field game theory.

3.4.1 Introduction

A great variety of phenomena in social and natural sciences is described and analyzed by agent-based models [109]. In many situations, the number of interacting agents is very large and the agents compete against each other, e.g. by maximizing their individual payoff [15]. We assume that the agents' dynamics can be modeled by differential equations. Thus, these agents play a differential game and we assume that a solution exists within the concept of Nash equilibria [191]. A setting like this can subsequently be well described and analyzed with mean field game (MFG) theory.

Models of this type can be found in many areas of research such as biology, engineering and economics. In the last decade, there has been a vast number of contributions to this field [148, 114, 130, 124, 44, 43, 42, 144, 149, 123, 122, 20, 2, 45]. The origin of mean field game theory dates back more than 20 years ago with some work of the economists Jovanovic and Rosenthal [130] as well as Bergin and Bernhardt [21]. The year 2006, when Caines et al. [124] in the engineering community and Lasry and Lions [148] in the mathematical literature independently published models of MFG type, can be seen as the moment of inception of this field. Mean field game models can be regarded as a special case of game theory since all agents play a differential game and their actions are characterized by the famous Nash equilibria [191, 114]. Furthermore, MFG theory considers an infinite number of players and can be seen as a further development of the continuous game theory invented by Aumann [14, 114].

In addition, we want to point out the connection to kinetic theory. The notion mean field describes the limit of infinitely interacting microscopic particles. This limit is crucial to derive time continuous mesoscopic description of particles and is necessary for tractable models. Classical applications in physics are plasmas and phase transitions where the number of particles in the original system is large and the mean field limit a very good approximation [112, 128].

Mean field game theory extends the mean field models by adding the social or game-theoretic perspective to the microscopic agents. The influence of an individual agent vanishes in the mean field limit as known from classical mean field theory. Nevertheless, this approximation is necessary in order to gain insights into large coupled systems of optimizing agents since the microscopic model is useless in the case of a large agent number.

Mathematically speaking, a mean field game model is characterized by two coupled partial differential equations (PDEs). One PDE associated to the optimal control problem is of Hamilton-Jacobi-Bellmann (HJB) type and is backwards in time. The second PDE is forward in time and is a forward Kolmogorov equation in the case of stochastic microscopic dynamics and a transport equation in case of deterministic dynamics.

In this work, we only consider deterministic microscopic dynamics. The prototype MFG model you may find in literature [41, 81] is given by:

$$\begin{aligned} \partial_t h(t, x) - H(x, \nabla h) &= 0, \quad \text{in } \mathbb{R}^d \times (0, T), \\ \partial_t g(t, x) - \operatorname{div}(\nabla_p H(x, g, \nabla g)) g(t, x) &= 0, \quad \text{in } \mathbb{R}^d \times (0, T), \\ g(0, x) = g_0, \quad h(x, T) &= \varphi(x, g(t)), \end{aligned}$$

where the Hamiltonian $H = H(x, g, p)$ needs to be convex with respect to the last variable. The function h describes the optimal action of a player at time t and position x , whereas g is a density function which characterizes the probability of finding an agent at time t at position x . Many research devoted to MFG starts with the MFG system stated above and focuses on analytical results such as existence and uniqueness. In our opinion and to our knowledge, there is a lack of proper derivations of MFG systems from microscopic agent dynamics. One of the few attempts to derive the MFG system from microscopic considerations is given by Cardaliaguet [41] and more recently by Degond et al. [81]. The reasons for several authors to neglect this derivation might be partially attributed to different interests and furthermore caused by the self-evidence of the derivation for many experts in this field.

We aim to explain the microscopic derivation in this manner that we hope to reach a broad audience. Furthermore, we hope to encourage researchers to use the MFG framework to build new models and investigate the results of many real-world applications.

The starting point of this study was the idea to derive a MFG model of the econophysical Levy-Levy-Solomon (LLS) model [154]. We had to realize early that the LLS model does not fit in the classical framework of MFG models and that such a scaling has not been considered before. This has lead us to the opinion that it is relevant to investigate the derivation of MFG models starting on the microscopic level and to study different scales.

In this work, we consider a well-known class of microscopic differential games [36] and study the mean field limit as well as the scaling behavior. In order to derive the MFG limit system, we need to require special symmetry and scaling assumptions on our microscopic model. Our research reveals that there is a large variety of scales leading us to different MFG limit systems. We especially want to point out that many MFG models discussed in literature are a subclass of our model.

The outline of the paper is as follows: In the next section, we summarize our main results. We define the microscopic differential game model and state the assumptions we need to derive the MFG limit system. We especially state the MFG limit system and discuss the scaling behavior of the microscopic model. The second part of this study is devoted to the proper derivation of the MFG system. We begin with the derivation of the corresponding set of HJB equations with the help of dynamic programming. In the next step, we use our assumptions in order to reduce this large system to one global HJB equation. Then we use the empirical measure to derive the MFG limit equations. Furthermore, we motivate the concept of measure-valued derivatives and connect our computations to the general case. In a next step, we study several examples of our model and make connections to known models in literature. We conclude this paper with a financial market model, inspired by the LLS model, to emphasize the importance of the new scale discovered in this work.

3.4.2 Main Results

We first define our microscopic model and formulate the needed assumption. As next step, we summarize the derivation of the MFG limit system and state the final result.

Microscopic Differential Game Model We consider N players which are each faced with the optimization problem

$$\underset{u_i: [0,T] \rightarrow \mathbb{R}}{\operatorname{argmax}} p_i(\mathbf{x}(T)) - \int_0^T L_i(t, \mathbf{x}, \mathbf{u}) dt, \quad (27)$$

where $\mathbf{x} = (x_1, \dots, x_N)^T \in \mathbb{R}^{dN}$, $x_i = (x_i^1, \dots, x_i^d)^T \in \mathbb{R}^d$, $1 \leq i \leq N$, $d \geq 1$, $\mathbf{u} = (u_1, \dots, u_N)^T \in \mathbb{R}^N$ and with the state dynamics

$$\dot{\mathbf{x}} = \mathbf{f}(t, \mathbf{x}, \mathbf{u}), \quad \mathbf{x}(0) = \mathbf{x}_0 \in \mathbb{R}^{dN}. \quad (28)$$

The functions $\mathbf{f} = (f_1, \dots, f_N)^T \in \mathbb{R}^{dN}$, $\mathbf{L} = (L_1, \dots, L_N)^T \in \mathbb{R}^N$, $\mathbf{p} = (p_1, \dots, p_N)^T \in \mathbb{R}^N$ are defined on:

$$\begin{aligned} f_i &: [0, T] \times \mathbb{R}^{dN} \times \mathbb{R}^N \rightarrow \mathbb{R}^d, \\ L_i &: [0, T] \times \mathbb{R}^{dN} \times \mathbb{R}^N \rightarrow \mathbb{R}, \\ p_i &: \mathbb{R}^{dN} \rightarrow \mathbb{R}. \end{aligned}$$

Nash Equilibria We assume that the players can observe the current state of the system, thus their strategies depend on time and state $u_i = u_i^*(t, \mathbf{x})$. Hence, the agents play a feedback or *Markovian strategy*. The corresponding equilibrium concept is known as *feedback Nash equilibrium*.

Definition 3.4.1. (see Bressan [36]) A vector of control functions

$(t, \mathbf{x}) \mapsto (u_1^*(t, \mathbf{x}), \dots, u_N^*(t, \mathbf{x}))^T$ is a Nash equilibrium for the game (27) in the class of feedback strategies if the following holds.

The control $u_i^*(t, \mathbf{x})$ provides a solution to the optimal control problem for player i :

$$\underset{u_i: [0,T] \times \mathbb{R}^{dN} \rightarrow \mathbb{R}}{\operatorname{argmax}} p_i(\mathbf{x}(T)) - \int_0^T L_i(t, \mathbf{x}, u_i, \mathbf{u}_{-i}^*(t, \mathbf{x}(t))) dt,$$

with the dynamics (28) and

$$\mathbf{u}_{-i}^*(t, \mathbf{x}(t)) := (u_1^*(t, \mathbf{x}), \dots, u_{i-1}^*(t, \mathbf{x}), u_{i+1}^*(t, \mathbf{x}), \dots, u_N^*(t, \mathbf{x}))^T \in \mathbb{R}^{N-1}.$$

We restrict ourselves to one important class of differential games.

Assumption 1. We assume that the dynamics and the running costs decouple in the following way:

$$\begin{aligned}\mathbf{f}(t, \mathbf{x}, \mathbf{u}) &= \mathbf{f}^0(t, \mathbf{x}) + \mathbf{M}(t, \mathbf{x}) \mathbf{u}(t, \mathbf{x}) \\ &= \mathbf{f}^0(t, \mathbf{x}) + \mathbf{M}^1(t, \mathbf{x}) u_1(t, \mathbf{x}) + \dots + \mathbf{M}^N(t, \mathbf{x}) u_N(t, \mathbf{x}), \\ L_i(t, \mathbf{x}, \mathbf{u}) &= L_i^1(t, \mathbf{x}, u_1) + \dots + L_i^N(t, \mathbf{x}, u_N),\end{aligned}$$

with $\mathbf{u}(t, \mathbf{x}) = (u_1(t, \mathbf{x}), \dots, u_N(t, \mathbf{x}))^T \in \mathbb{R}^N$, $\mathbf{M}(t, \mathbf{x}) \in \mathbb{R}^{dN \times N}$, $L_i(t, \mathbf{x}, \mathbf{u}) \in \mathbb{R}$, $\mathbf{f}^0(t, \mathbf{x}) \in \mathbb{R}^{dN}$, $\mathbf{M}^i \in \mathbb{R}^{dN}$, $i = 1, \dots, N$.

For this class of differential games, one can prove [36] the existence and uniqueness of *open-loop Nash* equilibrium solutions. Open-loop Nash equilibrium solutions can be interpreted as pointwise evaluations of feedback Nash solutions and thus the strategy u_i only depends on time $u_i = u_i(t)$.

Definition 3.4.2. (see Bressan[36]) A vector of control functions $t \mapsto (u_1^*, \dots, u_N^*)^T$ is a Nash equilibrium for the game (27) in the class of open-loop strategies if the following holds.

The control u_i^* provides a solution to the optimal control problem for player i :

$$\underset{u_i: [0, T] \rightarrow \mathbb{R}}{\operatorname{argmax}} p_i(\mathbf{x}(T)) - \int_0^T L_i(t, \mathbf{x}, u_i, \mathbf{u}_{-i}) dt,$$

with the dynamics (28).

We want to point out that the existence of an open-loop solution is necessary in order to obtain feedback Nash solutions. The following theorem, which one might find in Bressan [36], gives detailed conditions on the existence and uniqueness of open-loop Nash equilibrium solutions.

Theorem 3.4.1. We consider the microscopic model, defined in assumption 1, we assume that the vectors \mathbf{M}^i continuously depend on t and x and the functions $u_i \mapsto L_i^i(t, \mathbf{x}, u_i)$ are strictly convex. For every $(t, \mathbf{x}) \in [0, T] \times \mathbb{R}^{dN}$ and any vector $\lambda^i \in \mathbb{R}^{dN}$, $i = 1, \dots, N$, there exist a unique vector $\mathbf{u}^* \in \mathbb{R}^N$, respectively map: $(t, \lambda) \mapsto \mathbf{u}^*(t, \lambda)$. The control value u_i^* is determined as follows:

$$u_i^* = \underset{\omega \in \mathbb{R}}{\operatorname{argmax}} (\lambda^i)^T \mathbf{M}^i(t, \mathbf{x}) \omega - L_i^i(t, \mathbf{x}, \omega).$$

In order to compute the control explicitly, we restrict ourselves to the following class of running costs \mathbf{L} .

Assumption 2. We consider running costs of the form

$$L_i(t, \mathbf{x}, \mathbf{u}) = l_i(t, \mathbf{x}) + \frac{\hat{\alpha}}{2} u_i^2 + \frac{\bar{\alpha}}{2} \sum_{k=1, k \neq i}^N u_k^2,$$

with $\hat{\alpha} > 0$, $\bar{\alpha} \geq 0$ and $l_i : [0, T] \times \mathbb{R}^{dN} \rightarrow \mathbb{R}$.

Lemma 3.4.1. *Due to the special structure of our running cost, we can compute our optimal control explicitly. The optimal control u_i^* , $i = 1, \dots, N$ is given by:*

$$u_i^* = \frac{1}{\hat{\alpha}} (\lambda^i)^T \mathbf{M}^i(t, \mathbf{x}).$$

We solve the closed loop problem (feedback Nash equilibria) with the help of dynamic programming. In the closed loop setting, we want to have the optimal solution for arbitrary points in time and space. We can thus expect to get a PDE whose solution depends on time and space. This is done with the dynamic programming principle and we will obtain the HJB equations. The HJB equations are generally strongly non-linear and well-posedness is a difficult issue [36].

Assumption 3. *We assume that the HJB system of our differential game has a unique solution.*

Symmetry Assumptions The crucial assumption is that we consider identical, indistinguishable players. This translates in symmetry assumptions on our running costs \mathbf{L} and dynamic \mathbf{f} . These conditions are important to derive the mean field limit.

Definition 3.4.3. *We define the empirical moment $m_\Phi^N(\mathbf{x}) \in \mathbb{R}$, $\mathbf{x} \in \mathbb{R}^{dN}$ of the polynomial of order n*

$$\Phi(t, \mathbf{x}) = \sum_{|j| \leq n} \beta_j (x^1)^{j_1} (x^2)^{j_2} \dots (x^d)^{j_d}, \quad \beta_j \in \mathbb{R} \quad \mathbf{x} \in \mathbb{R}^d$$

with multi-index notation $|j| = j_1 + j_2 + \dots + j_d$, by

$$m_\Phi^N(\mathbf{x}) := \frac{1}{N} \sum_{k=1}^N \Phi(x_k).$$

Notice that the empirical moment m_Φ^N is fully symmetric with respect to the N variables x_k , $k = 1, \dots, N$. Full symmetry means that for any permutation $\sigma : \{1, \dots, N\} \rightarrow \{1, \dots, N\}$, $m_\Phi^N(\mathbf{x}) = m_\Phi^N(t, \mathbf{x}_\sigma)$ holds.

Assumption 4. *We model the dynamic and running costs as follows.*

- i) $\mathbf{f}_i^0(t, \mathbf{x}) = f(t, x_i, m_\Phi^N(\mathbf{x}))$ with $f : \mathbb{R}^{dN} \rightarrow \mathbb{R}^d$, $i = 1, \dots, N$.
- ii) $\mathbf{M}_i^i(t, \mathbf{x}) = \hat{m}(t, x_i, m_\Phi^N(\mathbf{x}))$, $\mathbf{M}_k^i(t, \mathbf{x}) = \bar{m}(t, x_k, m_\Phi^N(\mathbf{x}))$, $k \neq i$, $k = 1, \dots, N$ with $\hat{m} : \mathbb{R}^{dN} \rightarrow \mathbb{R}^d$, $\bar{m} : \mathbb{R}^{dN} \rightarrow \mathbb{R}^d$.
- iii) $l_i(t, \mathbf{x}) = l(x_i, m_\Phi^N(\mathbf{x}))$ with $l : \mathbb{R}^{dN} \rightarrow \mathbb{R}$ holds.
- iv) $p_i(t, \mathbf{x}) = p(t, x_i, m_\Phi^N(\mathbf{x}))$ with $p : \mathbb{R}^{dN} \rightarrow \mathbb{R}$.

Notice that all quantities denoted with a hat denote the self-interaction of agents, whereas the bar denotes the interaction with other agents. Furthermore, we want to emphasize that the functions f , \hat{m} , \bar{m} , l , p are symmetric in $(N - 1)$ variables.

MFG System In order to solve the optimization problem we use dynamic programming. We observe a N dimensional system of HJB equations. We then need the symmetry assumptions (assumption 4) to reduce the system to one global HJB equation. We call this equation global HJB equation, since we can deduce from the solution of the global HJB equation any solution of the N dimensional HJB equation.

Assumption 5. *We assume that a unique solution of the global HJB equation exists.*

Before we consider the mean field limit, we need to specify how each quantity scales with respect to the number of agents.

Assumption 6. *We require*

$$f, l, p \sim \mathcal{O}(1), \quad \hat{m} \sim \mathcal{O}\left(\frac{1}{N^\theta}\right), \quad \bar{m} \sim \mathcal{O}\left(\frac{1}{N^{\theta+1}}\right), \\ \hat{\alpha} \sim \mathcal{O}\left(\frac{1}{N^{2\theta}}\right), \quad \bar{\alpha} \sim \mathcal{O}\left(\frac{1}{N^{2\theta+1}}\right),$$

for $\theta \geq 0$.

As pointed out previously, the hat denotes the self interaction and the bar the interaction with the other agents. Thus, the additional factor N^{-1} of the quantities denoted with a bar is needed to scale the interactions with the other agents correctly. We can then rewrite the empirical moments with the help of the empirical measure to an integral, respectively moment of the corresponding density function. Here, we assume that the empirical measure converges in the mean field limit to an absolutely continuous measure and thus the corresponding probability density function exist. All functions are no longer acting only on the real line but also on function space. For this reason, we change the notation of all involved functions to calligraphic letters. The functions have become functionals. For example the function

$$v : \mathbb{R} \times \mathbb{R}^N \rightarrow \mathbb{R}, \quad v(y, \mathbf{x}) := y \frac{1}{N} \sum_{i=1}^N x_i$$

becomes the functional

$$\nu : \mathbb{R} \times \mathcal{P} \rightarrow \mathbb{R}, \quad \nu(y, g) := y \int x g(x) dx$$

for the corresponding probability density function $g \in \mathcal{P}$. We denote this density function by g and the MFG limit system is given by:

$$\begin{aligned} & \partial_t h(t, x) + \nabla_x h(t, x) \cdot \left(\ell(t, x, g) + \frac{1}{\bar{\alpha}} \bar{m}(t, x, g) \int g(t, z) \widehat{m}(t, z, g) \nabla_z h(t, z) dz \right) \\ &= \ell(t, x, g) - \frac{1}{2} \frac{1}{\bar{\alpha}} \left[\nabla_x h(t, x) \widehat{m}(t, x, g) \right]^2 + \frac{\bar{\alpha}}{2} \frac{1}{\bar{\alpha}^2} \int g(t, z) (\nabla_z h(t, z) \widehat{m}(t, z, g))^2 dz, \\ & \partial_t g(t, x) + \operatorname{div}_x \left(\left[\ell(t, x, g) + \frac{1}{\bar{\alpha}} (\widehat{m}(t, x, g))^2 \nabla_x h(t, x) \right. \right. \\ & \quad \left. \left. + \frac{1}{\bar{\alpha}} \bar{m}(t, x, g) \int g(t, z) \nabla_z h(t, z) \widehat{m}(t, z, g) dz \right] g(t, x) \right) = 0, \\ & g(0, x) = g_0, \quad h(T, x) = \varphi(t, x, g). \end{aligned}$$

The optimal strategy of an agent is given by the function h . Notice that there are several scales possible where the MFG limit exist but several terms vanish. We discuss several examples in section 3.4.4.

3.4.3 Derivation of Main Results

We use *dynamic programming* to solve the closed loop problem. The idea of dynamic programming is to start at final time and then going backwards in time with minimal costs. For a further introduction to dynamic programming we refer to [23]. We define the value function $V_i(\tau, \mathbf{y})$, $\tau \in [0, T]$, $\mathbf{y} \in \mathbb{R}^{dN}$ to be:

$$V_i(\tau, \mathbf{y}) := p_i(\mathbf{x}^*(T)) - \int_{\tau}^T L_i(t, \mathbf{x}^*(t), \mathbf{u}^*(t, \mathbf{x}^*(t))) dt,$$

where $x_i^*(t) = x_i^*(t, \tau, \mathbf{y})$ and the vector $\mathbf{y} \in \mathbb{R}^{dN}$ is the initial condition of our dynamics at time τ : $\mathbf{x}(\tau) = \mathbf{y}$. Consequently, the value function V_i is the total payoff for the i -th player at time τ with initial condition \mathbf{y} . We obtain a system of Hamilton-Jacobi-Bellmann equations:

$$\partial_{\tau} V_i(\tau, \mathbf{y}) + \nabla V_i(\tau, \mathbf{y}) \cdot \mathbf{f}(\tau, \mathbf{y}, \mathbf{u}^*) = L_i(\tau, \mathbf{y}, \mathbf{u}^*), \quad V_i(T, \mathbf{y}) = q_i(\mathbf{y}).$$

The system is closed by the equation for the optimal costs.

$$u_i^* = u_i^*(\tau, \mathbf{y}, \nabla V_i) = \frac{1}{\alpha} (\nabla V_i(\tau, \mathbf{y}))^T \mathbf{M}^i(\tau, \mathbf{y}).$$

Hence, we get:

$$\begin{aligned} \partial_{\tau} V_i + \nabla V_i \left(\mathbf{f}^0 + \sum_{k=1}^N \mathbf{M}^k \frac{1}{\bar{\alpha}} (\nabla V_k)^T \mathbf{M}^k \right) \\ = l_i + \frac{\bar{\alpha}}{2} \left(\frac{1}{\bar{\alpha}} (\nabla V_i)^T \mathbf{M}^i \right)^2 + \frac{\bar{\alpha}}{2} \sum_{k=1, k \neq i}^N \left(\frac{1}{\bar{\alpha}} (\nabla V_k)^T \mathbf{M}^k \right)^2, \end{aligned} \quad (29)$$

with terminal condition $V_i(T, \mathbf{y}) = p_i(\mathbf{y})$.

Global HJB equation In this section, we reduce the large system of HJB equation to one global HJB equation. We can use the symmetry assumption 4 and obtain for the state dynamics and running costs:

$$\begin{aligned} \mathbf{f}(\tau, \mathbf{y}) &= \mathbf{f}^0(\tau, \mathbf{y}) + \sum_{k=1}^N \mathbf{M}^k(\tau, \mathbf{y}) \frac{1}{\bar{\alpha}} (\nabla V_k(\tau, \mathbf{y}))^T \mathbf{M}^k(\tau, \mathbf{y}) \\ &= \mathbf{f}^0(\tau, \mathbf{y}) + \frac{1}{\bar{\alpha}} \sum_{k=1}^N \mathbf{M}^k(\tau, \mathbf{y}) \sum_{j=1}^N \nabla_{y_j} V_k(\tau, \mathbf{y}) \mathbf{M}_j^k(\tau, \mathbf{y}) \\ &= \mathbf{f}^0(\tau, \mathbf{y}) \\ &\quad + \frac{1}{\bar{\alpha}} \sum_{k=1}^N \mathbf{M}^k(\tau, \mathbf{y}) \left[\sum_{j=1, j \neq k}^N \nabla_{y_j} V_k(\tau, \mathbf{y}) \bar{m}(\tau, y_j, \mathbf{y}_{-j}) + \nabla_{y_k} V_k(\tau, \mathbf{y}) \hat{m}(\tau, y_k, \mathbf{y}_{-k}) \right]. \end{aligned}$$

We can rewrite the i -th component of f as:

$$\begin{aligned} f_i(\tau, \mathbf{y}) &= f(\tau, y_i, m_{\Phi}^N(\mathbf{y})) \\ &\quad + \frac{1}{\bar{\alpha}} \hat{m}(\tau, y_i, m_{\Phi}^N(\mathbf{y})) \left(\sum_{j=1, j \neq i}^N \nabla_{y_j} V_i(\tau, \mathbf{y}) \bar{m}(\tau, y_j, m_{\Phi}^N(\mathbf{y})) + \nabla_{y_i} V_i(\tau, \mathbf{y}) \hat{m}(\tau, y_i, m_{\Phi}^N(\mathbf{y})) \right) \\ &\quad + \frac{1}{\bar{\alpha}} \bar{m}(\tau, y_i, m_{\Phi}^N(\mathbf{y})) \sum_{k=1, k \neq i}^N \left(\sum_{j=1, j \neq k}^N \nabla_{y_j} V_k(\tau, \mathbf{y}) \bar{m}(\tau, y_j, m_{\Phi}^N(\mathbf{y})) + \nabla_{y_k} V_k(\tau, \mathbf{y}) \hat{m}(\tau, y_k, m_{\Phi}^N(\mathbf{y})) \right) \end{aligned}$$

Furthermore, for the objective functional we get:

$$\begin{aligned}
L_i(\tau, \mathbf{y}) &= l_i(\tau, \mathbf{y}) + \frac{\widehat{\alpha}}{2} \frac{1}{\widehat{\alpha}^2} (\nabla V_i(\tau, \mathbf{y})^T \mathbf{M}^i(t, \mathbf{y}))^2 + \frac{\bar{\alpha}}{2} \sum_{k=1, k \neq i}^N \frac{1}{\bar{\alpha}^2} (\nabla V_k(\tau, \mathbf{y})^T \mathbf{M}^k(t, \mathbf{y}))^2 \\
&= l(\tau, y_i, m_\Phi^N(\mathbf{y})) + \frac{1}{2\widehat{\alpha}} \left(\sum_{j=1}^N \nabla_{y_j} V_i(\tau, \mathbf{y}) \mathbf{M}_j^i(\tau, \mathbf{y}) \right)^2 + \frac{\bar{\alpha}}{2\widehat{\alpha}^2} \sum_{k=1, k \neq i}^N \left(\sum_{j=1}^N \nabla_{y_j} V_k(\tau, \mathbf{y}) \mathbf{M}_j^k(t, \mathbf{y}) \right)^2 \\
&= l(\tau, y_i, m_\Phi^N(\mathbf{y})) + \frac{1}{2\widehat{\alpha}} \left(\sum_{j=1, j \neq i}^N \nabla_{z_j} V_i(\tau, \mathbf{y}) \bar{m}(\tau, y_j, m_\Phi^N(\mathbf{y})) + \nabla_{y_i} V_i(\tau, \mathbf{y}) \widehat{m}(\tau, y_i, m_\Phi^N(\mathbf{y})) \right)^2 \\
&\quad + \frac{\bar{\alpha}}{2\widehat{\alpha}^2} \sum_{k=1, k \neq i}^N \left(\sum_{j=1, j \neq k, j \neq i}^N \nabla_{y_j} V_k(\tau, \mathbf{y}) \bar{m}(\tau, y_j, m_\Phi^N(\mathbf{y})) \right. \\
&\quad \left. + \nabla_{y_k} V_k(\tau, \mathbf{y}) \widehat{m}(\tau, y_k, m_\Phi^N(\mathbf{y})) \right)^2.
\end{aligned}$$

We can then rewrite the system of HJB equations (29) as follows.

$$\begin{aligned}
&\partial_\tau V_i(\tau, \mathbf{y}) + \sum_{l=1, l \neq i}^N \nabla_{y_l} V_i(\tau, \mathbf{y}) \left(f(\tau, y_l, m_\Phi^N(\mathbf{y})) \right. \\
&\quad \left. + \frac{1}{\widehat{\alpha}} \widehat{m}(\tau, y_l, m_\Phi^N(\mathbf{y})) \left[\sum_{j=1, j \neq l}^N \nabla_{y_j} V_l(\tau, \mathbf{y}) \bar{m}(\tau, y_j, m_\Phi^N(\mathbf{y})) + \nabla_{y_l} V_l(\tau, \mathbf{y}) \widehat{m}(\tau, y_l, m_\Phi^N(\mathbf{y})) \right] \right. \\
&\quad \left. + \frac{1}{\bar{\alpha}} \bar{m}(\tau, y_l, m_\Phi^N(\mathbf{y})) \sum_{k=1, k \neq l}^N \left[\sum_{j=1, j \neq k}^N \nabla_{y_j} V_k(\tau, \mathbf{y}) \bar{m}(\tau, y_j, m_\Phi^N(\mathbf{y})) \right. \right. \\
&\quad \left. \left. + \nabla_{y_k} V_k(\tau, \mathbf{y}) \widehat{m}(\tau, y_k, m_\Phi^N(\mathbf{y})) \right] \right) \\
&\quad + \nabla_{y_i} V_i(\tau, \mathbf{y}) \left(f(\tau, y_i, m_\Phi^N(\mathbf{y})) \right. \\
&\quad \left. + \frac{1}{\widehat{\alpha}} \widehat{m}(\tau, y_i, m_\Phi^N(\mathbf{y})) \left[\sum_{j=1, j \neq i}^N \nabla_{y_j} V_i(\tau, \mathbf{y}) \bar{m}(\tau, y_j, m_\Phi^N(\mathbf{y})) \right. \right. \\
&\quad \left. \left. + \nabla_{y_i} V_i(\tau, \mathbf{y}) \widehat{m}(\tau, y_i, m_\Phi^N(\mathbf{y})) \right] \right) \\
&\quad + \frac{1}{\bar{\alpha}} \bar{m}(\tau, y_i, m_\Phi^N(\mathbf{y})) \sum_{k=1, k \neq i}^N \left[\sum_{j=1, j \neq k}^N \nabla_{y_j} V_k(\tau, \mathbf{y}) \bar{m}(\tau, y_j, m_\Phi^N(\mathbf{y})) \right. \\
&\quad \left. + \nabla_{y_k} V_k(\tau, \mathbf{y}) \widehat{m}(\tau, y_k, m_\Phi^N(\mathbf{y})) \right] \Big) \\
&= l(\tau, y_i, m_\Phi^N(\mathbf{y})) + \frac{\widehat{\alpha}}{2} \left(\frac{1}{\widehat{\alpha}} \sum_{k=1, k \neq i}^N \nabla_{y_k} V_i(\tau, \mathbf{y}) \bar{m}(\tau, y_k, m_\Phi^N(\mathbf{y})) \right. \\
&\quad \left. + \frac{1}{\widehat{\alpha}} \nabla_{y_i} V_i(\tau, \mathbf{y}) \widehat{m}(\tau, y_i, m_\Phi^N(\mathbf{y})) \right)^2 \\
&\quad + \frac{\bar{\alpha}}{2} \sum_{k=1, k \neq i}^N \left(\frac{1}{\bar{\alpha}} \sum_{j=1, j \neq k}^N \nabla_{y_j} V_k(\tau, \mathbf{y}) \bar{m}(\tau, y_j, m_\Phi^N(\mathbf{y})) \right. \\
&\quad \left. + \frac{1}{\bar{\alpha}} \nabla_{y_k} V_k(\tau, \mathbf{y}) \widehat{m}(\tau, y_k, m_\Phi^N(\mathbf{y})) \right)^2
\end{aligned} \tag{30}$$

As a next step, we want to reduce the large system (30) of N equations to one PDE. We introduce a new function $W = W(t, y_i, m_\Phi^{N-1}(\mathbf{y}_{-i})) : [0, T] \times \mathbb{R}^d \times \mathbb{R}^{d(N-1)} \rightarrow \mathbb{R}$, with $\mathbf{y}_{-i} := (y_1, \dots, y_{i-1}, y_{i+1}, \dots, y_N)^T \in \mathbb{R}^{d(N-1)}$ that satisfies the following PDE (31), which we call

global HJB equation. We assume that W satisfies

$$\begin{aligned}
& \partial_t W(t, y_i, m_\Phi^{N-1}(\mathbf{y}_{-i})) + \sum_{l=1, l \neq i}^N \nabla_{y_l} W(t, y_i, m_\Phi^{N-1}(\mathbf{y}_{-i})) \left(f(t, y_l, m_\Phi^N(\mathbf{y})) \right. \\
& \quad \left. + \frac{\hat{m}(t, y_l, m_\Phi^N(\mathbf{y}))}{\hat{\alpha}} \left[\sum_{j=1, j \neq l}^N \nabla_{y_j} W(t, y_l, m_\Phi^{N-1}(\mathbf{y}_{-l})) \bar{m}(t, y_j, m_\Phi^N(\mathbf{y})) \right. \right. \\
& \quad \left. \left. + \nabla_{y_l} W(t, y_l, m_\Phi^{N-1}(\mathbf{y}_{-l})) \hat{m}(t, y_l, m_\Phi^N(\mathbf{y})) \right] \right. \\
& \quad \left. + \frac{1}{\hat{\alpha}} \bar{m}(t, y_l, m_\Phi^N(\mathbf{y})) \sum_{k=1, k \neq l}^N \left[\sum_{j=1, j \neq k}^N \nabla_{y_j} W(t, y_k, m_\Phi^{N-1}(\mathbf{y}_{-k})) \bar{m}(t, y_j, m_\Phi^N(\mathbf{y})) \right. \right. \\
& \quad \left. \left. + \nabla_{y_k} W(t, y_k, m_\Phi^{N-1}(\mathbf{y}_{-k})) \hat{m}(t, y_k, m_\Phi^N(\mathbf{y})) \right] \right) \\
& \quad + \nabla_{y_i} W(t, y_i, m_\Phi^{N-1}(\mathbf{y}_{-i})) \left(f(t, y_i, m_\Phi^N(\mathbf{y})) \right. \\
& \quad \left. + \frac{1}{\hat{\alpha}} \hat{m}(t, y_i, m_\Phi^N(\mathbf{y})) \left[\sum_{j=1, j \neq i}^N \nabla_{y_j} W(t, y_i, m_\Phi^{N-1}(\mathbf{y}_{-i})) \bar{m}(t, y_j, m_\Phi^N(\mathbf{y})) \right. \right. \\
& \quad \left. \left. + \nabla_{y_i} W(t, y_i, m_\Phi^{N-1}(\mathbf{y})) \hat{m}(t, y_i, m_\Phi^N(\mathbf{y})) \right] \right. \\
& \quad \left. + \frac{1}{\hat{\alpha}} \bar{m}(t, y_i, m_\Phi^N(\mathbf{y})) \sum_{k=1, k \neq i}^N \left[\sum_{j=1, j \neq k}^N \nabla_{y_j} W(t, y_k, m_\Phi^{N-1}(\mathbf{y}_{-k})) \bar{m}(t, y_j, m_\Phi^N(\mathbf{y})) \right. \right. \\
& \quad \left. \left. + \nabla_{y_k} W(t, y_k, m_\Phi^{N-1}(\mathbf{y}_{-k})) \hat{m}(t, y_k, m_\Phi^N(\mathbf{y})) \right] \right) \\
& = l(t, y_i, m_\Phi^N(\mathbf{y})) + \frac{1}{2 \hat{\alpha}} \left[\sum_{j=1, j \neq i}^N \nabla_{y_j} W(t, y_i, m_\Phi^{N-1}(\mathbf{y}_{-i})) \bar{m}(t, y_j, m_\Phi^N(\mathbf{y})) \right. \\
& \quad \left. + \nabla_{y_i} W(t, y_i, m_\Phi^{N-1}(\mathbf{y}_{-i})) \hat{m}(t, y_i, m_\Phi^N(\mathbf{y})) \right]^2 \\
& \quad + \frac{\bar{\alpha}}{2 \hat{\alpha}^2} \sum_{k=1, k \neq i}^N \left[\sum_{j=1, j \neq k}^N \nabla_{y_j} W(t, y_k, m_\Phi^{N-1}(\mathbf{y}_{-k})) \bar{m}(t, y_j, m_\Phi^N(\mathbf{y})) \right. \\
& \quad \left. + \nabla_{y_k} W(t, y_k, m_\Phi^{N-1}(\mathbf{y}_{-k})) \hat{m}(t, y_k, m_\Phi^N(\mathbf{y})) \right]^2.
\end{aligned} \tag{31}$$

with terminal condition $W(T, y_i, m_\Phi^{N-1}(\mathbf{y}_{-i})) = p(t, y_i, m_\Phi^N(\mathbf{y}))$.

Corollary 3.4.1. *We assume that a unique solution of equation (31) exist (see assumption 5). Then any solution of the HJB system (30) can be obtained by the solution of (31).*

Proof. We define

$$V_i(t, \mathbf{y}) := W(t, y_i, m_\Phi^{N-1}(\mathbf{y}_{-i})), \quad i = 1, \dots, N,$$

and assume that W solves (31). We compute the partial derivatives of V_i and get:

$$\begin{aligned}
\partial_t V_i(t, \mathbf{y}) &= \partial_t W(t, y_i, m_\Phi^{N-1}(\mathbf{y}_{-i})), \\
\nabla_{y_i} V_i(t, \mathbf{y}) &= \nabla_{y_i} W(t, y_i, m_\Phi^{N-1}(\mathbf{y}_{-i})), \\
\nabla_{y_k} V_i(t, \mathbf{y}) &= \nabla_{y_k} W(t, y_i, m_\Phi^{N-1}(\mathbf{y}_{-i})), \quad k \neq i,
\end{aligned}$$

holds. Thus, we can identify all functions in equation (30) with the solution of equation (31). We then apply the definition of V_i and obtain (31). \square

Proper Scaling An important aspect which arises before we can derive the mean field limit of equation (31) is the scaling properties of the functions \hat{m} , \bar{m} and weights $\hat{\alpha}$, $\bar{\alpha}$ with respect to the number of agents N . We demand the functions f_i and L_i to be of order one to ensure the existence of the mean field limit.

Theorem 3.4.2. We assume that $f \sim \mathcal{O}(1)$, $p \sim \mathcal{O}(1)$ and $l \sim \mathcal{O}(1)$ holds. We consider how $\hat{\alpha}, \bar{\alpha}, \hat{m}$ and \hat{m} scale with respect to the number of agents N ; we consider $\frac{1}{N^\theta}$, $\theta \geq 0$ and obtain

$$\begin{aligned}\hat{m} &\sim \mathcal{O}\left(\frac{1}{N^\theta}\right), \\ \bar{m} &\sim \mathcal{O}\left(\frac{1}{N^{\theta+1}}\right), \\ \hat{\alpha} &\sim \mathcal{O}\left(\frac{1}{N^{2\theta}}\right), \\ \bar{\alpha} &\sim \mathcal{O}\left(\frac{1}{N^{2\theta+1}}\right),\end{aligned}$$

to ensure $f_i, L_i \sim \mathcal{O}(1)$.

Proof. First, we analyze the scales of the quantities f_i and L_i . The different sums of f_i asymptotically satisfy:

$$\begin{aligned}i) \frac{1}{\hat{\alpha}} \hat{m}(\tau, y_i, m_\Phi^N(\mathbf{y})) \nabla_{y_i} V_i(\tau, \mathbf{y}) \hat{m}(\tau, y_i, m_\Phi^N(\mathbf{y})) &\sim \frac{\hat{m}^2}{\hat{\alpha}}, \\ ii) \frac{1}{\hat{\alpha}} \hat{m}(\tau, y_i, m_\Phi^N(\mathbf{y})) \sum_{j=1, j \neq i}^N \nabla_{y_j} V_i(\tau, \mathbf{y}) \bar{m}(\tau, y_j, m_\Phi^N(\mathbf{y})) &\sim \frac{N \bar{m} \hat{m}}{\hat{\alpha}}, \\ iii) \frac{1}{\hat{\alpha}} \sum_{k=1, k \neq i}^N \bar{m}(\tau, y_k, m_\Phi^N(\mathbf{y})) \sum_{j=1, j \neq k}^N \nabla_{y_j} V_k(\tau, \mathbf{y}) \bar{m}(\tau, y_j, m_\Phi^N(\mathbf{y})) &\sim \frac{N^2 \bar{m}^2}{\hat{\alpha}}.\end{aligned}$$

Respectively, the sums of L_i satisfy:

$$\begin{aligned}iv) \frac{1}{\sqrt{2\hat{\alpha}}} \nabla_{y_i} V_i(\tau, \mathbf{y}) \hat{m}(\tau, y_i, m_\Phi^N(\mathbf{y})) &\sim \frac{\hat{m}}{\sqrt{\hat{\alpha}}}, \\ v) \frac{1}{\sqrt{2\hat{\alpha}}} \sum_{j=1, j \neq i}^N \nabla_{z_j} V_i(\tau, \mathbf{y}) \bar{m}(\tau, y_j, m_\Phi^N(\mathbf{y})) &\sim \frac{N \bar{m}}{\sqrt{\hat{\alpha}}}, \\ vi) \frac{\sqrt{N \bar{\alpha}}}{\sqrt{2\hat{\alpha}}} \sum_{j=1, j \neq k, j \neq i}^N \nabla_{y_j} V_k(\tau, \mathbf{y}) \bar{m}(\tau, y_j, m_\Phi^N(\mathbf{y})) &\sim \frac{N^{\frac{3}{2}} \bar{m} \sqrt{\bar{\alpha}}}{\hat{\alpha}}, \\ vii) \frac{\sqrt{N \bar{\alpha}}}{\sqrt{2\hat{\alpha}}} \nabla_{y_k} V_k(\tau, \mathbf{y}) \hat{m}(\tau, y_k, m_\Phi^N(\mathbf{y})) &\sim \frac{N^{\frac{1}{2}} \hat{m} \sqrt{\bar{\alpha}}}{\hat{\alpha}}.\end{aligned}$$

Since

$$\begin{aligned}\left(\frac{\hat{m}}{\sqrt{\hat{\alpha}}}\right)^2 &= \frac{\hat{m}^2}{\hat{\alpha}}, \\ \left(\frac{N \bar{m}}{\sqrt{\hat{\alpha}}}\right)^2 &= \frac{N^2 \bar{m}^2}{\hat{\alpha}},\end{aligned}$$

holds the quantities *i*) and *iv*), and *iii*) and *v*) are asymptotically identical. For an arbitrary but fixed $\theta \geq 0$ we assume that $\hat{m} \sim \mathcal{O}\left(\frac{1}{N^\theta}\right)$ holds.

We require that $\frac{\widehat{m}^2}{\alpha} = 1$ holds and thus $\widehat{\alpha} \sim \mathcal{O}\left(\frac{1}{N^{2\theta}}\right)$ has to hold.

In the same manner, fraction *iii*) determines \bar{m} to be $\bar{m} \sim \mathcal{O}\left(\frac{1}{N^{\theta+1}}\right)$.

Then, finally, with the help of the quantities *vi*) or *vii*), we can conclude $\bar{\alpha} \sim \mathcal{O}\left(\frac{1}{N^{2\theta+1}}\right)$ \square

Scaled global HJB equation The mean field limit is well defined in the previously introduced scaling. We want to state the corresponding HJB-equation. We set

$$\begin{aligned}\widehat{m} &= \frac{1}{N^\theta} \widehat{\bar{m}}, \quad \widehat{\bar{m}} \sim \mathcal{O}(1), \\ \bar{m} &= \frac{1}{N^{\theta+1}} \bar{\bar{m}}, \quad \bar{\bar{m}} \sim \mathcal{O}(1), \\ \widehat{\alpha} &= \frac{1}{N^{2\theta}}, \quad \widehat{\bar{\alpha}}, \quad \widehat{\bar{\alpha}} \sim \mathcal{O}(1), \\ \bar{\alpha} &= \frac{1}{N^{2\theta+1}} \bar{\bar{\alpha}}, \quad \bar{\bar{m}} \sim \mathcal{O}(1).\end{aligned}$$

We neglect the second superscript and get the following global HJB-equation.

$$\begin{aligned}&\partial_t W(t, y_i, m_\Phi^{N-1}(\mathbf{y}_{-i})) + \sum_{l=1, l \neq i}^N \nabla_{y_l} W(t, y_i, m_\Phi^{N-1}(\mathbf{y}_{-i})) \left(f(t, y_l, m_\Phi^N(\mathbf{y})) \right. \\&\quad \left. + \frac{\widehat{m}(t, y_l, m_\Phi^N(\mathbf{y}))}{\widehat{\alpha}} \left[\frac{1}{N} \sum_{j=1, j \neq l}^N \nabla_{y_j} W(t, y_l, m_\Phi^{N-1}(\mathbf{y}_{-l})) \bar{m}(t, y_j, m_\Phi^N(\mathbf{y})) \right. \right. \\&\quad \left. \left. + \nabla_{y_l} W(t, y_l, m_\Phi^{N-1}(\mathbf{y}_{-l})) \widehat{m}(t, y_l, m_\Phi^N(\mathbf{y})) \right] \right) \\&\quad + \frac{1}{\widehat{\alpha}} \bar{m}(t, y_l, m_\Phi^N(\mathbf{y})) \frac{1}{N} \sum_{k=1, k \neq l}^N \left[\frac{1}{N} \sum_{j=1, j \neq k}^N \nabla_{y_j} W(t, y_k, m_\Phi^{N-1}(\mathbf{y}_{-k})) \bar{m}(t, y_j, m_\Phi^N(\mathbf{y})) \right. \\&\quad \left. + \nabla_{y_k} W(t, y_k, m_\Phi^{N-1}(\mathbf{y}_{-k})) \widehat{m}(t, y_k, m_\Phi^N(\mathbf{y})) \right] \\&\quad + \nabla_{y_i} W(t, y_i, m_\Phi^{N-1}(\mathbf{y}_{-i})) \left(f(t, y_i, m_\Phi^N(\mathbf{y})) \right. \\&\quad \left. + \frac{1}{\widehat{\alpha}} \widehat{m}(t, y_i, m_\Phi^N(\mathbf{y})) \left[\frac{1}{N} \sum_{j=1, j \neq i}^N \nabla_{y_j} W(t, y_i, m_\Phi^{N-1}(\mathbf{y}_{-i})) \bar{m}(t, y_j, m_\Phi^N(\mathbf{y})) \right. \right. \\&\quad \left. \left. + \nabla_{y_i} W(t, y_i, m_\Phi^{N-1}(\mathbf{y})) \widehat{m}(t, y_i, m_\Phi^N(\mathbf{y})) \right] \right) \\&\quad + \frac{1}{\widehat{\alpha}} \bar{m}(t, y_i, m_\Phi^N(\mathbf{y})) \frac{1}{N} \sum_{k=1, k \neq i}^N \left[\frac{1}{N} \sum_{j=1, j \neq k}^N \nabla_{y_j} W(t, y_k, m_\Phi^{N-1}(\mathbf{y}_{-k})) \bar{m}(t, y_j, m_\Phi^N(\mathbf{y})) \right. \\&\quad \left. + \nabla_{y_k} W(t, y_k, m_\Phi^{N-1}(\mathbf{y}_{-k})) \widehat{m}(t, y_k, m_\Phi^N(\mathbf{y})) \right] \\&= l(t, y_i, m_\Phi^N(\mathbf{y})) + \frac{1}{2 \widehat{\alpha}} \left[\frac{1}{N} \sum_{j=1, j \neq i}^N \nabla_{y_j} W(t, y_i, m_\Phi^{N-1}(\mathbf{y}_{-i})) \bar{m}(t, y_j, m_\Phi^N(\mathbf{y})) \right. \\&\quad \left. + \nabla_{y_i} W(t, y_i, m_\Phi^{N-1}(\mathbf{y}_{-i})) \widehat{m}(t, y_i, m_\Phi^N(\mathbf{y})) \right]^2 \\&\quad + \frac{\widehat{\alpha}}{2 \widehat{\alpha}^2} \frac{1}{N} \sum_{k=1, k \neq i}^N \left[\frac{1}{N} \sum_{j=1, j \neq k}^N \nabla_{y_j} W(t, y_k, m_\Phi^{N-1}(\mathbf{y}_{-k})) \bar{m}(t, y_j, m_\Phi^N(\mathbf{y})) \right. \\&\quad \left. + \nabla_{y_k} W(t, y_k, m_\Phi^{N-1}(\mathbf{y}_{-k})) \widehat{m}(t, y_k, m_\Phi^N(\mathbf{y})) \right]^2.\end{aligned}\tag{32}$$

Mean Field Limit The empirical measure is a tool to perform the key computation in the derivation of the mean field limit. This key computation is the transformation of an an

empirical moment into an integral. We have:

$$\begin{aligned}
m_\Phi^N(\mathbf{y}) &= \frac{1}{N} \sum_{k=1}^N \Phi(y_k) \\
&= \frac{1}{N} \sum_{k=1}^N \int \Phi(t, y^1, \dots, y^d) \delta(y^1 - y_k^1) \cdot \dots \cdot \delta(y^d - y_k^d) dy^1 \dots dy^d \\
&= \int \Phi(t, y^1, \dots, y^d) \mu_{\mathbf{y}}^N(y^1, \dots, y^d) dy^1 \dots dy^d.
\end{aligned}$$

We can apply this transformation to our functions $f, \hat{m}, \bar{m}, l, q$. Notice that due to our transformation the functions depend on the measure $\mu_{\mathbf{y}}^N$. The empirical measure is defined on: $\mu_{\mathbf{y}}^N : \mathbb{R}^d \rightarrow \mathbb{R}$. In order to emphasize the transformation, we define new functions in calligraphic notation. Due to assumption 4, we obtain:

$$\begin{aligned}
f(t, y, m_\phi^N(\mathbf{y})) &= f\left(t, y, \int \phi(z) \mu_{\mathbf{y}}^N(z) dz\right) =: \mathcal{f}(t, y, \mu_{\mathbf{y}}^N), \\
\hat{m}(t, y, m_\phi^N(\mathbf{y})) &= \hat{m}\left(t, y, \int \phi(z) \mu_{\mathbf{y}}^N(z) dz\right) =: \widehat{\mathbf{m}}(t, y, \mu_{\mathbf{y}}^N), \\
\bar{m}(t, y, m_\phi^N(\mathbf{y})) &= \bar{m}\left(t, y, \int \phi(z) \mu_{\mathbf{y}}^N(z) dz\right) =: \bar{\mathbf{m}}(t, y, \mu_{\mathbf{y}}^N), \\
l(t, y, m_\phi^N(\mathbf{y})) &= l\left(t, y, \int \phi(z) \mu_{\mathbf{y}}^N(z) dz\right) =: \ell(t, y, \mu_{\mathbf{y}}^N), \\
p(t, y, m_\phi^N(\mathbf{y})) &= p\left(t, y, \int \phi(z) \mu_{\mathbf{y}}^N(z) dz\right) =: \rho(t, y, \mu_{\mathbf{y}}^N).
\end{aligned}$$

We set $y := y_i$ and can replace the function $f, \hat{m}, \bar{m}, l, p$ in the scaled global HJB eqation (32) by $\mathcal{f}, \widehat{\mathbf{m}}, \bar{\mathbf{m}}, \ell, \rho$. In the same manner, we can rewrite the solution W .

$$W(t, y, m_\phi^{N-1}(\mathbf{y}_{-i})) = W\left(t, y, \int \phi(z) \mu_{\mathbf{y}_{-i}}^{N-1}(z) dz\right) =: \mathcal{W}(t, y, \mu_{\mathbf{y}_{-i}}^{N-1}),$$

Additionally, we have to assume that

$$\mathcal{W}(t, y, \mu_{\mathbf{y}_{-i}}^{N-1}) \approx \mathcal{W}(t, y, \mu_{\mathbf{y}}^N),$$

holds for large N .

We still need to discuss the remaining mixed terms of the form

$$\sum_{j=1, j \neq i}^N \nabla_{y_j} \mathcal{W}(t, y_i, \mu_{\mathbf{y}}^N) \ell(t, y_j, \mu_{\mathbf{y}}^N), \quad (33)$$

for any functional $\ell : [0, T] \times \mathbb{R}^d \times \mathcal{P} \rightarrow \mathbb{R}^d$.

Remark 3.4.1. *The sum of mixed derivatives (33) can be interpreted as measure derivatives. We refer to [81] for a formal discussion. A mathematically rigorous introduction to measure-valued derivatives can be found in [10] or [41].*

We show that (33) can be interpreted as directional derivative of the empirical measure along a flow, defined by the vector field \mathcal{O} . We define the mean field characteristic flow $\gamma_{y_i} : [a, a + \Delta T] \rightarrow \mathbb{R}^d$ by

$$\begin{cases} \dot{\gamma}_{y_i}(s) = \mathcal{O}(s, \gamma_{y_i}(s), \mu_{\gamma_y}^N(s)), \\ \gamma_{y_i}(a) = y_i, \end{cases}$$

with $\gamma_y = (\gamma_{y_1}, \dots, \gamma_{y_N})^T \in \mathbb{R}^{dN}$. Then we can rewrite the sum (33):

$$\begin{aligned} \sum_{j=1, j \neq i}^N \nabla_{y_j} \mathcal{W}(t, y_i, \mu_y^N) \mathcal{O}(t, x_j, \mu_y^N) &\approx \sum_{j=1, j \neq i}^N \nabla_{y_j} \mathcal{W}(t, y_i, \mu_{y_{-i}}^{N-1}) \mathcal{O}(t, x_j, \mu_y^N) \\ &= \sum_{j=1, j \neq i}^N \nabla_{y_j} \mathcal{W}(t, y_i, \mu_{\gamma_{y_{-i}}(a)}^{N-1}) \mathcal{O}(t, \gamma_{x_j}, \mu_y^N) \\ &= \frac{d}{ds} \mathcal{W}(t, y_i, \mu_{\gamma_{y_{-i}}}^{N-1}(s)) \Big|_{s=a} \\ &\approx \frac{d}{ds} \mathcal{W}(t, y_i, \mu_{\gamma_y}^N(s)) \Big|_{s=a} \end{aligned}$$

Furthermore, the measure $\mu_{\gamma_y}^N(t, y) = \frac{1}{N} \sum_{k=1}^N \delta(y^1 - \gamma_{y_k}^1(t)) \dots \delta(y^d - \gamma_{y_k}^d(t))$ satisfies the following transport equation:

$$\partial_t g(t, y) + \operatorname{div}_y(\mathcal{O}(t, y, g(t, y))) g(t, y) = 0, \quad g(a, y) = \mu_y^N(y) = \mu_{\gamma_y(a)}^N(y). \quad (34)$$

This can be verified by the subsequent computation. For any test function $\phi(y)$ we have:

$$\begin{aligned} \frac{d}{dt} \langle \mu_{\gamma_y}^N(t, y), \phi(y) \rangle &= \frac{d}{dt} \left\langle \frac{1}{N} \sum_{k=1}^N \delta(y^1 - \gamma_{y_k}^1(t)) \dots \delta(y^d - \gamma_{y_k}^d(t)), \phi(y) \right\rangle \\ &= \frac{1}{N} \sum_{k=1}^N \frac{d}{dt} \phi(\gamma_{y_k}(t)) = \frac{1}{N} \sum_{k=1}^N \nabla_y \phi(\gamma_{y_k}(t)) \dot{\gamma}_{y_k}(t) \\ &= \frac{1}{N} \sum_{k=1}^N \nabla_y \phi(\gamma_{y_k}(t)) \mathcal{O}(t, \gamma_{y_k}(t), \mu_{\gamma_y}^N(t, y)) \\ &= \langle \mu_{\gamma_y}^N(t, y), \nabla_y(\phi(y)) \mathcal{O}(t, y, \mu_{\gamma_y}^N(t, y)) \rangle. \end{aligned}$$

Mean Field Equation and Mixed Derivatives If we have a look at the global HJB equation, we observe several terms of the form (33). Interestingly, there is a composition of such mixed terms but because our scaling the inner sum vanishes as the next proposition reveals.

Proposition 3.4.1. *We assume that the empirical measure $\mu_{\gamma_y}^N$ defined through the vector field \bar{m} converges to a absolutely continuous measure μ as $N \rightarrow \infty$. The term*

$$\frac{1}{N} \sum_{j=1, j \neq i}^{N-1} \nabla_{y_j} W(t, y_i, m_\Phi^{N-1}(\mathbf{y}_{-i})) \bar{m}(t, y_j, m_\Phi^N(\mathbf{y})),$$

vanishes as $N \rightarrow \infty$.

Proof. We have seen that we can rewrite the term $\bar{m}(t, y_j, m_\Phi^N(\mathbf{y}))$ with the help of the empirical measure to $\bar{m}(t, y_j, \mu_{\gamma_y}^N)$. We define the mean field characteristic flow defined through the vector field \bar{m} .

$$\begin{cases} \dot{\gamma}_{y_i}(s) = \bar{m}(s, \gamma_{y_i}(s), \mu_{\gamma_y}^N(s)), \\ \gamma_{y_i}(t) = y_i. \end{cases}$$

Then we can rewrite the sum accordingly to

$$\begin{aligned} \sum_{j=1, j \neq i}^N \nabla_{y_j} W(t, y_i, m_\Phi^{N-1}(\mathbf{y}_{-i})) \bar{m}(t, y_j, m_\Phi^N(\mathbf{y})) &= \frac{d}{ds} \mathcal{W}(t, y_i, \mu_{\gamma_{\mathbf{y}_{-i}}(s)}^{N-1})|_{s=t} \\ &\approx \frac{d}{ds} \mathcal{W}(t, y_i, \mu_{\gamma_y}^N(s))|_{s=t}, \end{aligned}$$

Then in the limit $N \rightarrow \infty$ we have:

$$\lim_{N \rightarrow \infty} \frac{1}{N} \frac{d}{ds} \mathcal{W}(t, y_i, \mu_{\gamma_y}^N(s))|_{s=t} = 0,$$

since $\frac{d}{ds} \mathcal{W}(t, y_i, \mu_{\gamma_y}^N(s))|_{s=t} \sim \mathcal{O}(1)$ and $\lim_{N \rightarrow \infty} \mu_{\gamma_y}^N = \mu$ holds. \square

The remaining mixed term in the global HJB equation is given by:

$$\begin{aligned} MT^N := & \sum_{l=1, l \neq i}^N \nabla_{y_l} W(t, y_i, m_\Phi^{N-1}(\mathbf{y}_{-i})) \left(f(t, y_l, m_\Phi^N(\mathbf{y})) \right. \\ & + \frac{\widehat{m}(t, y_l, m_\Phi^N(\mathbf{y}))}{\widehat{\alpha}} \left[\frac{1}{N} \sum_{j=1, j \neq l}^N \nabla_{y_j} W(t, y_l, m_\Phi^{N-1}(\mathbf{y}_{-l})) \bar{m}(t, y_j, m_\Phi^N(\mathbf{y})) \right. \\ & \quad \left. \left. + \nabla_{y_l} W(t, y_l, m_\Phi^{N-1}(\mathbf{y}_{-l})) \widehat{m}(t, y_l, m_\Phi^N(\mathbf{y})) \right] \right] \\ & + \frac{1}{N} \frac{\bar{m}(t, y_l, m_\Phi^N(\mathbf{y}))}{\widehat{\alpha}} \sum_{k=1, k \neq l}^N \left[\frac{1}{N} \sum_{j=1, j \neq k}^N \nabla_{y_j} W(t, y_k, m_\Phi^{N-1}(\mathbf{y}_{-k})) \bar{m}(t, y_j, m_\Phi^N(\mathbf{y})) \right. \\ & \quad \left. + \nabla_{y_k} W(t, y_k, m_\Phi^{N-1}(\mathbf{y}_{-k})) \widehat{m}(t, y_k, m_\Phi^N(\mathbf{y})) \right]. \end{aligned}$$

Proposition 3.4.2. *We assume that the empirical measure $\mu_{\gamma_y}^N$ defined by the flow-field \mathcal{F} :*

$$\begin{aligned} \mathcal{F}(t, y_i, \mu_{\gamma_y}^N) := & \mathcal{F}(t, y_i, \mu_{\gamma_y}^N) + \frac{1}{\widehat{\alpha}} \widehat{m}(t, y_i, \mu_{\gamma_y}^N) \nabla_{y_i} \mathcal{W}(t, y_i, \mu_{\gamma_y}^N) \\ & + \frac{1}{\widehat{\alpha}} \bar{m}(t, y_i, \mu_{\gamma_y}^N) \int \nabla_z \mathcal{W}(t, z, \mu_{\gamma_y}^N) \widehat{m}(t, z, \mu_{\gamma_y}^N) \mu_{\gamma_y}^N dz. \end{aligned}$$

converges to the probability density function g in the limit $N \rightarrow \infty$. We can interpret the term MT^N in the mean field limit $N \rightarrow \infty$ as directional derivative,

$$\lim_{N \rightarrow \infty} MT^N = \frac{d}{ds} \mathcal{W}(t, y, g(s, y))|_{s=t}.$$

where the density g is defined as the solution of the transport equation

$$\partial_t g(t, y) + \operatorname{div}_y(\mathcal{F}(t, y, g)) g(t, y) = 0.$$

Proof. We have seen that we can rewrite the terms $f(t, y_l, m_\Phi^N(\mathbf{y}))$, $\hat{m}(t, y_l, m_\Phi^N(\mathbf{y}))$, $\bar{m}(t, y_j, m_\Phi^N(t, \mathbf{y}))$ with the help of the empirical measure to the corresponding functionals $\ell(t, y_l, \mu_{\gamma_y}^N)$, $\widehat{m}(t, y_l, \mu_{\gamma_y}^N)$, $\bar{m}(t, y_j, \mu_{\gamma_y}^N)$. Furthermore, the term

$$\frac{\bar{m}(t, y_l, m_\Phi^N(\mathbf{y}))}{\hat{\alpha}} \frac{1}{N} \sum_{k=1, k \neq l}^N \nabla_{y_k} W(t, y_k, m_\Phi^{N-1}(\mathbf{y}_{-k})) \widehat{m}(t, y_k, m_\Phi^N(\mathbf{y})),$$

can be reformulated as:

$$\frac{\bar{m}(t, y_l, \mu_{\gamma_y}^N)}{\hat{\alpha}} \int \nabla_z \mathcal{W}(t, z, \mu_{\gamma_{y-l}}^{N-1}) \widehat{m}(t, z, \mu_{\gamma_y}^N) \mu_{\gamma_{y-l}}^{N-1} dz.$$

We then define the mean field characteristic flow γ_{y_i} as

$$\begin{cases} \dot{\gamma}_{y_i}(s) = \mathcal{F}(s, \gamma_{y_i}(s), \mu_{\gamma_y}^N(s)), \\ \gamma_{y_i}(t) = y_i. \end{cases}$$

We can apply the proposition 3.4.1 and can conclude that for large N

$$\sum_{j=1, j \neq i}^N \nabla_{y_j} W(t, y_i, m_\Phi^{N-1}(\mathbf{y}_{-i})) \bar{m}(t, y_j, m_\Phi^N(\mathbf{y})) \sim 0,$$

holds. Thus, we can conclude that for large N

$$MT^N \approx \frac{d}{ds} \mathcal{W}(t, y_i, \mu_{\gamma_y}^N(s))|_{s=t},$$

holds. Furthermore, the empirical measure satisfies the transport equations

$$\partial_t \mu_{\gamma_y}^N(t, y) + \nabla_y (\mathcal{F}(t, y, \mu_{\gamma_y}^N) \mu_{\gamma_y}^N(t, y)) = 0.$$

since

$$\begin{aligned} \frac{d}{dt} \langle \mu_{\gamma_y}^N(t, x), \phi(y) \rangle &= \frac{d}{dt} \left\langle \frac{1}{N} \sum_{k=1}^N \delta(y^1 - \gamma_{y_k}^1(t)) \dots \delta(y^d - \gamma_{y_k}^d(t)), \phi(y) \right\rangle \\ &= \frac{1}{N} \sum_{k=1}^N \frac{d}{dt} \phi(\gamma_{y_k}(t)) = \frac{1}{N} \sum_{k=1}^N \nabla_y \phi(\gamma_{y_k}(t)) \dot{\gamma}_{y_k}(t) \\ &= \frac{1}{N} \sum_{k=1}^N \nabla_y \phi(\gamma_{y_k}(t)) \mathcal{F}(t, \gamma_{y_k}(t), \mu_{\gamma_y}^N(t, y)) \\ &= \langle \mu_{\gamma_y}^N(t, y), \nabla_y (\phi(y)) \mathcal{F}(t, y, \mu_{\gamma_y}^N(t, y)) \rangle. \end{aligned}$$

holds for any test function ϕ . By assumption $\lim_{N \rightarrow \infty} \mu_{\gamma_y}^N(t, y) = g(t, y)$ and hence, we get

$$\lim_{N \rightarrow \infty} MT^N = \frac{d}{ds} \mathcal{W}(t, y, g(s, y))|_{s=t},$$

and the measure g satisfies the transport equation

$$\partial_t g(t, y) + \operatorname{div}_y (\mathcal{F}(t, y, g) g(t, y)) = 0.$$

□

Finally, we can state the mean field equation.

Theorem 3.4.3. *We assume that assumptions 1-6 are fulfilled. Furthermore, we assume that the empirical measure defined by our dynamics converges to the density function g in the mean field limit. Then, the limit equation of our dynamics is given by:*

$$\begin{aligned} \partial_t h(t, x) + \nabla_x h(t, x) & \left(\ell(t, x, g) + \frac{1}{\bar{\alpha}} \bar{m}(t, x, g) \int g(t, z) \widehat{m}(t, z, g) \nabla_z h(t, z) dz \right) \\ & = \ell(t, x, g) - \frac{1}{2 \bar{\alpha}} \left[\nabla_x h(t, x) \widehat{m}(t, x, g) \right]^2 \\ & \quad + \frac{\bar{\alpha}}{2 \bar{\alpha}^2} \int g(t, z) (\nabla_z h(t, z) \widehat{m}(t, z, g))^2 dz, \\ \partial_t g(t, x) + \operatorname{div}_x & \left(\left[\ell(t, x, g) + \frac{1}{\bar{\alpha}} (\widehat{m}(t, x, g))^2 \nabla_x h(t, x) \right. \right. \\ & \quad \left. \left. + \frac{1}{\bar{\alpha}} \bar{m}(t, x, g) \int g(t, z) \nabla_z h(t, z) \widehat{m}(t, z, g) dz \right] g(t, x) \right) = 0, \\ g(0, x) & = g_0, \quad h(T, x) = p(t, x, g). \end{aligned} \tag{35}$$

Proof. The term

$$\frac{1}{N} \sum_{k=1, k \neq l}^N \nabla_{y_k} W(t, y_k, m_\Phi^{N-1}(\mathbf{y}_{-k})) \widehat{m}(t, y_k, m_\Phi^N(\mathbf{y}))$$

can be rewritten with the empirical measure to

$$\int \nabla_z \mathcal{W}(t, z, \mu_{\mathbf{y}_{-l}}^{N-1}) \widehat{m}(t, z, \mu_{\mathbf{y}}^N) \mu_{\mathbf{y}_{-l}}^{N-1} dz.$$

Then we apply proposition 3.4.1 and 3.4.2 and in the limit $N \rightarrow \infty$ we obtain:

$$\begin{aligned} \partial_t \mathcal{W}(t, x, g) & + \frac{d}{ds} \mathcal{W}(t, x, g(s, x)) \Big|_{s=t} \\ & + \nabla_x \mathcal{W}(t, x, g) \left(f(t, x, \mu) + \frac{1}{\bar{\alpha}} (\widehat{m}(t, x, g))^2 \nabla_x \mathcal{W}(t, x, g) \right. \\ & \quad \left. + \frac{1}{\bar{\alpha}} \bar{m}(t, x, g) \int g(t, z) \widehat{m}(t, z, g) \nabla_z \mathcal{W}(t, z, g) dz \right) \\ & = l(t, x, g) + \frac{1}{2 \bar{\alpha}} \left[\nabla_x \mathcal{W}(t, x, g) \widehat{m}(t, x, g) \right]^2 \\ & \quad + \frac{\bar{\alpha}}{2 \bar{\alpha}^2} \int g(t, z) (\nabla_z \mathcal{W}(t, z, g) \widehat{m}(t, z, g))^2 dz. \end{aligned} \tag{36}$$

where g is defined by the transport equation

$$\partial_t g(t, x) + \operatorname{div}_x \left(\left[\ell(t, x, g) + \frac{1}{\bar{\alpha}} (\widehat{m}(t, x, g))^2 \nabla_x h(t, x) \right. \right. \tag{37}$$

$$\left. \left. + \frac{1}{\bar{\alpha}} \bar{m}(t, x, g) \int g(t, z) \nabla_z h(t, z) \widehat{m}(t, z, g) dz \right] g(t, x) \right) = 0. \tag{38}$$

We define $h(t, x) := \mathcal{W}(t, x, g(t, \cdot))$ and since

$$\partial_t h(t, x) = \partial_t \mathcal{W}(t, x, g(t, \cdot)) + \frac{d}{ds} \mathcal{W}(t, x, g(s, \cdot)) \Big|_{s=t},$$

holds, we finally obtain (35). \square

Discussion The previous derivation shows that the strategy $h(t, x)$ can be interpreted as the control of one agent $\partial_{x_i} V_i(t, \mathbf{x})$. All the coupling to other agents are translated into the measure derivative, respectively the transport equation. The right hand side of equation (36) is the cost of the optimization in the mean field limit. The left hand side of the mean field HJB equation can be interpreted as a total time-space derivative along the mean field characteristic, defined by the vector field \mathcal{F} . The mean field characteristic is the characteristic of our transport equation (37) and defines the evolution of the density function.

3.4.4 Examples

We want to discuss several examples to make connections of known MFG results and demonstrate the huge variety of our derived MFG model.

Vanishing Coupling We assume that $\widehat{m} \equiv 0, \bar{\alpha} \equiv 0$ holds or that $\widehat{m}, \bar{\alpha}$ scale such that they vanish in the mean field limit. Then the MFG system reads:

$$\begin{aligned}\partial_t h(t, x) + \mathcal{J}(t, x, g) \nabla_x h(t, x) &= \ell(t, x, g) \\ \partial_t g(t, x) + \operatorname{div}_x(\mathcal{J}(t, x, g) g(t, x)) &= 0, \\ g(0, x) = g_0, \quad h(T, x) &= \rho(t, x, g).\end{aligned}$$

In this setting, the transport equation does not depend on the strategy h of the agent. Thus, the game theoretic component vanishes. To our knowledge, this scale has not been discussed in the literature earlier and might be interesting in special applications.

Classical Coupling In this setting, we assume $\bar{m} \equiv 0, \bar{\alpha} \equiv 0$ or again an appropriate scale such that $\bar{m}, \bar{\alpha}$ vanish in the limit. Then we obtain:

$$\begin{aligned}\partial_t h(t, x) + \mathcal{J}(t, x, g) \nabla_x h(t, x) &= \ell(t, x, g) - \frac{1}{2\bar{\alpha}} (\widehat{m}(t, x, g) \nabla_x h)^2 \\ \partial_t g(t, x) + \operatorname{div}_x \left(\left(\mathcal{J}(t, x, g) + \frac{1}{\bar{\alpha}} (\widehat{m}(t, x, g))^2 \nabla_x h(t, x) \right) g(t, x) \right) &= 0, \\ g(0, x) = g_0, \quad h(T, x) &= \rho(t, x, g).\end{aligned}$$

We call this limit system the classical coupling because many MFG models in literature such as [81, 41] fall in this class.

New Coupling One scale which falls in our new model class is: $\bar{m}, \bar{\alpha} \sim \mathcal{O}\left(\frac{1}{N}\right)$, $\hat{m}, \hat{\alpha} \sim \mathcal{O}(1)$. This choice corresponds to $\theta = 0$ and we observe:

$$\begin{aligned} \partial_t h(t, x) + & \left(\ell(t, x, g) + \frac{1}{\hat{\alpha}} \bar{m}(t, x, g) \int g(t, z) \widehat{m}(t, z, g) \nabla_z h(t, z) dz \right) \nabla_x h(t, x) \\ & = \ell(t, x, g) - \frac{1}{2\hat{\alpha}} (\widehat{m}(t, x, g) \nabla_x h)^2 \\ & + \frac{\bar{\alpha}}{2 \hat{\alpha}^2} \int g(t, z) (\nabla_z \mathcal{W}(t, z, g) \widehat{m}(t, z, g))^2 dz, \\ \partial_t g(t, x) + \operatorname{div}_x & \left(\left(\ell(t, x, g) + \frac{1}{\hat{\alpha}} (\widehat{m}(t, x, g))^2 \right) \nabla_x h(t, x) \right. \\ & \left. + \frac{1}{\hat{\alpha}} \bar{m}(t, x, g) \int g(t, z) \nabla_z h(t, z) \widehat{m}(t, z, g) dz \right) g(t, x) = 0, \\ g(0, x) = g_0, \quad h(T, x) & = p(t, x, g). \end{aligned}$$

A Financial Market Model In this section, we give an explicit example of our *new coupling* considered previously. Inspired by the econophysical Levy-Levy-Solomon model [154], we consider N financial agents. Each agent is equipped with two portfolios, one portfolio represents the investment in a risky stock, the other the investment in safe bonds. The sum of the risky investments $x \in \mathbb{R}_{\geq 0}$ and the risk-free investments $y \in \mathbb{R}_{\geq 0}$ is the overall wealth of the i -th agent $w_i := x_i + y_i$, $i = 1, \dots, N$. The system reads:

$$\begin{aligned} \dot{x}_i &= \theta \frac{\dot{S} + D}{S} x_i + u_i^*, \\ \dot{y}_i &= r y_i - u_i^*, \\ S &:= \lambda \frac{1}{N} \sum_{k=1}^N x_k, \\ u_i^* &= \underset{u_i: [0, T] \rightarrow \mathbb{R}}{\operatorname{argmax}} - \int_t^T \sum_{k=1}^N l_i^k(s, \mathbf{x}) + \frac{\alpha}{2} u_i^2 ds. \end{aligned}$$

Here, $\mathbf{x} := (x_1, \dots, x_N)^T \in \mathbb{R}^N$ and $r, D > 0$, $\lambda, \theta \in (0, 1)$ are positive constants. We denote by $S \in \mathbb{R}_{\geq}$ the stock price where D symbolizes a dividend. Furthermore, is r the interest rate of the safe asset, λ the market depth and θ expresses transaction costs.

Before we can derive the limit system, we need an explicit ODE for the risky portfolio. We define $e := (1, \dots, 1)^T \in \mathbb{R}^N$, $I := \operatorname{diag}(1) \in \mathbb{R}^{N \times N}$ and rewrite our risky asset equation:

$$\begin{aligned} \dot{\mathbf{x}} &= \operatorname{diag}(\theta) \frac{\frac{\lambda}{N} e^T \dot{\mathbf{x}} + D}{\frac{\lambda}{N} e^T \mathbf{x}} \mathbf{x} + \mathbf{u} \\ \left(I - \underbrace{\operatorname{diag}(\theta) \frac{\mathbf{x} e^T}{e^T \mathbf{x}}}_{=: P(\mathbf{x})} \right) \dot{\mathbf{x}} &= \operatorname{diag} \theta \frac{D}{\frac{\lambda}{N} e^T \mathbf{x}} \mathbf{x} + \mathbf{u} \end{aligned}$$

The matrix P is a rank one matrix and $\|P\|_1 = \theta < 0$ holds. Hence, the inverse of $\Sigma(\mathbf{x}) := I - P(\mathbf{x})$ exists and has a Neumann series expansion. We get:

$$\Sigma^{-1}(\mathbf{x}) = \sum_{k=0}^N P^k(\mathbf{x}) = I + \sum_{k=0}^N \alpha^k P(\mathbf{x}) = I + \frac{1}{1-\alpha} P(\mathbf{x}), \quad \alpha := \text{trace}(P(\mathbf{x})) = \theta.$$

Thus, the explicit stock ODE is given by:

$$\dot{\mathbf{x}} = \frac{D}{\frac{\lambda}{N} e^T \mathbf{x}} \Sigma^{-1}(\mathbf{x}) \text{ diag}(\theta) \mathbf{x} + \Sigma^{-1}(\mathbf{x}) \mathbf{u}.$$

For the i -th agent we observe:

$$\begin{aligned} \dot{x}_i &= \left(c_1 + c_2 \frac{1}{N} \sum_{k=1}^N u_k^* \right) \frac{x_i}{\frac{1}{N} \sum_{k=1}^N x_k} + u_i^*, \\ \dot{y}_i &= r y_i - u_i^*, \\ u_i^* &= \underset{u_i: [0,T] \rightarrow \mathbb{R}}{\text{argmax}} - \int_t^T \sum_{k=1}^N l_i^k(s, \mathbf{x}) + \frac{\alpha}{2} u_i^2 ds, \end{aligned}$$

where the constants c_1, c_2 are defined by: $c_1 := (1 + \frac{\theta}{1-\theta}) \theta \frac{D}{\lambda}, c_2 := \frac{\theta}{1-\theta}$. As one can immediately observe does this model fit into our framework. We check the symmetry assumptions and define the corresponding quantities.

$$\begin{aligned} f(x_i, \mathbf{x}_{-i}, y_i, \mathbf{y}_{-i}) &= \left(c_1 \frac{x_i}{\frac{1}{N} \sum_{k=1}^N x_k}, r y_i \right)^T, \\ M_i^i = \hat{m} &= \left(c_2 \frac{x_i}{\frac{1}{N} \sum_{k=1}^N x_k} \frac{1}{N} + 1, -1 \right)^T \in \mathcal{O}(1), \\ M_{k,k \neq i}^i = \bar{m} &= \left(c_2 \frac{x_i}{\frac{1}{N} \sum_{k=1}^N x_k} \frac{1}{N}, 0 \right)^T \in \mathcal{O}\left(\frac{1}{N}\right), \quad \bar{\alpha} \equiv 0, p \equiv 0 \quad k, i = 1, \dots, N. \end{aligned}$$

Due to the scaling properties the limit system reads:

$$\begin{aligned} \partial_t h(t, x, y) + \partial_x h(t, x, y) &\left(c_1 \frac{x}{\int z_1 f(t, z_1, z_2) dz_1 dz_2} \right. \\ &+ \left. \frac{c_2 x}{\alpha \int z_1 g(t, z_1, z_2) dz_1 dz_2} \int g(t, z_1, z_2) (\partial_{z_1} h(t, z_1, z_2) - \partial_{z_2} h(t, z_1, z_2)) dz_1 dz_2 \right) \\ &+ \partial_y h(t, x, y) r y = \ell(t, x, y, g) - \frac{1}{2\alpha} (\partial_x h(t, x, y) - \partial_y h(t, x, y))^2, \\ \partial_t g(t, x, y) + \partial_x \left(\left[c_1 \frac{x}{\int z_1 g(t, z_1, z_2) dz_1 dz_2} + \frac{1}{\alpha} (\partial_x h(t, x, y) - \partial_y h(t, x, y)) \right. \right. \\ &+ \left. \left. \frac{c_2 x}{\alpha \int z_1 g(t, z_1, z_2) dy dx} \int g(t, z_1, z_2) (\partial_{z_1} h(t, z_1, z_2) - \partial_{z_2} h(t, z_1, z_2)) dz_1 dz_2 \right] g(t, x, y) \right) \\ &+ \partial_y \left(\left[r y + \frac{1}{\alpha} (\partial_y h(t, x, y) - \partial_x h(t, x, y)) \right] g(t, x, y) \right) = 0. \end{aligned}$$

Simplified Model We simplify the previous model only by considering the risky portfolio. This might be realistic since the prime rate of many national banks are zero. Our microscopic system simplifies to:

$$\begin{aligned}\dot{x}_i &= \theta \frac{\dot{S} + D}{S} x_i + u_i^*, \\ S &:= \lambda \frac{1}{N} \sum_{k=1}^N x_k, \\ u_i^* &= \underset{u_i: [0, T] \rightarrow \mathbb{R}}{\operatorname{argmax}} - \int_t^T \sum_{k=1}^N l_i^k(s, \mathbf{x}) + \frac{\alpha}{2} u_i^2 ds.\end{aligned}$$

The explicit ODE system is then given by:

$$\begin{aligned}\dot{x}_i &= \left(c_1 + c_2 \frac{1}{N} \sum_{k=1}^N u_k^* \right) \frac{x_i}{\frac{1}{N} \sum_{k=1}^N x_k} + u_i^*, \\ u_i^* &= \underset{u_i \in \mathbb{R}}{\operatorname{argmax}} - \int_t^T \sum_{k=1}^N l_i^k(s, \mathbf{x}) + \frac{\alpha}{2} u_i^2 ds,\end{aligned}$$

The limit system is given by:

$$\begin{aligned}\partial_t h(t, x) + \partial_x h(t, x) &\left(c_1 \frac{x}{\int z g(t, z) dz} + \frac{c_2}{\alpha} \frac{x}{\int z g(t, z) dz} \int g(t, z) \partial_z h(t, z) dz \right) \\ &= \ell(t, x, g) - \frac{1}{2\alpha} (\partial_x h(t, x))^2, \\ \partial_t g(t, x) + \partial_x &\left(\left[c_1 \frac{x}{\int z g(t, z) dz} + \frac{1}{\alpha} \partial_x h(t, x) \right. \right. \\ &\quad \left. \left. + \frac{c_2}{\alpha} \frac{x}{\int z g(t, z) dz} \int g(t, z) \partial_z h(t, z) dz \right] g(t, x) \right) = 0.\end{aligned}$$

Discussion of financial market model This microscopic financial market model can be regarded as the rational version of kinetic portfolio optimization model introduced in [243]. In this context, rational means that the financial agents solve their optimization problem exactly. The model introduced in [243] considers boundedly rational agents in the sense of Simon [215]. Mathematically, the investors simplify their optimization problem with the help of model predictive control. The authors prove that the model can generate well known features of financial markets such as booms and crashes and fat-tails in asset returns. In economic research, there is an ongoing discussion if these phenomena, called stylized facts have their origin in the irrational behavior of market participants. A detailed analysis of the introduced rational portfolio model might help to answer this question. The elaborate discussion of this highly non-linear model is left open for further research.

3.4.5 Conclusion

In this study, we derived the MFG limit system out of microscopic dynamics. We have shown that it is possible to apply MFG theory to an important class of microscopic differential games. In addition, we have seen that the symmetry and the scaling behavior of our microscopic model is crucial in order to perform the limit. As demonstrated in the example section, it is possible to derive many different MFG models out of the discussed setting. Finally, we have shown that financial market models are a prototype candidate for MFG applications. Furthermore, this example motivates the discovery of new scales, we have conducted in this study.

We want to underline that all results of this study are on a formal level. Nevertheless, we believe that this work shows the great applicability of MFG theory to a large class of microscopic systems. We hope that this work clarifies the derivation of complex MFG models and furthermore enables the reader to apply MFG theory to a broad area of applications.

Reasonable extensions are the generalization of the microscopic differential game model. Such a new setting might include an infinite horizon optimization or stochastic state dynamics.

4 Portfolio Optimization and Model Predictive Control

In this paper, we introduce a large system of interacting financial agents in which each agent is faced with the decision of how to allocate his capital between a risky stock or a risk-less bond. The investment decision of investors, derived through an optimization, drives the stock price. The model has been inspired by the econophysical Levy-Levy-Solomon model [155]. The goal of this work is to gain insights into the stock price and wealth distribution. We especially want to discover the causes for the appearance of power-laws in financial data. We follow a kinetic approach similar to [166] and derive the mean field limit of our microscopic agent dynamics. The novelty in our approach is that the financial agents apply model predictive control (MPC) to approximate and solve the optimization of their utility function. Interestingly, the MPC approach gives a mathematical connection between the two opponent economic concepts of modeling financial agents to be rational or boundedly rational. We derive a moment model which is able to replicate the most prominent features of the financial markets: oscillatory price behavior, booms and crashes. Due to our kinetic approach, we can study the wealth and price distribution on a mesoscopic level. The wealth distribution is characterized by a lognormal law. For the stock price distribution, we can either observe a lognormal behavior in the case of long-term investors or a power-law in the case of high-frequency trader. Furthermore, the stock return data exhibits a fat-tail, which is a well known characteristic of real financial data.

4.1 Introduction

The question of allocating capital between a risky and risk-less asset is a well-known issue for private and institutional investors. This research question has a long tradition in economics: for example the famous works of Markowitz [174] or Merton [179, 180].

Another research field which has received a lot of attention in the last decade is the modeling of financial markets. Several financial crashes (Black Monday 1987, Dot-com Bubble 2000, Global Financial Crisis 2007) have shown that classical financial market models fail to replicate financial data properly [61, 102]. Since the 1970s, econometricians have detected empirical artifacts in financial data known as *stylized facts*. Stylized facts are universal statistical properties of financial data which can be observed all over the world [62]. The most prominent examples are: booms and crashes of stock prices, the inequality of wealth and fat-tails in the stock return distribution. Several researchers point out that stylized facts play an important role in the creation of financial crisis [162, 222]. For that reason, the discovery of the origin of stylized facts has become a prospering field of economic research. Up to now, this question could only be answered partially and remains widely open [195].

First attempts to discover the origin of stylized facts were made by agent-based financial market models. These models consider a large number of interacting financial agents and share more similarities with particle models in physics than with classical asset-pricing models [164, 222]. These models use tools from statistical physics like Monte Carlo simulations and are part of the new research field econophysics. Major contributions in this field are [155, 164, 209, 64, 121]. These complex systems of interacting agents are not only inspired by physical theories but also by behavioral finance. Thus, the agents are modeled to be boundedly rational in the sense of Simon [212]. These modern market models are capable of reproducing stylized facts. In physics, one might call stylized facts scaling laws [164], which is

the motivation to apply tools from physics onto financial models. Numerical experiments of agent-based models indicate that psychological misperceptions of investors can be accounted to be one reason for the appearance of stylized facts [71, 162].

The disadvantage of these particle models is the need to study the complex behavior empirically through computer simulations. In addition, many studies have shown [93, 254, 143, 119] that in several agent-based models stylized facts are caused by finite-size effects of the model and are thus only numerical artifacts. To overcome these problems, it is possible to derive kinetic PDE models out of the microscopic particle models, which give us the possibility to study the appearance of stylized facts analytically. There are several examples of such a kinetic approach [166, 34, 67, 66, 88, 175, 25].

The starting point of our work is an agent-based model of financial agents who want to optimize their investment decision. They are faced with the decision of how to allocate their capital in a risky stock or a risk-less bond. To determine the investment strategy, the agents minimize the badness of their portfolio where they estimate the future stock return by a convex combination of a fundamental and chartist return estimate. The stock price is driven by the aggregated demand of financial agents. To fix the stock price, we use a relaxation of Walras equilibrium law [250], utilized in many econophysical models [19, 71, 164]. The microscopic model is inspired by the famous Levy-Levy-Solomon model [154, 155]. Further closely related agent-based models are [60, 38]. One novelty of our model is to apply model predictive control (MPC) to simplify the optimization process and derive the investment decision of agents. This methodology, often applied in the engineering community, has been recently applied to a kinetic opinion formation model [4] but, to our knowledge, never before to a kinetic financial market model. We consider a large system of coupled constrained optimization problems. In order to reduce this system to a set of ordinary differential equations (ODEs), we introduce the game-theoretic concept of Nash equilibria and apply MPC. From the perspective of agent modeling, we first consider rational financial agents and derive through the MPC approach boundedly rational agents.

Mathematically, we perform the mean field limit of our microscopic model to derive a mesoscopic description of our dynamics. This means that we look at the limiting case of infinitely many agents and instead of considering each agent individually we can study the dynamics through probability densities. This limit often provides us with Fokker-Planck type equations which enable us to derive analytic solutions and study the long time behavior of our model. This work is closely related to the kinetic financial market model of Maldarella and Pareschi [166]. Besides other approaches, we apply the Boltzmann methodology as performed in [166] and well described in [198] to derive a Fokker-Planck model. We want to point out that, to our knowledge, this is the first model which translates a portfolio model in a kinetic PDE model and consequently considers a wealth and a stock price evolution. We thus are able to analyze the wealth and stock price distribution simultaneously and thus study possible interrelations.

We consider three modeling stages. First, we consider a deterministic model and derive the mean field limit. In addition, we derive a macroscopic moment model which describes the evolution of the stock prices and the average amount of wealth in stocks and bonds. We show

that the stock price evolution can create oscillatory solutions, booms and crashes and can thus replicate prominent characteristics of financial markets.

Secondly, we add noise to the investment decision of investors and study the outcome on the mesoscopic level. At the final modeling stage, we introduce a new population of financial brokers, equipped with microscopic stock prices. These stock prices are modeled as stochastic differential equations (SDEs). In the mean field limit of infinitely many brokers, we observe a Fokker-Planck equation. This enables us to study the stock price distribution. We distinguish between long-term investors and high-frequency trader. In the case of long-term investors, the stock price distribution is of lognormal type, whereas in the case of high-frequency trader we observe an inverse-gamma distribution. The same distribution has been previously discovered in other financial market models [166, 34, 67]. We want to point out that the inverse-gamma distribution asymptotically satisfies a power-law for large stock prices. In addition, we show numerically that the stock return distributions have a fat-tail. Finally, we want to emphasize that we can observe in all of our models a wealth or portfolio distribution of normal or log-normal type. This is an interesting result, as one might expect to observe a power-law in the portfolio, presumed one has a power-law in the stock return distribution.

The outline of our paper is as follows: in the next section, we first define the microscopic portfolio model. We then apply the MPC approach to simplify the optimization and derive the investment decision of each financial agent. Then, we derive the mean field limit equation in section three and analyze the portfolio distribution. In addition, we derive a moment model which we discuss analytically and numerically. As a next step, we extend our model by adding noise to the investment decision and analyze the resulting PDE-ODE system. In section six, we introduce a population of broker, so that the microscopic stock prices are described by a stochastic process. As it has been done for the previous modeling stages, we perform the mean field limit in order to analyze the stock price distribution. In section seven, we give numerical examples of our model and verify our previous computations. We finish the paper with a short discussion of our results and possible model extensions.

4.2 Microscopic Model

We consider N financial agents equipped with their personal monetary wealth $w_i \geq 0$. We assume non-negative wealth, and thus do not allow debts. The agents have to allocate their wealth between a risky asset (stock) and a risk-free asset (bond). The wealth in the risky asset is denoted by $x_i \geq 0$ and the wealth in the risk-free asset by $y_i \geq 0$. Thus, the wealth of the i -th agent at time $t > 0$ is given by $w_i(t) = x_i(t) + y_i(t)$.

The time evolution of the risk-free asset is described by a fixed non-negative interest rate $r \geq 0$ and the evolution of the risky asset by the stock return,

$$\frac{\dot{S}(t) + D(t)}{S(t)},$$

where $S(t)$ is the stock price at time t and $D(t) \geq 0$ the dividend. We denote all macroscopic quantities with capital letters. For now, we assume that the stock price and the dividend are given and that the stock price is a differentiable function of time. The agent can shift capital between the two assets. We denote the shift from bonds into stocks by u_i . Thus we have the

dynamics

$$\begin{aligned}\dot{x}_i(t) &= \frac{\dot{S}(t) + D(t)}{S(t)} x_i(t) + u_i(t) \\ \dot{y}_i(t) &= r y_i(t) - u_i(t).\end{aligned}$$

We still need to describe the time evolution of the stock price S . The investment decisions of the agents drive the price through the excess demand

$$ED_N(t) := \frac{1}{N} \sum_{i=1}^N u_i(t).$$

The excess demand is positive if the investors buy more stocks than they sell. Thus the **macroscopic stock price evolution** is given by

$$\dot{S}(t) = \kappa ED_N(t) S(t). \quad (39)$$

where the constant $\kappa > 0$ measures the market depth. This model for the stock price is commonly accepted among economists. The ODE (39) can be interpreted as a relaxation of the well known equilibrium law, supply equals demand, dating back to the economist Walras [250].

Investment strategy Next, we describe how an agent determines his investment strategy. As in classical economic theory, u_i will be a solution of a risk or cost minimization. First, in order to make an investment decision, an agent has to estimate future returns. We take two possible strategies into account, a chartist estimate and a fundamentalist estimate. The estimates need to depend on the current stock price.

Fundamentalists believe in a fundamental value of the stock price denoted by $s^f > 0$ and assume that the stock price will converge in the future to this specific value. The investor therefore estimates the future return of stocks versus the return of bonds as

$$K^f := U_\gamma \left(\omega \frac{s^f - S}{S} \right) - r.$$

Here, U_γ is a value function in the sense of Kahnemann and Tversky [134] which depends on the risk tolerance γ of an investor. A typical example is $U_\gamma(x) = sgn(x)|x|^\gamma$ with $0 < \gamma < 1$ and sign function sgn . The constant $\omega > 0$ measures the expected speed of mean reversion to the fundamental value s^f of fundamental. We want to point out that this stock return estimate is a rate and thus ω needs to scale with time.

Chartists assume that the future stock return is best approximated by the current or past stock return. They estimate the return rate of stocks over bonds by

$$K^c := U_\gamma \left(\frac{\dot{S}/\rho + D}{S} \right) - r.$$

The constant $\rho > 0$ measures the frequency of exchange rates [166]. Both estimates are aggregated into one estimate of stock return over bond return by a convex combination

$$K = \chi K^f + (1 - \chi) K^c.$$

This idea has been previously applied to a kinetic model of opinion formation [5]. The weight χ is determined from an instantaneous comparison as modeled in [164]. We let

$$\chi = W(K^f - K^c),$$

where $W : \mathbb{R} \rightarrow [0, 1]$ is a continuous function. If for example, $W = \frac{1}{2}\tanh + \frac{1}{2}$, the investor optimistically believes in the higher estimate. Together, if $K > 0$, the investor believes that stocks will perform better and if $K < 0$ that bonds will perform better.

Objective function Next, we can define the minimization problem that determines the agent's actions. We define the “badness” of the portfolio by

$$\Psi_i := \begin{cases} |K| \frac{x_i^2}{2}, & K < 0, \\ 0, & K = 0, \\ |K| \frac{y_i^2}{2}, & K > 0, \end{cases}$$

which can be conveniently rewritten to $\Psi_i = K \cdot \left(-H(-K) \frac{x_i^2}{2} + H(K) \frac{y_i^2}{2} \right)$, where H is the Heaviside step function, zero at the origin. If stocks are believed to be better ($K > 0$), then being invested in bonds ($y_i > 0$) is bad, and vice versa. The badness is larger, the larger the estimated difference between returns K . The agent tries to minimize the running costs

$$\int_0^T \left(\frac{\mu}{2} u_i(t)^2 + \Psi_i(t) \right) dt.$$

We consider a finite time interval $[0, T]$ and have added a penalty term that punishes transactions. The penalty term is necessary to convexify the problem but is also reasonable, because it describes transaction costs. The transaction costs are modeled to be quadratic which is an often used assumption in portfolio optimization [24, 186].

Hence, in summary, our microscopic model is given by

$$\dot{x}_i(t) = \frac{\dot{S}(t) + D(t)}{S(t)} x_i(t) + u_i^*(t) \quad (40a)$$

$$\dot{y}_i(t) = r y_i(t) - u_i^*(t) \quad (40b)$$

$$\dot{S}(t) = \kappa E D_N(t) S(t) \quad (40c)$$

$$u_i^* := \underset{u_i: [0, T] \rightarrow \mathbb{R}}{\operatorname{argmax}} \int_0^T \left(\frac{\mu}{2} u_i(t)^2 + \Psi_i(t) \right) dt. \quad (40d)$$

The microscopic model is an optimal control problem. The dynamics are strongly coupled by the stock price in a non-linear fashion. Since all investors want to minimize their individual badness function, one needs to solve the optimal control problem in a game-theoretic context. We choose the concept of Nash equilibria which will be explained in detail in the next section.

4.3 MPC for Microscopic Model

In case of many agents, we have a large system of optimization problems (40). Such a system is very expensive to solve. For that reason, we approximate the objective functional (40d) by model-predictive control (MPC). In the MPC framework, one assumes that the investor only

optimizes on the time interval $[\bar{t}, \bar{t} + \Delta t]$ for a small $\Delta t > 0$ and fixed \bar{t} . One thus assumes that one can approximate the control u on $[0, T]$ by piecewise constant functions on time intervals of length Δt . We can only expect to observe a suboptimal strategy since we perform an approximation of (40d).

We choose the penalty parameter μ in the running costs to be proportional to the time interval so that $\mu = \nu \Delta t$ for some ν . This can be motivated by checking the units of the variables in the cost functional (K is a rate, thus measured in 1/time, Ψ is wealth²/time, u wealth/time). We see that the penalty parameter μ must be a time unit. Furthermore, we insert the right-hand side of the stock price equation into the stock return. Thus, the constrained optimization problem reads

$$\begin{aligned} & \int_{\bar{t}}^{\bar{t}+\Delta t} \left(\frac{\nu \Delta t}{2} u_i^2(t) + \Psi_i(t) \right) dt \rightarrow \min \\ & \dot{x}_i(t) = \kappa ED_N(t) x_i(t) + \frac{D(t)}{S(t)} x_i(t) + u_i(t), \quad x_i(\bar{t}) = \bar{x}_i, \\ & \dot{y}_i(t) = r y_i(t) - u_i(t), \quad y_i(\bar{t}) = \bar{y}_i, \\ & \dot{S}(t) = \kappa ED_N(t) S(t), \quad S(\bar{t}) = \bar{S}. \end{aligned}$$

Game theoretic setting We want to solve our MPC problem in a game theoretic setting. All agents are coupled by the stock price respectively excess demand ED_N . As pointed out previously, it is impossible that all agents act optimal since all agents play a game against each other. In fact, we are faced with a noncooperative differential game. Thus, a reasonable equilibrium concept is needed to solve our optimal control problem. We want to search for Nash equilibria. In this setting, each agent assumes that the strategies of the other players are fixed and optimal. Thus, we get N optimization problems which need to be solved simultaneously. Hence, we have a N -dimensional Lagrangian $L \in \mathbb{R}^N$. The i -th entry L_i corresponds to the i -th player and reads:

$$\begin{aligned} L_i(x_i, y_i, S, u_i, \lambda_{x_i}, \lambda_{y_i}, \lambda_S) = & \int_{\bar{t}}^{\bar{t}+\Delta t} \left(\frac{\nu \Delta t}{2} u_i^2(t) + \Psi_i(t) \right) dt \\ & + \int_{\bar{t}}^{\bar{t}+\Delta t} \dot{\lambda}_{x_i} x_i + \lambda_{x_i} \kappa ED_N x_i + \lambda_{x_i} \frac{D}{S} x_i + \lambda_{x_i} u_i dt - \lambda_{x_i} \bar{x}_i \\ & + \int_{\bar{t}}^{\bar{t}+\Delta t} \dot{\lambda}_{y_i} y_i + \lambda_{y_i} r y_i - \lambda_{y_i} u_i dt - \lambda_{y_i} \bar{y}_i, \\ & + \int_{\bar{t}}^{\bar{t}+\Delta t} \dot{\lambda}_S S + \lambda_S \kappa ED_N S dt - \lambda_S \bar{S}, \end{aligned}$$

with Lagrange multiplier $\lambda_{x_i}, \lambda_{y_i}, \lambda_S$. Notice that the quantities (x_j^*, y_j^*, u_j^*) , $j = 1, \dots, i-1, i+1, \dots, N$ are assumed to be optimal in the i -th optimization and therefore only enter as

parameters in the i -th Lagrangian L_i . We assume $\lambda_{x_i}(\bar{t} + \Delta t) = \lambda_{y_i}(\bar{t} + \Delta t) = \lambda_S(\bar{t} + \Delta t) = 0$ and thus the optimality conditions are given by

$$\begin{aligned}\dot{x}(t) &= \kappa ED_N(t) x_i(t) + \frac{D(t)}{S(t)} x_i + u_i, \quad x_i(\bar{t}) = \bar{x}_i, \\ \dot{y}_i(t) &= r y_i(t) - u_i(t), \quad y_i(\bar{t}) = \bar{y}_i, \\ \dot{S}(t) &= \kappa ED_N(t) S(t), \quad S(\bar{t}) = \bar{S}, \\ \nu \Delta t u_i(t) &= -\lambda_{x_i}(t) - \lambda_{x_i}(t) \frac{\kappa}{N} x_i(t) + \lambda_{y_i}(t) - \frac{\kappa}{N} S(t) \lambda_S(t), \\ \dot{\lambda}_{x_i}(t) &= -\kappa ED_N(t) \lambda_{x_i}(t) - \frac{D(t)}{S(t)} \lambda_{x_i}(t) - \partial_{x_i} \Psi_i(t), \\ \dot{\lambda}_{y_i}(t) &= -r \lambda_{y_i}(t) - \partial_{y_i} \Psi_i(t), \\ \dot{\lambda}_S(t) &= \lambda_{x_i}(t) \frac{D(t)}{S^2(t)} x_i - \kappa ED_N(t) \lambda_S(t) - \partial_S \Psi_i(t).\end{aligned}$$

Then we apply a backward Euler discretization to the adjoint equations and get

$$\begin{aligned}\lambda_{x_i}(\bar{t}) &= \Delta t \partial_{x_i} \Psi_i(\bar{t} + \Delta t), \\ \lambda_{y_i}(\bar{t}) &= \Delta t \partial_{y_i} \Psi_i(\bar{t} + \Delta t), \\ \lambda_S(\bar{t}) &= \Delta t \partial_S \Psi_i(\bar{t} + \Delta t).\end{aligned}$$

Hence, the optimal strategy is given by

$$u_N^*(x_i, y_i, S) = \begin{cases} \frac{1}{\nu} (K y_i - \frac{\kappa}{N} S (\partial_S K) \frac{y_i^2}{2}), & K > 0, \\ 0, & K = 0, \\ \frac{1}{\nu} (K x_i + K \frac{\kappa}{N} x_i^2 + \frac{\kappa}{N} S (\partial_S K) \frac{x_i^2}{2}), & K < 0. \end{cases}$$

Feedback controlled model The feedback controlled model reads

$$\dot{x}_i(t) = \kappa ED_N(t) x_i(t) + \frac{D(t)}{S(t)} x_i(t) + u_N^*(t, x_i, y_i, S) \quad (41a)$$

$$\dot{y}_i(t) = r y_i(t) - u_N^*(t, x_i, y_i, S) \quad (41b)$$

$$\dot{S}(t) = \kappa ED_N(t) S(t). \quad (41c)$$

Here, we have inserted the right-hand side of our stock equation (39) into the stock return.

Remark 4.3.1. *Alternatively, one might first discretize the system and then optimize. The corresponding optimal control is identical.*

4.4 Mean Field Limit of Feedback Controlled Model

In this section, we want to perform the limit of infinitely many agents $N \rightarrow \infty$, known as mean field limit. Classical literature on this topic are [35, 85, 192]. The goal is to derive a mesoscopic description of the financial agents instead of considering each agent in the N particle phase space individually. Thus, instead of considering the agents' dynamics in a large

dynamical system, we want to describe our dynamics with the help of a density function $f(t, x, y)$, $x, y \in \mathbb{R}_{\geq 0}$. The density $f(t, x, y)$ describes the probability that an agent at time t has an amount $x \in \mathbb{R}_{\geq 0}$ of wealth invested in his risky portfolio and $y \in \mathbb{R}_{\geq 0}$ wealth in his risk-free portfolio. The empirical measure is a nice tool to connect the solution of the dynamical system to the mean field limit equation.

Definition 4.4.1. *The two-dimensional empirical measure $f_{(\mathbf{x}, \mathbf{y})}^N(x, y)$ for given vectors $\mathbf{x} := (x_1, \dots, x_N)^T \in \mathbb{R}^N$ and $\mathbf{y} := (y_1, \dots, y_N)^T \in \mathbb{R}^N$ is defined by:*

$$f_{(\mathbf{x}, \mathbf{y})}^N(x, y) := \frac{1}{N} \sum_{k=1}^N \delta(x - x_k) \delta(y - y_k).$$

We use the empirical measure to derive the mean field limit equation formally. This is done partially because of the elegance of the method and mainly to clarify the process to the reader. We assume that the microscopic model has a unique solution. Furthermore, we denote the solution of the wealth evolution by $\mathbf{x}(t) := (x_1(t), \dots, x_N(t))^T \in \mathbb{R}^N$ and $\mathbf{y}(t) := (y_1(t), \dots, y_N(t))^T \in \mathbb{R}^N$. We consider a test function $\phi(x, y)$, $x, y \in \mathbb{R}_{\geq 0}$ and compute

$$\begin{aligned} \frac{d}{dt} \langle f_{(\mathbf{x}(t), \mathbf{y}(t))}^N(t, x, y), \phi(x, y) \rangle &= \frac{1}{N} \sum_{k=1}^N \frac{d}{dt} \phi(x_k(t), y_k(t)) \\ &= \frac{1}{N} \sum_{k=1}^N \partial_x \phi(x_k(t), y_k(t)) \dot{x}_k(t) + \partial_y \phi(x_k(t), y_k(t)) \dot{y}_k(t) \\ &= \frac{1}{N} \sum_{k=1}^N \partial_x \phi(x_k(t), y_k(t)) \left(\kappa ED_N(t) x_k(t) + \frac{D(t)}{S(t)} x_k(t) + u^*(t, x_k, y_k, S) \right) \\ &\quad + \frac{1}{N} \sum_{k=1}^N \partial_y \phi(x_k(t), y_k(t)) (r y_k(t) - u^*(t, x_k, y_k, S)) \\ &= \left\langle f_{(\mathbf{x}(t), \mathbf{y}(t))}^N(t, x, y), \partial_x \phi(x, y) \left(\kappa ED(t, f, S) x + \frac{D(t)}{S(t)} x + u^*(t, x, y, S) \right) \right\rangle \\ &\quad + \left\langle f_{(\mathbf{x}(t), \mathbf{y}(t))}^N(t, x, y), \partial_y \phi(x, y) (r y - u^*(t, x, y, S)) \right\rangle. \end{aligned}$$

Here, $\langle \cdot \rangle$ denotes the integration over x and y . Furthermore, the excess demand ED and optimal control u^* is given by:

$$\begin{aligned} ED(t, f, S) &:= \int \int u^*(t, x, y, S) f_{(\mathbf{x}(t), \mathbf{y}(t))}^N(t, x, y) dx dy \\ &= \frac{1}{N} \sum_{k=1}^N u^*(t, x_k, y_k, S), \\ u^*(t, x, y, S) &:= \begin{cases} \frac{1}{\nu} K(t, S) x, & K < 0, \\ 0, & K = 0, \\ \frac{1}{\nu} K(t, S) y, & K > 0, \end{cases} \\ &= \lim_{N \rightarrow \infty} u_N^*. \end{aligned}$$

Hence, the empirical measure $f_{(\mathbf{x}(t), \mathbf{y}(t))}^N(t, x, y)$ satisfies the equation

$$\partial_t f(t, x, y) + \partial_x \left(\left[\kappa ED(t, f, S) x + \frac{D(t)}{S(t)} x + u^*(t, x, y, S) \right] f(t, x, y) \right) \quad (42a)$$

$$+ \partial_y ([r y + u^*(t, x, y, S)] f(t, x, y)) = 0, \quad (42b)$$

in the weak sense, equipped with the excess demand

$$ED(t, f, S) = \int \int u^*(x, y, S) f(t, x, y) dx dy.$$

We call the PDE (42) the **mean field portfolio equation**. Thus the mean field portfolio stock price evolution is described by the PDE (42) coupled with the macroscopic stock price ODE.

$$\dot{S}(t) = \kappa ED(t, f, S) S(t).$$

Remark 4.4.1. We want to emphasize that the mean field limit optimal control u^* is identical to a best reply strategy of our microscopic model. In a best reply strategy, the optimal control is given by the gradient of the objective function.

4.4.1 Moment Model

The objective of this section is to derive a macroscopic ODE system of our PDE-ODE system of the previous section. Furthermore, we analyze the moment system and verify with the help of simulations that our stylized model can reproduce reasonable financial data. We define the average amount of wealth in stocks X and wealth in bonds Y by

$$X(t) = \int \int x f(t, x, y) dx dy, \quad Y(t) = \int \int y f(t, x, y) dx dy.$$

Thus, the excess demand simplifies to

$$\begin{aligned} ED(t, X, Y, S) &= \frac{1}{\nu} K(S) \int \int (H(-K(t, S)) x + H(K(t, S)) y) f(t, x, y) dx dy \\ &= \begin{cases} \frac{1}{\nu} K(t, S) X(t), & K(t, S) < 0, \\ 0, & K(t, S) = 0, \\ \frac{1}{\nu} K(t, S) Y(t), & K(t, S) > 0. \end{cases} \end{aligned}$$

where we have used the simple affine-linear form of the control in x and y . The mean field portfolio equation reads

$$\begin{aligned} \partial_t f(t, x, y) + \partial_x \left((\kappa ED(t, X, Y, S) x + \frac{D(t)}{S(t)} x + u^*(t, x, y, S) f(t, x, y)) \right) \\ + \partial_y ((r y - u^*(t, x, y, S)) f(t, x, y)) = 0. \end{aligned} \quad (43)$$

We can derive a moment system. We multiply (43) by x , y respectively and integrate over all variables to get the ODE system

$$\frac{d}{dt}X(t) = \kappa ED(t, X, Y, S) X(t) + \frac{D(t)}{S(t)} X(t) + ED(t, X, Y, S) \quad (44a)$$

$$\frac{d}{dt}Y(t) = r Y(t) - ED(t, X, Y, S) \quad (44b)$$

$$\frac{d}{dt}S(t) = \kappa ED(t, X, Y, S) S(t). \quad (44c)$$

Booms, crashes and oscillatory solutions We want to study whether our stock price satisfies the most prominent features of stock markets. These are crashes, booms and oscillatory solutions. Mathematically, a boom or crash is described by exponential growth or decay of the price. In order to study the price evolution, we assume that the weight $W \in [0, 1]$ is constant, the exchange rate frequency is $\rho \equiv 1$ and that the value function U_γ is given by the identity. The corresponding equations and solutions can be found in the appendix 4.9.1.

- Fundamentalists merely ($\chi = 1$) influence the price by their fundamental value s^f . The price is driven to the steady state $S_\infty = \frac{\omega s^f}{\omega+r}$ exponentially. Interestingly, the convergence speed depends on the market depth κ , the interest rate r , the expected speed of mean reversion ω and the amount of wealth invested.
- Chartists merely ($\chi = 0$) build their investment decision on the current stock return. The price gets driven exponentially to the equilibrium stock price $S_\infty = \frac{D}{r}$ or away from the equilibrium stock price. This behavior is determined by the average wealth invested in stocks or bonds. In general, we observe exponential growth or decay of the stock price (e.g. $D \equiv 0$). Hence, the chartist behavior can create market booms or crashes. We can thus expect that an interplay of fundamental and chartist strategies leads to oscillatory behavior around the equilibrium prices.
- In our last case, we consider a mix of chartist and fundamental return expectations with a constant weight $\chi \in (0, 1)$. In that case, the price converges to the equilibrium price $S_\infty = \frac{\chi \omega s^f + (1-\chi) D}{\chi \omega + r}$ which is a combination of the previous equilibrium prices. Thus, the weight χ heavily influences the price dynamic. Furthermore, we can expect to observe oscillatory solutions if we consider a non constant weight $\chi(t, S)$.

Wealth evolution We can analyze the wealth evolution in the same manner as previously the stock price equation. We consider each portfolio separately. The computation can be found in the appendix 4.9.1, as well.

- We have exponential growth in the stock portfolio, if the wealth gets transferred from bonds to stocks. In the opposite case, the decay of wealth is described by an exponential as well.
- In the bond portfolio, we also observe an exponential increase if the wealth gets shifted into the bond portfolio. If stocks are assumed to perform substantially better ($K(S) > r$), we have exponential decay in the bond portfolio.

Simulations We want to provide first insights into the portfolio dynamics. The goal is to verify the existence of oscillatory solutions of this simple ODE model. Our previous analysis indicates that there is an interplay between different steady states. We choose the value function U_γ and the weight function W as follows:

$$W(K^f - K^c) := \beta \left(\frac{1}{2} \tanh \left(\frac{K^f - K^c}{\alpha} \right) + \frac{1}{2} \right) + (1 - \beta) \left(\frac{1}{2} \tanh \left(-\frac{K^f - K^c}{\alpha} \right) + \frac{1}{2} \right),$$

$$\alpha > 0, \beta \in [0, 1],$$

$$U_\gamma(x) := \begin{cases} x^{\gamma+0.05}, & x > 0, \\ -(|x|)^{\gamma-0.05}, & x \leq 0, \end{cases} \quad \gamma \in [0.05, 0.95].$$

The weight function W models the instantaneous comparison of the fundamental and chartist return estimate. The constant $\beta \in [0, 1]$ determines if the investor trusts in the higher ($\beta = 1$) or lower estimate ($\beta = 0$) and we thus call this constant the trust coefficient. The constant $\alpha > 0$ simply scales the estimated returns.

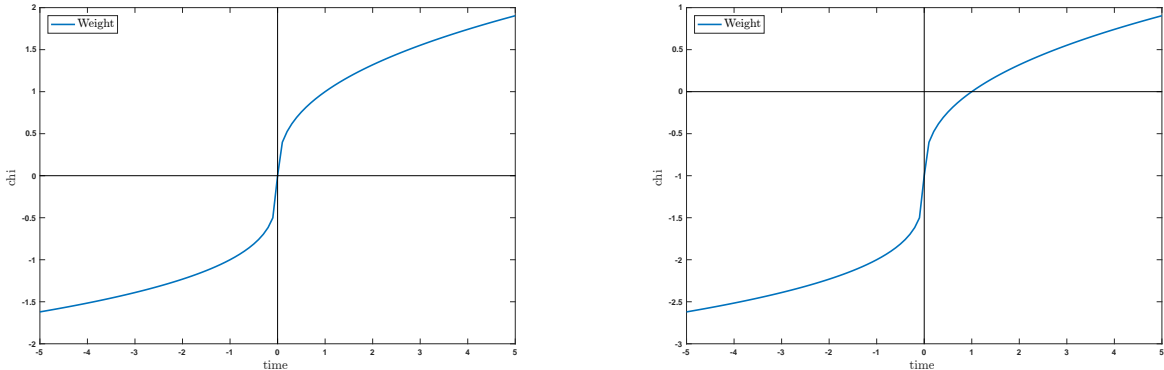


Figure 40: Example of Value functions with different reference points.

The value function U_γ models psychological behavior of an investor towards gains and losses. In order to derive the value function, one needs to measure the attitude of an individual as a deviation from a reference point. We have chosen the reference point to be zero, since $U_\gamma(0) = 0$ holds. In figure 40 we have plotted U_γ and $\bar{U}_\gamma := U_\gamma - 1$. The value function \bar{U}_γ is an example of a value function with a negative reference point. Our choice of value function satisfies the usual assumptions: the function is concave for gains and convex for losses, which corresponds to risk aversion and risk seeking behavior of investors. Furthermore, our value function is steeper for losses than for gains, which models the psychological loss aversion of financial agents (see figure 40).

We have solved the moment system with a simple forward Euler discretization. The time step has been chosen sufficiently small to exclude stability problems due to stiffness. We verified the results with the `ode15i` Matlab solver. We have chosen a trust coefficient $\beta = 0.25$ for the simulations in figure 41 and 42. We refer to the appendix 4.9.2 for further settings. The oscillations of the stock price is caused by oscillations in the excess demand. The stock price is always less than or equal to the fundamental price. In addition, the oscillations get translated

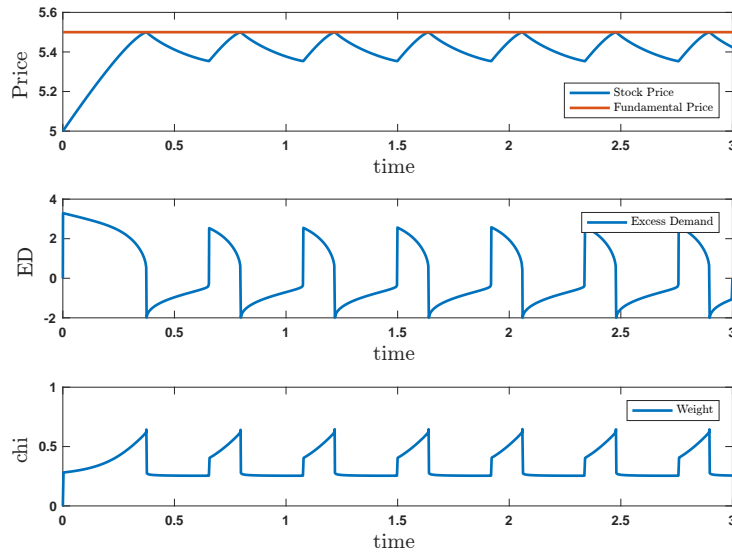


Figure 41: Stock price

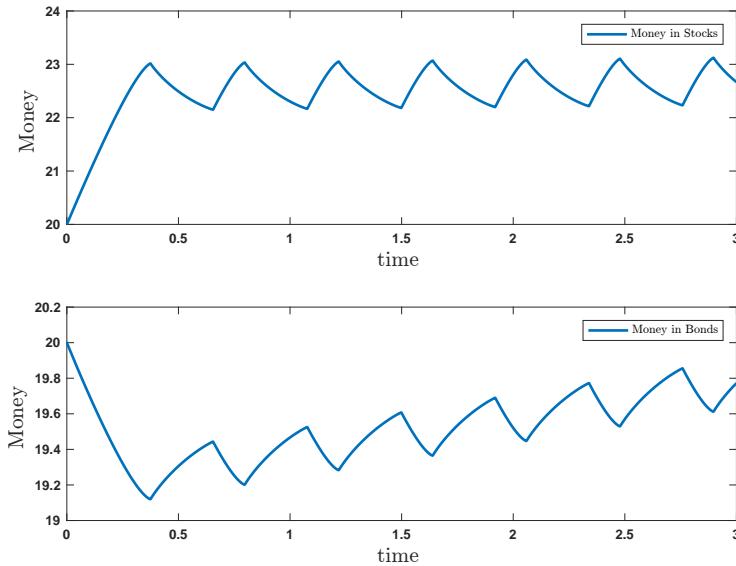


Figure 42: Wealth evolution.

to the wealth evolution of the portfolios. Increasing wealth in the stock portfolio leads to decreasing wealth in the bond portfolio. Furthermore, we can observe on average a small positive slope of the wealth invested in bonds (see figure 42). This is caused by the positive

interest rate r . In our next simulations (figure 43), we have altered the trust coefficient to study the impact on the price behavior. As figure 43 reveals, the trust coefficient β influences

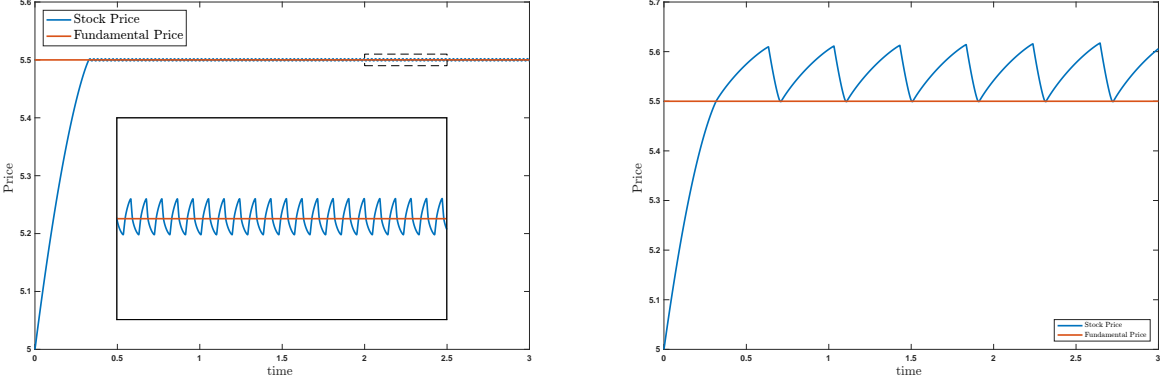


Figure 43: Stock price with trust coefficient $\beta = 0.7$ (left figure) and trust coefficient $\beta = 0.85$ (right figure).

the amplitude and frequency of our oscillations. In addition, β determines the location of the oscillatory stock price evolution with respect to the fundamental value s^f . A low trust coefficient leads to oscillations located below the fundamental price and a high trust coefficient to oscillations above the fundamental value.

We want to point out that the price behavior is very sensitive with respect to the parameters $\gamma, \kappa, \omega, \alpha$ and β .

Remark 4.4.2. *The parameters influence the price dynamics as follows:*

- A larger risk tolerance γ leads to smaller wave periods and smaller amplitudes. A high risk tolerance heavily changes the price characteristics. We could thus observe convergence of the price to the fundamental value.
- The market depth κ influences the amplitude of the oscillations. A bigger κ value leads to a larger amplitude.
- The speed of mean reversion ω and the scale parameter α influence the wave period and amplitude. The wave period and amplitude decrease with increasing ω , respectively α .

Macroscopic steady states In order to obtain steady states, the equations

$$\begin{aligned} 0 &= \kappa ED(X, Y, S)X + \frac{D}{S}X + ED(X, Y, S) \\ 0 &= rY - ED(X, Y, S) \\ 0 &= \kappa ED(X, Y, S) S, \end{aligned}$$

need to be fulfilled. Besides the trivial solution the following steady state configurations are possible.

- i) $X = 0, Y = 0, S$ arbitrary

- ii) $K(S) = 0, Y = 0, D = 0, X$ arbitrary
- iii) $K(S) = 0, r = 0, D = 0, X$ and Y arbitrary
- iv) $K(S) > 0, Y = 0, D = 0, X$ arbitrary
- v) $K(S) < 0, X = 0, r = 0, Y$ arbitrary

The case *i*) corresponds to the situation when all investors are bankrupt. In the cases *ii*) and *iii*), the investors expect to have no benefit of shifting the capital between both portfolios. This means that the expected return $K(S)$ is zero, which is equivalent to

$$U_\gamma \left(\omega \frac{s^f - S}{S} \right) \chi + (1 - \chi) U_\gamma(0) = r.$$

If we choose the value function U_γ to be the identity, we observe

$$S^\infty = \frac{\chi \omega s^f}{1 + r},$$

as the equilibrium stock price. One might assume that the reference point of the value function is not zero. This means that the financial agent has a fixed bias towards potential gains or losses in his opinion. Mathematically, $U_\gamma(0) \neq 0$ holds and thus the steady state would be shifted by the reference point. Hence, psychological misperceptions of investors lead to changes of the equilibrium price. The case *iv*) corresponds to the situation that the investor wants to shift wealth from the bond portfolio into the stock portfolio. In fact, no transaction takes place, since there is no wealth left in the bond portfolio. Thus $K(S) > 0$ has to hold, which means

$$U_\gamma \left(\omega \frac{s^f - S}{S} \right) \chi + (1 - \chi) U_\gamma(0) > r.$$

In the simple case of the identity function as utility function, we obtain:

$$\frac{\omega \chi s^f}{r + \omega \chi} > S. \quad (45)$$

In this equilibrium case, the amount of transactions have been too low to push the price above a certain threshold defined by inequality (45). The reason for the steady state is the bankruptcy in the bond portfolio. Such a situation does not reflect a usual situation in financial markets. In case *v*), we face the opposite situation. Here, the investor wants to shift wealth from stocks to bonds although there is no wealth left in the stock portfolio.

4.4.2 Marginals of Mean Field Portfolio Equation

In the previous section, we have analyzed the macroscopic properties of our model. In addition, we want to study the distribution of wealth. The mesoscopic behavior can be studied by the mean field portfolio equation. Compared to models, which only consider ODEs, this is a huge benefit of our kinetic approach. We are interested in discovering the marginal distributions of the mean field portfolio equation

$$\begin{aligned} \partial_t f(t, x, y) + \partial_x ((\kappa ED(t, X, Y, S) x + \frac{D(t)}{S(t)} x + u^*(t, x, y, S)) f(t, x, y)) \\ + \partial_y ((r y - u^*(t, x, y, S)) f(t, x, y)) = 0. \end{aligned}$$

In fact, we can derive equations for the distribution of wealth in stocks and wealth in bonds. The corresponding marginals of f are defined by

$$g(t, x) := \int f(t, x, y) dy, \quad h(t, y) := \int f(t, x, y) dx.$$

Hence, g is a probability density function of the wealth invested in stocks and h is the probability density function of wealth invested in bonds. We then integrate the mean field portfolio equation over y respectively x to observe equations for g and h . Since the optimal control u^* depends on both microscopic quantities, we cannot expect to get a closed equation for g or h in general.

Nevertheless, in the special case $K < 0$, the control u^* only depends on x and the time evolution of g reads

$$\partial_t g(t, x) + \partial_x \left(\left[\frac{K(S(t))}{\nu} (\kappa X(t) + 1) + \frac{D(t)}{S(t)} \right] x g(t, x) \right) = 0.$$

One solution of the equation is given by:

$$g(t, x) = \frac{c}{\sqrt{\pi}x} \exp \left\{ - \left(\log(x) - \int_0^t \frac{K(S(\tau))}{\nu} (\kappa X(\tau) + 1) + \frac{D(\tau)}{S(\tau)} d\tau \right)^2 \right\}, \quad c > 0,$$

Notice that g is the distribution function of a lognormal law.

We get a closed equation for h , in the case $K > 0$, in the same way. The solution h is of lognormal type as well. We refer to the appendix 4.9.3 for a detailed discussion.

4.5 Feedback Controlled Model with Noise

We have seen that our model can reproduce the most prominent features of stock price data, namely oscillatory prices, which replicate booms and crashes. Furthermore, we have shown that the distribution of wealth in bonds and stocks can be represented in special cases by lognormal distributions.

So far, we have considered a fully deterministic model. This does not seem to capture all characteristics of financial markets completely. It is generally accepted that stock prices are unpredictable and e.g. news and political decisions influence the behavior of market participants in an uncertain fashion. For that reason, we want to add randomness to our deterministic model. The optimal control of the i -th agent was given by

$$u^*(x_i, y_i, S) = \begin{cases} \frac{1}{\nu} K(S) x_i, & K < 0, \\ 0, & K = 0, \\ \frac{1}{\nu} K(S) y_i, & K > 0. \end{cases}$$

Notice that the investment decision of agents only differs through different personal wealth. Thus, the estimate of stock return over bond return was identical for all investors. This assumption seems to be too simple, so each individual should differ in their return estimate. Hence, we add white noise to our returns estimate. Since the return estimate is a rate, the random variable also needs to scale with time. We use symbolic notation of integrals adopted from the common notation of SDEs to define the integrated noisy optimal control

$$u_{\eta_i}^*(x_i, y_i, S) dt = \begin{cases} \frac{1}{\nu} K(S) dt + \frac{1}{\nu} x_i dW_i & K < 0, \\ 0, & K = 0, \\ \frac{1}{\nu} K(S) dt + \frac{1}{\nu} y_i dW_i, & K > 0. \end{cases}$$

Here, dW_i denotes the stochastic Itô integral and thus the feedback controlled microscopic system with noise is given by

$$dx_i = (\kappa E D_N x_i + u_i^*) dt + \frac{1}{\nu} (H(-K)x_i + H(K)y_i) dW_i \quad (46a)$$

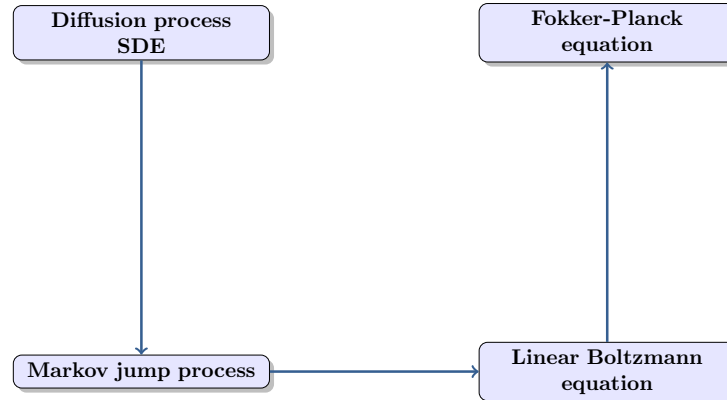
$$dy_i = (r y_i - u_i^*) dt - \frac{1}{\nu} (H(-K)x_i + H(K)y_i) dW_i \quad (46b)$$

$$dS = (\kappa E D_N S) dt. \quad (46c)$$

4.5.1 Mean Field Limit

The goal of this section is to derive a mesoscopic description of our particle dynamics with noise. The classical mean field approaches by Braun, Hepp, Neunzert and Dobrushin [192, 35, 85] do not apply because of the white noise. The only known mean field result in the case of diffusion processes is the convergence of N interacting processes to the kinetic McKean-Vlasov equation [230]. Unfortunately, our model (46) does not satisfy the classical assumptions since our N -particle dynamics are coupled with the macroscopic stock price ODE.

The following modeling approach, well described in [198], is an alternative method to derive the mean field limit of the microscopic model (46) at least formally. The idea is to discretize the diffusion process and interpret it as a Markov jump process. Then, one can derive the corresponding master equation, which can be also interpreted as a linear Boltzmann equation. With the right scaling, known in kinetic theory as grazing limit, one observes in the limit the Fokker-Planck equation. The following diagram illustrates the modeling process.



Boltzmann model As seen before, we consider the probability density $f(t, x, y)$ which describes an investor to have monetary wealth $x \in \mathbb{R}_{\geq 0}$ in his risky portfolio and wealth $y \in \mathbb{R}_{\geq 0}$ in his risk-free portfolio. The portfolio dynamics are characterized by the following linear in-

teractions $(x, y) \mapsto (x', y')$.

$$\begin{aligned} x' &= x + a \left(\kappa ED(t) + \frac{D(t)}{S(t)} \right) x + a u_\eta^*(t, x, y, S), & \text{if } x' > 0, \\ y' &= y + a y r - a u_\eta^*(t, x, y, S), & \text{if } y' > 0, \end{aligned}$$

with

$$\begin{aligned} u_\eta^* &:= u^*(t, x, y, S) + \frac{1}{\sqrt{a} \nu} (H(-K) x + H(K) y) \eta, \\ a &:= \Delta t, \end{aligned}$$

and a normally distributed random variable η with zero mean and variance one. The time step $\Delta t > 0$ is fixed and originates from the Euler-Maruyama discretization of the SDE. The time evolution of the density function $f(t, x, y)$ is then described by an integro-differential equation of Boltzmann type. In weak form, the equation reads

$$\frac{d}{dt} \int \phi(x, y) f(t, x, y) dx dy = (L(f), \phi), \quad (47)$$

$$(L(f), \phi) := \left\langle \int \mathcal{K}(x, y, S, ED, D, \eta) (\phi(x', y') - \phi(x, y)) f(t, x, y) dx dy \right\rangle, \quad (48)$$

with a suitable test function $\phi(x, y)$ and $\langle \cdot \rangle$ denotes the expectation with respect to the random variable $\eta \in \mathbb{R}$. The interaction kernel \mathcal{K} has to ensure that the post interaction portfolio values remain positive:

$$\mathcal{K}(x, x', y, y', S, ED, D, \eta) := \theta \mathbf{1}_{\{x' > 0\}} \mathbf{1}_{\{y' > 0\}} \eta,$$

where $\theta > 0$ is the collision rate and $\mathbf{1}(\cdot)$ the indicator function. The interaction kernel can be simplified if there is no dependence on x and y . This case corresponds to the case of Maxwellian molecules in the classical Boltzmann equation. This can be achieved by truncating the random variable η in a way that the post interaction wealth always remains positive. In our case, it is not possible to state explicit bounds for our random variable η since the stock return is not bounded. In fact, for a sufficiently small step size Δt , it is always possible to truncate the random variable in a way that the kernel is independent of x, y . Then, the interaction operator reads:

$$(L(f), \phi) := \left\langle \theta \int (\phi(x', y') - \phi(x, y)) f(t, x, y) dx dy \right\rangle.$$

We can immediately observe that our model conserves the number of agents, which corresponds to the choice $\phi(x, y) = 1$.

We are interested in the asymptotic behavior of the density function f .

Asymptotic limit The goal of the asymptotic procedure is to derive a model of Fokker-Planck type. Thus, the integral operator gets translated into a second order differential operator. The procedure can be described in two steps. First, we perform a second order Taylor expansion of the test function $\phi(x', y')$. Secondly, we rescale characteristic parameters of the model, preserving the main macroscopic properties of the original kinetic equation (47). A closely

related approach in kinetic theory is the famous grazing collision limit [244]. We introduce the scaling

$$\theta = \frac{1}{\epsilon}, \quad a = \epsilon,$$

where $\epsilon > 0$ and perform the limit $\epsilon \rightarrow 0$. The limit equation is given by the the following Fokker-Planck equation

$$\begin{aligned} & \partial_t f(t, x, y) + \partial_x((\kappa ED(t, f, S) x + u^*(t, x, y, S)) f(t, x, y)) \\ & + \partial_y((r y - u^*(t, x, y, S)) f(t, x, y)) + \frac{1}{2 \nu^2} \partial_{yx}^2 ((H(-K)x + H(K)y) f(t, x, y)) \\ & = \frac{1}{2 \nu^2} \partial_x^2 ((H(-K)x + H(K)y) f(t, x, y)) + \frac{1}{2 \nu^2} \partial_y^2 ((H(-K)x + H(K)y) f(t, x, y)), \end{aligned}$$

coupled with the macroscopic stock price ODE

$$\dot{S}(t) = \kappa ED(t, f, S) S(t).$$

We call the previously introduced PDE the **diffusive mean field portfolio equation**. In the appendix 4.9.5, we provide a detailed discussion of the derivation of the diffusive mean field portfolio equation.

4.5.2 Marginals of Diffusive Mean Field Portfolio Equation

Again, we are interested in the behavior of the marginal distributions g and h . In the special case $K < 0$, the control u^* only depends on x and the time evolution of g reads.

$$\partial_t g(t, x) + \partial_x \left(\left[\frac{K(S(t))}{\nu} (\kappa X(t) + 1) + \frac{D(t)}{S(t)} \right] x g(t, x) \right) - \partial_x^2 \left(\frac{x^2}{2 \nu^2} g(t, x) \right) = 0.$$

In order to search for self-similar solutions, we introduce the scaling $\bar{g}(t, \bar{x}) = x g(t, x)$, $\bar{x} = \log(x)$ and define $b(t) := \frac{K(S(t))}{\nu} (\kappa X(t) + 1) + \frac{D(t)}{S(t)}$. We observe a linear convection-diffusion equation for the evolution of $\bar{g}(t, \bar{x})$

$$\partial_t \bar{g}(t, \bar{x}) + \left(b(t) - \frac{1}{2 \nu^2} \right) \partial_{\bar{x}} \bar{g}(t, \bar{x}) = \frac{1}{2 \nu^2} \partial_{\bar{x}}^2 \bar{g}(t, \bar{x}).$$

The solution is given by

$$\bar{g}(t, \bar{x}) = \frac{1}{(2 (\frac{t}{\nu^2} + c) \pi)^{\frac{1}{2}}} \exp \left\{ -\frac{(\bar{x} + \frac{\frac{t}{\nu^2} + c}{2} - B(t))^2}{2 (\frac{t}{\nu^2} + c)} \right\}, \quad c > 0,$$

with $B(t) := \int_0^t b(\tau) d\tau + \bar{c}$, $\bar{c} > 0$. After reverting to the original variables, we get

$$g(t, x) = \frac{1}{x (2 (\frac{t}{\nu^2} + c) \pi)^{\frac{1}{2}}} \exp \left\{ -\frac{\left(\log(x) + \frac{\frac{t}{\nu^2} + c}{2} - B(t) \right)^2}{2 (\frac{t}{\nu^2} + c)} \right\}, \quad c > 0.$$

Thus, the wealth in bonds admits a lognormal asymptotic behavior as well.

Analogously, we obtain a similar equation for h in the case $K > 0$. The solution also satisfies a lognormal law. For details, we refer to the appendix 4.9.4. At first glance, we did not gain any new information compared to the marginals of the mean field portfolio equation. In both cases, we have observed lognormal behavior. However, this is not true, in the diffusive case, our solution admits a time dependent variance and is not constant in contrast to the deterministic case. In addition, we have observed that adding multiplicative noise does not change the portfolio distribution drastically.

4.6 Stock Price as Random Process

Until now, the macroscopic stock price evolution has been given by the ODE (39) and was deterministic. We aim to analyze the price behavior in a probabilistic setting and analyze the price distribution. We modify the model by adding a microscopic stochastic model beneath the macroscopic stock price equation (39). To do so, we introduce a new population of $M \in \mathbb{N}$ market makers or brokers. Each broker is equipped with a microscopic stock price $s_j > 0$. The microscopic stock prices are modeled as random processes. The average of broker prices generates the macroscopic stock price S_M .

$$S_M := \frac{1}{M} \sum_{j=1}^M s_j.$$

The stochastic nature of microscopic stock prices can be explained by different market accessibility of each broker. Their individual stock price is given by

$$ds_j = \kappa ED s_j dt + s_j dW_j, \quad j = 1, \dots, M, \quad (49)$$

where W_j is a Wiener process and equation (49) has to be interpreted in the Itô sense. Compared to the macroscopic stock price equation (39), there is multiplicative noise added to the price evolution of brokers.

The stock price evolution is coupled with the portfolio evolution in two different ways: First, by the stock return in the stock portfolio and secondly by the investment decision u^* .

$$\begin{aligned} \partial_t f + \partial_x((\kappa ED x + u^*) f) + \partial_y((r y - u^*) f) + \frac{1}{2 \nu^2} \partial_{yx}^2 ((-H(-K)x + H(K)y) f) \\ = \frac{1}{2 \nu^2} \partial_x^2 ((H(-K)x + H(K)y) f) + \frac{1}{2 \nu^2} \partial_y^2 ((H(-K)x + H(K)y) f), \\ ds_j = \kappa ED s_j dt + s_j dW_j, \quad j = 1, \dots, M. \end{aligned}$$

We need to specify whether the investors' decisions are based on the microscopic or macroscopic stock price. The macroscopic stock price determines the stock return of the agents' portfolio, because this is the global market price. In the case of the investment decision, one can argue that an investor might trade on the microscopic or macroscopic stock price. Arbitrage opportunities are a reason to act on the microscopic scale. In addition, one can argue that the microscopic stock prices have in fact a smaller time scale than the macroscopic stock price since the latter is the average of the former. This leads us to the characterization that investors acting on the micro prices are **high-frequency traders**, whereas agents action on the macro price can be accounted to be **long-term investors**.

Mean field limit As seen before, we want to consider the mean field limit of our microscopic stock price equations. In fact, the microscopic brokers only differ in their initial conditions and multiplicative noise. We have:

$$ds_j(t) = \kappa ED(t, f, (\cdot)) s_j(t) dt + s_j(t) dW_j, \quad s_j(0) = s_j^0. \quad (50)$$

Thus, there is no coupling between broker and we have a simple setting of McKean-Vlasov type equations. We have written the excess demand as $ED(t, f, (\cdot))$ since we can have $ED(t, f, s_j)$ in the high-frequency case or $ED(t, f, S_M)$ for long-term investors. We assume that the empirical measure $V_{\mathbf{s}(\mathbf{0})}^N(0, s)$, which is defined by the initial conditions of the microscopic system

$$V^N(0, s) := \frac{1}{M} \sum_{k=1}^M \delta(s - s_k^0),$$

converges to a distribution function $V(0, s)$. Then, the system (49) converges in expectation to the mean field SDE

$$d\bar{s}_j(t) = \kappa ED(t, f, \bar{s}_j) \bar{s}_j(t) dt + \bar{s}_j(t) dW_j, \quad \bar{s}_j(0) = \mathfrak{s}_j, \quad \mathfrak{s}_j \sim V(0, s). \quad (51)$$

Due to the Wiener process, the above set of stochastic processes is independent and in particular identically distributed. We can thus apply the Feynman-Kac formula and the distribution $V(t, s)$, $s > 0$ evolves accordingly to

$$\partial_t V(t, s) + \partial_s (\kappa ED(t, f, (\cdot)) s V(t, s)) = \frac{1}{2} \partial_s^2(s^2 V(t, s)). \quad (52)$$

Notice that the macroscopic stock price is the first moment of V .

$$S(t) = \int s V(t, s) ds.$$

Hence, our **diffusive mean field portfolio stock price** system is given by:

$$\begin{aligned} \partial_t f(t, x, y) + \partial_x ((\kappa ED(t, f, S) x + u^*(t, x, y, (\cdot))) f(t, x, y, s)) \\ - \frac{1}{2} \frac{1}{\nu^2} \partial_x^2 ((H(-K)x + H(K)y) f(t, x, y)) + \frac{1}{2} \frac{1}{\nu^2} \partial_{yx}^2 ((H(-K)x + H(K)y) f(t, x, y)) \\ + \partial_y ((r y - u^*(t, x, y, (\cdot))) f(t, x, y)) - \frac{1}{2} \frac{1}{\nu^2} \partial_y^2 ((H(-K)x + H(K)y) f(t, x, y)) = 0, \\ \partial_t V(t, s) + \partial_s (\kappa ED(t, f, (\cdot)) s V(t, s)) = \frac{1}{2} \partial_s^2(s^2 V(t, s)). \end{aligned}$$

Remember that the influence of the investment decision enters in the stock-price evolution through the excess demand. In the next sections, we want to study the influence of a high-frequency or long-term strategy of investors on the price distribution V .

4.6.1 Long-term investors

In the case of long-term investors, the investment decision $u^* = u^*(t, x, y, S)$ depends on the macroscopic stock price S . The stock price equation is given by:

$$\partial_t V + \partial_s \left(\frac{\kappa}{\nu} K(S) \left[\int \int [H(-K(S))x + H(K(S))y] f(t, x, y) dx dy \right] s V \right) = \frac{1}{2} \partial_s^2(s^2 V). \quad (53)$$

We can take the first moment of the previous equation and obtain the macroscopic stock price ODE (39) considered in the previous sections. In addition, we want to point out that in the case of long-term investors, we can derive the same moment system (44), discussed previously.

Asymptotic behavior Due to the fact that the stock price is a stochastic process, we can study the distribution function of our stock price PDE. We define

$$P(t) := \int \int [H(-K(S))x + H(K(S))y] f(t, x, y) dx dy,$$

$$R(t) := \frac{\kappa}{\nu} K(S(t)) P(t),$$

and search for self-similar solutions of equation (53). The quantity P is the average amount of wealth in the bond or stock portfolio and R is the average amount of wealth invested in stocks. We consider the scaling $\mathcal{V}(p, t) = s V(t, s)$, $p = \log(s)$ and \mathcal{V} thus satisfies the following linear convection-diffusion equation

$$\partial_t \mathcal{V}(t, p) + \left(R(t) - \frac{1}{2} \right) \partial_p \mathcal{V}(t, p) = \frac{1}{2} \partial_p^2 \mathcal{V}(t, p).$$

The solution of the previous equation is given by

$$\mathcal{V}(t, p) = \frac{1}{\sqrt{2 \pi}} \exp \left\{ - \frac{(p + \frac{t+c_1}{2} - \bar{R}(t))^2}{2} \right\},$$

for a constant $c_1 > 0$ and $\bar{R}(t) := \int_0^t R(\tau) d\tau + c_2$, $c_2 > 0$. Hence, by reverting to the original variables, we get

$$V(t, s) = \frac{1}{s \sqrt{2 \pi (t + c_1)}} \exp \left\{ - \frac{(\log(s) + \frac{t+c_1}{2} - \bar{R}(t))^2}{2 (t + c_1)} \right\}.$$

We thus observe lognormal asymptotic behavior of the model.

4.6.2 High-frequency Traders

In the case of high-frequency investors, we have to clarify the dependence of the optimal control u^* on the microscopic stock price s . The investment strategy of **high-frequency fundamentalists** can be translated one to one. We have

$$k^f(t, s) := U_\gamma \left(\omega \frac{s^f(t) - s}{s} \right) - r.$$

The chartist estimated return is more difficult. In fact, the chartists estimate involves a time derivative of the stock price. On the microscopic level, we can insert the right-hand side of the microscopic stock price equation. In addition, we assume that the investor averages over the uncertainty. Thus, for **high-frequency chartists** we get:

$$k^c(t, s) := U_\gamma \left(\frac{\kappa/\rho ED(t, f, s) + D(t)}{s} \right) - r,$$

We define the aggregated high-frequency estimate of stock return over bond return by

$$k(t, s) := \chi k^f(t, s) + (1 - \chi) k^c(t, s).$$

Hence, the **high-frequency stock price equation** reads

$$\begin{aligned}\partial_t V(t, s) + \partial_s \left(\frac{\kappa}{\nu} k(t, s) \left[\int \int [H(-k(t, s)) x + H(k(t, s)) y] f(t, x, y) dx dy \right] s V(t, s) \right) \\ = \frac{1}{2} \partial_s^2 (s^2 V(t, s)).\end{aligned}$$

Notice that we cannot find a closed equation for the first moment of this equation. In general, it is difficult to solve the high-frequency stock price equation. We want to study admissible states of the high-frequency stock price equation in order to obtain a solution.

In addition, we have to specify the dependence of the diffusive mean field portfolio equation on the microscopic stock price. We want to point out that the diffusive mean field portfolio equation, solely coupled with the high-frequency stock price equation, is not well-defined. This is because of the fact that it is unclear how to interpret the variable s in the optimal control of the diffusive mean field portfolio equation. One solution to this problem is to add the mean field SDE (51) to our model. The diffusive mean field portfolio equation is then coupled with the mean field SDE through the microscopic stock prices \bar{s} in the optimal control. In addition, the diffusive mean field portfolio equation is coupled with the high-frequency stock price equation by the macroscopic stock price S . We get:

$$\begin{aligned}\partial_t f(t, x, y) + \partial_x ((\kappa ED(t, f, S) x + u^*(t, x, y, \bar{s})) f(t, x, y)) \\ - \frac{1}{2 \nu^2} \partial_x^2 ((H(-K)x + H(K)y) f(t, x, y)) + \frac{1}{2 \nu^2} \partial_{yx}^2 ((H(-K)x + H(K)y) f(t, x, y)) \\ + \partial_y ((r y - u^*(t, x, y, \bar{s})) f(t, x, y)) - \frac{1}{2 \nu^2} \partial_y^2 ((H(-K)x + H(K)y) f(t, x, y)) = 0, \\ d\bar{s}(t) = \kappa ED(t, f, \bar{s}) \bar{s}(t) dt + \bar{s}(t) dW, \\ \partial_t V(t, s) + \partial_s \left(\frac{\kappa}{\nu} k(t, s) \left[\int \int [H(-k(t, s))x + H(k(t, s))y] f(t, x, y) dx dy \right] s V(t, s) \right) \\ = \frac{1}{2} \partial_s^2 (s^2 V(t, s)).\end{aligned}$$

Since the solution of our high-frequency stock price equation is the density of the stochastic process \bar{s} , we can substitute this PDE by the expected value of the stochastic process \bar{S} . The alternative model reads:

$$\begin{aligned}\partial_t f(t, x, y) + \partial_x ((\kappa ED(t, f, S) x + u^*(t, x, y, \bar{s})) f(t, x, y)) \\ - \frac{1}{2 \nu^2} \partial_x^2 ((H(-K)x + H(K)y) f(t, x, y)) + \frac{1}{2 \nu^2} \partial_{yx}^2 ((H(-K)x + H(K)y) f(t, x, y)) \\ + \partial_y ((r y - u^*(t, x, y, \bar{s})) f(t, x, y)) - \frac{1}{2 \nu^2} \partial_y^2 ((H(-K)x + H(K)y) f(t, x, y)) = 0, \\ d\bar{s}(t) = \kappa ED(t, f, \bar{s}) \bar{s}(t) dt + \bar{s}(t) dW, \\ S = E[\bar{s}].\end{aligned}$$

We consider the former model instead of the latter as we can analyze the stock price distribution due to the high-frequency stock price equation.

Steady state We want to show that in special cases the steady state distribution is described by an inverse gamma distribution. We assume that $\chi \equiv 1$, $s^f \equiv c > 0$, $U_\gamma(x) = x$ holds. The stock price equation is then simplified to

$$\begin{aligned} \partial_t V(t, s) + \partial_s \left(\frac{\kappa}{\nu} [\omega s^f - s (\omega + r)] \left[\int \int [H(-k(s))x + H(k(s))y] f(t, x, y) dx dy \right] V(t, s) \right) \\ = \frac{1}{2} \partial_s^2 (s^2 V(t, s)). \end{aligned}$$

Furthermore, we assume that the portfolio distribution f has reached a steady state f_∞ . We define

$$\begin{aligned} P_x^\infty &:= \int \int x f_\infty(x, y) dx dy > 0, \quad k < 0, \\ P_y^\infty &:= \int \int y f_\infty(x, y) dx dy > 0, \quad k > 0. \end{aligned}$$

and assume $P^\infty := P_x^\infty = P_y^\infty$. Hence, the steady state distribution $V_\infty(s)$ satisfies

$$\frac{1}{2} \partial_s^2 (s^2 V_\infty(s)) - \frac{\kappa}{\nu} P^\infty \partial_s ([\omega s^f - s (\omega + r)] V_\infty(s)) = 0. \quad (54)$$

The solution of (54) is given by the inverse gamma distribution

$$V_\infty(s) = C \frac{1}{(s)^{2(1+\frac{\kappa}{\nu} P_\infty(\omega+r))}} \exp \left\{ -\frac{2 \frac{\kappa}{\nu} \omega P_\infty s^f}{s} \right\}, \quad s > 0,$$

where the constant C should be chosen as

$$C := \frac{(2 \kappa \omega P_\infty s^f)^{1+2\frac{\kappa}{\nu} P_\infty(\omega+r)}}{\Gamma(1 + 2\frac{\kappa}{\nu} P_\infty(\omega+r))},$$

such that the mass of V_∞ is equal to one. Here, $\Gamma(\cdot)$ denotes the gamma function. We immediately observe that for large stock prices s , the distribution function asymptotically satisfies

$$V_\infty \sim \frac{1}{s^{2(1+\frac{\kappa}{\nu} P_\infty(\omega+r))}}.$$

Hence, the equilibrium distribution is described by a power-law.

Remark 4.6.1. • We have observed that the presence of high-frequency fundamentalists leads to power-law behavior in the stock price distribution. This coincides with earlier findings in the closely related Pareschi-Maldarella model [166]. Furthermore, the shape of the steady state (inverse-gamma distribution) is identical to wealth distributions observed in [34, 67].

• The universal features which create power-law tails are multiplicative noise and additionally an external force on the microscopic level. In our case, this force is given by the fundamental value s^f of the fundamental trading strategy.

- The presence of chartists may also lead to fat-tails in the stock price distribution. Their estimated stock return was given by

$$k^c(t, s) = U_\gamma \left(\frac{\kappa/\rho \cdot ED(t, f, s) + D(t)}{s} \right).$$

We assume that the value function is given by $U_\gamma(\cdot) = (\cdot) - \mathfrak{r}$, where $-\mathfrak{r} < 0$ is the reference point. Then, it is possible to observe a steady state distribution of inverse-gamma type. Thus, a fixed overestimation of risk also leads to power-law tails.

4.7 Numerics

In this section, we want to present some numerical examples of our mean field model. We always consider the final kinetic model, namely the diffusive mean field portfolio stock price model. Our simulations have been conducted with a standard Monte Carlo solver. Furthermore, we use the weighting function W and value function U_γ as defined previously. First, we have a look at the price and portfolio dynamics in the case of long-term investors. Secondly, we consider the case of high-frequency trader. Detailed information of our parameter choice can be found in the appendix 4.9.6.

Long-Term Investors In order to observe more realistic price behavior compared to our moment model, we introduce a time varying fundamental price $s^f(t)$. We choose a stationary lognormally distributed fundamental price, modeled by the following SDE

$$ds^f = 0.1 \cdot s^f \cdot dW.$$

Again, W denotes the Wiener process and the integrals need to be interpreted in the Itô sense. In the case of a constant fundamental price, we observe oscillatory behavior (see figure

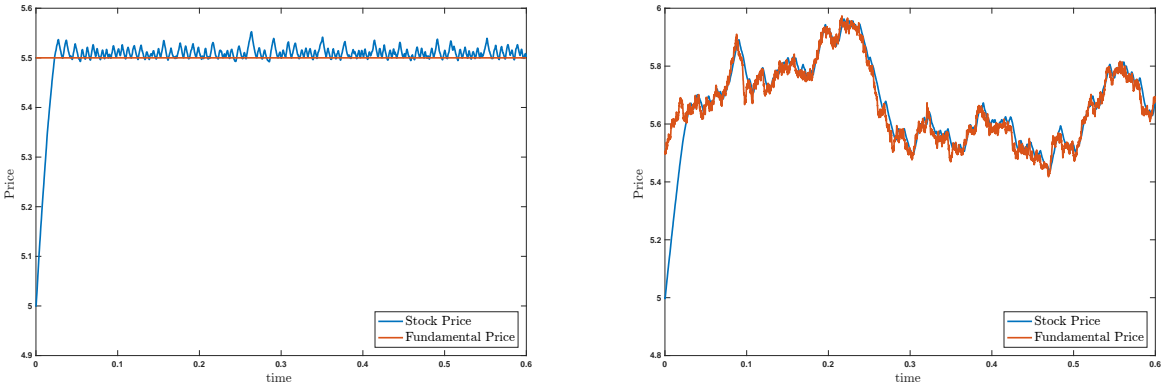


Figure 44: Stock price with a constant fundamental price s^f (left figure) and a time varying fundamental price (right figure).

44). We have already seen this characteristic price behavior in our simulations of the moment model. The asymmetries in the peaks are caused by the noise of the Monte Carlo solver. The price behavior rapidly changes for a time varying fundamental price. The stock price follows the fundamental price but has some overshoots (see figure 44). These overshoots are essential

to observe a fat-tail in the stock return distribution. To quantify this, we look at a quantile-quantile plot of logarithmic stock returns. We easily recognize that the stock return exhibits

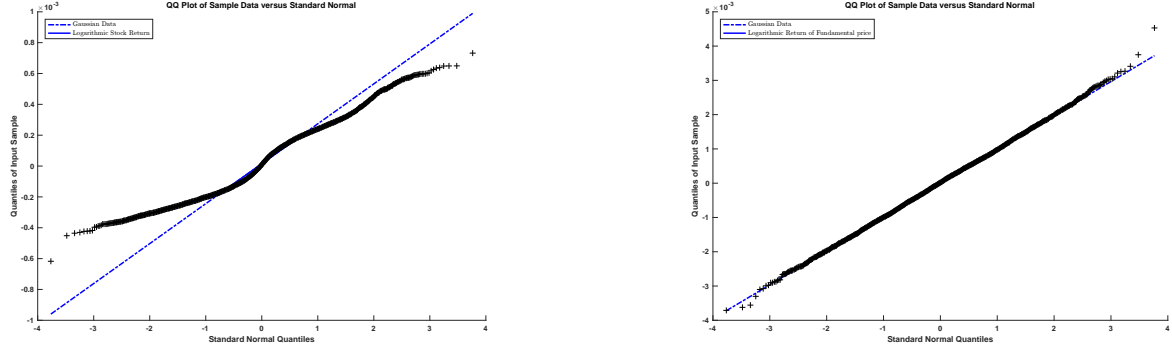


Figure 45: Quantile-quantile plot of logarithmic stock return distribution (left-hand side) and logarithmic return of fundamental prices (right-hand side).

heavy tails (see figure 45). In comparison to the stock return, the return of fundamental prices is well fitted by a Gaussian distribution.

Due to the mesoscopic kinetic model, we can analyze the price and wealth distributions. In the previous paragraph, we could show that the stock price distribution is given by lognormal law. Our simulations (see figure 46) verify this result. In addition, we want to have a look at the

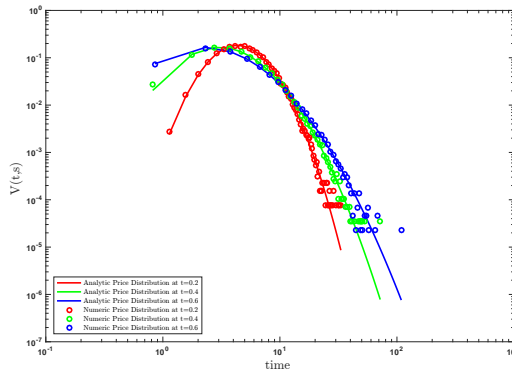


Figure 46: Stock price distribution.

marginal distribution $g(t, x)$ which describes the wealth of the stock portfolio. Unfortunately, we cannot give an analytic solution in the general case. Interestingly, the distribution of stock investments is well fitted by a normal distribution (see figure 47). In the special situation that the aggregated estimate of stock return over bond return, denoted by K , is strictly positive or strictly negative, we can compute marginal distributions analytically. Then the marginal distribution admits lognormal behavior. For our example, we consider the case $K > 0$, thus, we observe the marginal distribution of wealth in bonds h . In order to ensure $K > 0$, we have set the fundamental stock price to $s^f \equiv 10$ and fixed the weight $\chi \equiv 1$. As figure 48 illustrates, our numerical simulations certify our analytic result.

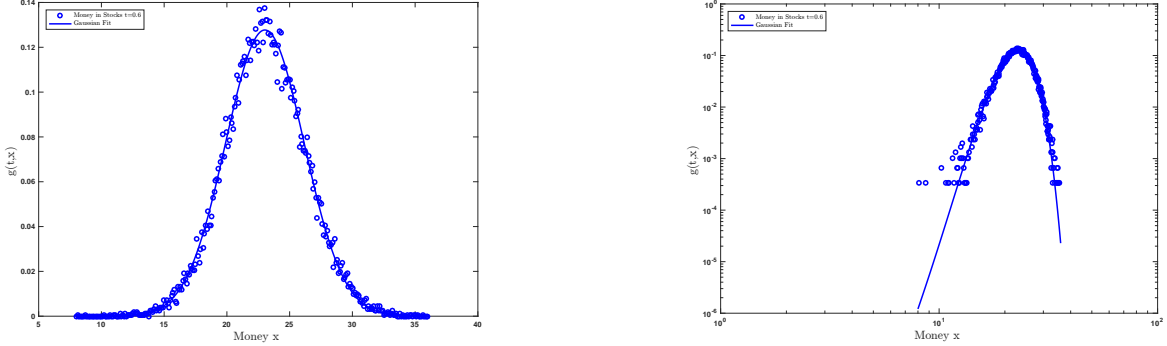


Figure 47: Distribution of the wealth invested in stocks with a gaussian fit. Left figure has a linear scale, whereas the right figure shows the distribution in log-log scale.

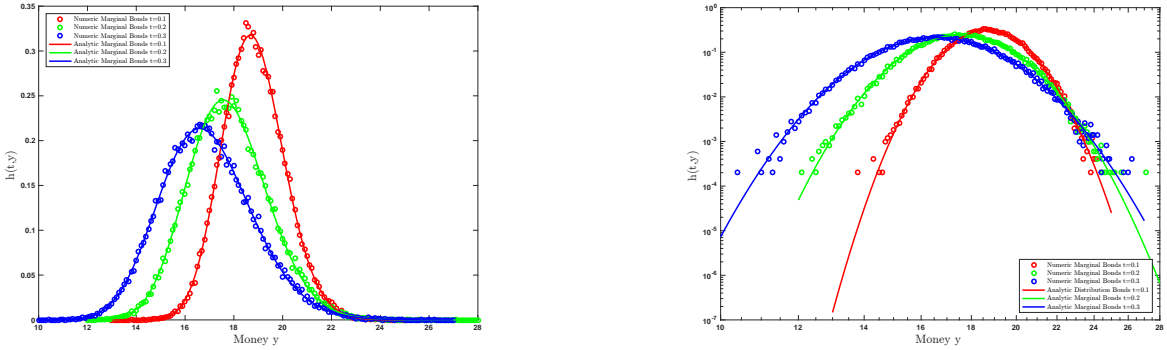


Figure 48: Distribution of the wealth invested in bonds plotted with the lognormal analytic self-similar solution.

High-Frequency Investors In the high-frequency investor case, we numerically observe a fat-tail (see figure 49). The fit by the inverse-gamma distribution reveals that the fit underestimates the tail probabilities. Furthermore, the wealth distributions are in both portfolios well-fitted by a Gaussian distribution as you can see in figure (50). The shape of the wealth coincides with the marginal portfolio distributions we computed in the long-term investor case.

In the previous section, we could compute an admissible steady state distribution analytically. We have observed that the inverse-gamma distribution is a steady state, which is asymptotically well characterized by a power-law for large stock prices s . In order to compute the steady state numerically, the constants r and D must be chosen in an unrealistic manner to guarantee a steady state in the portfolio dynamics. Furthermore, we do not consider the diffusive portfolio equation, but instead the mean field portfolio. In addition, the value function has been chosen as the identity and the weight is fixed as $\chi \equiv 1$. Figure (51) shows that the stock price distribution converges to the analytically computed steady state of inverse-gamma type.

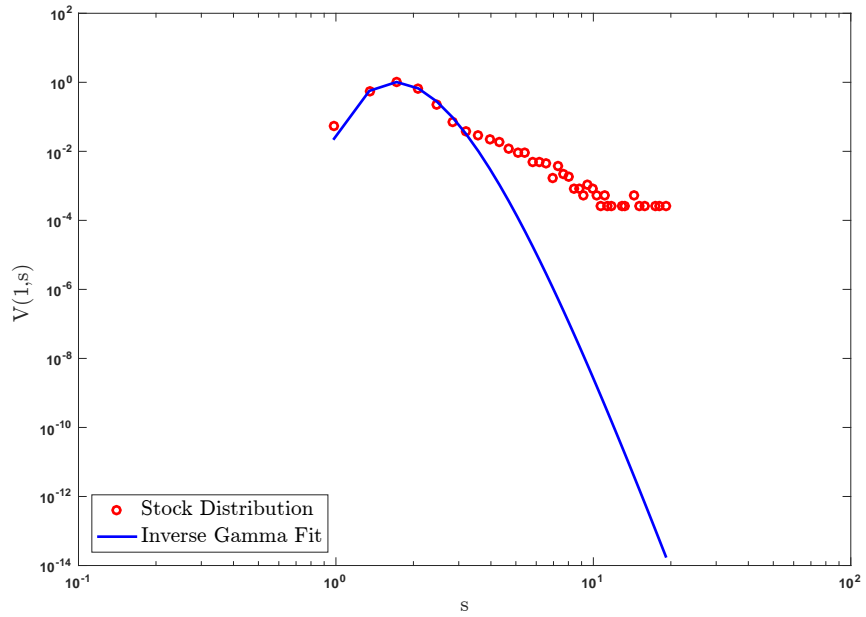


Figure 49: Stock price distribution.

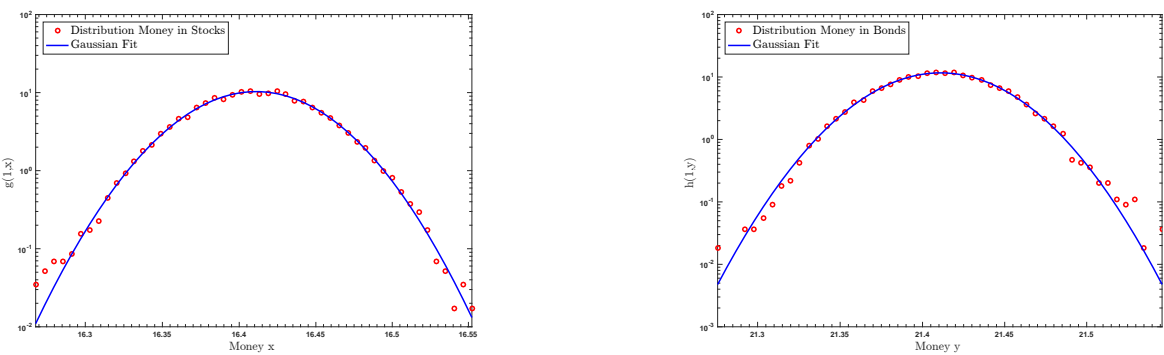


Figure 50: Distributions of the wealth invested in stocks (left-hand side) and wealth invested in bonds (right-hand side) at $t = 1$.

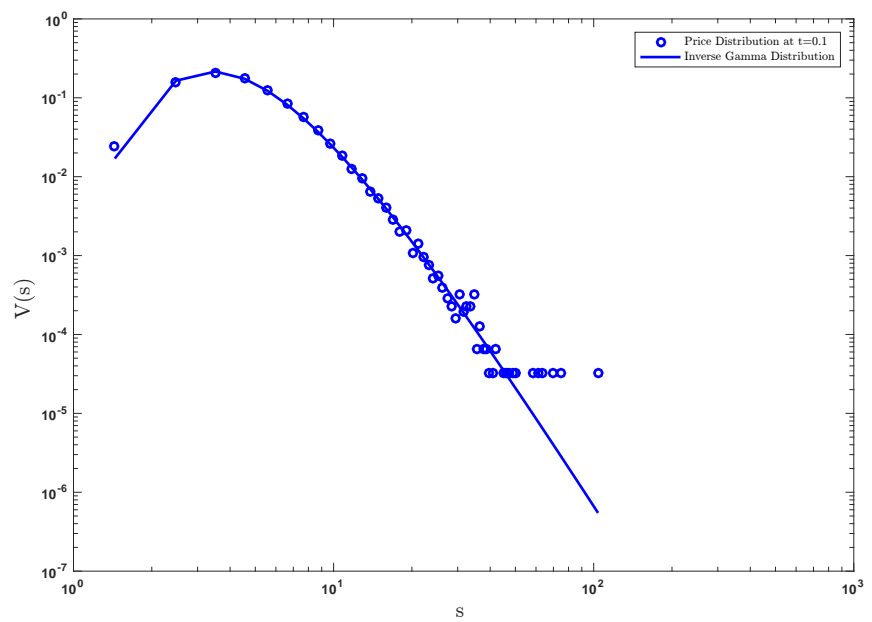


Figure 51: Steady state distribution.

4.8 Conclusion

The starting point of our investigation was a microscopic portfolio model coupled with the macroscopic stock price equation. Each financial agent was equipped with an optimization problem in order to derive his investment decision. We used the MPC approach in a game theoretical concept to simplify and solve the optimization. The MPC approach has given us a mathematical connection between the two economic concepts of rational and boundedly rational financial agents. Then, starting from the feedback controlled model, we derived a kinetic model. In three modeling stages we derived the mean field portfolio model, the diffusive mean field portfolio model and the diffusive mean field portfolio stock price model.

We first considered a macroscopic perspective and derived and analyzed a three-dimensional moment model. We have seen that this simple ODE model can already replicate financial data exhibiting prominent features like oscillatory solutions, booms and crashes. Then, the three kinetic portfolio models have been analyzed to discover insights in the portfolio distribution. The marginal distributions of wealth in bonds or wealth in stocks can be characterized by a lognormal distribution in special cases. These findings have been supported by our simulations. We have employed the diffusive mean field portfolio stock price model to investigate the price behavior. In the case of long-term investors, the price distribution is given by a lognormal law. In addition, we have computed a steady state of inverse gamma type in the stock price distribution for high-frequency trader. We have seen that for large stock prices the distribution asymptotically satisfies a power-law.

The possibility to analyze the underlying distribution functions means a huge advantage of the chosen kinetic approach. We want to conclude that kinetic modeling is a good tool to reveal insights in the stock price and wealth distributions.

Our model provides an explicit explanation for the creation of power-laws in the stock price distribution. Furthermore, we have observed fat-tails in the stock return distribution, which is a universal feature in real return data. Interestingly, we do not observe fat-tails in the portfolio distribution. This is a surprising result as one could expect to see the same distribution in the stock price and portfolio dynamics. A likely reason is the reallocation of wealth between the two assets which leads to a balance of wealth in both portfolios. We need to remark that regarding the wealth distribution, our model fails to replicate power-laws present in real financial data.

In order to observe a power-law in the wealth distribution, there are several possible model extensions. One idea is to add earnings to the microscopic model. Thus, one would add an external force on the microscopic level. This might give a fat-tail in the portfolio distribution. Alternatively, one could introduce wealth interactions among agents. There are several kinetic models which consider wealth distributions where a power-law has been observed [34, 67, 54, 197]. These models consider interacting financial agents who are performing binary trades. We leave this question open for further research.

4.9 Appendix

4.9.1 Moment Model

We summarize the solutions of the moment model in the following propositions.

Proposition 4.9.1. *In special cases, we can compute solutions of our stock price equation. We assume constant weights χ , a fixed frequency $\rho \equiv 1$ and assume that the utility function is described by the identity.*

- *Fundamentalists alone ($\chi = 1$): The stock price equation reads*

$$\dot{S} = \begin{cases} \kappa (\omega s^f - (\omega + r) S) Y, & \frac{\omega s^f}{\omega+r} > S, \\ \kappa (\omega s^f - (\omega + r) S) X, & \frac{\omega s^f}{\omega+r} < S. \end{cases}$$

This equation seems reasonable, so the investor shifts his capital into stocks if he expects a positive stock return, and vice versa. The solution is given by

$$S(t) = \begin{cases} (1 - \exp\{-\kappa (\omega + r) \int_0^t Y(\tau) d\tau\}) \frac{\omega s^f}{\omega+r} + S(0) \exp\{-\kappa (\omega + r) \int_0^t Y(\tau) d\tau\}, \\ \text{for } \frac{\omega s^f}{\omega+r} > S, \\ (1 - \exp\{-\kappa (\omega + r) \int_0^t X(\tau) d\tau\}) \frac{\omega s^f}{\omega+r} + S(0) \exp\{-\kappa (\omega + r) \int_0^t X(\tau) d\tau\}, \\ \text{for } \frac{\omega s^f}{\omega+r} < S. \end{cases}$$

Hence, the price is driven exponentially fast to the steady state $S_\infty = \frac{\omega s^f}{\omega+r}$.

- *Chartists alone ($\chi = 0$): We get*

$$\dot{S} = \begin{cases} \frac{\kappa D Y}{1-\kappa Y} - \frac{r \kappa Y}{1-\kappa Y} S, & \text{for } \kappa D Y + D (1 - \kappa Y) > S, \\ \frac{\kappa D X}{1-\kappa X} - \frac{r \kappa X}{1-\kappa X} S, & \text{for } \kappa D X + D (1 - \kappa X) < S. \end{cases}$$

The solution is given by

$$S(t) = \begin{cases} \left(1 - \exp\left\{-r \kappa \int_0^t \frac{Y(\tau)}{1-\kappa Y(\tau)} d\tau\right\}\right) \frac{D}{r} + S(0) \exp\left\{-r \kappa \int_0^t \frac{Y(\tau)}{1-\kappa Y(\tau)} d\tau\right\}, \\ \text{for } \kappa D Y + D (1 - \kappa Y) > S, \\ \left(1 + \exp\left\{-r \kappa \int_0^t \frac{X(\tau)}{1-\kappa X(\tau)} d\tau\right\}\right) \frac{D}{r} + S(0) \exp\left\{-r \kappa \int_0^t \frac{X(\tau)}{1-\kappa X(\tau)} d\tau\right\}, \\ \text{for } \kappa D X + D (1 - \kappa X) < S. \end{cases}$$

- *Chartists and fundamentalists with a constant weight $\chi \in (0, 1)$: The corresponding stock price equation reads*

$$\dot{S} = \begin{cases} \kappa (\chi \omega s^f + (1 - \chi) D - (r + \chi \omega) S) \frac{Y}{1+(1-\chi)\kappa Y}, & K(S) > 0, \\ \kappa (\chi \omega s^f + (1 - \chi) D - (r + \chi \omega) S) \frac{X}{1+(1-\chi)\kappa X}, & K(S) < 0. \end{cases}$$

The solution is given by

$$S(t) = \begin{cases} \left(1 - \exp\{-\kappa (\chi \omega + r) \int_0^t \frac{Y(\tau)}{1+\kappa(1-\chi)Y(\tau)} d\tau\}\right) \frac{\chi \omega s^f + (1 - \chi) D}{\chi \omega + r} \\ + S(0) \exp\{-\kappa (\chi \omega + r) \int_0^t \frac{Y(\tau)}{1+\kappa(1-\chi)Y(\tau)} d\tau\}, \quad \text{for } K(S) > 0, \\ \left(1 - \exp\{-\kappa (\chi \omega + r) \int_0^t \frac{X(\tau)}{1+\kappa(1-\chi)X(\tau)} d\tau\}\right) \frac{\chi \omega s^f + (1 - \chi) D}{\chi \omega + r} \\ + S(0) \exp\{-\kappa (\chi \omega + r) \int_0^t \frac{X(\tau)}{1+\kappa(1-\chi)X(\tau)} d\tau\}, \quad \text{for } K(S) < 0. \end{cases}$$

Proposition 4.9.2. *For the wealth evolution, we consider the stock and bond portfolio separately.*

- In the stock portfolio, the wealth evolution is given by

$$\dot{X} = \begin{cases} (\kappa K(S) Y + \frac{D}{S}) X + K(S) Y, & \text{for } K(S) > 0, \\ (\kappa K(S) X + \frac{D}{S}) X + K(S) X, & \text{for } K(S) < 0. \end{cases}$$

The solution is given by

$$X(t) = \begin{cases} X(0) \exp \left\{ \int_0^t \kappa K(S) Y + \frac{D}{S} d\tau \right\} + \left(1 - \exp \left\{ - \int_0^t \kappa K(S) Y d\tau \right\} \right) \frac{1}{\kappa}, & \text{for } K(S) > 0, \\ \frac{X(0) \exp \left\{ \int_0^t K(S) + \frac{D}{S} d\tau \right\}}{1 + \kappa \int_0^t K(S) \exp \left\{ \int_0^\zeta K(S) + \frac{D}{S} d\zeta \right\} d\tau}, & \text{for } K(S) < 0. \end{cases}$$

- The bond portfolio is given by

$$\dot{Y} = \begin{cases} r Y - K(S) Y, & \text{for } K(S) > 0, \\ r Y - K(S) X, & \text{for } K(S) < 0, \end{cases}$$

with the solution

$$Y(t) = \begin{cases} Y(0) \exp \left\{ \int_0^t (r - K(S)) d\tau \right\}, & \text{for } K(S) > 0, \\ \exp \{r t\} \left(Y(0) - \int_0^t K(S) X \exp \{-r \tau\} d\tau \right), & \text{for } K(S) < 0. \end{cases}$$

4.9.2 Parameters of Moment Simulation

If not indicated differently the parameters are set to:

Δt	0.0001	κ	0.1
D	0.01	ν	5
r	0.01	S_0	5
α	0.5	Y_0	20
ω	20	X_0	20
s^f	5.5	T_{end}	3
γ	0.35	ρ	1

4.9.3 Marginals of Mean Field Portfolio Model

For $K > 0$, we get a closed equation for h :

$$\partial_t h(t, y) + \partial_y \left(\left(r - \frac{K(S(t))}{\nu} \right) y h(t, y) \right) = 0.$$

This advection equation can also be solved by the lognormal density function

$$h(t, y) = \frac{\hat{c}}{\sqrt{\pi}y} \exp \left\{ - \left(\log(y) - \int_0^t r - \frac{K(S(\tau))}{\nu} d\tau \right)^2 \right\}, \quad \hat{c} > 0,$$

which can be verified by simple computations.

4.9.4 Marginals of Diffusive Mean Field Portfolio Model

In the case $K > 0$, we obtain for h the equation

$$\partial_t h(t, y) + \partial_x \left(\left[r - \frac{K(S(t))}{\nu} \right] y h(t, y) \right) = \frac{1}{2\nu^2} \partial_y^2 (y^2 h(t, y)).$$

Again, we consider the scaling $\bar{h}(t, \bar{y}) = y h(t, y)$, $\bar{y} = \log(y)$ and define $e(t) := r - \frac{K(S(t))}{\nu}$. Simple computations reveal that \bar{h} satisfies

$$\partial_t \bar{h}(t, \bar{x}) + \left(e(t) - \frac{1}{2\nu^2} \right) \partial_{\bar{y}} \bar{h}(t, \bar{y}) = \frac{1}{2\nu^2} \partial_{\bar{y}}^2 \bar{h}(t, \bar{y}).$$

We define $E(t) := \int_0^t e(\tau) d\tau + c_2$, $c_2 > 0$ and

$$\bar{h}(t, \bar{y}) = \frac{1}{(2(\frac{t}{\nu^2} + c_1)\pi)^{\frac{1}{2}}} \exp \left\{ - \frac{(\bar{y} + \frac{(\frac{t}{\nu^2} + c_1)}{2} - E(t))^2}{2(\frac{t}{\nu^2} + c_1)} \right\}, \quad c_1 > 0,$$

solves the previous convection-diffusion equation. Then, reverting to the original variables, we observe a lognormal law.

$$h(t, y) = \frac{1}{y(2(\frac{t}{\nu^2} + c_1)\pi)^{\frac{1}{2}}} \exp \left\{ - \frac{\left(\log(y) + \frac{(\frac{t}{\nu^2} + c_1)}{2} - E(t) \right)^2}{2(\frac{t}{\nu^2} + c_1)} \right\}, \quad c_1 > 0.$$

4.9.5 Asymptotic Limit of Boltzmann Model

We expand the test function $\phi(x', y')$ in a Taylor series up to order two.

$$\begin{aligned} \phi(x', y') - \phi(x, y) &= (x' - x) \frac{\partial \phi(x, y)}{\partial x} + (y' - y) \frac{\partial \phi(x, y)}{\partial y} + \\ &\quad (x' - x)(y' - y) \frac{\partial^2 \phi(x, y)}{\partial y \partial x} + \frac{1}{2}(y' - y)^2 \frac{\partial^2 \phi(x, y)}{\partial y^2} + \\ &\quad \frac{1}{2}(x' - x)^2 \frac{\partial^2 \phi(x, y)}{\partial x^2} + R(x, y). \end{aligned}$$

Here, R denotes the remainder of the Taylor series. The right-hand side of our kinetic equation is then given by:

$$\begin{aligned} (L(f), \phi) = & \left\langle \theta \int a \left[x \left(\kappa ED + \frac{D}{S} \right) + u_\eta^*(t, x, y, S) \right] \frac{\partial \phi(x, y)}{\partial x} f(t, x, y) dx dy \right\rangle \\ & + \left\langle \theta \int a [y r - u_\eta^*(t, x, y, S)] \frac{\partial \phi(x, y)}{\partial y} f(t, x, y) dx dy \right\rangle \\ & + \left\langle \theta \int \left[(x' - x) (y' - y) \frac{\partial^2 \phi(x, y)}{\partial y \partial x} + \frac{1}{2} (y' - y)^2 \frac{\partial^2 \phi(x, y)}{\partial y^2} \right] f(t, x, y) dx dy \right\rangle \\ & + \left\langle \theta \int \left[\frac{1}{2} (x' - x)^2 \frac{\partial^2 \phi(x, y)}{\partial x^2} + R(x, y) \right] f(t, x, y) dx dy \right\rangle. \end{aligned}$$

We make the following scaling assumptions:

$$\theta = \frac{1}{\epsilon}, \quad a = \epsilon.$$

The interaction operator is consequently given by:

$$\begin{aligned} (L(f), \phi) = & \int \left[x \left(\kappa ED + \frac{D}{S} \right) + u^*(x, y, S) \right] \frac{\partial \phi(x, y)}{\partial x} f(t, x, y) dx dy \\ & + \int [y r - u^*(x, y, S)] \frac{\partial \phi(x, y)}{\partial y} f(t, x, y) dx dy \\ & + \int \left[\epsilon x \left(\kappa ED + \frac{D}{S} \right) y r - \frac{1}{\nu^2} (H(-K)x + H(K)y)^2 \right] \frac{\partial^2 \phi(x, y)}{\partial y \partial x} f(t, x, y) dx dy \\ & + \int \frac{1}{2} [\epsilon y^2 r^2 - 2 \epsilon y r u^*(x, y, S) + \epsilon u^*(x, y, S) + \frac{1}{\nu^2} (H(-K)x + H(K)y)^2] \frac{\partial^2 \phi(x, y)}{\partial y^2} f(t, x, y) dx dy \\ & + \int \frac{1}{2} [\epsilon \left(x \left(\kappa ED + \frac{D}{S} \right) + u^*(x, y, S) \right)^2 + \frac{1}{\nu^2} (H(-K)x + H(K)y)^2] \frac{\partial^2 \phi(x, y)}{\partial x^2} f(t, x, y) dx dy \\ & + R_\epsilon(t). \end{aligned}$$

Here, we have used the fact that our random variable has zero mean. We assume that the remainder

$$R_\epsilon(t) := \left\langle \theta \int R_\epsilon(x, y, \gamma) f(t, x, y) dx dy \right\rangle,$$

vanishes in the limit $\epsilon \rightarrow 0$. Consequently, our integral operator simplifies to

$$\begin{aligned} (L(f), \phi) = & \int \left[x \left(\kappa ED(t) + \frac{D}{S} \right) + u^*(x, y, S) \right] \frac{\partial \phi(x, y)}{\partial x} f(t, x, y) dx dy + \\ & \int [y r - u^*(x, y, S)] \frac{\partial \phi(x, y)}{\partial y} f(t, x, y) dx dy + \\ & \int \frac{1}{2} \frac{1}{\nu^2} (H(-K)x + H(K)y)^2 \left[\frac{\partial^2 \phi(x, y)}{\partial x^2} + \frac{\partial^2 \phi(x, y)}{\partial y^2} - \frac{\partial^2 \phi(x, y)}{\partial y \partial x} \right] f(t, x, y) dx dy, \end{aligned}$$

as $\epsilon \rightarrow 0$. Then we integrate by parts and observe the weak form of the following Fokker-Planck equation

$$\begin{aligned}
& \frac{\partial}{\partial t} f(t, x, y) + \frac{\partial}{\partial x} \left(\left[x \left(\kappa ED(t) + \frac{D}{S} \right) + u^*(x, y, S) \right] f(t, x, y) \right) + \\
& \frac{\partial}{\partial y} ([y r - u^*(x, y, S)] f(t, x, y)) + \frac{1}{\nu^2} \frac{\partial^2}{2 \partial x \partial y} ((H(-K)x + H(K)y)^2 f(t, x, y)) \\
= & \frac{1}{\nu^2} \frac{\partial^2}{2 \partial x^2} ((H(-K)x + H(K)y)^2 f(t, x, y)) + \frac{1}{\nu^2} \frac{\partial^2}{2 \partial y^2} ((H(-K)x + H(K)y)^2 f(t, x, y)).
\end{aligned}$$

4.9.6 Parameters of Simulations

The parameters of our simulations are set to:

Random Fundamental Price

Δt	0.0001	κ	0.4
D	0.01	ν	5
r	0.01	S_0	5
α	0.5	Y_0	20
β	0.65	X_0	20
ω	80	T_{end}	0.6
γ	0.55	Samples	$3 \cdot 10^4$
ρ	$\frac{2}{3}$		

Computation of Marginal

Δt	0.0001	κ	0.1
D	0.01	ν	5
r	0.01	S_0	5
χ	1	Y_0	20
s^f	10	X_0	20
ω	20	T_{end}	0.3
γ	0.35	Samples	$5 \cdot 10^4$
ρ	$\frac{2}{3}$		

High-frequency trader

Δt	0.001	κ	0.4
D	0.01	ν	5
r	0.01	S_0	5
α	1	Y_0	20
β	0.2	X_0	20
ω	80	T_{end}	1
γ	0.55	Samples	$5 * 10^3$
ρ	$\frac{2}{3}$		

5 Mean Field Limit of a Behavioral Financial Market Model

In the past decade there has been a growing interest in agent-based econophysical financial market models. The goal of these models is to gain further insights into stylized facts of financial data. We derive the mean field limit of the econophysical Cross model [71] and show that the kinetic limit is a good approximation of the original model. Our kinetic model is able to replicate some of the most prominent stylized facts, namely fat-tails of asset returns, uncorrelated stock price returns and volatility clustering. Interestingly, psychological misperceptions of investors can be accounted to be the origin of the appearance of stylized facts. The mesoscopic model allows us to study the model analytically. We derive steady state solutions and entropy bounds of the deterministic skeleton. These first analytical results already guide us to explanations for the complex dynamics of the model.

5.1 Introduction

In the past years, there has been a number of financial crises (Black Monday 1987, Dot-com Bubble 2000, Global Financial Crisis 2007). Unfortunately, these crises all have in common that classical financial market models fail to explain their origin and existence [61, 102]. Additionally, these models fail to explain the existence of *stylized facts*, which are assumed to be one important aspect to the creation of market crashes [152]. Stylized facts are statistical properties of financial data observable all over the world [62]. The most prominent examples are *fat-tails* in asset returns and *volatility clustering* [63, 30]. In physics, stylized facts might be viewed as scaling laws [162], which is the reason why physicists became more and more interested in economic models [226].

This has lead to the new field of research called econophysics which can be traced back to the Dow Jones crash (Black Monday) in 1987. Generally speaking, physicists and economists apply physical theories such as kinetic theory, mean field theory or percolation theory to economic issues. One tool of econophysics are so called agent-based financial market models. Many researchers believe that these models help to gain more insights into financial markets [102, 162]. These modern models of financial markets consist of many interacting agents which are studied with the help of Monte Carlo simulations [151].

These models do not consider rational financial agents, often called *homo oeconomicus*, which have been considered in the classical financial market models. They rather consider so called bounded rational agents in the sense of Simon [214] and are often inspired by the prospect theory founded by Kahnemann and Tversky [134]. These modern financial market models can reproduce stylized facts and they seem to indicate that psychological misperceptions of agents are one reason for their appearance. However, until now the origin of stylized facts is not completely understood [162].

Time continuous, in particular kinetic partial differential equations (PDEs), can help to understand the connection between the microscopic modeling of investors (agents) and the existence of stylized facts. One reason is the possibility to study the long time behavior of PDE models. This can be done by studying the steady state solutions of the PDE model. In the last decade, there have been several attempts from the physical and mathematical community to translate financial market models into time continuous PDE models. Examples are [166, 66] and more recently [243]. There are many mathematical methods to translate microscopic ordinary dif-

ferential equations (ODEs) into PDEs. A popular approach in economic applications is the kinetic Boltzmann method, mainly advanced by Toscani and Pareschi [198]. This ansatz is mathematically well understood and has been applied to many different applications in life sciences and social sciences [198]. In this paper, we follow a closely related approach. Instead of considering the kinetic Boltzmann description, we perform the mean field limit. The mean field limit is one of the classical kinetic limits as well, and describes the limit of infinitely many microscopic agents. The reason for that choice is that the microscopic coupling of agents in financial market models is induced by averaging of the agents' investment decisions. Hence, no binary interactions among agents, as considered in the kinetic Boltzmann approach, but rather a force field induced by the actions of all investors drives the microscopic dynamics.

The goal of this work is to derive the mean field limit of a microscopic econophysical financial market model. We show that the mesoscopic model is a good approximation of the original agent-based model. We have chosen a microscopic econophysical model which considers behavioral aspects of investors and reveals that they are the reasons for the existence of stylized facts. Thus, the starting point of our investigations is an agent-based model published by Cross et al. [71] in 2005. In Monte Carlo simulations, this model can reproduce the most prominent *stylized facts* of financial data, namely: *fat-tails in stock price return data, uncorrelated price returns and volatility clustering*. The benefit of this model is that it shows, by means of computer simulation, that the psychological herding pressure of investors causes the appearance of fat-tails . In absence of the herding pressure, the stock price behavior is characterized by a Gaussian return distribution. The financial agents are modeled as bounded rational agents in the sense of Simon [214]. Each financial agent is described by his investment decision on the stock market, meaning if they are in a short position (sell stocks) or long position (buy stocks). Since each agent is characterized through two possible orientations, there is an obvious connection to the Ising spin model [126] known in statistical physics. It is important to emphasize that this model follows a bottom up approach [71] and develops the aggregated stock price behavior from reasonable microscopic interactions. These microscopic interactions can be interpreted as a simple trading strategy of investors. Nevertheless, we still consider a basic model. The model is simple in the sense that there are no binary interactions between agents and the agents have no learning ability [71]. Furthermore, we want to underline that the goal of Cross et al. is not to predict prices or understand how to fit historic prices best [71], but rather gain insights into the creation of stylized facts. We also want to mention that there has been an earlier attempt to derive a mean field model of the original model [70]. In fact, the mean field model [70] follows a different philosophy and does not use a bottom up approach. In particular, the model [70] is substantially different compared to the original model [71]. Before we can derive the mean field limit of the model of Cross et al., we need to ensure that there are no finite size effects regarding the number of agents. Earlier studies [93, 254, 143, 119] and recently by Otte et al. [242] show that many agent-based econophysical models have finite size effects. Pleasingly, this is not the case in the original Cross model, as the simulations of Otte et al. [242] revealed. In this study, simulations with up to five million agents of the original Cross model have been conducted. For further simulation results we refer to the original papers [71, 72, 145] and the recently introduced SABCEMM tool [242].

The result of the kinetic limit is a system of PDEs coupled with a stochastic differential equation (SDE). The SDE defines the time evolution of the market price, whereas the PDEs

governs the investment decision of agents. We derive the space-homogeneous PDE-SDE system and the space-heterogeneous PDE-SDE system. The former corresponds to the *ratio-*
nal agent model with no herding, whereas the latter takes herding into account. In fact, the space-homogeneous model generates Gaussian stock price data while the heterogeneous model can create fat-tails in asset returns. Thus, our mesoscopic model exhibits the same characteristics and can reproduce qualitatively the same stylized facts as the original model [71]. Additionally, to its economic relevance this PDE-SDE system is already interesting for pure mathematical considerations. This model is very similar to models of animal aggregation originally introduced by Eftimie et al. [92]. Furthermore, our model is closely related to *structured population dynamics* as discussed in [183, 203]. This type of kinetic model has been probably first introduced by Kac [132]. In addition, there is also an obvious similarity to the famous Goldstein-Taylor model [110, 231].

The structure of the paper is as follows: First, we introduce the econophysical model of Cross et al. [71] which we denote *Cross model*. We then introduce a microscopic approximation of the original Cross model which we call *kinetic particle model*. In section 4, we derive the time continuous space-homogeneous and space-heterogeneous *mean field Cross model*. Throughout the paper we give numerical simulations of the different models. In section 5, we extensively study the mean field Cross model numerically. In addition, we show that the mean field Cross model is qualitatively identical to the original Cross model. In section 6, we present a qualitative study of the mesoscopic model. We finish the paper with a short discussion of this work and a presentation of further research directions.

5.2 The Original Model

In this section, we provide a brief definition of the original Cross model [71]. There is a fixed number of $N \in \mathbb{N}$ agents. Each agent has to decide in each time step whether he wants to be long or short in the market, meaning if he wants to buy or sell stocks. Thus, the investment propensity γ_i of each agent switches between a buy position $\gamma_i = 1$ and a sell position $\gamma_i = -1$. The excess demand function at time $t \in [0, \infty)$ is defined as the average of all investment decisions γ_i .

$$ED_N(t) := \frac{1}{N} \sum_{i=1}^N \gamma_i(t). \quad (55)$$

Hence, ED_N measures the fraction of long respectively short investors. Furthermore, the model introduces two *psychological* pressures, the *herding pressure* and the *inaction pressure*, which control the switching mechanism of investment decisions. The *inaction pressure* is defined by the interval

$$I_i = \left[\frac{m_i}{1 + \alpha_i}, m_i (1 + \alpha_i) \right],$$

where m_i denotes the stock price of the last switch of agent i and $\alpha_i > 0$ is the so called *inaction threshold*. The investor switches position if the current stock price $S(t) > 0$ leaves the interval I_i . This trading strategy can be interpreted as an agent *taking his profits* or *cutting his losses*. The model is discrete in time with fixed increments of time $\Delta t > 0$.

The *herding pressure* is given by:

$$\begin{cases} c_i(t + \Delta t) = c_i(t) + \Delta t |ED_N(t)|, & \text{if } \gamma_i(t) ED_N(t) < 0, \\ c_i(t + \Delta t) = c_i(t), & \text{otherwise.} \end{cases} \quad (56)$$

Thus, the herding pressure is increased if the financial agent is in the minority position. The switch is induced if the herding pressure exceeds the *herding threshold* β_i . The thresholds α_i, β_i are drawn from uniformly, independently and identically distributed random variables.

$$\begin{aligned} \alpha_i &\sim \text{Unif}(A_1, A_2), \quad A_2 > A_1 > 0, \\ \beta_i &\sim \text{Unif}(B_1, B_2), \quad B_2 > B_1 > 0. \end{aligned}$$

We assume that α_i and β_i are uncorrelated and fixed after the initial choice. The constants B_1 and B_2 have to scale with time, since they correspond to the time units an investor can resist the herding pressure.

$$\begin{aligned} B_1 &:= b_1 \cdot \Delta t, \quad b_1 > 0, \\ B_2 &:= b_2 \cdot \Delta t, \quad b_2 > 0. \end{aligned}$$

In summary, the switching mechanism can be described as follows.

The switch is induced if

$$c_i > \beta_i \text{ or } S(t) \notin I_i.$$

After each switch the *herding pressure* gets reset to zero and the memory variable m_i gets updated to the current stock price.

The stock price is then driven by the excess demand:

$$S(t + \Delta t) = S(t) \exp \left\{ (1 + \theta |ED_N(t)|) \left(\sqrt{\Delta t} \eta - \frac{\Delta t}{2} \right) + \kappa \Delta t \frac{\Delta ED_N(t)}{\Delta t} \right\}, \quad (57)$$

$$\eta \sim \mathcal{N}(0, 1), \quad (58)$$

$$\Delta ED_N(t) := \frac{1}{N} \sum_{i=1}^N \gamma_i(t) - \frac{1}{N} \sum_{i=1}^N \gamma_i(t - \Delta t), \quad (59)$$

where the constant $\kappa > 0$ is known as market depth measuring the impact of a change in excess demand on the stock price. The *heteroskedasticity parameter* $\theta \geq 0$ models the impact of the excess demand on the random external market information modeled by the Gaussian random variable. The reason for that choice is that “*periods of extreme market volatility often coincide with periods of extreme*” [71] excess demand. We refer to the original papers [71, 72, 145] for further modeling details.

5.2.1 Microscopic Simulations

In this section, we shortly present the outcome of simulations of the original Cross model. We investigate the most prominent stylized facts of financial data, namely fat-tails of asset returns, uncorrelated stock price returns and volatility clustering. A fat-tailed distribution is characterized by an algebraic decay of the tails of the distribution. This can be well illustrated by a qq-plot, where the data is fitted against a Gaussian distribution. Uncorrelated price returns and volatility clustering can be deduced from the auto-correlation function of stock price returns. The former corresponds to an auto-correlation of zero and the latter to a slow decaying positive correlation of absolute log-returns for increasing time lags.

If only the inaction pressure is active (blue graph in figure 52), we obtain Gaussian behavior of the stock price since the excess demand is approximately zero. In fact, this trading rule can be regarded as in some sense *rational*. If the herding pressure is added, the stock price behavior rapidly changes and we obtain non-Gaussian return distributions (green graph in figure 52). In both cases we observe uncorrelated raw price returns which can be deduced

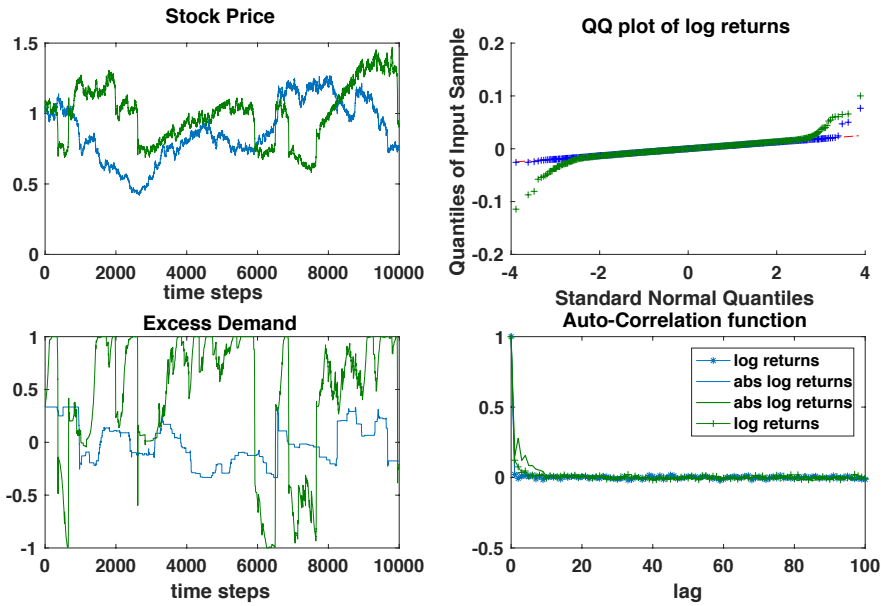


Figure 52: Simulations of the original Cross model. The blue graph represents simulations only conducted with the inaction pressure, whereas the model output conducted with the inaction and herding pressure are colored green. The heteroskedasticity parameter is set to $\theta = 2$ and we refer to table 9 for further details.

from the auto-correlation plot in figure 52. Furthermore, there is only a minor correlation in the case where both pressures are active. Figure 53 reveals, adding a dependence on the excess demand to the diffusion ($\theta = 2$), that we obtain volatility clustering. In agreement with earlier studies [71, 72], we obtain no qualitative change in the simulations in cases where

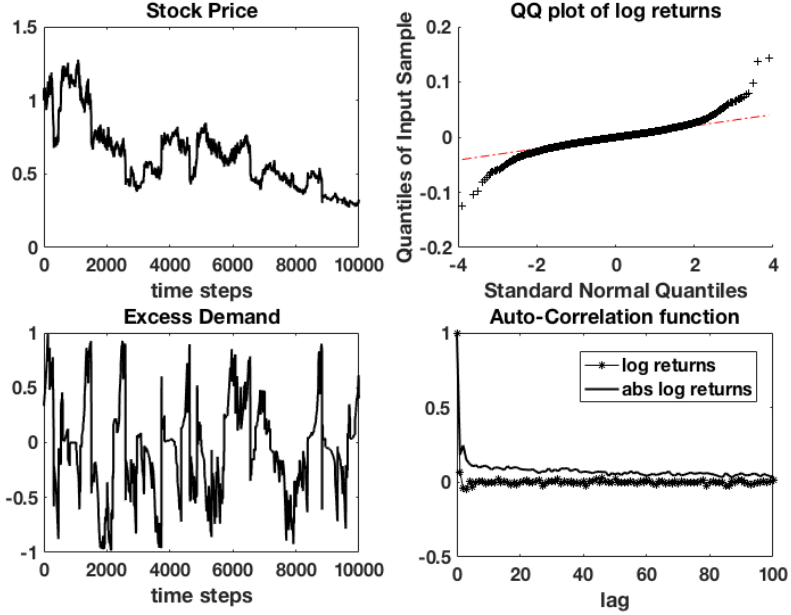


Figure 53: Simulations of the original Cross model with inaction and herding pressure. The heteroskedasticity parameter is set to $\theta = 2$. For further choices of parameters we refer to table 9.

the herding thresholds are correlated or the thresholds get resampled after each switch. For these reasons, we have used the simplest, previously introduced setting.

In summary, we want to record that the model with only active inaction pressure and constant diffusion function produces Gaussian stock return behavior. In comparison to that, adding the herding pressure changes the price behavior and we obtain fat-tails in the stock return. Furthermore, adding an excess demand depending diffusion function, results in volatility clustering.

5.3 Kinetic Particle Model

As pointed out previously, our goal is to derive a mesoscopic description of the agents' dynamics. From a mathematical perspective, the original Cross model is a highly non-linear dynamical system. In order to derive a kinetic PDE model, we need to consider the continuum limit $\Delta t \rightarrow 0$ and the mean field limit $N \rightarrow \infty$. The mean field limit, is well known in statistical physics and is concerned with the description of large particle systems by probabilistic quantities. Famous physical examples are the Ising model [126] or the Vlasov [246] equation. Before we derive the kinetic model, we first derive a particle game. Secondly, we translate the particle game into a PDE. In fact, our financial agents are described by three quantities; the market position $\gamma_i \in \{-1, 1\}$, the herding pressure $c_i \geq 0$ and the memory variable $m_i \geq 0$. The two quantities, the herding pressure and the memory variable, can take continuous values whereas the market position is discrete. Consequently, it is reasonable to divide the population into two groups, the agents holding a long position and the agents holding a short position. In a next step, we want to derive a switching probability of each agent to

change his market position during a fixed time interval. This means that we want to neglect any dependencies of each agent on his personal past action. Hence, each agent rolls the dice at each time step and the switching probability of the agent only depends on the position of the agent in the (m, c) space and the external stock price. This simplification is crucial in order to derive a kinetic PDE system. First, we aim to derive the switching probability based on the herding pressure denoted by $p(c) \in [0, 1]$, $c \in \mathbb{R}$. In fact, the herding thresholds are all realizations of a uniformly distributed random variable on $[B_1, B_2]$. Consequently, the probability for a switch is simply given by the cumulative distribution function of the random variable $\beta \sim \text{Unif}(B_1, B_2)$.

$$p(c) := P(\beta \leq c) = \int_{-\infty}^c \frac{x - B_1}{B_2 - B_1} dx = \begin{cases} 0, & c < B_1, \\ \frac{c - B_1}{B_2 - B_1}, & c \in [B_1, B_2], \\ 1, & c > B_2. \end{cases}$$

Equivalently, we define two random variables

$$\psi \sim \text{Unif}(M_1(m), M_2(m)), \quad M_1(m) := \frac{m}{1 + A_2}, \quad M_2(m) := \frac{m}{1 + A_1}$$

and

$$\eta \sim \text{Unif}(M_3(m), M_4(m)), \quad M_3(m) := m(1 + A_1), \quad M_4(m) := m(1 + A_2)$$

for an arbitrary but fixed $m > 0$. Notice that $M_1 < M_2 < M_3 < M_4$ holds and consequently the probability of a switch for a given stock price $S > 0$ and memory $m > 0$ can be modeled by:

$$q(m, S) := 1 - P(\psi \leq S) + P(\eta \leq S) = \begin{cases} 1, & S < M_1(m), \\ 1 - \frac{S - M_1(m)}{M_2(m) - M_1(m)}, & S \in [M_1(m), M_2(m)], \\ 0, & S \in (M_2(m), M_3(m)), \\ \frac{S - M_3(m)}{M_4(m) - M_3(m)}, & S \in [M_3(m), M_4(m)], \\ 1, & S > M_4(m). \end{cases}$$

We define the switching probability to be the linear combination of these two probabilities.

$$\lambda_P(t, c, m, S) := \lambda_1 p(c) + \lambda_2 q(t, m, S), \quad \lambda_1, \lambda_2 > 0, \quad \text{with } \lambda_1 + \lambda_2 = 1.$$

This choice has been made partially for simplicity and as a result of simulations that indicate a good performance of this choice. We want to summarize the new kinetic particle model.

Each agent is described by the three properties (γ_i, c_i, m_i) . The excess demand is simply the average of the investment propensities (55) and the time evolution of the herding pressure is given by (56). At each time step $t_k := k \Delta t$, $k \in \mathbb{N}$, the agent switches his market position with the probability $\lambda_P(t_k, c_i, m_i, S)$. The memory variable m_i and the herding pressure c_i get updated after a switch as in the original model. The time evolution of the stock price equation is given by

$$S(t_{k+1}) = S(t_k) + \Delta t \kappa \frac{\Delta ED_N}{\Delta t} S(t_k) + \sqrt{\Delta t} (1 + \theta |ED_N|) S(t_k) \eta. \quad (60)$$

The pricing equation (58) of the original Cross model approximates the underlying time continuous model by an explicit exponential integrator. We approximate the time continuous SDE by an Euler-Maruyama discretization.

In some sense, the derived switching probabilities can already be seen as the mean field limit of our system. In fact, our approximation is only good if we consider a sufficiently large number of agents. Thus this kinetic particle model should be seen as a realization of a random process of interacting agents. It is worthwhile to notice that this kinetic approximation leads to a noticeable reduction of computational costs in comparison to the original Cross model. The model outputs are qualitatively identical and both models compute the same quantities. The simulations have been conducted on the same machine. In our MATLAB implementation, we obtain a speedup of the factor 72.

5.3.1 Microscopic Simulations of Kinetic Particle Model

In this section, we want to show that the kinetic particle model must be regarded a good approximation of the original Cross model at least on a qualitative level. Remember that we have introduced a switching rate for the investment decisions of agents and changed the pricing formula.

As in our previous microscopic simulations, we see a Gaussian behavior of the stock return distribution in the pure inaction case (blue graph in figure 54). When adding the herding pressure (green graph in figure 54) the behavior of the price rapidly changes and we obtain fat-tails in the price return distribution. These results coincide with the findings in the original Cross model. We obtain that the additional psychological herding effect forms jumps in the price process, respectively oscillations in the excess demand.

In the next simulation, see figure 55, we consider a positive heteroskedasticity parameter, setting $\theta = 2$. As in the original Cross model, we obtain additional volatility clustering which can be deduced from the auto-correlation plot in figure 55.

5.4 Kinetic Model

We introduce two groups of agents. One investor group is long $\gamma_i = 1$ and the other short $\gamma_i = -1$ in the market. Hence, we consider the two densities $f^+(t, m, c)$ and $f^-(t, m, c)$. The variable $m \in \mathbb{R}$ we call memory variable which considers the stock price of the last switch. The variable $c \in \mathbb{R}$ is the herding pressure which is increased if the personal market position is in the opposite direction of the excess demand. We have not chosen the half space $m, c \in \mathbb{R}_{\geq 0}$ to avoid non-standard boundary conditions at zero. Due to our choice, we can pose simple Dirichlet boundary conditions. Furthermore, we assume for a moment that the stock price $S(t)$ is externally provided. The time evolution of the densities is described by two phenomena:

Transport There is an advection of the herding pressure which is proportional to the excess demand if the agent's decision contradicts the average opinion. Mathematically, this can be modeled by:

$$\begin{aligned}\partial_t f^+(t, m, c) + \partial_c (H(-ED[f^+, f^-](t)) f^+(t, m, c)) &= 0, \\ \partial_t f^-(t, m, c) + \partial_c (H(ED[f^+, f^-](t)) f^-(t, m, c)) &= 0,\end{aligned}$$

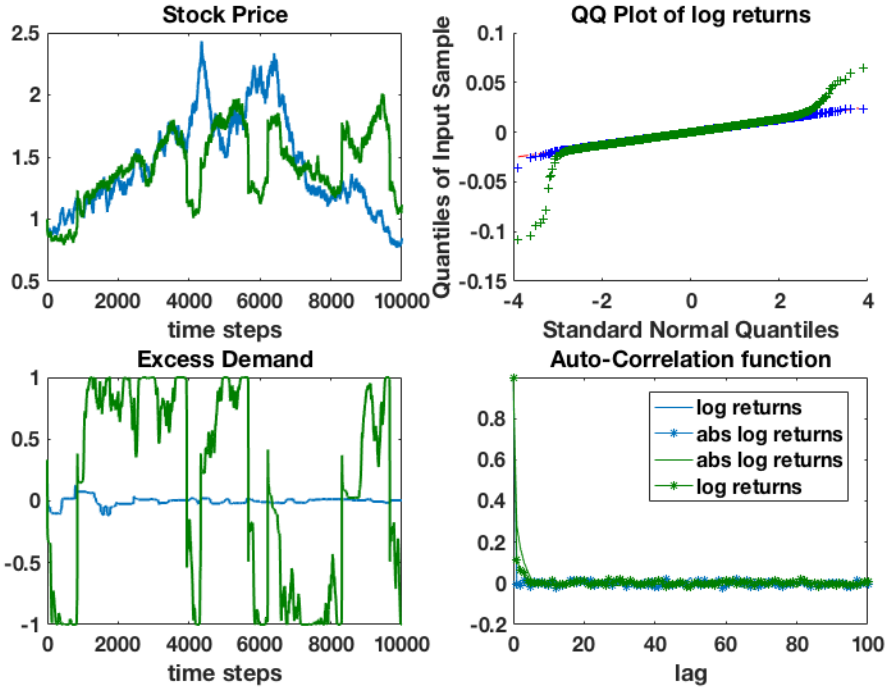


Figure 54: Simulations of the kinetic particle model with inaction and herding pressure (green graph) and only inaction pressure (blue graph). We have set the heteroskedasticity parameter $\theta = 0$, for further details we refer to table 10.

with

$$ED[f^+, f^-](t) := \int f^+(t, m, c) - f^-(t, m, c) dm dc.$$

Here, the shape function $H(\cdot)$ has the following properties

- $H(x) = 0, \forall x \leq 0,$
- $H(x) > 0, \forall x > 0,$
- $\dot{H}(x) \geq 0, \forall x \geq 0.$

In order to approximate the original Cross model best, we choose the shape function as follows:

$$H_C(x) := \begin{cases} 0, & x \leq 0, \\ x, & x > 0. \end{cases}$$

The second effect of our particle dynamics are the interactions through the switching rate.

Switching Mechanism As derived previously, the switching of investors between a long ($\gamma=1$) and short ($\gamma = -1$) position is fully determined by the switching rate λ . Since we are faced with a rate, we need to scale the probability λ_P by the characteristic time step of the Cross model $\Delta t_C > 0$, we define: $\lambda(t, c, m, S) := \frac{\lambda_P(t, c, m, S)}{\Delta t_C}$.

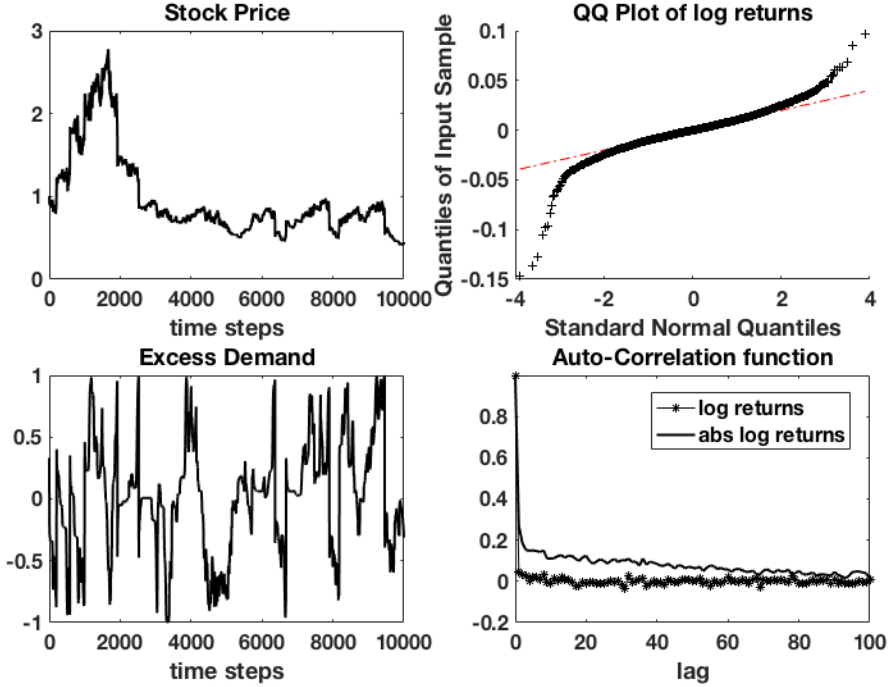


Figure 55: Simulations of the kinetic particle model with inaction and herding pressure (green graph) and only inaction pressure (blue graph). We have set the heteroskedasticity parameter $\theta = 2$, for further details we refer to table 10.

The loss of agents with a long, respectively short position, is simply described by multiplication of the rate λ with the corresponding density function.

$$Q_{loss}[f^{(\cdot)}](t, m, c, S) := f^{(\cdot)}(t, m, c) \lambda(t, m, c, S).$$

The gain term is more complex. As determined by the particle dynamic, all agents which have switched are re-emitted in the (c, m) space at the point $(0, S)$. Hence, translated into our continuous dynamics we get:

$$Q_{gain}[f^{(\cdot)}](t, m, c, S) := \delta(m - S(t)) \delta(c) \int Q_{loss}[f^{(\cdot)}](t, m, c, S) dm dc.$$

Thus, e.g. in the case of f^+ the switching dynamic is given by:

$$\partial_t f^+(t, m, c) = Q_{gain}[f^-](t, m, c, S) - Q_{loss}[f^+](t, m, c, S).$$

The Model Finally, the complete evolutionary dynamics of the densities f^+ , f^- are described by the system:

$$\begin{aligned} \partial_t f^+(t, m, c) + \partial_c (H(-ED[f^+, f^-](t)) f^+(t, m, c)) &= Q_{gain}[f^-](t, m, c, S) - Q_{loss}[f^+](t, m, c, S), \\ \partial_t f^-(t, m, c) + \partial_c (H(ED[f^+, f^-](t)) f^-(t, m, c)) &= Q_{gain}[f^+](t, m, c, S) - Q_{loss}[f^-](t, m, c, S). \end{aligned} \quad (61)$$

This PDE system is coupled with the SDE

$$dS = \kappa \dot{ED} S dt + (1 + \theta |ED|) S dW, \quad (62)$$

where W denotes the Wiener process and we interpret the stochastic integral in the Itô sense. The SDE (62) is the time continuous version of the previously introduced stock price equation (60). The PDE-SDE systems is coupled through the excess demand ED . Besides initial conditions, we pose Dirichlet boundary conditions

$$\begin{aligned} \lim_{c \rightarrow \pm\infty} f^+(t, m, c) &= \lim_{c \rightarrow \pm\infty} f^-(t, m, c) = 0, \\ \lim_{m \rightarrow \pm\infty} f^+(t, m, c) &= \lim_{m \rightarrow \pm\infty} f^-(t, m, c) = 0. \end{aligned}$$

Thus, we can simplify the time derivative of the excess demand as follows:

$$\begin{aligned} \frac{d}{dt} ED[f^+, f^-](t) &= \int \frac{\partial}{\partial t} f^+(t, m, c) - \frac{\partial}{\partial t} f^-(t, m, c) dm dc \\ &= \int -\partial_c (H(-ED[f^+, f^-](t)) f^+(t, m, c)) + \partial_c (H(ED[f^+, f^-](t)) f^-(t, m, c)) \\ &\quad + Q_{gain}^+(t, m, c, S) - Q_{loss}^+(t, m, c, S) - Q_{gain}^-(t, m, c, S) + Q_{loss}^-(t, m, c, S) dm dc \\ &= 2 \int f^-(t, m, c) \lambda(t, m, c, S) - f^+(t, m, c) \lambda(t, m, c, S) dm dc. \end{aligned}$$

Space-homogeneous Model In this paragraph, we define the space-homogeneous model. Here, we mean by space variable the herding variable c , although this is no physical space. The reason for that choice is the analogy to kinetic theory, since the mean field Cross model has an advection in the herding variable c . The investment decision does no longer depend on the two dimensional (m, c) space but only on the memory variable m . Therefore, the space-homogeneous model does not include the herding effect and corresponds to the only inaction dynamics of the original Cross model. Thus, we define the space-homogeneous model by:

$$\begin{aligned} \partial_t g^+(t, m) &= Q_{gain}^h[g^-](t, m, S) - Q_{loss}^h[g^+](t, m, S), \\ \partial_t g^-(t, m) &= Q_{gain}^h[g^+](t, m, S) - Q_{loss}^h[g^-](t, m, S), \\ Q_{gain}^h[g^{(\cdot)}](t, m, S) &:= \delta(m - S(t)) \int g^{(\cdot)}(t, m) \lambda_h(t, m, S) dm, \\ Q_{loss}^h[g^{(\cdot)}](t, m, S) &:= g^{(\cdot)}(t, m) \lambda_h(t, m, S). \end{aligned} \quad (63)$$

The homogeneous model can be directly derived from the full model by integrating out the herding variable and setting the switching rate to $\lambda_h := \frac{q}{\Delta t_C}$. Here, one uses the linearity of the collision integral. In fact, $g^{(\cdot)}(t, m) := \int_{\mathbb{R}} f^{(\cdot)}(t, m, c) dc$ holds if $\lambda = \lambda_h$.

5.5 Numerics

In this section, we give numerical examples of our proposed mean field Cross model. We show that the kinetic model exhibits the same characteristic behavior as the original Cross model. We solve the PDE system with a standard finite volume discretization. We use a first order upwind scheme and apply the trapezoidal quadrature formula to evaluate the integrals

of our model. The resulting ODEs are solved by an explicit Euler method. Notice that due to the stiff source term caused by the dirac deltas we get an additional stability condition to the classical Courant-Friedrich-Lowy condition. We approximate the dirac deltas by a uniform distribution with support on one grid cell. The SDE is approximated by a simple Euler-Maruyama discretization.

First we present test cases of the space-homogeneous and secondly of the space-heterogeneous mean field Cross model. Finally, we present the corresponding Monte Carlo solver of our mean field Cross model and give further examples.

Space-homogeneous Model Figure 56 shows that in the space-homogeneous setting we obtain Gaussian distributed stock returns. Furthermore, there is no auto-correlation present (see figure 56). The simulation in figure 56 have been conducted with $\theta = 0$ but we want

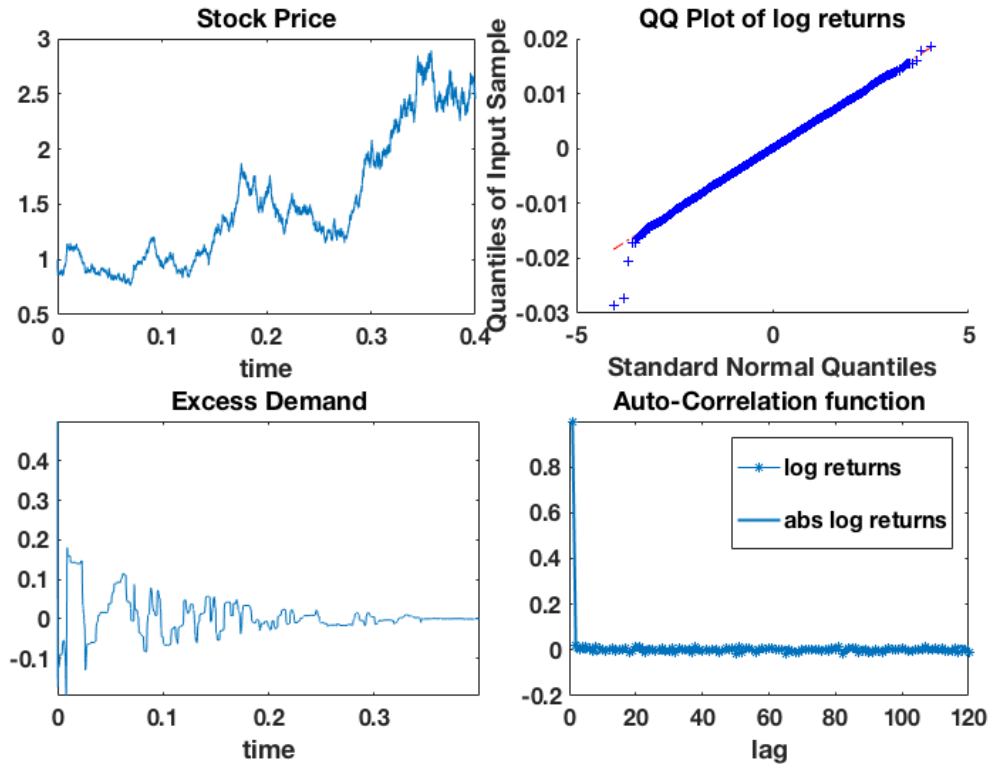


Figure 56: Space-homogeneous model with $\theta = 0$. For further parameters we refer to table 11.

to point out that for $\theta = 2$ we obtain qualitatively the same result. We want to emphasize that the simulation results are qualitatively identical to the simulations of the original Cross model.

Space-heterogeneous Model Figure 57 shows that the space-heterogeneous model output is characterized by a non-Gaussian return distribution. The heteroskedasticity parameter is set to zero and thus we see in figure 57 an auto-correlation of approximately zero.

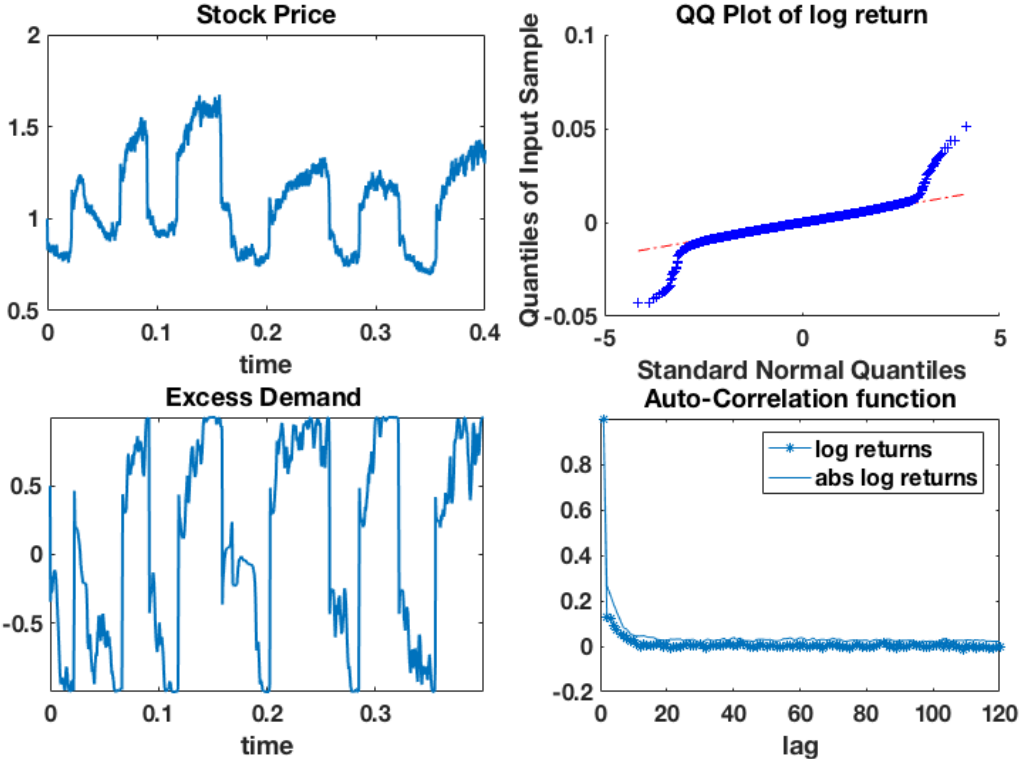


Figure 57: Space-heterogeneous model with $\theta = 0$. Further parameters are given in table 11.

By setting the heteroskedasticity parameter to $\theta = 2$ we then obtain a positive auto-correlation of absolute returns (see figure 58). The other characteristics of the model remain unchanged, thus figure 58 shows a non-Gaussian return distributions and oscillating excess demand as well. In summary, we can state that the mean field Cross model exhibits the same qualitative behavior as the original Cross model.

5.5.1 Deterministic Stock Price Equation

The following test cases are conducted with a deterministic stock price equation. We do this in order to investigate if the homogeneous and heterogeneous models already behave differently in a fully deterministic setting. Thus, the mean field Cross model becomes a PDE-ODE system.

Space-homogeneous Model From figure 59 we deduce that the dynamics converge to a steady profile. In addition, figure 59 reveals that the masses of both populations average before they reach a steady state.

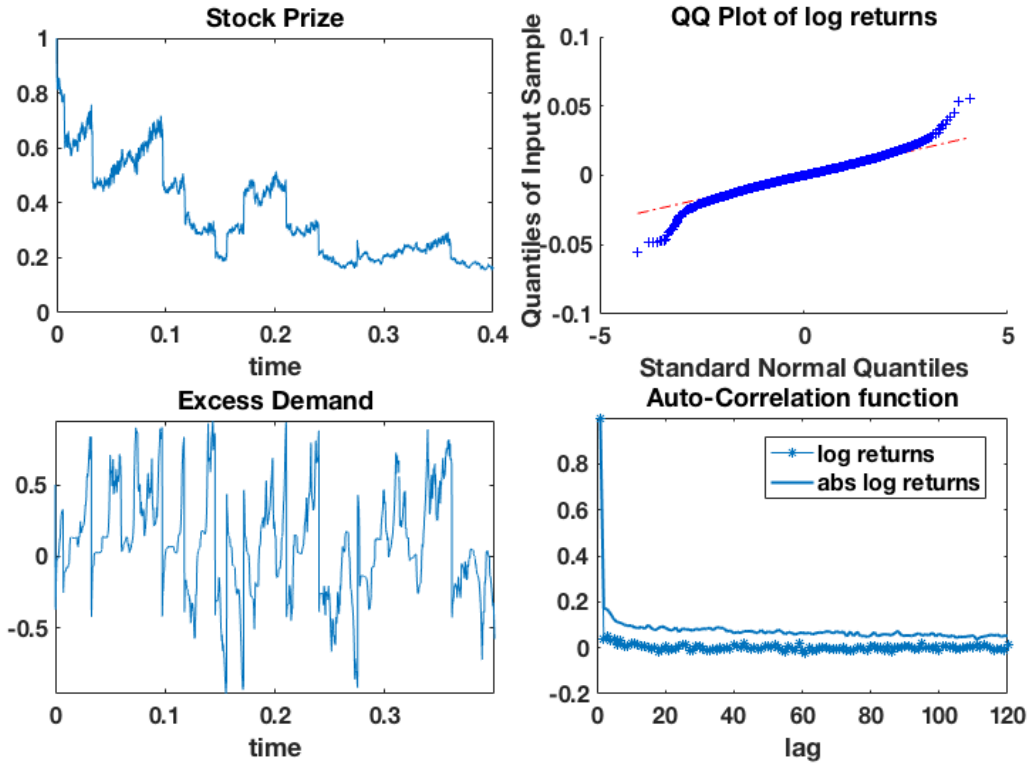


Figure 58: Space-heterogeneous model with $\theta = 2$. Further parameters are given in table 11.

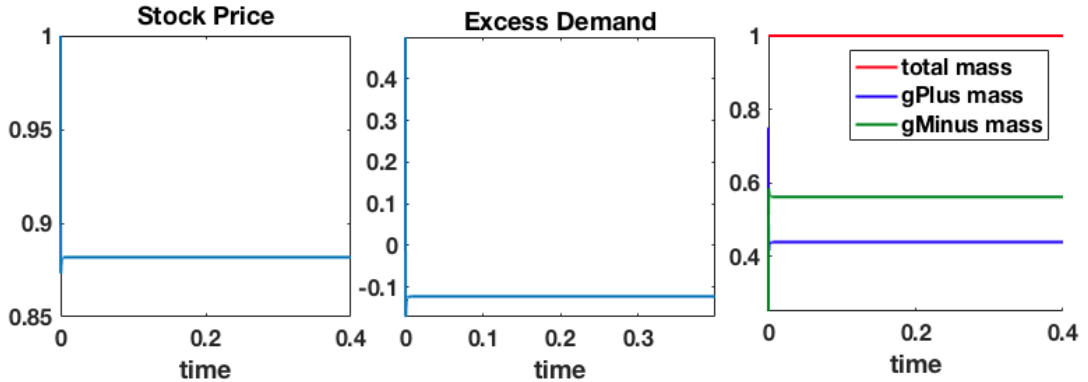


Figure 59: Space-homogeneous model with deterministic stock price equation and $\theta = 0$. For further parameters we refer to table 11.

Space-heterogeneous Model As in the space-homogeneous model, the dynamics of the space-heterogeneous model reaches a steady state as well (see figure 60). In figure 60, we obtain that the excess demand becomes -1 . Thus, all agents have the same position. Hence, we can conclude that already the deterministic skeleton of the space-homogeneous and space-

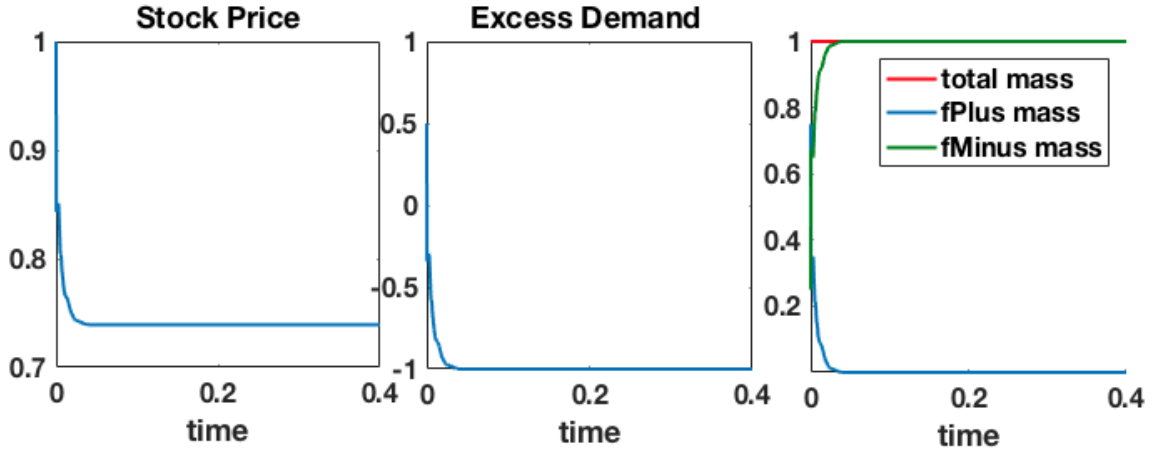


Figure 60: Space-heterogeneous model with deterministic stock price equation and $\theta = 2$. For further parameters we refer to table 11.

heterogeneous model behave differently. In the next section, we will analyze the steady states of both models in detail.

5.5.2 Monte Carlo Solver

In this section we present a Monte Carlo solver of our space-heterogeneous mean field Cross model. Although the Monte Carlo solvers have a poor convergence rate, there is at least one advantage. In comparison to most deterministic schemes, Monte Carlo solvers do not add any dissipation to the numerical solution [198]. This is an important feature, e.g. when analyzing the tail behavior of the density function.

In order to derive the Monte Carlo solver, we need to interpret the mean field Cross model as the master equation of a stochastic process. The main feature of the stochastic process is the switching mechanism. We summarize the Monte Carlo algorithm as follows.

Monte Carlo Algorithm
<ol style="list-style-type: none"> Generate sample $X_i^0 = (\gamma_i^0, m_i^0, c_i^0) \in \{-1, 1\} \times \mathbb{R}_{\geq 0} \times \mathbb{R}_{\geq 0}$, $i = 1, \dots, N$ from initial distribution. For each time step $k \in \{1, \dots, \frac{T}{\Delta t}\}$ <ol style="list-style-type: none"> calculate ED_N^k see (55), S^{k+1} see equation 60, $\hat{\lambda}_i^k := 1 - \exp(-\Delta t \lambda_i^k)$ update sample X_i^k to X_i^{k+1} and set <ol style="list-style-type: none"> with probability $\hat{\lambda}_i^k$ $\gamma_i^{k+1} = -\gamma_i^k$, $m_i^{k+1} = S^{k+1}$, $c_i^{k+1} = 0$. otherwise $\gamma_i^{k+1} = \gamma_i^k$, $m_i^{k+1} = m_i^k$ and calculate c_i^{k+1} by (56). Reconstruct densities f_{k+1}^+, f_{k+1}^-.

Notice that the switching rate of our particle model $\lambda_P = \Delta t_C \lambda$ is a first order Taylor approximation of $\hat{\lambda}$. The advantage of $\hat{\lambda}$ compared to λ_P is that $\hat{\lambda} \in (0, 1)$ holds for arbitrary

time steps Δt . Thus, there are no time step restrictions which is an advantage compared to the finite volume method. Qualitatively, the model output in figure 61 coincide with the

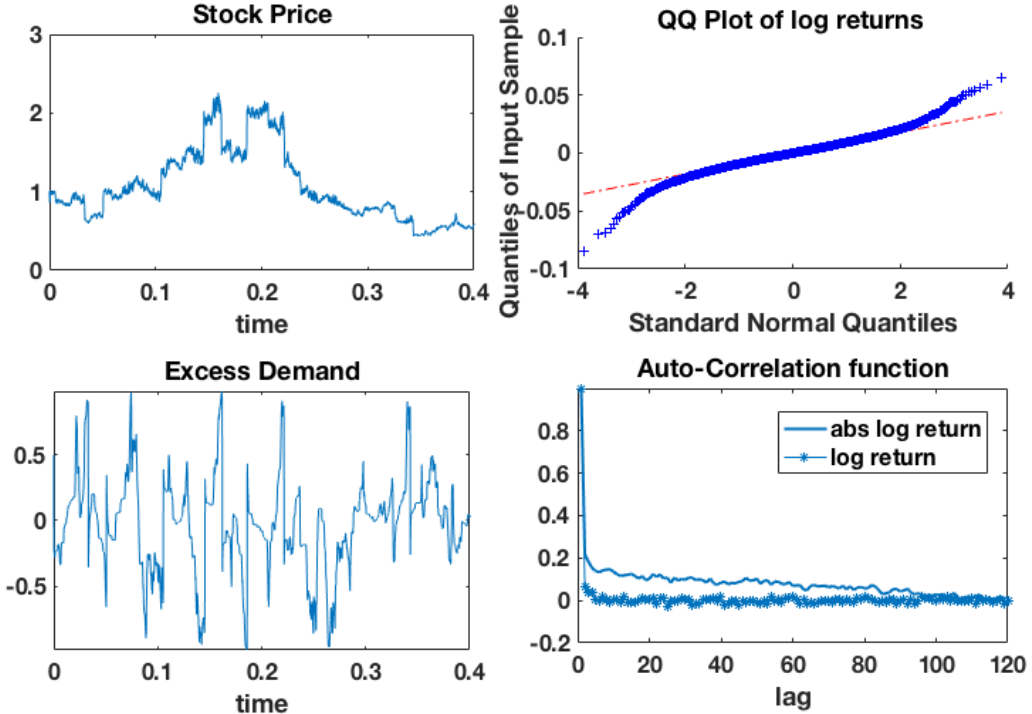


Figure 61: Space-heterogeneous mean field Cross model with $\theta = 2$. The simulation has been performed with a Monte Carlo solver with 10^5 samples. For further parameter settings we refer to table 11.

previous simulations conducted with a finite volume scheme. Consequently, the results in figure 61 coincide qualitatively to the results of the original Cross model.

5.6 Qualitative Behavior of the Model

In this section, we want to study the analytical behavior of the space-homogeneous and space-heterogeneous mean field Cross model. The goal is to confirm our previous findings and to understand the complex model behavior in more detail.

Both models are integro-differential equations equipped with a linear interaction integral. The number of agents is conserved for both models, which corresponds to the mass of the system. Furthermore, we prove that the only collision invariants of both models are given by constant functions. We refer to the appendix for details.

We divide our analysis in two parts, first we study the space-homogeneous model and secondly the space-heterogeneous model.

Space-homogeneous Model The null space at time t and stock price S of the collision operator $Q^h[g](t, m, S) := Q_{gain}^h[g](t, m, S) - Q_{loss}^h[g](t, m, S)$ is given by

$$N(Q^h)(t, S) = \{g \in Y : \text{supp}(g) \subseteq \{m \in \mathbb{R} : \lambda_h(t, m, S) \equiv 0\}\},$$

where $Y(\mathbb{R}, \mathbb{R})$ denotes the set of young measures. We have chosen this function space since dirac delta functions are a subset of young measures. Notice that especially $g = \delta(m - S)$ is in the null space.

The previous simulations presented in figure 59 indicate that in the case of a deterministic stock price evolution our system (63) reaches a steady profile.

Steady States We assume that the stock price $S \equiv s_0 > 0$ is constant. This is reasonable because in equilibrium the excess demand is constant and thus the time derivative is zero. Hence, the right-hand side of the deterministic stock price equation is zero. Then all equilibrium solutions g_∞^+, g_∞^- of the model are described by

- a) $ED[g_\infty^+, g_\infty^-] = 0$
 - i) $g_\infty^+ = g_\infty^- = 0$.
 - ii) $g_\infty^+, g_\infty^- > 0$ and $g_\infty^+, g_\infty^- \in N(Q^h)(s_0)$ with $\int g_\infty^+ dm = \int g_\infty^- dm$.
- b) $ED[g_\infty^+, g_\infty^-] < 0$
 - i) $g_\infty^+ = 0$ and $g_\infty^- > 0$, $g_\infty^- \in N(Q^h)(s_0)$.
 - ii) $g_\infty^+, g_\infty^- > 0$ and $g_\infty^+, g_\infty^- \in N(Q^h)(s_0)$ with $\int g_\infty^+ dm \neq \int g_\infty^- dm$.
- c) $ED[g_\infty^+, g_\infty^-] > 0$
 - i) $g_\infty^- = 0$ and $g_\infty^+ > 0$, $g_\infty^+ \in N(Q^h)(s_0)$.
 - ii) $g_\infty^+, g_\infty^- > 0$ and $g_\infty^+, g_\infty^- \in N(Q^h)(s_0)$ with $\int g_\infty^+ dm \neq \int g_\infty^- dm$.

If the steady state solutions g_∞^+, g_∞^- are elements of the null space $N(Q^h)(s_0)$, this means that they do not switch their market position any longer. The reason is that the memory variable or more precisely the stock price of the last switch is sufficiently close to the equilibrium price such that the agent does not feel the tension to change position.

Entropy Bound As frequently done in kinetic theory, we want to show the entropy dissipation of our system (63). Such an entropy inequality is the key ingredient in order to prove uniqueness and asymptotic behavior in kinetic models. Mathematically, an entropy of a kinetic equation is a special kind of Lyapunov functional. We use the notion of general relative entropy [183, 203]. The dual equation of our system for a constant stock price $S \equiv s_0$ is given by

$$\begin{aligned} -\partial_t \psi^+(t, m) &= \psi^-(t, S) \lambda^h(m, S) - \psi^+(t, m) \lambda^h(m, S) \\ -\partial_t \psi^-(t, m) &= \psi^+(t, S) \lambda^h(m, S) - \psi^-(t, m) \lambda^h(m, S). \end{aligned} \tag{64}$$

We define the general relative entropy for positive functions ψ, p and a convex function K to be

$$t \mapsto \mathcal{K}_\psi(g, p) := \int_{\mathbb{R}} \psi(p) K\left(\frac{g}{p}\right) dm.$$

We can then formulate the following theorem.

Theorem 5.6.1. *For all convex functions $K : \mathbb{R} \rightarrow \mathbb{R}$ and any solutions $p^+, p^- > 0$, g^+, g^- of equation (63) and solutions $\psi^+, \psi^- > 0$ of the dual equation (64), the general relative entropy inequality*

$$\frac{d}{dt} (\mathcal{K}_{\psi^+}(g^+, p^+) + \mathcal{K}_{\psi^-}(g^-, p^-)) \leq 0, \quad (65)$$

holds.

For the detailed proof we refer to the appendix 5.8.2. As a direct consequence, we can state the following a-priori bound:

Lemma 5.6.1. *For any functions satisfying theorem 5.6.1 and any convex function K we can state the following inequality.*

$$\begin{aligned} & \int_{\mathbb{R}} \psi^+(t, m) p^+(t, m) K\left(\frac{g^+(t, m)}{p^+(t, m)}\right) + \psi^-(t, m) p^-(t, m) K\left(\frac{g^-(t, m)}{p^-(t, m)}\right) dm \\ & \leq \int_{\mathbb{R}} \psi^+(0, m) p^+(0, m) K\left(\frac{g^+(0, m)}{p^+(0, m)}\right) + \psi^-(0, m) p^-(0, m) K\left(\frac{g^-(0, m)}{p^-(0, m)}\right) dm \end{aligned}$$

Remark 5.6.1. *The application of the entropy inequality (65) in order to prove convergence to the equilibrium distributions is not straightforward. The difficulty is that all possible steady state solutions are not strictly positive. We expect, the long time asymptotics of system (63) to be determined by the positive eigenvector of the largest non-negative eigenvalue [203]. The entropy inequality in theorem 5.6.1 is the appropriate tool to show the long time convergence or even the rate of convergence to a steady state.*

Space-heterogeneous Model We can analyze the heterogeneous model in the same manner as before. The null space at time t and stock Price S of the collision operator

$$Q[f](t, m, c, S) := Q_{gain}[f](t, m, c, S) - Q_{loss}[f](t, m, c, S),$$

is given by

$$N(Q)(t, S) = \{f \in \bar{Y} : \text{supp}(f) \subseteq \{(m, c) \in \mathbb{R}^2 : \lambda(t, m, c, S) \equiv 0\}\},$$

where $\bar{Y}(\mathbb{R}^2, \mathbb{R})$ is again the set of young measures.

Steady States As before, we assume $S \equiv s_0 > 0$ and all equilibrium solutions f_∞^+, f_∞^- are characterized by:

- A) $ED[f_\infty^+, f_\infty^-] = 0$
 - $f_\infty^+ = f_\infty^- = 0$.
 - $f_\infty^+, f_\infty^- > 0$ and $f_\infty^+, f_\infty^- \in N(Q)(s_0)$ with $\int f_\infty^+ dm dc = \int f_\infty^- dm dc$.
- B) $ED[f_\infty^+, f_\infty^-] < 0$
 - $f_\infty^+ = 0$ and $f_\infty^- > 0$, $f_\infty^- \in N(Q)(s_0)$.

- C) $ED[f_\infty^+, f_\infty^-] > 0$
 – $f_\infty^- = 0$ and $f_\infty^+ > 0$, $f_\infty^+ \in N(Q)(s_0)$.

In comparison to the homogeneous setting, the case $ED[f_\infty^+, f_\infty^+] \neq 0$ with $f_\infty^+, f_\infty^- > 0$ cannot be a steady state. The reason is that due to the advection (increase of herding pressure), the partial derivative with respect to the herding pressure c must be constant. Thus, for any test function $\phi(m, c)$ and $ED[f_\infty^+, f_\infty^+] < 0$

$$\int \phi(m, c) \partial_c \left(H(-ED[f_\infty^+, f_\infty^+]) f_\infty^+ \right) dm dc = 0,$$

has to hold. This constant has to be zero, otherwise this would be a contradiction to our boundary condition.

$$\lim_{m, c \rightarrow \infty} f_\infty^{(\cdot)}(m, c) = 0.$$

Hence, the excess demand can only take the values $\{-1, 0, 1\}$ in the equilibrium. This guides us to the explanation that the interplay of these steady states creates the characteristic oscillatory behavior in the stochastic simulations.

Entropy Bound In the two dimensional case the definition of the generalized entropy can be translated one to one. Thus, for positive functions Φ , n and any convex function K we have

$$t \mapsto \mathcal{K}_\Phi(f, n) := \int_{\mathbb{R}} \int_{\mathbb{R}} \Phi(n) K\left(\frac{f}{n}\right) dm dc.$$

The dual equation of the heterogeneous model is given by

$$\begin{aligned} -\partial_t \Phi^+(t, m, c) - H(-ED) \partial_c \Phi^+(t, m, c) &= \Phi^-(t, S, c) \lambda(m, c, S) - \Phi^+(t, m, c) \lambda(m, c, S) \\ -\partial_t \Phi^-(t, m, c) - H(ED) \partial_c \Phi^-(t, m, c) &= \Phi^+(t, S, c) \lambda(m, c, S) - \Phi^-(t, m, c) \lambda(m, c, S). \end{aligned} \quad (66)$$

Theorem 5.6.2. *For all convex functions $K : \mathbb{R} \rightarrow \mathbb{R}$ and any solutions $n^+, n^- > 0$, f^+, f^- of equation (61) and solutions $\Phi^+, \Phi^- > 0$ of the dual equation (66) the general relative entropy inequality*

$$\frac{d}{dt} (\mathcal{K}_{\Phi^+}(f^+, n^+) + \mathcal{K}_{\Phi^-}(f^-, n^-)) \leq 0,$$

holds.

Proof. The proof is similar to the homogeneous case. The only difference is an additional advection term. Due to the growth assumption on our densities the advection terms vanish after integration over c -space. \square

As direct consequence we get a a-priori bound.

Lemma 5.6.2. *For any functions satisfying theorem 5.6.2 and any convex function K we can state the following inequality.*

$$\begin{aligned} &\int_{\mathbb{R}} \Phi^+(t, m, c) n^+(t, m, c) K\left(\frac{f^+(t, m, c)}{n^+(t, m, c)}\right) + \Phi^-(t, m, c) n^-(t, m, c) K\left(\frac{f^-(t, m, c)}{n^-(t, m, c)}\right) dm dc \\ &\leq \int_{\mathbb{R}} \Phi^+(0, m, c) n^+(0, m, c) K\left(\frac{f^+(0, m, c)}{n^+(0, m, c)}\right) + \Phi^-(0, m, c) n^-(0, m, c) K\left(\frac{f^-(0, m, c)}{n^-(0, m, c)}\right) dm dc. \end{aligned}$$

In order to study the stability properties of the space-heterogeneous system (61) and space-homogeneous system (63), we would need to analyze the eigenvalue problem. This study is left open for further research. As the steady state discussion of the space-heterogeneous and space-homogeneous model reveals, we expect to obtain fundamental different convergence and stability results in both models.

Numerics This paragraph is devoted to confirm the findings and conjectures, we achieved in the previous investigations.

In the steady state discussion of the space-homogeneous model, we obtained that the steady state densities are identical zero or in the null space of the collision operator. Figure 62 clearly shows that the dynamics are steady as long the support of the density functions is in the null space of the collision operator.

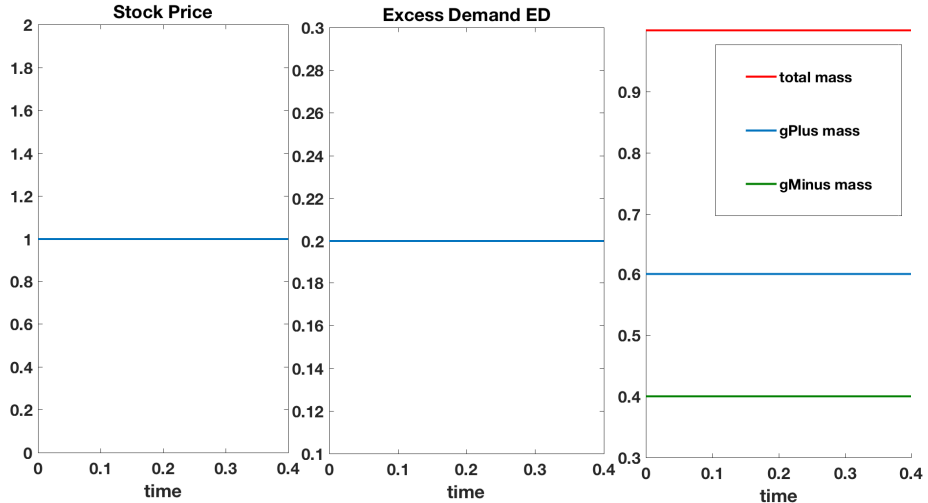


Figure 62: Space-homogeneous deterministic mean field Cross model. The initial densities have their support in the null space of the collision operator. Further parameters are given in table 11.

The figures 59 and 63 indicate the convergence of the solutions g^+, g^- to the steady states $b) - ii)$ or $c) - ii)$ for general initial data. Interestingly, we see in figure 63 a convergence to the steady state of type $b) - ii)$ although the initial mass of g^- is close to zero. Thus, we conjecture that $b) - ii), c) - ii)$ are stable steady states, whereas $b) - i), c) - i)$ are unstable steady states. A proper proof of this numerical observation is left open for further research.

The steady-state analysis of the space-heterogeneous model has shown that the excess demand can only reach the values $\{-1, 0, 1\}$ in equilibrium. Our deterministic simulations, visualized in figures 60, 64 and 65, reveal that the excess demand always converges to the

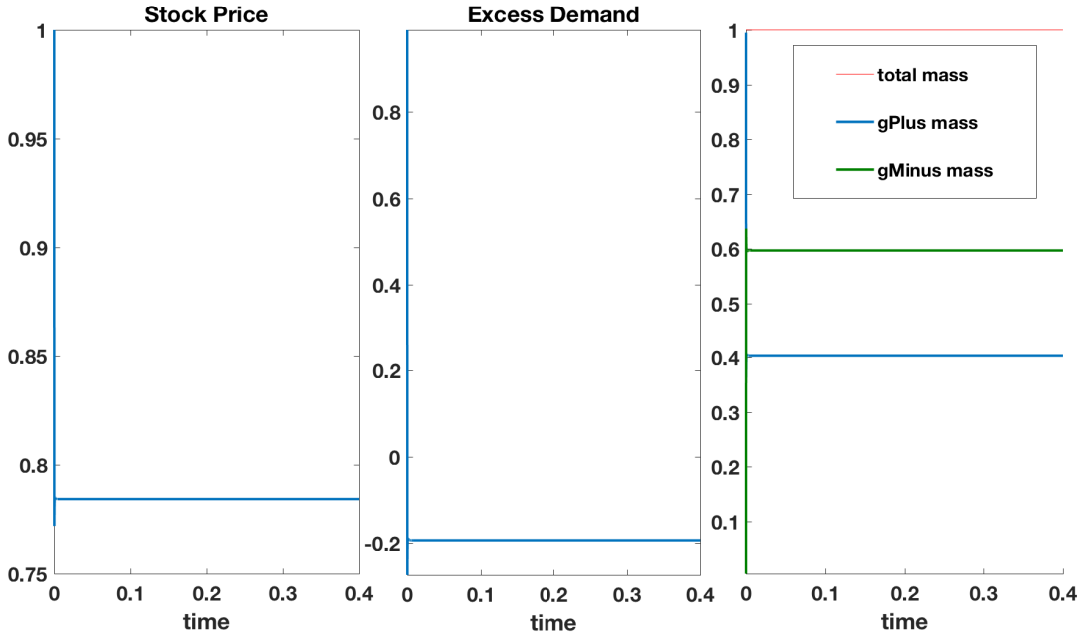


Figure 63: Space-homogeneous deterministic mean field Cross model. The initial excess demand is given by $ED[g_0^+, g_0^-](0) = 0.99$. Further parameters are given in table 11.

extreme values $\{1, -1\}$. This is even the case if the initial densities have their support in the null space $N(Q)(t, S)$, see figure 65. This observation coincides with the steady states in B) or C) and again the initial values determine the convergence to one or another. Furthermore, the results in figure 64 indicate the stability of the steady states B), respectively C), in comparison to A).

5.7 Conclusion and Outlook

We have introduced a kinetic model and have shown that the model is a good approximation of the original Cross model at least on a qualitative level. We have derived the continuum and mean field limit of the particle model and have obtained the mean field Cross model. Our numerical investigations have revealed that the mean field Cross model exhibits identical characteristics as the original econophysical Cross model. The appearance of fat-tails is a direct consequence of the herding pressure. In the space-homogeneous case, where only the inaction pressure was active, we observe Gaussian behavior of stock returns. Interestingly, we only obtain volatility clustering in the space-heterogeneous model if we add the dependency of the diffusion function on the excess demand.

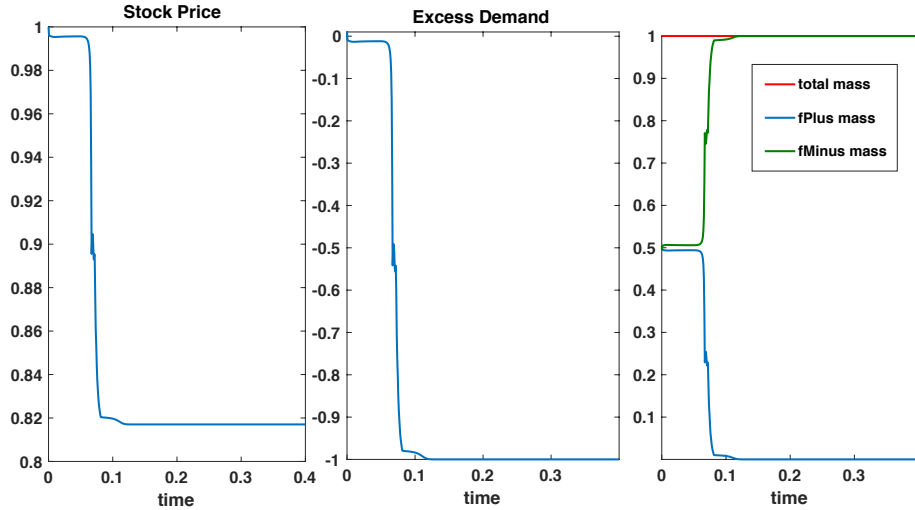


Figure 64: Space-heterogeneous deterministic mean field Cross model. The initial excess demand is given by $ED[f_0^+, f_0^-](0) = 0.01$. Further parameters are given in table 11.

Furthermore, we have analyzed the PDE system with respect to steady states. We have shown that in the space-homogeneous case the excess demand can take various values compared to the heterogeneous case. In the heterogeneous case, the excess demand can only reach $\{-1, 0, 1\}$ in the equilibrium case. Hence, we conclude that this behavior of the deterministic skeleton explains the oscillatory behavior of the stochastic model. In addition, we could derive entropy bounds for the space-homogeneous and space-heterogeneous model as well.

We want to briefly discuss the advantages of the mean field Cross model compared to the microscopic Cross model. The PDE-SDE system most obviously enables us to do mathematical analysis, e.g. we could study the steady states of the deterministic PDE-ODE model. Furthermore, we have gained a reduction of dimensions. Thus, instead of considering N agents separately, we only consider two three-dimensional distribution functions. This can also be observed in the reduction of numerical complexity of the mean field model compared to the original Cross model. Of course we have to assume a large number of agents. Finally, we also want to point out the reduction of parameters of the SDE-PDE system in contrast to the original microscopic model.

Further research directions are to quantify the influence of several parameters such as the market depth κ on the statistical properties of the stock price. A sensitivity analysis or stochastic collocation might be performed to do uncertainty quantification. In addition, one might want to solve the inverse problem and fit several parameters to original stock price data. Again the advantages of the Cross model become obvious since we have reduced the number of

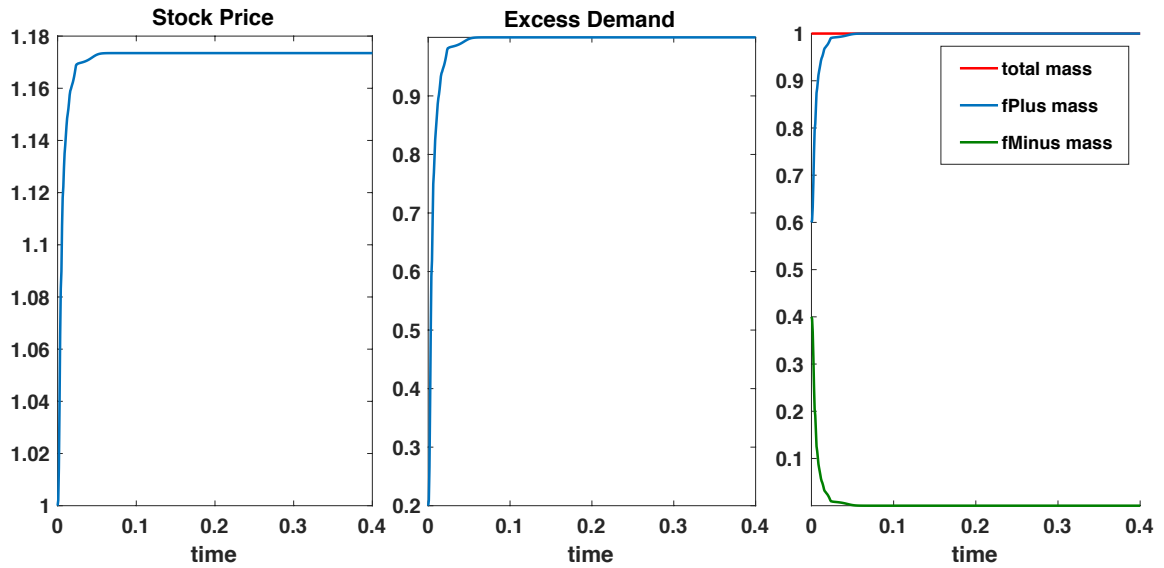


Figure 65: Space-heterogeneous deterministic mean field Cross model. The initial densities have their support in the null space of the collision operator. For further parameter settings we refer to table 11.

unknowns remarkably. Finally, we want to point out the possibility to extend the analysis of the model. Thus, the questions of existence, uniqueness and asymptotic convergence remain open.

5.8 Appendix

5.8.1 Numerics

Parameter	Value
κ	0.2
A_1	0.1
A_2	0.3
b_1	25
b_2	100
Δt	$4 \cdot 10^{-5}$
N	1000
Time Interval	$[0, 0.4]$

Variable	Initial Value
α	0 or 2
$S(0)$	1
$\gamma_i(0)$	$\gamma_i(0) = 1, 1 \leq i \leq 667, \gamma_i(0) = -1, 668 \leq i \leq N$
$ED(0)$	$\frac{1}{N} \sum_{i=1}^N \gamma_i(0)$
$c_i(t)$	$B_1, \forall 1 \leq i \leq N$
$m_i(t)$	$S(0), \forall 1 \leq i \leq N$

Table 9: Parameter settings of the original Cross model.

Parameter	Value
κ	0.2
A_1	0.1
A_2	0.3
b_1	25
b_2	100
Δt	$4 \cdot 10^{-5}$
N	30.000
Time Interval	$[0, 0.4]$

Variable	Initial Value
α	0 or 2
λ_1, λ_2	$\lambda_1 = \lambda_2 = 0.5$ or $\lambda_1 = 0, \lambda_2 = 1$
$S(0)$	1
$\gamma_i(0)$	$\gamma_i(0) = 1, 1 \leq i \leq 667, \gamma_i(0) = -1, 668 \leq i \leq N$
$ED(0)$	$\frac{1}{N} \sum_{i=1}^N \gamma_i(0)$
$c_i(t)$	$B_1, \forall 1 \leq i \leq N$
$m_i(t)$	$S(0), \forall 1 \leq i \leq N$

Table 10: Parameter setting of the kinetic particle model.

Parameter	Value
κ	0.2
A_1	0.1
A_2	0.3
b_1	25
b_2	100
Δt	$4 \cdot 10^{-5}$
N_c, N_m grid points	400
Time Interval	$[0, 0.4]$

Variable	Initial Value
α	0 or 2
λ_1, λ_2	$\lambda_1 = \lambda_2 = 0.5$
$S(0)$	1
$ED(0)$	$\int f^+(0, m, c) - f^-(0, m, c) dm dc$
$f^+(0, m, c)$	$\text{Unif}(M_1, m_4) \times \text{Unif}(B_1, B_2)$
$f^-(0, m, c)$	$\text{Unif}(M_1, m_4) \times \text{Unif}(B_1, B_2)$

Table 11: Parameter settings of the mean field Cross model.

5.8.2 Qualitative Studies

We give the following definitions for space and velocity dependent distribution functions. They can be immediately transferred into the space-homogeneous setting.

Definition 5.8.1. Given any function $\phi(v, x)$, $x, v \in \mathbb{R}^d$ and a density function $f(t, v, x)$, $x, v \in \mathbb{R}^d$. Then we call the average value with respect to the function $\phi(\cdot)$, an observable.

$$\langle \phi(v, x), f(t, v, x) \rangle := \int_{\mathbb{R}^d \times \mathbb{R}^d} \phi(v, x) f(t, v, x) dv dx.$$

Definition 5.8.2. We call the function $\psi(v, x) \in \mathbb{R}^n$, $x, v \in \mathbb{R}^d$, $n, d \in \mathbb{N}$ a collision invariant of the kinetic equation

$$\partial_t f(t, v, x) + \nabla_x (G[f](t, v, x)) = Q[f](t, v, x),$$

where $f : [0, \infty) \times \mathbb{R}^d \times \mathbb{R}^d \rightarrow \mathbb{R}^n$ is the density function, $G[f](t, v, x) \in \mathbb{R}^n$ the flux and $Q[f](t, v, x)$ the collision operator, if

$$\int_{\mathbb{R}^d} \psi(v, x) \cdot Q[f](t, v, x) dv dx = 0,$$

holds for all functions f . Furthermore, we call all observables of the kinetic density with respect to any collision invariant

$$\langle \psi(v, x), f(t, v, x) \rangle = \int_{\mathbb{R}^d} \psi(v, x) Q[f](t, v, x) dv dx,$$

a conserved quantity.

Remark 5.8.1. Due to our growth assumption on the densities f^+, f^- we get:

$$\begin{aligned} \partial_t \int_{\mathbb{R} \times \mathbb{R}} \phi_1(m, c) f^+(t, m, c) + \phi_2(m, c) f^-(t, m, c) dm dc &= \\ \int_{\mathbb{R} \times \mathbb{R}} \phi_1(m, c) (Q_{gain}[f^-](t, m, c, S) - Q_{loss}[f^+](t, m, c, S)) dm dc \\ &+ \int_{\mathbb{R} \times \mathbb{R}} \phi_2(m, c) (Q_{gain}[f^+](t, m, c, S) - Q_{loss}[f^-](t, m, c, S)) dm dc. \end{aligned}$$

If ϕ_1, ϕ_2 are collision invariants we have:

$$\partial_t \int_{\mathbb{R} \times \mathbb{R}} \phi_1(m, c) f^+(t, m, c) + \phi_2(m, c) f^-(t, m, c) dm dc = 0.$$

Thus, the conserved quantities are constant in time, which reveals the motivation of their name.

Theorem 5.8.1. All collision invariants of our homogeneous model are given by

$$\begin{aligned} \psi_1(m) &= c_1, \\ \psi_2(m) &= c_2, \end{aligned}$$

and in the space-heterogeneous case we get:

$$\begin{aligned}\psi_1(m, c) &= c_1, \\ \psi_2(m, c) &= c_2,\end{aligned}$$

where $c_1, c_2 \in \mathbb{R}$ are constants. Thus, the only conserved quantity of our system is the mass, respectively the number of agents.

Proof. We perform the proof for the space-heterogeneous setting, but one can translate the results one to one to the one dimensional case. The functions $\psi_1(m, c), \psi_2(m, c)$ have to satisfy:

$$\begin{aligned}& \int_{\mathbb{R} \times \mathbb{R}} \psi_1(m, c) (Q_{gain}[f^-](t, m, c, S) - Q_{loss}[f^+](t, m, c, S)) dm dc + \\ & + \int_{\mathbb{R} \times \mathbb{R}} \psi_2(m, c) (Q_{gain}[f^+](t, m, c, S) - Q_{loss}[f^-](t, m, c, S)) dm dc = 0\end{aligned}$$

This is equivalent to

$$\begin{aligned}& \psi_1(S, 0) \int_{\mathbb{R} \times \mathbb{R}} \lambda(t, c, m, S) f^-(t, m, c) dm dc - \int_{\mathbb{R}^2} \psi_1(m, c) \lambda(t, c, m, S) f^+(t, m, c) dm dc \\ & + \psi_2(S, 0) \int_{\mathbb{R} \times \mathbb{R}} \lambda(t, c, m, S) f^+(t, m, c) dm dc - \int_{\mathbb{R} \times \mathbb{R}} \psi_2(m, c) \lambda(t, c, m, S) f^-(t, m, c) dm dc = 0\end{aligned}$$

This equation can be rewritten.

$$\begin{aligned}& \int_{\mathbb{R} \times \mathbb{R}} \lambda(t, c, m, S) f^-(t, m, c) (\psi_1(S, 0) - \psi_2(m, c)) dm dc \\ & + \int_{\mathbb{R} \times \mathbb{R}} \lambda(t, c, m, S) f^+(t, m, c) (\psi_2(S, 0) - \psi_1(m, c)) dm dc = 0.\end{aligned}$$

The previous equation has to hold for all functions f . Thus, by the lemma of variational calculus, we can conclude that

$$\begin{aligned}\psi_1(S, 0) &= \psi_2(m, c), \\ \psi_2(S, 0) &= \psi_1(m, c),\end{aligned}$$

has to hold. Hence, we define $c_2 := \psi_1(S, 0)$ and $c_1 := \psi_2(S, 0)$ and the proof is completed. \square

The proof of theorem 5.6.1 is given by:

Proof. A straightforward computations shows.

$$\begin{aligned}
& \partial_t \left[\psi^+(t, m) p^+(t, m) K \left(\frac{g^+(t, m)}{p^+(t, m)} \right) \right] + \partial_t \left[\psi^-(t, m) p^-(t, m) K \left(\frac{g^-(t, m)}{p^-(t, m)} \right) \right] \\
& + \psi^+(t, S) p^-(t, m) K \left(\frac{g^-(t, m)}{p^-(t, m)} \right) \lambda^h(m, S) \\
& - \psi^+(t, m) \delta(m - S) \int_{\mathbb{R}} \lambda^h(t, m') p^-(t, m') K \left(\frac{g^-(t, m')}{p^-(t, m')} \right) dm' \\
& + \psi^-(t, S) p^+(t, m) K \left(\frac{g^+(t, m)}{p^-(t, m)} \right) \lambda^h(m, S) \\
& - \psi^-(t, m) \delta(m - S) \int_{\mathbb{R}} \lambda^h(t, m') p^+(t, m') K \left(\frac{g^+(t, m')}{p^+(t, m')} \right) dm' \\
& = \psi^+(t, m) \delta(m - S) \int_{\mathbb{R}} \lambda^h(m', S) p^-(t, m') \left(\left[K \left(\frac{g^+(t, m)}{p^+(t, m)} \right) - K \left(\frac{g^-(t, m')}{p^-(t, m')} \right) \right] \right. \\
& \quad \left. + K' \left(\frac{g^+(t, m)}{p^+(t, m)} \right) \left[\frac{g^-(t, m')}{p^-(t, m')} - \frac{g^+(t, m)}{p^+(t, m)} \right] \right) dm' \\
& + \psi^-(t, m) \delta(m - S) \int_{\mathbb{R}} \lambda^h(m', S) p^+(t, m') \left(\left[K \left(\frac{g^-(t, m)}{p^-(t, m)} \right) - K \left(\frac{g^+(t, m')}{p^+(t, m')} \right) \right] \right. \\
& \quad \left. + K' \left(\frac{g^-(t, m)}{p^-(t, m)} \right) \left[\frac{g^+(t, m')}{p^+(t, m')} - \frac{g^-(t, m)}{p^-(t, m)} \right] \right) dm'.
\end{aligned}$$

Then we integrate over m and get.

$$\begin{aligned}
& \frac{d}{dt} \int_{\mathbb{R}} \psi^+(t, m) p^+(t, m) K \left(\frac{g^+(t, m)}{p^+(t, m)} \right) dm + \frac{d}{dt} \int_{\mathbb{R}} \psi^-(t, m) p^-(t, m) K \left(\frac{g^-(t, m)}{p^-(t, m)} \right) dm \\
& = \psi^+(t, S) \int_{\mathbb{R}} \lambda^h(m', S) p^-(t, m') \left(\left[K \left(\frac{g^+(t, S)}{p^+(t, S)} \right) - K \left(\frac{g^-(t, m')}{p^-(t, m')} \right) \right] \right. \\
& \quad \left. + K' \left(\frac{g^+(t, S)}{p^+(t, S)} \right) \left[\frac{g^-(t, m')}{p^-(t, m')} - \frac{g^+(t, S)}{p^+(t, S)} \right] \right) dm' \\
& + \psi^-(t, S) \int_{\mathbb{R}} \lambda^h(m', S) p^+(t, m') \left(\left[K \left(\frac{g^-(t, S)}{p^-(t, S)} \right) - K \left(\frac{g^+(t, m')}{p^+(t, m')} \right) \right] \right. \\
& \quad \left. + K' \left(\frac{g^-(t, S)}{p^-(t, S)} \right) \left[\frac{g^+(t, m')}{p^+(t, m')} - \frac{g^-(t, S)}{p^-(t, S)} \right] \right) dm'.
\end{aligned}$$

Thanks to the convexity of K the inequality

$$0 \geq K(y) - K(x) + K'(y)(x - y),$$

holds for any differentiable function K . Thus, the right-hand side is negative and the entropy inequality (65) holds. \square

6 Conclusion and Outlook

In this work, we have studied different facets of kinetic financial market modeling. On the microscopic level, our SABCEMM tool has revealed the drawbacks of microscopic agent-based models. First of all, many models exhibit numerical artifacts, potentially falsify the result. Secondly, our studies have shown the computational costs of the simulations and the drawbacks of Monte Carlo sampling as well. The theoretical results in chapter 3 verify the applicability of mean field limits in the context of financial markets. We want to point out that this new field of applications has led to new limit systems which are thus new in literature. Finally, we have derived kinetic models of two microscopic agent-based models. We have provided a detailed analysis of man field models focusing on the origin of stylized facts. In both models, the emergence of stylized facts can be attributed to the investment behavior of financial agents.

The essence of this work can be summarized as follows:

- Kinetic models significantly reduce the computational costs.
- Agent-based financial market models can be well approximated by kinetic models.
- Analytical results can be derived within each kinetic model and offer new insights regarding the origin of stylized facts.
- Wealth or stock price distribution can be obtained as solutions of the kinetic model.

Below, we will provide a detailed discussion of the previous chapters and give an outlook for further research perspectives.

6.1 SABCEMM

We have introduced the simulation framework SABCEMM, a tool designed for a large class of agent-based computational financial market models. As far as we know, this software is the first simulator especially designed for econophysical financial market models. Its object-orientation allows the user to easily add and create new models. This facilitates the comparison of different financial market models on an objective basis. The efficient implementation has been verified by simulations considering several million of agents as well as speed tests of SABCEMM. Furthermore, we have shown that the generation of random numbers constitutes a severe issue regarding computational time and model output. A clever integration of the random number generator may reduce the computation time up to 35%. Additionally, we have obtained that the qualitative simulation outputs can vary when utilizing a unreliable random number generator.

Beyond that, we ran several test cases to present our tool's great applicability and provided an example an example of finite size effects, which clearly shows the disadvantages of microscopic simulations.

This framework's overall objective is to compare and validate the large amount of different

agent-based financial market models prevalent in literature. This can only be achieved if more models will be added to the framework, which must be regarded the main task for the future. Further improvement of SABCEMM will be constituted by the acceleration of the simulation process which can be accomplished by a parallelization with respect to financial agents and by a parallel generation of random numbers.

6.2 Mean Field Limit and Mean Field Games

Chapter 3 introduced stochastic diffusion processes and kinetic theory. Additionally, we provided a brief discussion of stochastic stock price equations and the corresponding master equations. We have seen that multiplicative noise is essential in order to obtain an inverse gamma distribution as steady state. This is an important observation and market mechanisms like this have been used in several agent-based models. The centerpiece of this chapter was the derivation of mean field models starting at deterministic microscopic dynamics. First, we considered a simple financial market model and rigorously performed the mean filed limit. We here demonstrated the applicability of mean field theory for this kind of financial market models. Furthermore, we studied the mean field limit of differential games. Each agent is thus not only characterized by an ODE but additionally solves an optimization problem. We considered a general model and formally derived the mean field limit system. The discussion of the scaling behavior of our microscopic system led to the discovery of new reasonable settings. Therefore, we have extended the class of mean field game models to a considerable extent. In fact, we show that our financial market model satisfies the scaling assumptions and derive the limit system. This clearly shows the adaptability of mean field game theory to agent-based financial market models. A reasonable next step would then be concerned with the extension to stochastic microscopic dynamics, a desirable generalization especially in the context of financial market models.

6.3 Portfolio Optimization and Model Predictive Control

In a first step, we have developed a microscopic asset allocation model inspired by the econophysical Levy-Levy-Solomon model [155]. We then simplified the optimization with the help of model predictive control and thus reduced our model's complexity to a considerable degree. This has revealed the mathematical connection between a fully rational agent and a bounded rational agent. Thus, the investment decision of bounded rational agents can be interpreted as an approximation of a utility maximization. We performed the mean field limit of this microscopic system and derived mesoscopic and macroscopic kinetic models. More precisely, the macroscopic model is a moment model which can replicate prominent features of financial markets, i.e. oscillatory price behavior, booms and crashes. The mesoscopic models have revealed that the wealth distribution is characterized by a lognormal law. In the case of long term investors, the stock price distribution is given by a lognormal law as well. Interestingly, in the case of high-frequency traders, the steady state stock price distribution is characterized by an inverse gamma distribution. Hence, in our model, the power-laws in stock price distribution can be attributed to high-frequency traders. This power-law in stock price, however, does not generate a power- law in the portfolio dynamics. This is a remarkable observation and deserves to be investigated in detail in the future. We could thus extend the microscopic model in order to generate power-laws in the portfolio as well. More precisely, we could add earnings or microscopic interactions among the agents. In summary, we want to point

out that the kinetic model allowed us to analyze the stock price and portfolio distributions. Furthermore, the computational costs for our kinetic model and especially the moment mode have been reduced drastically compared to the original microscopic model. Remarkably, we have discovered the origins of fat-tails in our model and supported this finding analytically. We can thus conclude that kinetic theory and, more precisely, the mean field limit must be regarded an appropriate tool to gain more insights into the complex behavior of agent-based financial market models.

6.4 Behavioral Financial Market Model

In chapter 5, we have derived the field limit of the econophysical Cross model [71] and demonstrated that the kinetic model approximates the original model well. The mean field model reveals that the appearance of fat-tails in the stock return distribution is to be attributed to agents' herding pressure. The existence of stylized facts can thus be constituted by the agents' behavioral misperceptions. These observations correspond with earlier finds by Cross et al. [71, 72]. Apart from the reduction of computational costs, the possibility to study the model analytically constitutes the crucial advantage of the kinetic model over the original. We have investigated the steady state behavior of the deterministic skeleton of the mean field Cross model. We have thus found that the additional advection term in the mean field Cross model, which is only present when the investors are influenced by herding, reduces the set of possible steady states. This creates the complex oscillatory price behavior when noise is added to the model. These findings and observations open a whole variety of possible (promising) directions for further research: the proof of existence and uniqueness, which in the context of this coupled PDE-SDE model must not be regarded as trivial or irrelevant. Another possibility could be the performance of uncertainty quantification of several model parameters to determine the sensitivity of the obtained stylized facts with respect to those. Finally, an attempt to solve the inverse problem and fit the artificial stock price data to real financial data seems a promising venture.

6.5 Economic Perspectives

We aimed to answer the economic question concerned with the origins of stylized facts. In essence, the reasons of their appearance can only be found in the market mechanism or in the agents' investment decision. The results obtained in chapter 3 revealed that the mere market mechanism itself has the potential to generate fat-tails. We checked that the obtained stylized facts in our kinetic financial market models derived in chapters 4 and 5 originate from agent dynamics and not merely from the market mechanism. Both kinetic models revealed that the origin of fat-tails lie in investors' investment decisions. In the mean field Cross model, fat-tails in stock return data must be attributed to herding behavior. We can therefore support the economic assumption that behavioral influence on the investment decision of financial agents leads to stylized facts. In our portfolio model, we found that high-frequency traders must be considered in order to obtain fat-tails in the stock price distribution. We considered a fundamental and chartist trading strategy. We could prove the existence of a fat-tail for the case of a fundamental strategy and for a chartist strategy at least in special cases. More precisely, a power-law behavior is caused by a negative shift in the reference point of the utility function of chartists, which corresponds to high risk aversion. We want to point out again that we have not discovered a power-law in the portfolio dynamics. This is a striking result

since the portfolio constantly interacts with the stock price. One possible explanation is that the shift between both portfolios prevents the creation of fat-tails. Further investigations might help to arrive at a better understanding of the correlation between stock price and wealth distribution. Finally, we want to emphasize that our kinetic models in chapters 4 and 5 considered bounded rational agents. We could obtain stylized facts in both models. In contrast, classical financial market models consisting of rational agents fail to reproduce prominent stylized facts. In chapter 3, we discussed mean field games, a new field of research. We showed that the model ideally displays rational agents playing a differential game against each other. The question whether a scenario like this may create fat-tails or stylized facts must be left open for further research. We nevertheless want to stress that a model of rational agents which allows the creation of stylized facts is very likely to have an enormous impact on economic research. We conclude that kinetic theory helps to approximate a solution to the riddle the phenomenon of stylized facts imposes on mathematicians and economists alike. However, many questions remain unanswered. What is the impact of different market mechanism on the appearance of stylized facts? Is it possible to obtain stylized facts in a rational agent environment? Which models in literature replicate financial data best?

References

- [1] Google test. <https://github.com/google/googletest>. Accessed: 2017-08-24.
- [2] Y. Achdou and I. Capuzzo-Dolcetta. Mean field games: Numerical methods. *SIAM Journal on Numerical Analysis*, 48(3):1136–1162, 2010.
- [3] F. Ackerman. Still dead after all these years: interpreting the failure of general equilibrium theory. *Journal of Economic Methodology*, 9(2):119–139, 2002.
- [4] G. Albi, M. Herty, and L. Pareschi. Kinetic description of optimal control problems and applications to opinion consensus. *arXiv preprint arXiv:1401.7798*, 2014.
- [5] G. Albi, L. Pareschi, and M. Zanella. Boltzmann-type control of opinion consensus through leaders. *Philosophical Transactions of the Royal Society of London A: Mathematical, Physical and Engineering Sciences*, 372(2028):20140138, 2014.
- [6] R. Alexandre and C. Villani. On the landau approximation in plasma physics. In *Annales de l’Institut Henri Poincaré (C) Non Linear Analysis*, volume 21, pages 61–95. Elsevier, 2004.
- [7] S. Alfarano. *An agent-based stochastic volatility model*. PhD thesis, 2006.
- [8] S. Alfarano, T. Lux, and F. Wagner. Estimation of agent-based models: the case of an asymmetric herding model. *Computational Economics*, 26(1):19–49, 2005.
- [9] S. Alfarano, T. Lux, and F. Wagner. Time variation of higher moments in a financial market with heterogeneous agents: An analytical approach. *Journal of Economic Dynamics and Control*, 32(1):101–136, 2008.
- [10] L. Ambrosio, N. Gigli, and G. Savaré. *Gradient flows: in metric spaces and in the space of probability measures*. Springer Science & Business Media, 2008.
- [11] J. V. Andersen and D. Sornette. The \$-game. *The European Physical Journal B-Condensed Matter and Complex Systems*, 31(1):141–145, 2003.
- [12] A. Arnold, P. Markowich, G. Toscani, and A. Unterreiter. On convex sobolev inequalities and the rate of convergence to equilibrium for fokker-planck type equations. 2001.
- [13] A. B. Atkinson, T. Piketty, and E. Saez. Top incomes in the long run of history. Technical report, National Bureau of Economic Research, 2009.
- [14] R. J. Aumann. Markets with a continuum of traders. *Econometrica: Journal of the Econometric Society*, pages 39–50, 1964.
- [15] R. M. Axelrod. *The complexity of cooperation: Agent-based models of competition and collaboration*. Princeton University Press, 1997.
- [16] S. Bach, M. Beznoska, and V. Steiner. A wealth tax on the rich to bring down public debt? revenue and distributional effects of a capital levy. Technical report, Discussion papers//German Institute for Economic Research, 2011.
- [17] L. Bachelier. *Théorie de la spéculation*. Gauthier-Villars, 1900.

- [18] F. Bassetti and G. Toscani. Explicit equilibria in a kinetic model of gambling. *Physical Review E*, 81(6):066115, 2010.
- [19] A. Beja and M. B. Goldman. On the dynamic behavior of prices in disequilibrium. *The Journal of Finance*, 35(2):235–248, 1980.
- [20] A. Bensoussan, J. Frehse, P. Yam, et al. *Mean field games and mean field type control theory*, volume 101. Springer, 2013.
- [21] J. Bergin and D. Bernhardt. Anonymous sequential games with aggregate uncertainty. *Journal of Mathematical Economics*, 21(6):543–562, 1992.
- [22] B. Bernanke. Interview with the international herald tribune, 5 2010.
- [23] D. P. Bertsekas, D. P. Bertsekas, D. P. Bertsekas, and D. P. Bertsekas. *Dynamic programming and optimal control*, volume 1. Athena scientific Belmont, MA, 1995.
- [24] D. Bertsimas and D. Pachamanova. Robust multiperiod portfolio management in the presence of transaction costs. *Computers & Operations Research*, 35(1):3–17, 2008.
- [25] M. Bisi, G. Spiga, G. Toscani, et al. Kinetic models of conservative economies with wealth redistribution. *Communications in Mathematical Sciences*, 7(4):901–916, 2009.
- [26] F. Black and M. Scholes. The pricing of options and corporate liabilities. *Journal of political economy*, 81(3):637–654, 1973.
- [27] F. Bolley, J. A. Canizo, and J. A. Carrillo. Stochastic mean-field limit: non-lipschitz forces and swarming. *Mathematical Models and Methods in Applied Sciences*, 21(11):2179–2210, 2011.
- [28] L. Boltzmann. Weitere studien über das wärmegleichgewicht unter gasmolekülen. In *Kinetische Theorie II*, pages 115–225. Springer, 1970.
- [29] W. F. Bondt and R. Thaler. Does the stock market overreact? *The Journal of finance*, 40(3):793–805, 1985.
- [30] J.-P. Bouchaud. Power laws in economics and finance: some ideas from physics. 2001.
- [31] J.-P. Bouchaud. An introduction to statistical finance. *Physica A: Statistical Mechanics and its Applications*, 313(1):238–251, 2002.
- [32] J.-P. Bouchaud. Economics needs a scientific revolution. *Nature*, 455(7217):1181–1181, 2008.
- [33] J.-P. Bouchaud and R. Cont. A langevin approach to stock market fluctuations and crashes. *The European Physical Journal B-Condensed Matter and Complex Systems*, 6(4):543–550, 1998.
- [34] J.-P. Bouchaud and M. Mézard. Wealth condensation in a simple model of economy. *Physica A: Statistical Mechanics and its Applications*, 282(3):536–545, 2000.
- [35] W. Braun and K. Hepp. The vlasov dynamics and its fluctuations in the 1/n limit of interacting classical particles. *Communications in mathematical physics*, 56(2):101–113, 1977.

- [36] A. Bressan. Noncooperative differential games. *Milan Journal of Mathematics*, 79(2):357–427, 2011.
- [37] W. A. Brock and C. H. Hommes. A rational route to randomness. *Econometrica: Journal of the Econometric Society*, pages 1059–1095, 1997.
- [38] W. A. Brock and C. H. Hommes. Heterogeneous beliefs and routes to chaos in a simple asset pricing model. *Journal of Economic dynamics and Control*, 22(8-9):1235–1274, 1998.
- [39] P.-L. Buono and R. Eftimie. Analysis of hopf/hopf bifurcations in nonlocal hyperbolic models for self-organised aggregations. *Mathematical Models and Methods in Applied Sciences*, 24(02):327–357, 2014.
- [40] J. Y. Campbell. *The econometrics of financial markets*. princeton University press, 1997.
- [41] P. Cardaliaguet. Notes on mean field games. Technical report, Technical report, 2010.
- [42] P. Cardaliaguet, F. Delarue, J.-M. Lasry, and P.-L. Lions. The master equation and the convergence problem in mean field games. *arXiv preprint arXiv:1509.02505*, 2015.
- [43] P. Cardaliaguet, J.-M. Lasry, P.-L. Lions, and A. Porretta. Long time average of mean field games with a nonlocal coupling. *SIAM Journal on Control and Optimization*, 51(5):3558–3591, 2013.
- [44] P. Cardaliaguet, J.-M. Lasry, P.-L. Lions, A. Porretta, et al. Long time average of mean field games. *NHM*, 7(2):279–301, 2012.
- [45] R. Carmona and F. Delarue. Probabilistic analysis of mean-field games. *SIAM Journal on Control and Optimization*, 51(4):2705–2734, 2013.
- [46] J. A. Carrillo, Y.-P. Choi, and M. Hauray. The derivation of swarming models: mean-field limit and wasserstein distances. *Collective dynamics from bacteria to crowds*, 553:1–46, 2014.
- [47] J. A. Carrillo, M. Fornasier, J. Rosado, and G. Toscani. Asymptotic flocking dynamics for the kinetic cucker–smale model. *SIAM Journal on Mathematical Analysis*, 42(1):218–236, 2010.
- [48] C. Cercignani. The boltzmann equation. In *The Boltzmann Equation and Its Applications*, pages 40–103. Springer, 1988.
- [49] M. Cesa. A brief history of quantitative finance. *Probability, Uncertainty and Quantitative Risk*, 2(1):6, 2017.
- [50] A. Chakraborti, I. M. Toke, M. Patriarca, and F. Abergel. Econophysics review: II. agent-based models. *Quantitative Finance*, 11(7):1013–1041, 2011.
- [51] D. Challet, M. Marsili, and Y.-C. Zhang. Stylized facts of financial markets and market crashes in minority games. *Physica A: Statistical Mechanics and its Applications*, 294(3):514–524, 2001.

- [52] D. Challet and M. Marslii. Criticality and finite size effects in a simple realistic model of stock market. *Working Paper Department of Theoretical Physics, Oxford University, INFM, Trieste-SISSA Unit, Trieste*, 2002.
- [53] F. A. Chalub, P. A. Markowich, B. Perthame, and C. Schmeiser. Kinetic models for chemotaxis and their drift-diffusion limits. *Monatshefte für Mathematik*, 142(1-2):123–141, 2004.
- [54] A. Chatterjee and B. K. Chakrabarti. Kinetic exchange models for income and wealth distributions. *The European Physical Journal B-Condensed Matter and Complex Systems*, 60(2):135–149, 2007.
- [55] A. Chatterjee, B. K. Chakrabarti, and S. Manna. Pareto law in a kinetic model of market with random saving propensity. *Physica A: Statistical Mechanics and its Applications*, 335(1):155–163, 2004.
- [56] S.-H. Chen, C.-L. Chang, and Y.-R. Du. Agent-based economic models and econometrics. *Knowledge Engineering Review*, 27(2):187–219, 2012.
- [57] C. Chiarella, R. Dieci, and L. Gardini. Speculative behaviour and complex asset price dynamics: a global analysis. *Journal of Economic Behavior & Organization*, 49(2):173–197, 2002.
- [58] C. Chiarella, R. Dieci, and L. Gardini. The dynamic interaction of speculation and diversification. *Applied Mathematical Finance*, 12(1):17–52, 2005.
- [59] C. Chiarella, R. Dieci, and L. Gardini. Asset price and wealth dynamics in a financial market with heterogeneous agents. *Journal of Economic Dynamics and Control*, 30(9):1755–1786, 2006.
- [60] C. Chiarella, R. Dieci, and X.-Z. He. Heterogeneous expectations and speculative behavior in a dynamic multi-asset framework. *Journal of Economic Behavior & Organization*, 62(3):408–427, 2007.
- [61] D. Colander, H. Föllmer, A. Haas, M. D. Goldberg, K. Juselius, A. Kirman, T. Lux, and B. Sloth. The financial crisis and the systemic failure of academic economics. 2009.
- [62] R. Cont. Empirical properties of asset returns: stylized facts and statistical issues. 2001.
- [63] R. Cont. Volatility clustering in financial markets: empirical facts and agent-based models. In *Long memory in economics*, pages 289–309. Springer, 2007.
- [64] R. Cont and J.-P. Bouchaud. Herd behavior and aggregate fluctuations in financial markets. *Macroeconomic dynamics*, 4(2):170–196, 2000.
- [65] R. Cont, M. Potters, and J.-P. Bouchaud. Scaling in stock market data: stable laws and beyond. In *Scale invariance and beyond*, pages 75–85. Springer, 1997.
- [66] S. Cordier, L. Pareschi, and C. Piatecki. Mesoscopic modelling of financial markets. *Journal of Statistical Physics*, 134(1):161–184, 2009.
- [67] S. Cordier, L. Pareschi, and G. Toscani. On a kinetic model for a simple market economy. *Journal of Statistical Physics*, 120(1-2):253–277, 2005.

- [68] I. Corporation. Intel math kernel library.
- [69] R. Cowan and N. Jonard. *Heterogenous agents, interactions and economic performance*, volume 521. Springer Science & Business Media, 2002.
- [70] R. Cross, M. Grinfeld, and H. Lamba. A mean-field model of investor behaviour. In *J. Phys. Conf. Ser.*, volume 55, pages 55–62, 2006.
- [71] R. Cross, M. Grinfeld, H. Lamba, and T. Seaman. A threshold model of investor psychology. *Physica A: Statistical Mechanics and its Applications*, 354:463–478, 2005.
- [72] R. Cross, M. Grinfeld, H. Lamba, and T. Seaman. Stylized facts from a threshold-based heterogeneous agent model. *The European Physical Journal B-Condensed Matter and Complex Systems*, 57(2):213–218, 2007.
- [73] F. Cucker and S. Smale. Emergent behavior in flocks. *Automatic Control, IEEE Transactions on*, 52(5):852–862, 2007.
- [74] P. Curie. Sur la symétrie dans les phénomènes physiques, symétrie d'un champ électrique et d'un champ magnétique. *Journal de physique théorique et appliquée*, 3(1):393–415, 1894.
- [75] M. A. Da Silva, G. T. Lima, et al. Combining monetary policy and prudential regulation: an agent-based modeling approach. *Banco Central Do Brasil Working Papers (394)*, 2015.
- [76] M. E. Dabla-Norris, M. K. Kochhar, M. N. Suphaphiphat, M. F. Ricka, and E. Tsounta. *Causes and consequences of income inequality: a global perspective*. International Monetary Fund, 2015.
- [77] J. B. Davies. *Personal wealth from a global perspective*. Oxford University Press, 2008.
- [78] R. H. Day and W. Huang. Bulls, bears and market sheep. *Journal of Economic Behavior & Organization*, 14(3):299–329, 1990.
- [79] P. De Grauwe and M. Grimaldi. *Heterogeneity of agents and the exchange rate: a nonlinear approach*. MIT Press, 2005.
- [80] G. Debreu. Excess demand functions. *Journal of mathematical economics*, 1(1):15–21, 1974.
- [81] P. Degond, M. Herty, and J.-G. Liu. Mean-field games and model predictive control. *Communications in Mathematical Sciences*, 15(5), 2017.
- [82] R. Dieci, I. Foroni, L. Gardini, and X.-Z. He. Market mood, adaptive beliefs and asset price dynamics. *Chaos, Solitons & Fractals*, 29(3):520–534, 2006.
- [83] E. W. Dijkstra. On the role of scientific thought. In *Selected writings on computing: a personal perspective*, pages 60–66. Springer, 1982.
- [84] Z. Ding, C. W. Granger, and R. F. Engle. A long memory property of stock market returns and a new model. *Journal of empirical finance*, 1(1):83–106, 1993.

- [85] R. L. Dobrushin. Vlasov equations. *Functional Analysis and Its Applications*, 13(2):115–123, 1979.
- [86] A. Dragulescu and V. M. Yakovenko. Statistical mechanics of money. *The European Physical Journal B-Condensed Matter and Complex Systems*, 17(4):723–729, 2000.
- [87] A. Drăgulescu and V. M. Yakovenko. Exponential and power-law probability distributions of wealth and income in the united kingdom and the united states. *Physica A: Statistical Mechanics and its Applications*, 299(1):213–221, 2001.
- [88] B. Düring, D. Matthes, and G. Toscani. Kinetic equations modelling wealth redistribution: a comparison of approaches. *Physical Review E*, 78(5):056103, 2008.
- [89] B. Düring and G. Toscani. Hydrodynamics from kinetic models of conservative economies. *Physica A: Statistical Mechanics and its Applications*, 384(2):493–506, 2007.
- [90] B. During, G. Toscani, et al. International and domestic trading and wealth distribution. *Communications in Mathematical Sciences*, 6(4):1043–1058, 2008.
- [91] F. Y. Edgeworth. *Mathematical psychics: An essay on the application of mathematics to the moral sciences*. Number 10. CK Paul, 1881.
- [92] R. Eftimie, G. De Vries, M. Lewis, and F. Lutscher. Modeling group formation and activity patterns in self-organizing collectives of individuals. *Bulletin of mathematical biology*, 69(5):1537, 2007.
- [93] E. Egenter, T. Lux, and D. Stauffer. Finite-size effects in monte carlo simulations of two stock market models. *Physica A: Statistical Mechanics and its Applications*, 268(1):250–256, 1999.
- [94] N. Ehrentreich. *Agent-based modeling: The Santa Fe Institute artificial stock market model revisited*, volume 602. Springer Science & Business Media, 2007.
- [95] N. Ehrentreich. Agent-based modeling. *Lecture Notes in Economics and Mathematical Systems*, 602, 2008.
- [96] M. Ernst and R. Brito. Scaling solutions of inelastic boltzmann equations with overpopulated high energy tails. *Journal of Statistical Physics*, 109(3):407–432, 2002.
- [97] M. H. Ernst and R. Brito. High-energy tails for inelastic maxwell models. *EPL (Euro-physics Letters)*, 58(2):182, 2002.
- [98] L. C. Evans. An introduction to stochastic differential equations version 1.2. *Lecture Notes, UC Berkeley*, 2006.
- [99] E. F. Fama. Mandelbrot and the stable paretian hypothesis. *Journal of Business*, pages 420–429, 1963.
- [100] E. F. Fama. Efficient capital markets: A review of theory and empirical work*. *The journal of Finance*, 25(2):383–417, 1970.
- [101] D. Farmer. Seminar presented at université de paris vi, 1997.

- [102] J. D. Farmer and D. Foley. The economy needs agent-based modelling. *Nature*, 460(7256):685–686, 2009.
- [103] J. D. Farmer and S. Joshi. The price dynamics of common trading strategies. *Journal of Economic Behavior & Organization*, 49(2):149–171, 2002.
- [104] M. Frank, A. Klar, E. Larsen, and S. Yasuda. Approximate models for radiative transfer. *Bulletin-institute of mathematics academia sinica*, 2(2):409, 2007.
- [105] R. Franke and F. Westerhoff. Structural stochastic volatility in asset pricing dynamics: Estimation and model contest. *Journal of Economic Dynamics and Control*, 36(8):1193–1211, 2012.
- [106] Y. Fujiwara, W. Souma, H. Aoyama, T. Kaizoji, and M. Aoki. Growth and fluctuations of personal income. *Physica A: Statistical Mechanics and its Applications*, 321(3):598–604, 2003.
- [107] G. Furioli, A. Pulvirenti, E. Terraneo, and G. Toscani. Fokker–planck equations in the modeling of socio-economic phenomena. *Mathematical Models and Methods in Applied Sciences*, 27(01):115–158, 2017.
- [108] R. Gibrat. Les inégalités économiques. 1931.
- [109] N. Gilbert. *Agent-based models*. Number 153. Sage, 2008.
- [110] S. Goldstein. On diffusion by discontinuous movements, and on the telegraph equation. *The Quarterly Journal of Mechanics and Applied Mathematics*, 4(2):129–156, 1951.
- [111] F. Golse. The mean-field limit for the dynamics of large particle systems. *Journées équations aux dérivées partielles*, 9:1–47, 2003.
- [112] F. Golse. On the dynamics of large particle systems in the mean field limit. In *Macroscopic and Large Scale Phenomena: Coarse Graining, Mean Field Limits and Ergodicity*, pages 1–144. Springer, 2016.
- [113] P. Gopikrishnan, V. Plerou, L. A. N. Amaral, M. Meyer, and H. E. Stanley. Scaling of the distribution of fluctuations of financial market indices. *Physical Review E*, 60(5):5305, 1999.
- [114] O. Guéant, J.-M. Lasry, and P.-L. Lions. Mean field games and applications. *Paris-Princeton lectures on mathematical finance 2010*, pages 205–266, 2011.
- [115] G. Harras and D. Sornette. How to grow a bubble: A model of myopic adapting agents. *Journal of Economic Behavior & Organization*, 80(1):137–152, 2011.
- [116] C. C. R. D. X.-Z. He. The dynamic behaviour of asset prices in disequilibrium: a survey. *International Journal of Behavioural Accounting and Finance*, 2(2):101–139, 2011.
- [117] A. Heertje. Recent criticism of general equilibrium theory. In *Equilibrium, Markets and Dynamics*, pages 51–60. Springer, 2002.
- [118] P. Hellekalek. Good random number generators are (not so) easy to find. *Mathematics and Computers in Simulation*, 46(5):485–505, 1998.

- [119] T. Hellthaler. The influence of investor number on a microscopic market model. *International Journal of Modern Physics C*, 6(06):845–852, 1996.
- [120] M. Herty and A. Klar. Modeling, simulation, and optimization of traffic flow networks. *SIAM Journal on Scientific Computing*, 25(3):1066–1087, 2003.
- [121] C. H. Hommes. Heterogeneous agent models in economics and finance. *Handbook of computational economics*, 2:1109–1186, 2006.
- [122] M. Huang, P. E. Caines, and R. P. Malhamé. An invariance principle in large population stochastic dynamic games. *Journal of Systems Science and Complexity*, 20(2):162–172, 2007.
- [123] M. Huang, R. P. Malhamé, and P. E. Caines. Nash certainty equivalence in large population stochastic dynamic games: Connections with the physics of interacting particle systems. In *Decision and Control, 2006 45th IEEE Conference on*, pages 4921–4926. IEEE, 2006.
- [124] M. Huang, R. P. Malhamé, P. E. Caines, et al. Large population stochastic dynamic games: closed-loop mckean-vlasov systems and the nash certainty equivalence principle. *Communications in Information & Systems*, 6(3):221–252, 2006.
- [125] G. Iori and J. Porter. Agent-based modelling for financial markets. *Chapter prepared for the Handbook on Computational Economics and Finance*, 2012.
- [126] E. Ising. Beitrag zur theorie des ferromagnetismus. *Zeitschrift für Physik A Hadrons and Nuclei*, 31(1):253–258, 1925.
- [127] K. Itō. *On stochastic differential equations*, volume 4. American Mathematical Soc., 1951.
- [128] P.-E. Jabin. A review of the mean field limits for vlasov equations. *Kinet. Relat. Models*, 7(4):661–711, 2014.
- [129] M. C. Jensen. Some anomalous evidence regarding market efficiency. *Journal of financial economics*, 6(2-3):95–101, 1978.
- [130] B. Jovanovic and R. W. Rosenthal. Anonymous sequential games. *Journal of Mathematical Economics*, 17(1):77–87, 1988.
- [131] M. Kac. Foundations of kinetic theory. In *Proceedings of the Third Berkeley Symposium on Mathematical Statistics and Probability*, volume 1955, pages 171–197, 1954.
- [132] M. Kac. A stochastic model related to the telegrapher’s equation. *Rocky Mountain Journal of Mathematics*, 4(3), 1974.
- [133] D. Kahneman. Maps of bounded rationality: Psychology for behavioral economics. *The American economic review*, 93(5):1449–1475, 2003.
- [134] D. Kahneman and A. Tversky. Prospect theory: An analysis of decision under risk. *Econometrica: Journal of the Econometric Society*, pages 263–291, 1979.

- [135] T. Kaizoji. Speculative bubbles and crashes in stock markets: an interacting-agent model of speculative activity. *Physica A: Statistical Mechanics and its Applications*, 287(3):493–506, 2000.
- [136] T. Kaizoji, S. Bornholdt, and Y. Fujiwara. Dynamics of price and trading volume in a spin model of stock markets with heterogeneous agents. *Physica A: Statistical Mechanics and its Applications*, 316(1):441–452, 2002.
- [137] T. L. Karl. Economic inequality and democratic instability. *Journal of Democracy*, 11(1):149–156, 2000.
- [138] E. Kashdan and L. Pareschi. Mean field mutation dynamics and the continuous luria–delbrück distribution. *Mathematical biosciences*, 240(2):223–230, 2012.
- [139] A. Kempf and O. Korn. Market depth and order size. *Journal of Financial Markets*, 2(1):29–48, 1999.
- [140] G.-r. Kim and H. M. Markowitz. Investment rules, margin, and market volatility. *The Journal of Portfolio Management*, 16(1):45–52, 1989.
- [141] A. Kirman. Ants, rationality, and recruitment. *The Quarterly Journal of Economics*, 108(1):137–156, 1993.
- [142] A. P. Kirman, G. Teyssiére, et al. Microeconomic models for long-memory in the volatility of financial time series. Technical report, Society for Computational Economics, 2001.
- [143] R. Kohl. The influence of the number of different stocks on the levy–levy–solomon model. *International Journal of Modern Physics C*, 8(06):1309–1316, 1997.
- [144] A. Lachapelle, J.-M. Lasry, C.-A. Lehalle, and P.-L. Lions. Efficiency of the price formation process in presence of high frequency participants: a mean field game analysis. *Mathematics and Financial Economics*, 10(3):223–262, 2016.
- [145] H. Lamba and T. Seaman. Market statistics of a psychology-based heterogeneous agent model. *International Journal of Theoretical and Applied Finance*, 11(07):717–737, 2008.
- [146] O. E. Lanford III. Time evolution of large classical systems. In *Dynamical systems, theory and applications*, pages 1–111. Springer, 1975.
- [147] B. Lapeyre, E. Pardoux, and R. Sentis. *Introduction to Monte Carlo methods for transport and diffusion equations*, volume 6. Oxford University Press on Demand, 2003.
- [148] J.-M. Lasry and P.-L. Lions. Mean field games. *Japanese journal of mathematics*, 2(1):229–260, 2007.
- [149] J.-M. Lasry, P.-L. Lions, and O. Guéant. Application of mean field games to growth theory. 2008.
- [150] B. LeBaron. Agent-based computational finance: Suggested readings and early research. *Journal of Economic Dynamics and Control*, 24(5):679–702, 2000.

- [151] B. LeBaron. Agent-based financial markets: Matching stylized facts with style. *Post Walrasian Macroeconomics: Beyond the DSGE Model*, pages 221–235, 2006.
- [152] B. LeBaron. Agent-based financial markets: Matching stylized facts with style. *Post Walrasian Macroeconomics: Beyond the DSGE Model*, pages 221–235, 2006.
- [153] D. Leopold. *The young Karl Marx: German philosophy, modern politics, and human flourishing*, volume 81. Cambridge University Press, 2007.
- [154] H. Levy, M. Levy, and S. Solomon. *Microscopic simulation of financial markets: from investor behavior to market phenomena*. Academic Press, 2000.
- [155] M. Levy, H. Levy, and S. Solomon. A microscopic model of the stock market: cycles, booms, and crashes. *Economics Letters*, 45(1):103–111, 1994.
- [156] M. Levy, H. Levy, and S. Solomon. Microscopic simulation of the stock market: the effect of microscopic diversity. *Journal de Physique I*, 5(8):1087–1107, 1995.
- [157] M. Levy, N. Persky, and S. Solomon. The complex dynamics of a simple stock market model. *International Journal of High Speed Computing*, 8(01):93–113, 1996.
- [158] A. W. Lo. The adaptive markets hypothesis: Market efficiency from an evolutionary perspective. *Journal of Portfolio Management, Forthcoming*, 2004.
- [159] R. E. Lucas. Econometric policy evaluation: A critique. In *Carnegie-Rochester conference series on public policy*, volume 1, pages 19–46. Elsevier, 1976.
- [160] T. Lux. Herd behaviour, bubbles and crashes. *The economic journal*, pages 881–896, 1995.
- [161] T. Lux. Financial power laws: Empirical evidence, models, and mechanism. Technical report, Economics working paper/Christian-Albrechts-Universität Kiel, Department of Economics, 2006.
- [162] T. Lux. Stochastic behavioral asset pricing models and the stylized facts. Technical report, Economics working paper/Christian-Albrechts-Universität Kiel, Department of Economics, 2008.
- [163] T. Lux. Stochastic behavioral asset pricing models and the stylized facts. *Handbook of financial markets: Dynamics and evolution*, 1:161, 2009.
- [164] T. Lux and M. Marchesi. Scaling and criticality in a stochastic multi-agent model of a financial market. *Nature*, 397(6719):498–500, 1999.
- [165] T. Lux and M. Marchesi. Volatility clustering in financial markets: A microsimulation of interacting agents. *International Journal of Theoretical and Applied Finance*, 3(04):675–702, 2000.
- [166] D. Maldarella and L. Pareschi. Kinetic models for socio-economic dynamics of speculative markets. *Physica A: Statistical Mechanics and its Applications*, 391(3):715–730, 2012.

- [167] B. G. Malkiel. The efficient market hypothesis and its critics. *The Journal of Economic Perspectives*, 17(1):59–82, 2003.
- [168] B. G. Malkiel and E. F. Fama. Efficient capital markets: A review of theory and empirical work. *The journal of Finance*, 25(2):383–417, 1970.
- [169] B. B. Mandelbrot. *The variation of certain speculative prices*. Springer, 1997.
- [170] B. B. Mandelbrot. A multifractalwalkdown. *Scientific American*, page 71, 1999.
- [171] R. N. Mantegna and H. E. Stanley. Scaling behaviour in the dynamics of an economic index. *Nature*, 376(6535):46–49, 1995.
- [172] R. N. Mantegna and H. E. Stanley. *Introduction to econophysics: correlations and complexity in finance*. Cambridge university press, 1999.
- [173] R. R. Mantel. On the characterization of aggregate excess demand. *Journal of economic theory*, 7(3):348–353, 1974.
- [174] H. Markowitz. Portfolio selection. *The journal of finance*, 7(1):77–91, 1952.
- [175] D. Matthes and G. Toscani. Analysis of a model for wealth redistribution. *Kinetic and related Models*, 1:1–22, 2008.
- [176] D. Matthes and G. Toscani. On steady distributions of kinetic models of conservative economies. *Journal of Statistical Physics*, 130(6):1087–1117, 2008.
- [177] H. P. McKean. Propagation of chaos for a class of non-linear parabolic equations. *Stochastic Differential Equations (Lecture Series in Differential Equations, Session 7, Catholic Univ., 1967)*, pages 41–57, 1967.
- [178] S. Méléard. Asymptotic behaviour of some interacting particle systems; mckean-vlasov and boltzmann models. In *Probabilistic models for nonlinear partial differential equations*, pages 42–95. Springer, 1996.
- [179] R. C. Merton. Lifetime portfolio selection under uncertainty: The continuous-time case. *The review of Economics and Statistics*, pages 247–257, 1969.
- [180] R. C. Merton. Optimum consumption and portfolio rules in a continuous-time model. *Journal of economic theory*, 3(4):373–413, 1971.
- [181] R. C. Merton. Theory of rational option pricing. *The Bell Journal of economics and management science*, pages 141–183, 1973.
- [182] R. C. Merton. On the pricing of corporate debt: The risk structure of interest rates. *The Journal of finance*, 29(2):449–470, 1974.
- [183] P. Michel, S. Mischler, and B. Perthame. General relative entropy inequality: an illustration on growth models. *Journal de mathématiques pures et appliquées*, 84(9):1235–1260, 2005.
- [184] J. S. Mill. On the definition of political economy and method of investigation proper to it (1836). *Collected Works of John Stuart Mill*, 4:120–164, 1994.

- [185] K. S. Miller. On the inverse of the sum of matrices. *Mathematics Magazine*, pages 67–72, 1981.
- [186] J. E. Mitchell and S. Braun. Rebalancing an investment portfolio in the presence of convex transaction costs, including market impact costs. *Optimization Methods and Software*, 28(3):523–542, 2013.
- [187] J. F. Muth. Rational expectations and the theory of price movements. *Econometrica: Journal of the Econometric Society*, pages 315–335, 1961.
- [188] G. J. Myers, C. Sandler, and T. Badgett. *The art of software testing*. John Wiley & Sons, 2011.
- [189] N. A. G. (NAG). Nag c library.
- [190] G. Naldi, L. Pareschi, and G. Toscani. *Mathematical modeling of collective behavior in socio-economic and life sciences*. Springer, 2010.
- [191] J. Nash. Non-cooperative games. *Annals of mathematics*, pages 286–295, 1951.
- [192] H. Neunzert. The vlasov equation as a limit of hamiltonian classical mechanical systems of interacting particles. *Trans. Fluid Dynamics*, 18:663–678, 1977.
- [193] M. J. D. Ostry, M. A. Berg, and M. C. G. Tsangarides. *Redistribution, Inequality, and Growth*. International Monetary Fund, 2014.
- [194] R. Owen. *Observations on the Effect of the Manufacturing System...* 1815.
- [195] A. Pagan. The econometrics of financial markets. *Journal of empirical finance*, 3(1):15–102, 1996.
- [196] R. Palmer, W. Brian Arthur, J. H. Holland, B. LeBaron, and P. Tayler. Artificial economic life: a simple model of a stockmarket. *Physica D: Nonlinear Phenomena*, 75(1):264–274, 1994.
- [197] L. Pareschi and G. Toscani. Self-similarity and power-like tails in nonconservative kinetic models. *Journal of statistical physics*, 124(2-4):747–779, 2006.
- [198] L. Pareschi and G. Toscani. *Interacting Multiagent Systems: Kinetic Equations and Monte Carlo Methods*. Oxford University Press, 2013.
- [199] L. Pareschi and G. Toscani. Wealth distribution and collective knowledge: a boltzmann approach. *Phil. Trans. R. Soc. A*, 372(2028):20130396, 2014.
- [200] V. Pareto. Course d’ economie politique professé a l’ université de lausanne. 1896-1897.
- [201] V. Pareto. Cours d’économie politique, professé à l’université de lausanne. tome second, 1897.
- [202] F. Pérez and B. E. Granger. IPython: a system for interactive scientific computing. *Computing in Science and Engineering*, 9(3):21–29, May 2007.

- [203] B. Perthame. The general relative entropy principle—applications in perron-frobenius and floquet theories and a parabolic system for biomotors. *Rend. Accad. Naz. Sci. XL Mem. Mat. Appl.*(5), 29(1):307–325, 2005.
- [204] T. Piketty. Capital in the 21st century. 2014.
- [205] T. Piketty and G. Zucman. Capital is back: Wealth-income ratios in rich countries 1700–2010. *The Quarterly Journal of Economics*, 129(3):1255–1310, 2014.
- [206] A. Rubinstein. *Modeling bounded rationality*, volume 1. MIT press, 1998.
- [207] J. Rumbaugh, M. Blaha, W. Premerlani, F. Eddy, W. E. Lorensen, et al. *Object-oriented modeling and design*, volume 199. Prentice-hall Englewood Cliffs, NJ, 1991.
- [208] L. Saint-Raymond. *Hydrodynamic limits of the Boltzmann equation*. Number 1971. Springer, 2009.
- [209] E. Samanidou, E. Zschischang, D. Stauffer, and T. Lux. Agent-based models of financial markets. *Reports on Progress in Physics*, 70(3):409, 2007.
- [210] M. Segnon and T. Lux. Multifractal models in finance: Their origin, properties, and applications. Technical report, Kiel Working Paper, 2013.
- [211] R. J. Shiller. From efficient markets theory to behavioral finance. *The Journal of Economic Perspectives*, 17(1):83–104, 2003.
- [212] H. A. Simon. A behavioral model of rational choice. *The quarterly journal of economics*, pages 99–118, 1955.
- [213] H. A. Simon. Models of man; social and rational. 1957.
- [214] H. A. Simon. Theories of bounded rationality. *Decision and organization*, 1(1):161–176, 1972.
- [215] H. A. Simon. *Models of bounded rationality: Empirically grounded economic reason*, volume 3. MIT press, 1982.
- [216] S. Sinha, A. Chatterjee, A. Chakraborti, and B. K. Chakrabarti. *Econophysics: an introduction*. John Wiley & Sons, 2010.
- [217] J. C. L. Sismondi. *Nouveaux principes d'économie politique, ou de la richesse dans ses rapports avec la population*. Delaunay, 1827.
- [218] F. Slanina. Inelastically scattering particles and wealth distribution in an open economy. *Physical Review E*, 69(4):046102, 2004.
- [219] A. Smith. *The wealth of nations [1776]*. na, 1937.
- [220] F. Solt. Economic inequality and democratic political engagement. *American Journal of Political Science*, 52(1):48–60, 2008.
- [221] H. Sonnenschein. Market excess demand functions. *Econometrica: Journal of the Econometric Society*, pages 549–563, 1972.

- [222] D. Sornette. Physics and financial economics (1776–2014): puzzles, ising and agent-based models. *Reports on Progress in Physics*, 77(6):062001, 2014.
- [223] D. Sornette and W.-X. Zhou. Importance of positive feedbacks and overconfidence in a self-fulfilling ising model of financial markets. *Physica A: Statistical Mechanics and its Applications*, 370(2):704–726, 2006.
- [224] H. Spohn. *Large scale dynamics of interacting particles*, volume 825. Springer, 1991.
- [225] H. E. Stanley, V. Afanasyev, L. A. N. Amaral, S. Buldyrev, A. Goldberger, S. Havlin, H. Leschhorn, P. Maass, R. N. Mantegna, C.-K. Peng, et al. Anomalous fluctuations in the dynamics of complex systems: from dna and physiology to econophysics. *Physica A: Statistical Mechanics and its Applications*, 224(1-2):302–321, 1996.
- [226] H. E. Stanley, L. A. N. Amaral, D. Canning, P. Gopikrishnan, Y. Lee, and Y. Liu. Econophysics: Can physicists contribute to the science of economics? *Physica A: Statistical Mechanics and its Applications*, 269(1):156–169, 1999.
- [227] M. H. STANLEY, L. A. Amaral, S. V. Buldyrev, S. Havlin, H. Leschhorn, P. Maass, M. A. SALINGER, and H. EUGENE STANLEY. Can statistical physics contribute to the science of economics? *Fractals*, 4(03):415–425, 1996.
- [228] G. J. Stigler. The development of utility theory. i. *The Journal of Political Economy*, pages 307–327, 1950.
- [229] G. J. Stigler. Public regulation of the securities markets. *The Journal of Business*, 37(2):117–142, 1964.
- [230] A.-S. Sznitman. Topics in propagation of chaos. In *Ecole d’Eté de Probabilités de Saint-Flour XIX—1989*, pages 165–251. Springer, 1991.
- [231] G. I. Taylor. Diffusion by continuous movements. *Proceedings of the London Mathematical Society*, 2(1):196–212, 1922.
- [232] A. Teglio, M. Raberto, and S. Cincotti. The impact of banks’capital adequacy regulation on the economic system: An agent-based approach. *Advances in Complex Systems*, 15(supp02):1250040, 2012.
- [233] A. Tiwana, J. Wang, M. Keil, and P. Ahluwalia. The bounded rationality bias in managerial valuation of real options: Theory and evidence from it projects. *Decision Sciences*, 38(1):157–181, 2007.
- [234] M. Torregrossa and G. Toscani. On a fokker–planck equation for wealth distribution. 2017.
- [235] G. Toscani. Wealth redistribution in conservative linear kinetic models. *EPL (Euro-physics Letters)*, 88(1):10007, 2009.
- [236] G. Toscani, C. Brugna, and S. Demichelis. Kinetic models for the trading of goods. *Journal of Statistical Physics*, 151(3-4):549–566, 2013.
- [237] G. Toscani et al. Kinetic models of opinion formation. *Communications in mathematical sciences*, 4(3):481–496, 2006.

- [238] J.-C. Trichet. Reflections on the nature of monetary policy non-standard measures and finance theory, 11 2010. Introductory speech at the ECB Central Banking Conference, Frankfurt [Accessed: 2016 05 13].
- [239] T. Trimborn, M. Frank, and S. Martin. Mean field limit of a behavioral financial market model. manuscript submitted for publication, arXiv preprint, <http://arxiv.org/abs/1711.02573>.
- [240] T. Trimborn, M. Herty, and M. Frank. Microscopic derivation of mean field game models. in preparation.
- [241] T. Trimborn, P. Otte, S. Cramer, M. Beikirch, E. Pabich, and M. Frank. Data set of sabcemm- a simulation framework for agent-based computational economic market models. <http://dx.doi.org/10.18154/RWTH-2017-09142>.
- [242] T. Trimborn, P. Otte, S. Cramer, M. Beikirch, E. Pabich, and M. Frank. Sabcemm- a simulation framework for agent-based computational economic market models. manuscript submitted for publication.
- [243] T. Trimborn, L. Pareschi, and M. Frank. Portfolio optimization and model predictive control: A kinetic approach. arXiv preprint.
- [244] C. Villani. On a new class of weak solutions to the spatially homogeneous boltzmann and landau equations. *Archive for rational mechanics and analysis*, 143(3):273–307, 1998.
- [245] A. Vlasov. Vibration properties of the electron gas and its application. *Scientific notes of the Moscow State University, Physics*, 75, 1945.
- [246] A. A. Vlasov. *The oscillation properties of an electron gas*. US Atomic Energy Commission, 1938.
- [247] J. Von Neumann and O. Morgenstern. *Theory of games and economic behavior (60th Anniversary Commemorative Edition)*. Princeton university press, 2007.
- [248] D. A. Walker. *Walrasian Economics*. Cambridge University Press, 2006.
- [249] L. Walras. *Études d'économie sociale:(Théorie de la répartition de la richesse sociale.)*. F. Rouge, 1896.
- [250] L. Walras. *Études d'économie politique appliquée:(Théorie de la production de la richesse sociale)*. F. Rouge, 1898.
- [251] L. Walras. *Elements of pure economics*. Routledge, 2013.
- [252] P. Weiss. L'hypothèse du champ moléculaire et la propriété ferromagnétique. *J. phys. theor. appl.*, 6(1):661–690, 1907.
- [253] W.-X. Zhou and D. Sornette. Self-organizing ising model of financial markets. *The European Physical Journal B-Condensed Matter and Complex Systems*, 55(2):175–181, 2007.

- [254] E. Zschischang and T. Lux. Some new results on the levy, levy and solomon microscopic stock market model. *Physica A: Statistical Mechanics and its Applications*, 291(1):563–573, 2001.